University of Alberta

APPLICATION OF PERFLUORINATED ACID ISOMER PROFILES FOR MANUFACTURING AND EXPOSURE SOURCE DETERMINATION

by

Jonathan P. Benskin

A thesis submitted to the Faculty of Graduate Studies and Research
in partial fulfillment of the requirements for the degree of

Doctor of Philosophy

in

Medical Sciences

Department of Laboratory Medicine and Pathology

©Jonathan P. Benskin
Spring 2011
Edmonton, Alberta

Canada

EXAMINING COMMITTEE

Dr. Andrew Holt; University of Alberta, Department of Pharmacology

Dr. X. Chris Le; University of Alberta, Department of Laboratory Medicine and

Pathology

Dr. Robert J. Letcher; Carleton University, National Wildlife Research Center

Dr. Vincent St. Louis; University of Alberta, Department of Biological Sciences

Dr. Jonathan W. Martin; University of Alberta, Department of Laboratory

Medicine and Pathology

ABSTRACT

Perfluorinated acids (PFAs) constitute a diverse class of compounds which have been manufactured for over 50 years and are now globally disseminated in the environment, including remote arctic food webs. The two most commonly detected PFAs in the environment, perfluorooctane sulfonate (PFOS, $C_8F_{17}SO_3^-$) and perfluorooctanoate (PFOA, $C_7F_{15}COO^-$) display significant adverse health effects in lab animals, and continue to garner concern from international regulatory agencies. Historical PFOS and PFOA manufacturing was predominantly by electrochemical fluorination (ECF), a process which results in 20-30% branched / 70-80% linear isomers. While ECF was for the most part phased-out in 2002, production of strictly linear PFOA continues today by a telomerization process. Among the questions pertaining to future regulation of these chemicals is to what extent PFOA in the environment can be attributed to ECF (mostly historical production) versus telomerization (ongoing production), and to what extent precursors (i.e. indirect exposure) contribute to environmental PFOS concentrations. It was hypothesised that PFA isomer profiles in humans and environmental samples may be useful as a tool for manufacturing and/or exposure source determination. To explore this, an LC-MS/MS method was developed to characterize the major PFA and PFA-precursor isomers in human and environmental samples. Whilst PFOA isomer profiles are predominantly linear in humans and wildlife, PFOS isomer profiles can be enriched or deficient in branched content, relative to historically manufactured formulations. These profiles were partially explained by isomer-specific pharmacokinetic and

biotransformation experiments, whereby branching of the perfluoroalkyl chain typically resulted in faster elimination of PFAs in rodents, while branching of a PFOS-precursor typically resulted in faster biotransformation in human liver microsomes. Based on these results, quantitative assessment of manufacturing source in biological samples is expected to be difficult; therefore, we examined water samples in which isomer profiles were expected to be largely conserved. PFOA in sub-Arctic and Atlantic regions was found to be predominantly of ECF-origin, which confirms model predictions on the global release and transport of PFAs. Nonetheless, linear-telomer contributions were significant in most locations, suggesting that current production may represent a significant source of PFAs to remote arctic food-webs in the future.

This thesis is structured as a series of manuscripts which have been published, submitted, and/or are in preparation for submission to peer-reviewed journals. Accordingly, repetition of prefatory sections (introduction, materials, methods, etc.) was inevitable. All manuscripts were written by Jonathan P. Benskin with critical comments provided by Jonathan W. Martin. Contributions of all co-authors are provided in detail below.

Chapter One – Manufacturing of Perfluorinated Acids and Their Precursors

Excerpts Published in – Rev Environ Contam Toxicol. 208: 111–160.

Author List – Jonathan P. Benskin, Amila O. De Silva, Jonathan W. Martin

Contributions – Jonathan Benskin prepared this manuscript with editorial comments by Amila O. De Silva and Jonathan W. Martin

Chapter Two – Simultaneous Characterization of Perfluoroalkyl Carboxylate, Sulfonate, and Sulfonamide Isomers by Liquid Chromatography-Tandem Mass Spectrometry.

Published in – Anal Chem. 79: 6455–6464.

Author List – Jonathan P. Benskin, Mahmoud Bataineh, Jonathan W. Martin

Contributions – Jonathan Benskin conducted method development, data collection, interpretation, and manuscript preparation. Mahmoud Bataineh

provided helpful suggestions on mobile phase conditions and gradient. This work was conducted under the guidance of Jonathan Martin.

Chapter Three – Disposition of Perfluorinated Acid Isomers in Sprague-Dawley Rats following a Single Dose

Published in – *Environ Toxicol Chem.* 28(3): 542–554.

Author List – Jonathan P. Benskin, Amila O. De Silva, Leah J. Martin, Gilles Arsenault, Robert McCrindle, Nicole Riddell, Scott A. Mabury, and Jonathan W. Martin

Contributions – Jonathan Benskin was responsible for animal husbandry, preparation of the administered dose, sample acquisition, analysis of perfluorocarboxylate and sulfonate isomers, and data interpretation. Leah Martin provided statistical analysis. Gilles Arsenault, Robert McCrindle, and Nicole Riddell prepared and provided purified isomers of PFOS and PFOA for identification of ECF composition. Each author contributed to the design of the study and provided comments on the manuscript prepared by Jonathan Benskin. This work was conducted under the guidance of Jonathan Martin.

Chapter Four – Isomer-Specific Biotransformation Rates of a Perfluorooctane Sulfonate (PFOS)-Precursor by Cytochrome P450 Isozymes and Human Liver Microsomes

Published in – *Environ Sci Technol.* 43(22): 8566–8572.

Author List – Jonathan P. Benskin, Andrew Holt, Jonathan W. Martin

Contributions – Jonathan Benskin conducted method development, data collection, interpretation, and manuscript preparation. Andrew Holt provided helpful comments on experimental design, and kinetic modelling experiments. This work was conducted under the guidance of Jonathan Martin.

Chapter Five – Perfluorinated Acid Isomer Profiling in Water and Quantitative Assessment of Manufacturing Source

Published in – *Environ Sci Technol.* 44(23): 9049–9054.

Author List – Jonathan P. Benskin, Leo W.Y. Yeung, Nobuyoshi Yamashita, Sachi Taniyasu, Paul Lam, and Jonathan W. Martin

Contributions – Jonathan Benskin collected Mississippi River water, conducted method development, data collection, interpretation, and manuscript preparation. Leo Yeung, Nobuyoshi Yamashita, Sachi Taniyasu, and Paul Lam provided coastal Asia water extracts. This work was conducted under the guidance of Jonathan Martin.

Chapter Six – Perfluorinated Acid Isomer Profiling in Water from Remote Locations

To be submitted to – *Environ Sci Technol.*

Author List – Jonathan P. Benskin, Lutz Ahrens, Gregg Tomy, Derek Muir, Brian Scott, Christine Spencer, Bruno Rosenburg and Jonathan W. Martin

Contributions – Jonathan Benskin conducted method development, data collection, interpretation, and manuscript preparation. Lutz Ahrens provided

extracts from the Eastern Atlantic. Gregg Tomy, Derek Muir, Brian Scott, Christine Spencer, and Bruno Rosenburg provided Atlantic and Arctic Ocean extracts. This work was conducted under the guidance of Jonathan Martin.

Chapter Seven – Summary, Conclusions and Future Work

Excerpts Published in – Rev Environ Contam Toxicol. 208: 111–160.

Author List – Jonathan P. Benskin, Amila O. De Silva, Jonathan W. Martin

Contributions – Jonathan Benskin prepared this manuscript with editorial comments by Amila O. De Silva and Jonathan W. Martin.

ACKNOWLEDGEMENTS

TABLE OF CONTENTS

LIST OF TABLES

LIST OF FIGURES

LIST OF APPENDICES

Chapter 1. Manufacturing of Perfluorinated Acids

Excerpts of this chapter have been published with kind permission from Springer Science+Business Media: *Rev. Environ. Contam. Toxicol.* Isomer Profiling of Perfluorinated Substances as a Tool for Source Tracking: A Review of Early Findings and Future Applications, 208, 111-160, Benskin, J.P.; De Silva, A.O.; Martin, J.W. Copyright Springer Science+Business Media, LLC 2010.

1.1   Introduction

Perfluorinated compounds (PFCs) constitute a diverse class of chemicals which have been manufactured for over 60 years for use in various commercial products and processes. The presence of PFCs in human blood was first detected by Taves et al.[1] in 1968 using nuclear magnetic resonance (NMR) spectroscopy, albeit analytical capabilities at the time prevented structural confirmation of these materials. Over thirty years later, perfluorinated acids (PFAs) were first identified in the blood of humans[2] and wildlife[3] using liquid chromatography-tandem mass spectrometry. Since then, the widespread distribution of PFAs in the global environment has been corroborated, with PFA concentrations in the blood of humans and remote arctic wildlife exceeding those of most legacy persistent organic pollutants (POPs)[4,5]. PFAs combine persistence with significant chain-length dependent bioaccumulation[6] and long-range transport potentials[7-11] and have also displayed significant adverse health effects in animal models. Due to the hazard profile associated with these chemicals, perfluorooctane sulfonate (PFOS; one of the most commonly detected PFAs in the environment) and its precursors

1

were recently listed as Annex B persistent organic pollutants under the International Stockholm Convention Treaty[12]. Elucidating sources of exposure to PFAs is necessary to help mitigate future risks associated with these chemicals.

1.2   Potential Health Implications

Interestingly, perfluorinated carboxylates (including perfluorooctanoate, PFOA) were studied for over a decade prior to their identification in humans and wildlife due to their potency as peroxisome proliferators[13]. More recently, PFAs have been associated with serum cholesterol reduction, disruption of intracellular communication, hepatotoxicity, tumors, and developmental abnormalities in animal models[14]. Despite these clear links to adverse health effects, assessing the risk that PFAs pose to humans is difficult due to vast differences in their toxicological profile between species. For example, PFOS and PFOA have extremely long half lives in humans (4-5 years[15]), which is in sharp contrast to the half life observed in cynomolgus monkeys for PFOS (200 days following 6 months of oral dosing[16]) and PFOA (14-42 days for male or female monkeys following oral or IV administration[17]). In rodents, PFOS and PFOA elimination half lives are on the order of days, depending on sex and route of exposure[18-20]. The route of elimination also varies between species; rodents excrete perfluorinated carboxylates primarily via the urine, while for humans and monkeys, excretion is predominantly in the feces[21]. Andersen et al.[22] suggested that differences in elimination half lives between species are a result of higher reabsorption efficiency in humans.

The mechanism of toxicity can also be markedly different between humans and animal models. In rodents, PFAs activate peroxisome proliferator-activated receptor alpha (PPARα), which induces peroxisome proliferation and an increased incidence of tumors[21]. While PFAs have been found to activate human PPARα to a greater extent than rat PPARα[23], this receptor is not highly expressed in humans, and following activation operates under a different pathway than in rodents. In general, the PPARα mode of action, which induces tumors in rats is thought to be largely irrelevant in humans, and associations between PFA exposure and incidence of cancer have been largely inconsistent in occupational exposure studies. For example, a recent study by Lundin et al.[24] observed no association between occupational exposure to PFOA and liver, pancreatic and testicular cancer or liver cirrhosis but did find an association (albeit inconsistently) with prostate cancer, cerebrovasular disease, and diabetes. This latter result appears consistent with an earlier study, which also observed a correlation between PFOA exposure and mortality from prostate cancer[25].

The link between PFA exposure and developmental toxicity in humans has also been largely inconclusive thus far, although PFAs have been observed to cross the placenta[26,27] and have also been observed in breast milk[28,29]. Appelberg et al.[30,31] observed statistically significant negative associations between PFOS and PFOA concentrations with birth weight, ponderal index (measure of leanness), and head circumference, but no associations with newborn length or gestational age. In contrast, Grice et al.[32] observed no associations between women occupationally exposed to PFOS and the birth weight of their offspring.

Nolan et al.[33] concluded that exposure to PFOA-contaminated drinking water was not associated with an increased risk of congenital anomalies, labour or delivery complications, or maternal risk factors. Similarly, in a study of 1400 non-occupationally exposed women from Denmark, Fei et al.[34] also observed no correlation between PFOS concentrations and birth weight, but did observe an association between PFOA and birth weight.

The ability of PFOS and PFOA to bind nuclear receptors[35] and displace serum protein-ligand binding[36,37] has also led to speculation that these compounds may act as endocrine disruptors. Multiple studies have demonstrated the toxicity of PFAs towards the thyroid at high doses in animal models[16,38-40]. In humans, Melzer et al.[41] observed a correlation between higher concentrations of serum PFOS and PFOA and incidence of thyroid disease. This contrasts the results of Bloom et al.[42], in which non-occupational exposure to PFAs was not associated with thyroid function, albeit a weak association was observed with free thyroxine and perfluorodecanoate and perfluorundecanoate.

Overall, it is still unclear whether exposure to PFAs leads to adverse health effects in humans. Of concern are the inconsistencies between human and animal models, exposure to presently unidentified PFAs or PFA-precursors, as well as possible synergistic effects of multiple PFAs of different chain length or functional group, which cannot be accounted for in toxicological studies involving single substances.

1.3   Perfluoralkyl Chain Branching

In the over half-century of global perfluorochemical manufacturing, the two most commonly used synthetic methods have produced products with very different isomeric purities. Despite the fact that both branched and linear PFA and PFA-precursor isomers exist in the environment, quantitative analysis of these chemicals is, for the most part, still conducted by eluting all isomers together and integrating them as a single peak. This practice has continued despite the fact that emerging literature suggests that more accurate and informative data can be generated by isomer-specific analysis.

The extent to which perfluoromethyl branching patterns affect the physical, chemical, and biological properties of perfluorinated substances is of increasing scientific interest. It is hypothesized that branching patterns may affect properties such as environmental transport and degradation, partitioning, bioaccumulation, pharmacokinetics, and toxicity. It may even influence total PFA quantification, thus perhaps leading to questions about the accuracy of current human and environmental exposure assessments. Of particular focus in this thesis is the measurement and interpretation of isomer signatures in the environment to gain new knowledge on emission sources, to differentiate between historical versus current exposure sources, or to identify direct versus indirect pathways of exposure for humans and wildlife. To do this effectively requires adequate analytical methods, and a fundamental knowledge of the properties that may affect the environmental fate of individual isomers.

1.4   Isomer Nomenclature

PFA and PFA-precursor acronyms and empirical formulae are listed in Table 1.1. While a comprehensive numbering system was recently proposed for all isomers of perfluoroalkyl sulfonates and carboxylates[43], herein we have adopted an earlier, more rudimentary, system developed by Langlois and Oehme[44] (2006), and modified by Benskin et al.[45] for the limited number of isomers actually present in the commercially manufactured PFA- and PFA-precursor formulations (see section on *Historical and Current Manufacturing Sources of Perfluoroalkyl Isomers*). Using perfluorooctane sulfonate (PFOS, Table 1.1) as an example, linear, perfluoroisopropyl, and *tert*-perfluorobutyl are abbreviated as *n*-, *iso*-, and *tb*-PFOS, respectively. For the remaining monomethyl branched isomers, *m* refers to a perfluoromethyl branch and the number preceding it indicates the carbon position on which the branch resides. Likewise, dimethyl substituted branched isomers are labelled as m_2 and the preceding numbers refer to the location of the CF_3 branching points. For example, 5-perfluoromethyl-PFOS is abbreviated as 5*m*-PFOS, while 5,3-perfluorodimethyl-PFOS is abbreviated as 5,3m_2-PFOS. The same nomenclature system was adopted for perfluoroalkyl carboxylates (PFCAs), however it should be noted that 1*m*-PFCAs do not exist, since the carbon in the 1-position corresponds to the carboxylate moiety.

Table 1.1 Acronyms and empirical formulas for perfluoroalkyl sulfonates, sulfonamides, and carboxylates

Chemical	Formula	Acronyms
Perfluoroalkyl sulfonates		
Perfluorobutane sulfonate	$F(CF_2)_4SO_3^-$	PFBS
Perfluoropentane sulfonate	$F(CF_2)_5SO_3^-$	PFPeS
Perfluorohexane sulfonate	$F(CF_2)_6SO_3^-$	PFHxS
Perfluoroheptane sulfonate	$F(CF_2)_7SO_3^-$	PFHpS
Perfluorooctane sulfonate	$F(CF_2)_8SO_3^-$	PFOS
Perfluorodecane sulfonate	$F(CF_2)_{10}SO_3^-$	PFDS
Perfluoroalkyl sulfonamides		
N-methyl perfluorooctanesulfonamidoethanol	$F(CF_2)_8SO_2N(CH_3)(CH_2CH_2OH)$	NMeFOSE
N-ethyl perfluorooctanesulfonamidoethanol	$F(CF_2)_8SO_2N(CH_2CH_3)(CH_2CH_2OH)$	NEtFOSE
Perfluorooctanesulfonamide	$F(CF_2)_8SO_2NH_2$	PFOSA
N-ethyl perfluorooctanesulfonamide	$F(CF_2)_8SO_2N(CH_2CH_3)H$	NEtFOSA
N-methyl perfluorooctanesulfonamide	$F(CF_2)_8SO_2N(CH_3)H$	NMeFOSA
Perfluorooctanesulfonamidoethanol	$F(CF_2)_8SO_2NH(CH_2CH_2OH)$	FOSE
Perfluorooctanesulfonamidoacetate	$F(CF_2)_8SO_2NH(CH_2C(O)OH)$	FOSAA
N-ethyl perfluorooctanesulfonamidoacetate	$F(CF_2)_8SO_2N(CH_2CH_3)(CH_2C(O)OH)$	NEtFOSAA
N-methyl perfluorooctanesulfonamidoacetate	$F(CF_2)_8SO_2N(CH_3)(CH_2C(O)OH)$	NMeFOSAA
Perfluoroalkyl carboxylates		
Trifluoroacetate	$F(CF_2)C(O)O^-$	TFA
Perfluoropropanoate	$F(CF_2)_2C(O)O^-$	PFPrA
Perfluorobutanoate	$F(CF_2)_3C(O)O^-$	PFBA
Perfluoropentanoate	$F(CF_2)_4C(O)O^-$	PFPeA
Perfluorohexanoate	$F(CF_2)_5C(O)O^-$	PFHxA
Perfluoroheptanoate	$F(CF_2)_6C(O)O^-$	PFHpA
Perfluorooctanoate	$F(CF_2)_7C(O)O^-$	PFOA
Perfluorononanoate	$F(CF_2)_8C(O)O^-$	PFNA
Perfluorodecanoate	$F(CF_2)_9C(O)O^-$	PFDA
Perfluoroundecanoate	$F(CF_2)_{10}C(O)O^-$	PFUnA
Pefluorododecanoate	$F(CF_2)_{11}C(O)O^-$	PFDoA
Perfluorotridecanoate	$F(CF_2)_{12}C(O)O^-$	PFTrA
Perfluorotetradecanoate	$F(CF_2)_{13}C(O)O^-$	PFTA

1.5 Historical and Current Manufacturing Sources of Perfluoroalkyl Isomers

The various synthetic routes and their estimated contributions to the global environmental mass balance of perfluorochemicals have been recently reviewed[46-48]. The following section focuses on the relevance of perfluorochemical manufacturing to isomer profiles and the implications for source tracking. The major production of perfluorochemicals has historically occurred by either Simons electrochemical fluorination (ECF), or by telomerization. Telomerization is a synthetic process that results in an isomerically pure product, which retains

7

the structure of the starting material (typically linear), whereas ECF results in a mixture of branched and linear isomers and by-products. ECF was used to produce all 3M-manufactured perfluorooctane sulfonyl fluoride (PFOSF, $C_8F_{17}SO_2F$)-based products since 1949[47], and the majority of 3M perfluorooctanoic acid since 1947[48]. Although 3M phased out their perfluorooctyl-based chemistries in 2002, the company continues to manufacture perfluorobutyl-based products by this method[49]. Telomerization, which was originally developed by DuPont,[50] saw minor use beginning in the 1970s for the production of PFOA; however, it was not until the 2002 phase out of 3M ECF-PFOA that DuPont began the large-scale manufacturing of PFOA by this alternative technique. Telomerization continues to be the dominant production method today for producing PFOA and perfluorononanoic acid (PFNA), however Prevedouros et al.[48] indicated that minor ECF manufacturing of ammonium perfluorooctanoate (APFO) has continued since 2002 in Asia and Europe. Although it is not clear how much ECF production continues today, in this thesis ECF will be generally regarded as the 'historical' manufacturing process, whereas telomerization will be regarded as the 'current' production method, despite it's minor use from the 1970s-2002[51,52].

It is only germane to note that other synthetic routes to branched PFCAs have been reported in the patent literature, as reviewed elsewhere[46]. For example, liquid phase direct fluorination (LPDF) can produce minor quantities of branched isomers of perfluoroalkyl substances and this may explain the small quantities of branched isomers in PFOA purchased from supplier Sigma Aldrich/Fluka

8

(Steinhiem, Switzerland) (Table 1.2). However, it is unclear what contribution, if any, these minor manufacturing sources make to global PFA loadings.

Table 1.2 Principally manufactured PFOS/PFOA isomer compositions, compared to specialty chemical isomer compositions determined by ^{19}F NMR. Note that in some cases, companies listed are the suppliers and not necessarily the manufacturers. Isomers are abbreviated as normal (*n*), internal monomethyl (*im*), isopropyl (*iso*), alpha (*α*), t-butyl (*tb*), dimethyl (*dm*), and total branched ($\sum br$).

Isomer	Principle manufactured isomer profiles (wt %)		Specialty chemical isomer profiles (wt %)							
	PFOA 3M[a]	PFOS 3M[b]	PFOS TCI[c]	PFOS Matrix[d]	PFOS Sigma Aldrich Fluka[e]	T-PFOS Wellington[f]	br-PFOS Wellington[g]	PFOS Sigma Aldrich/ Fluka[h]	PFOS Oakwood[i]	PFOA Sigma Aldrich/ Fluka[j]
Lot #	Assumed equivalent in all lots[53]		GJ01	P15D	436098/1	TPFOS04 05	brPFOSK 1106	batch # 312421000	batch # 008577, lot # XO8M	n/a
n	77.6	70	67.0	68.3	78.9	68.9	78.8	82.2	72.4	98.9
im	12.6	17.0	18.7	17.9	9.3	17.9		9.8	17.7	
iso	9.0	10.3	9.6	10.9	10.0	10.8	10.0	10.0	9.4	
α	0.1	1.6	3.2	1.2	1.1	1.9	1.2	1.2	3.4	
tb	0.2	0.2	0.3	0.3	0.2	0.2	0.2	0.4	0.4	
dm	0.1	0.2	1.4	1.3	0.5	0.3	0.6	0.5		
$\sum br$	22.0	29.3	33.1	31.7	21.1	31.1	21.1	21.4	30.9	1.1

n/a – not available   [a] St. Paul, MN, USA[54]   [b] St. Paul, MN, USA[55]
[c] Portland, OR, USA[56]   [d] Columbia, SC,USA[56]   [e] Milwaukee, WI, USA, n=2 measurements[56]
[f] Guelph, ON, Canada[57]   [g] Guelph, ON, Canada[58]   [h] Buchs, Switzerland[59]
[i] West Columbia, SC, USA[59]   [j] Steinhiem, Switzerland[60]

The telomerization process involves free radical addition of a starting telogen (e.g., perfluoroethyl iodide, CF_3CF_2I) with an unsaturated taxogen (e.g., tetrafluoroethylene, $CF_2=CF_2$), thereby lengthening the perfluoroalkyl moiety by units of CF_2CF_2[50]. The major product of this reaction is typically an eight-carbon, straight-chain perfluoroalkyl iodide which is then subjected to oxidation with oleum to form PFOA[61], or carboxylation to form PFNA, the latter of which is used by several companies in the US, France, and Japan[48] for the manufacturing of polyvinylidene fluoride. Fluoroalkyl iodides can also be reacted to form

fluorotelomer olefins $(F(CF_2)_nCH=CH_2)$, alcohols $(F(CF_2)_nCH_2CH_2OH)$ and fluoroacrylate monomers $(F(CF_2CF_2)_nCH_2CH_2OC(O)CHR=CH_2)$, which are subsequently incorporated into polymeric material and/or surfactants for consumer product applications. Although telomerization retains the geometry of the starting telogen and thus produces a more isomerically pure product than ECF, telomerized products usually contain chain-length impurities which can be both even and/or odd chain-lengths and varying from 4-15 carbons[48]. Despite this, there are reports in the scientific and patent literature of odd numbered and branched chain perfluoroalkyl iodides being produced by telomerization using branched telogens (e.g., $(CF_3)_2CI$) and single carbon taxogens[62-64], which could result in isopropyl PFAs.

In comparison to telomerization, ECF results in numerous by-products, including branched and linear isomers of various even and odd chain lengths (Table 1.3). This method was used by 3M for perfluorination of n-octanoyl halide $(H(CH_2)_7C(O)X, X = Cl$ or $F)$ to form $F(CF_2)_7C(O)F$, which was then subjected to base-catalyzed hydrolysis to yield PFOA. The primary use of PFOA was, and still is, as an emulsifier in fluoropolymer manufacturing[48]. Similarly, ECF of n-octanesulfonyl fluoride was used to produce PFOSF, which was subsequently used as a starting material for various consumer and industrial chemical formulations. For example, base-catalyzed hydrolysis of PFOSF yields PFOS, which had minor uses, predominantly in fire-fighting foams and metal plating. It was also used intentionally to some extent in various consumer products, and can be observed as an unintentional residual in many PFOSF-derived products.

10

Reaction of PFOSF with ethylamine was used to form N-ethyl perfluorooctane sulfonamide (NEtFOSA; Table 1.1), commonly marketed as an insecticide[65]. The major use of PFOSF was reaction with ethyl or methyl amine, followed by ethylene carbonate, to yield *N*-ethyl perfluorooctane sulfonamidoethanol (NEtFOSE) and *N*-methyl perfluorooctane sulfonamidoethanol (NMeFOSE), respectively (Table 1.1). NMeFOSE was subsequently reacted to form urethane, acrylate and/or adipate monomers which were subsequently polymerized to form surface treatment products (marketed under 3M's ScotchGard™ brand)[66]. Paper protectors used in food packaging and commercial applications consisted of either NMeFOSE-acrylate polymer, or a mixture of 10% mono-, 85% di- and 5% tri-phosphate esters of NEtFOSE[66]. It is unknown if the isomeric profile of PFOSF is preserved in subsequent consumer products that are synthetically derived from PFOSF (e.g., fluroacrylate polymers, phosphate esters, etc.). Furthermore, while the degradation of such polymers or PFOSF derivatives has been hypothesised as a source of PFAs in the environment, it is unclear whether such degradation rates would be isomer-specific. The isomer profile of residual impurities may reflect the affinity of certain isomers to undergo polymerization, or alternatively, to cause selective weakening of the fluorinated polymer and cause isomer-specific degradation. Analysis of short and long-chain perfluoroalkyl sulfonate and carboxylate impurities in standards of 3M ECF PFOA and PFOS reveal branched content of up to 75% (Table 1.3). Unreacted residual monomers (<1 - 2%) reported in polymers containing PFOSF derived materials[66,67] also contain significant quantities of branched material of various chain lengths[50,68]. This

discussion is important because it is uncertain what contribution residual impurities make to overall human or environmental exposures; however it may be possible to distinguish residuals from intentionally produced products based on isomer profile. Such differences may be useful for elucidating the role of residuals in human and environmental exposure scenarios, although further validation is necessary.

Table 1.3 Impurities and branched-isomer content in 3M ECF PFOS and PFOA.

Impurity in 3 M ECF PFOS (lot 217)	% impurity (wt)	% branched of the impurity	Impurity in 3 M ECF PFOA (lot 332)	% impurity (wt)	% branched of the impurity
PFBS	1.2 [f]	0 [a]	PFHxA	0 73 [h]	18 [e]
PFPeS	1.3 [f]	N/A	PFHpA	3.7 [h]	N/A
PFHxS	4.7 [f]	18 [b]	PFNA	0 2 [g]	65 [g]
PFHpS	1.1 [f]	28 [c]	PFDA	0.0005 [g]	54 [g]
PFDS	N/A	75 [d]	PFUnA	0.0008 [g]	28 [g]
PFOA	0.79 [g]	19 [g]	PFDoA	0.0008 [g]	32 [g]
PFNA	0.002 [g]	70 [g]			
PFDA	0.0005 [g]	51 [g]			
PFUnA	0.0002 [g]	46 [g]			
PFDoA	0.0004 [g]	33 [g]			

[a]As determined by LC-MS/MS peak area, monitoring m/z 299/80 transition
[b]As determined by LC MS/MS peak area peak area, monitoring m/z 399/80 transition
[c]As determined by LC-MS/MS peak area peak area, monitoring m/z 399/80 transition
[d]As determined by LC-MS/MS peak area peak area, monitoring m/z 599/80 transition
[e] As determined by LC-MS/MS peak area peak area, monitoring m/z 313/269 transition
[f]Seacat et al [16]
[g]Reagen et al [53]
[h]Butenhoff et al [38]

In 2002, 16 companies were known to manufacture perfluorochemicals at 33 manufacturing sites worldwide[48,69]. Of these, Asahi Glass, Clariant, Daikin, and DuPont produced fluorochemicals via telomerization, while Dyneon (a subsidiary of 3M), Bayer, Dainippon Ink & Chemicals, and Miteni were known to have, or are currently producing fluorochemicals by ECF[49]. Little is known about production, use, or emissions of perfluorochemicals by these manufacturers,

however it is widely reported that 3M produced 85%, or more, of total worldwide volumes of APFO by ECF since 1949[69]. ECF manufacturing by 3M took place in plants in Cottage Grove, MN, (ECF PFOA pilot production only), Cordova, IL, Decatur, AL, and Antwerp (Belgium)[66]. All PFOS emissions from 1951 – 1964 are assumed to have occurred in the US, however as production in other plants increased from 1965 – 1974, this figure decreased to 75%, and by 1975 only 50% of total emissions occurred from the US[10]. Although the isomer composition of ECF-fluorochemicals can vary from manufacturer to manufacturer[59] (Table 1.2), isomer profiles of 3M ECF PFOS and PFOA were consistent between manufacturing locations, and showed minimal inter-lot variability from year to year. For example, 3M ECF PFOS reportedly had a consistent isomer composition of 70% linear (standard deviation (SD) 1.1%) and 30% branched (SD 0.8%) in eight production lots over 10 yr[53]. Likewise, 3M ECF PFOA had a consistent isomer composition of 78% linear (SD 1.2%) and 22% branched (SD 1.2%) in 18 production lots over a 20 yr period, as determined by ^{19}F nuclear magnetic resonance (NMR). This batch-to-batch consistency may allow researchers to distinguish sources to the environment based on isomer profiles. It is important to note from a source tracking perspective, that while 3M may have produced most of the historical global ECF PFOA, between 1992 and 2002 more than 95% of 3M ECF PFOA was being used by other companies for fluoropolymer manufacturing[70]. DuPont, for example, used 3M ECF PFOA for fluoropolymer manufacturing, beginning in the 1950s[48].

Of the 89 possible PFOS isomers described by Rayne et al.[43], only ~11 appear to be present in measurable concentrations in 3M standards[56]. The structures of these isomers are *n*, *iso*, *5m*, *4m*, *3m*, *2m*, *1m*, *tb*, *4,4m$_2$*, *5,3m$_2$* and *5,4m$_2$*. While less effort has gone into the characterization of ECF PFOA, out of 39 possible PFOA isomers[43] it appears that *n*, *iso*, *5m*, *4m*, and *3m*-PFOA make up 99.2% in 3M ECF standards with minor contributions (<0.8%) from *2m*, *tb*, *4,4m$_2$*, *5,3m$_2$* and *5,4m$_2$*[54] (Table 1.2). While other isomers are theoretically possible, these are unlikely to be present at measurable concentrations in the environment since they are virtually undetectable in the commercially manufactured material.

The isomer profile of 3M ECF perfluorooctane sulfonamides and sulfonamido-alcohols are also fairly consistent with 3M ECF PFOS, despite the additional synthetic production steps (Table 1.4). The isomer composition of these products reportedly varied from 70-75% straight chain isomers, although this could increase up to 80% linear in some cases depending on the final chemical form and customer specifications for the final product use. NMR characterization of 3M ECF perfluorooctane sulfonamide (FOSA; Table 1.1), PFOS, and NEtFOSE (Table 1.4) indicated reproducible batch-to-batch, and product-to-product consistency in isomer profile. This may imply that directly emitted PFOS may be indistinguishable from precursor-derived PFOS based on isomer profile, provided the degradation pathways are not isomer-selective (studied in Chapter 4). While non-isomer selective degradation pathways may prevent the contributions of the various abiotic pathways (e.g., atmospheric transport and

oxidation of precursors versus direct emission of PFAs) from being easily elucidated by isomer profile, abiotic degradation of PFOS-precursors is noted to be a minor source of PFOS[71].

Table 1.4 Isomer composition (relative weight %) of 3M perfluorooctane suflonyl fluoride (PFOSF)-derived products determined by ^{19}F NMR

Isomer	FOSA[a]			PFOS[b]	NEtFOSE[a]	Mean ± 1 SD
	Lot 15312	TN-A-1584[c]	Lot 2353	Lot 217	Lot 30107	
Normal	67.3	70.9	67.1	70	69.9	69.1 ± 1.81
Monomethyl	17.9	15.2	18.2	17.0	17.4	17.2 ± 1.18
Isopropyl	9.9	9.1	9.4	10.3	10.7	9.90 ± 0.67
Alpha	3.7	3.2	3.5	1.6	1.6	2.72 ± 1.04
t-butyl	0.24	0.21	0.27	0.2	0.23	0.24 ± 0.02
dimethyl	0.14	0.12	0.13	0.2	0.13	0.13 ± 0.01
total branched	31.88	27.83	31.5	29.3	30.06	30.1 ± 1.63

[a]Korkowski and Kestner[72]
[b]Kestner[55]
[c]Lot number was not available for this standard.

PFOSF-derived fluorochemicals can contribute to both perfluoro-carboxylate (major pathway) and sulfonate (minor pathway, only under certain conditions) loadings via abiotic degradation[7,73-75] and to environmental PFOS concentrations via biotransformation[76-79]. Thus, PFOA isomer profiles in the environment (expected to be ~80% linear if contribution is exclusively from ECF PFOA; Table 1.2) could be influenced by the isomer pattern of PFOSF-derived fluorochemicals such as perfluorooctane sulfonamides (~70% linear; Table 1.4). If contributions from PFOSF-derived fluorochemicals to PFOA are significant, one might expect PFOA isomer profiles to be slightly enriched in branched content (i.e., up to 30% branched isomer content) in samples, relative to 3M ECF PFOA. However, not all branched PFOSF isomers are expected to degrade to the same corresponding branched perfluorocarboxylate. Atmospheric oxidation of α-branched perfluorooctyl sulfonamides (e.g. 1m-NEtFOSA, 1m-NMeFOSE) is

expected to produce linear PFCAs due to loss of both the α-carbon and its

monoperfluoromethyl branch, provided degradation of branched chains proceeds

via the same mechanism as the linear molecule (Figure 1.1).
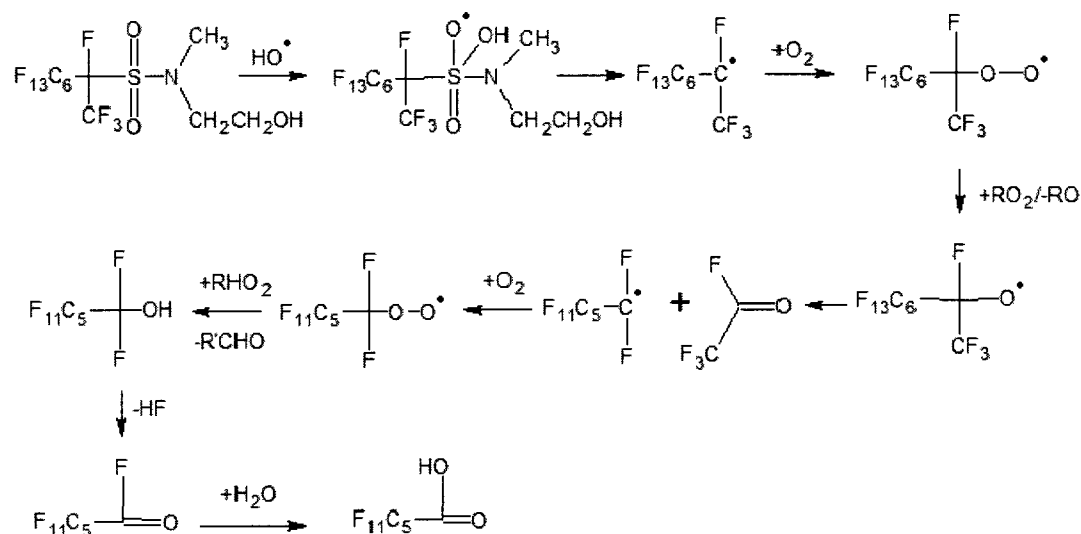
Figure 1.1 Hypothesized pathway for formation of a linear perfluorocarboxylate from a branched precursor. Reaction scheme shown is based on atmospheric oxidation pathway for linear N-methylperfluorooctanesulfonamidoethanol provided by D'eon et al.[80]

Compared to what is known about the historical manufacturing of PFOS,

surprisingly little is known about current production. Miteni (Italy) is known to be

currently producing perfluoroalkyl sulfonates and carboxylates by ECF, and

according to documents recently submitted to the International Stockholm

Convention on Persistent Organic Pollutants, China began the large-scale

production of PFOSF-products in 2003. By 2006, 15 Chinese enterprises were

producing more than 200 tonnes (t) of PFOSF, approximately half of which was

exported to Brazil, the EU, and Japan[81]. While this is substantially less than the

3665 t of PFOSF produced by the 3M Co. in 2000 alone[47], it is similar to the 260 t of APFO produced by 3M in 1999[82]. It is not currently clear how much PFOS is being produced by China or by what method (ECF vs. telomer). If isomer profiles in new Chinese PFOSF material are unique from other manufacturers and continue to increase to pre-2002 production levels, we could expect to see changes in environmental isomer patterns in the future. To our knowledge, this 'new PFOS' has yet to be taken into account in models that estimate future global PFOS production. Paul et al.[47] estimated $\sim$1000 t yr^{-1} PFOS/PFOSF manufactured globally since 2002, provided production by remaining companies has not increased.

Information recently presented at the Workshop on Managing Perfluorinated Chemicals and Transitioning to Safer Alternatives (Geneva, Switzerland, February 12-13, 2009), suggested that most manufacturers have begun substituting perfluorooctyl-based products with perfluorinated chains of four[83] and six[84,85] carbons in length. One such alternative, PFBS, has demonstrated lower toxicity[86] and faster elimination[87] in rodents than its corresponding longer chain homologues. However, PFBS is nevertheless still detectable in water, often in concentrations higher than PFOS or PFOA[88,89]. It has also been reported in children[90], and its effects on humans are largely unknown. Residual PFBS impurities, a by-product of ECF PFOSF synthesis, did not appear to contain any branched isomers, despite the clear presence of branched C6, C7, and C10 perfluoralkyl sulfonate impurities in commercially manufactured PFOS (Table 1.3). The rearrangement of the fluoroalkyl chain to form branched isomers

17

tends to decrease with chain length[59], and thus the lack of branched isomers in currently manufactured ECF PFBS (based on ^{19}F NMR analysis,[59]), is not necessarily surprising; albeit this implies that differentiating between historical, residual, and current intentionally-manufactured PFBS using isomer profiles will be difficult, if not impossible.

Other sources of branched PFAs may also contribute to environmental loadings. For example, thermolysis of fluoropolymers is known to be a potential source of PFAs in the environment,[91] and is thought to proceed via a carbene radical, which, while still requiring further investigation, may have the potential to form branched PFCAs. In fact, in a follow-up study by Ellis et al.[92], GC-MS analysis of aqueous PTFE thermolysis extracts revealed some evidence of branched perfluorocarboxylate formation. No authentic branched standards were available at the time of this study, and therefore this finding should be re-examined using current isomer profiling methods.

1.6 Current Analytical PFA Isomer Separation Methods

The earliest reported perfluoroalkyl isomer separations were conducted by Bastosa et al.[93] in which GC-MS was used to partially separate a mixture of ECF NEtFOSA isomers in ant bait marketed under the name Sulfuramid[TM]. 3M also reported HPLC-MS/MS separations of total branched from linear perfluoroalkyl carboxylates and sulfonates in human blood[94] as well as ^{19}F NMR characterizations of technical mixtures[54]. These latter methods, while effective for

characterizing the isomer composition in standards, lacked the sensitivity to be applied to environmental samples.

The first methods suitable for isomer-specific analysis in environmental samples were developed by De Silva and Mabury[51] and employed GC-MS to chromatographically separate a range of perfluoroalkyl carboxylates (C_8–C_{13}). Their original method employed a 90 m ZB-35 column, and was capable of separating seven PFOA isomers along with a suite of PFCAs up to and including PFTrA in less than 100 min. This method was later optimized by substituting in a 105 m Rtx-35 column (Restek Corp., Bellefonte, PA, USA), which reduced method time to under 80 min and allowed for the detection of an additional PFOA isomer (total of 8 PFOA isomers)[52]. The advantage of GC-MS based isomer analysis is, most obviously, the high chromatographic resolution associated with GC, but also that it is less prone to matrix effects which can hinder electrospray ionization (ESI) sources. Ionization efficiencies in GC-MS may have minimal differences based on comparison between pure standards of *n*-PFNA and *iso*-PFNA[52]. As such, the quantitative isomer composition of a sample may be possible by comparison of relative peak areas of the molecular ion. This approach is prone to errors in HPLC-ESI-MS methods because the relative peak areas are also affected by the physical properties of each isomer in the mixture. The major disadvantage of the GC-MS method is that the derivatization procedure is relatively laborious, and that perfluoroalkyl sulfonates cannot be analyzed simultaneously because they are not efficiently derivatized with 2,4-difluoroaniline. Langlois and Oehme[95] addressed this latter deficiency by

developing a novel PFOS derivatization method in which PFOS was reacted with isopropanol and sulfuric acid to form volatile isopropyl derivatives. When a derivatized technical standard of PFOS was analyzed by GC-MS, 11 isomers were separated in under 8 min. This procedure proved viable for PFHxS and various PFCAs, however chromatographic isomer separation was not evaluated for these latter compounds. Furthermore, it was unclear whether this method is suitable for application to environmental samples, since isomer-specific derivatization yield and stability was not investigated and no complex matrix was tested. A similar procedure producing silane derivatives for GC-MS analysis was recently used to determine PFOS and PFOA in packaging materials and textiles[96]. Derivatives were noted to be stable within 2 d and limits of detection were 13.9 and 1.6 ng/mL for silated PFOS and PFOA, respectively, but the method was not validated for isomer-specific analysis. Recently, Chu and Letcher[97] developed an in-port derivatization GC-MS method for PFOS isomers, using tetrabutyl ammonium hydroxide to produce volatile butyl PFOS isomer derivatives. Application of this method to a technical standard resulted in the separation and identification of 11 PFOS isomers in <15 min, and while detection limits were notably higher than most current LC-MS/MS methods, the authors were able to validate the method using environmental samples from the Great Lakes and Arctic.

Isomer-specific PFOS-precursor analysis by GC has also beenconducted by De Silva et al.[98]. This method utilized a 60 m DB-WAX (0.25 mm ID x 0.25

μm FT, Phenomenex, Torrance, CA, USA) column to provide near baseline resolution of nine NEtFOSE isomers in under 15 min.

In 2004, Martin et al.[99] presented early chromatograms of PFOS isomer separation by HPLC-MS/MS, using an octadecasilyl (C_{18}) stationary phase. This was followed up in 2006 by Langlois and Oehme[44], who carried out the first isomer-specific characterization of a technical PFOS standard using purified isomer fractions and HPLC-MS/MS with perfluorophenyl (PFP) and C_{18} columns. This relatively fast method (<30 min with PFP column for 10 isomers), was later used to examine FOSA isomer patterns in standards, as well as PFOA isomer patterns in standards, human blood, and water[100]. Ultra-pressure liquid chromatography (UPLC) has demonstrated promise in achieving simultaneous chromatographic separations of PFOS and PFOA isomers in less than 20 min[101,102]. While some co-elution appears to occur between 1*m*- and *n*-PFOS, and 4*m*- and *iso*-PFOA isomers, these can likely be resolved using knowledge of isomer-specific collision-induced dissociation patterns[44,45]. These methods also appear to suffer from co-eluting matrix interferences, and thus some work is still needed to refine them before they can be applied to environmental samples.

1.7 Goals and Hypotheses

There were two overall goals of this thesis. The first was to elucidate the contributions of ECF (primarily historical) versus telomer (primarily current) manufacturing to total PFOA concentrations in the environment. The second goal

was to determine to what extent PFOS in humans and wildlife is a result of exposure to precursors (i.e. indirect exposure) versus direct exposure to PFOS itself. Addressing these objectives has important implications from both a regulatory and risk management perspective. For example, unless historically-manufactured PFOA can be differentiated from contemporary PFOA, the overall effectiveness of past and present industry phase-out initiatives will remain difficult to assess. Likewise, determining to what extent humans and wildlife are exposed directly versus indirectly is the first step in identifying routes and pathways of exposure, which can then be used to mitigate exposure.

It is hypothesized that PFA isomer profiles can be used as a tool for estimating contributions from historical (primarily ECF) and current (primarily telomer) manufacturing sources, while also providing a biomarker of PFOS exposure source (i.e. indirect exposure to precursors versus direct exposure to PFAs themselves). As discussed in Chapter 1, the isomer profile of historically (ECF) manufactured PFOA can be differentiated from that of contemporary (telomer) PFOA, and provided this profile remains conserved in environmental samples, may provide a "fingerprint" of manufacturing source in samples. On the other hand, PFOS and PFOS precursors were manufactured exclusively by ECF to produce a consistent mixture of ~70% linear / 30% branched isomers. Deviations from these percentages may be resultant from isomer specific biotransformation and/or pharmacokinetics which may in turn provide a biomarker of precursor and/or direct exposure.

Despite the potential of this tool, several major hurdles must be overcome before interpretation of PFA isomer profiles can yield meaningful results. As highlighted in the section on current analytical PFA isomer separation methods, few techniques exist for separation of PFA and/or PFA-precursor isomers, and those that were developed prior to the work presented here were suitable for either perfluoroalkyl sulfonates or carboxylates (not both) and were not optimized for resolving PFA-precursor isomers. The objective of Chapter 2 was to develop and apply a method for characterization of the major perfluoroalkyl carboxylate, sulfonate, and sulfonamide isomers in a single injection. Using the analogy that 'like dissolves like', we hypothesised that a long, linear perfluorinated stationary phase would have the greatest intermolecular interaction with linear PFAs, and ultimately the greatest potential for success in separating branched from linear PFA isomers. The method was validated with standards and human serum, and while unique PFOS and PFOA isomer profiles were observed, it was difficult to interpret these patterns without knowledge of isomer specific pharmacokinetics or biotransformation.

The objective of Chapters 3 and 4 was to investigate the influence of perfluoroalkyl chain branching on isomer-specific pharmacokinetics and biotransformation. In these Chapters, we hypothesized that the 3-dimensional structure of individual PFA isomers would influence both pharmacokinetics and biotransformation, respectively, and we tested these hypotheses using both *in vivo* and *in vitro* models. These data were then used to interpret isomer profiles in biological samples (discussed in Chapter 7).

23

From the experiments conducted in Chapters 3 and 4, it was concluded that quantitative assessment of manufacturing source was not possible in biological samples. We therefore hypothesised that isomer profiles may be conserved in abiotic samples such as seawater, and in Chapter 5, a method is presented that is capable of examining isomer profiles in these low concentrations samples. In this work, the relative ratio of branched isomers in samples from coastal Asia, the Mississippi River, and the North Sea Canal were examined for evidence of abiotic or biological fractionation, and a method was developed to quantitatively assess the contributions from historical versus current manufacturing to PFA concentrations in these samples.

Once this isomer profiling method was validated for low concentration seawater samples, in Chapter 6 we applied it to samples from remote regions (Baffin Bay, Lancaster sound, North Sea, Atlantic Ocean, etc.). The objective of this work was to determine whether Arctic Ocean PFOA is from a historical (i.e. from slow, oceanic transport) or current (i.e. from fast, atmospheric transport and degradation of telomer-precursors) manufacturing source. Based on model predictions, we hypothesised that samples in remote regions should contain isomer profiles resembling ECF PFOA. Isomer profiles in samples collected from the Atlantic Ocean, Baffin Bay, Lancaster Sound, North Sea, and Norwegian Sea were examined, and the contribution of ECF manufacturing to total PFOA concentrations was quantified.

Chapter 7 presents a review of thesis findings and relevant literature on PFA and PFA-precursor isomers. Interpretation of isomer profiles in the context

of manufacturing and exposure source determination is discussed. Current challenges and future avenues of research are also presented.

1.8   References

1.   Taves, D.R. *Nature.* **1968**, *217*, 1050-1051.

2.   Hansen, K.J.; Clemen, L.A.; Ellefson, M.E.; Johnson, H.O. *Environ. Sci. Technol.* **2001**, *35*, 766-770.

3.   Giesy, J.P.; Kannan, K. *Environ. Sci. Technol.* **2001**, *35*, 1339-1342.

4.   Calafat, A.M.; Kuklenyik, Z.; Reidy, J.A.; Caudill, S.P.; Tully, J.S.; Needham, L.L. *Environ. Sci. Technol.* **2007**, *41*, 2237-2242.

5.   Center for Disease Control (CDC). Third National Report on Human Exposure to Environmental Chemicals; NCEH Pub. No. 05-0570; Department of Health and Human Services, Centers for Disease Control and Prevention, National Center for Environmental Health, Division of Laboratory Sciences, U.S. Government Printing Office: Washington, DC, **2005**.

6.   Houde, M.; Martin, J.W.; Letcher, R.J.; Solomon, K.R.; Muir, D.C. *Environ. Sci. Technol.* **2006**, *40*, 3463-3473.

7.   Wallington, T.J.; Hurley, M.D.; Xia, J.; Wuebbles, D.J.; Sillman, S.; Ito, A.; Penner, J.E.; Ellis, D.A.; Martin, J.; Mabury, S.A.; Nielsen, O.J.; Sulbaek Andersen, M.P. *Environ. Sci. Technol.* **2006**, *40*, 924-930.

8.   Wania, F. *Environ. Sci. Technol.* **2007**, *41*, 4529-4535.

9.   Armitage, J.; Cousins, I.T.; Buck, R.C.; Prevedouros, K.; Russell, M.H.; MacLeod, M.; Korzeniowski, S.H. *Environ. Sci. Technol.* **2006**, *40*, 6969-6975.

10.   Armitage, J.M.; MacLeod, M.; Cousins, I.T. *Environ.Sci.Technol.* **2009**, 1134-1136.

11.   Armitage, J.M.; Schenker, U.; Scheringer, M.; Martin, J.W.; Macleod, M.; Cousins, I.T. *Environ. Sci. Technol.* **2009**, *43*, 9274-9280.

12.   United Nations Environmental Protection Secretariat of the Stockholm Convention on Persistent Organic Pollutants Pollutants. Geneva, Switzerland, **2009**.

13.   Abdellatif, A.G.; Preat, V.; Taper, H.S.; Roberfroid, M. *Toxicol. Appl. Pharmacol.* **1991**, *111*, 530-537.

14.   Kennedy, G.L., Jr.; Butenhoff, J.L.; Olsen, G.W.; O'Connor, J.C.; Seacat, A.M.; Perkins, R.G.; Biegel, L.B.; Murphy, S.R.; Farrar, D.G. *Cri. Rev. Toxicol.* **2004**, *34*, 351-384.

15.   Olsen, G.W.; Burris, J.M.; Ehresman, D.J.; Froehlich, J.W.; Seacat, A.M.; Butenhoff, J.L.; Zobel, L.R. *Environ. Health Perspect.* **2007**, *115*, 1298-1305.

16.   Seacat, A.M.; Thomford, P.J.; Hansen, K.J.; Olsen, G.W.; Case, M.T.; Butenhoff, J.L. *Toxicol. Sci.* **2002**, *68*, 249-264.

17.   Butenhoff, J.L.; Kennedy, G.L., Jr.; Hinderliter, P.M.; Lieder, P.H.; Jung, R.; Hansen, K.J.; Gorman, G.S.; Noker, P.E.; Thomford, P.J. *Toxicol. Sci.* **2004**, *82*, 394-406.

18.   Vanden Heuvel, J.P.; Kuslikis, B.I.; Van Rafelghem, M.J.; Peterson, R.E. *J. Biochem. Toxicol.* **1991**, *6*, 83-92.

19.   Vanden Heuvel, J.P.; Davis, J.W.; Sommers, R.; Peterson, R.E. *J. Biochem. Toxicol.* **1992**, *7*, 31-36.

20.   Ohmori, K.; Kudo, N.; Katayama, K.; Kawashima, Y. *Toxicol.* **2003**, *184*, 135-140.

21.   Andersen, M.E.; Butenhoff, J.L.; Chang, S.C.; Farrar, D.G.; Kennedy, G.L., Jr.; Lau, C.; Olsen, G.W.; Seed, J.; Wallace, K.B. *Toxicol. Sci.* **2008**, *102*, 3-14.

22.   Andersen, M.E.; Clewell, H.J., 3rd; Tan, Y.M.; Butenhoff, J.L.; Olsen, G.W. *Toxicol.* **2006**, *227*, 156-164.

23.   Vanden Heuvel, J.P.; Thompson, J.T.; Frame, S.R.; Gillies, P.J. *Toxicol. Sci.* **2006**, *92*, 476-489.

24. Lundin, J.I.; Alexander, B.H.; Olsen, G.W.; Church, T.R. *Epidemiol.* **2009**, *20*, 921-928.

25. Gilliland, F.D.; Mandel, J.S. *J. Occup. Med.* **1993**, *35*, 950-954.

26. Midasch, O.; Drexler, H.; Hart, N.; Beckmann, M.W.; Angerer, J. *Int. Arch. Occup. Environ. Health.* **2007**, *80*, 643-648.

27. Inoue, K.; Okada, F.; Ito, R.; Kato, S.; Sasaki, S.; Nakajima, S.; Uno, A.; Saijo, Y.; Sata, F.; Yoshimura, Y.; Kishi, R.; Nakazawa, H. *Environ. Health Perspect.* **2004**, *112*, 1204-1207.

28. Tao, L.; Ma, J.; Kunisue, T.; Libelo, E.L.; Tanabe, S.; Kannan, K. *Environ. Sci. Technol.* **2008**, *42*, 8597-8602.

29. Llorca, M.; Farre, M.; Pico, Y.; Teijon, M.L.; Alvarez, J.G.; Barcelo, D. *Environ. Int.* **2010**, *36*, 584-592.

30. Apelberg, B.J.; Witter, F.R.; Herbstman, J.B.; Calafat, A.M.; Halden, R.U.; Needham, L.L.; Goldman, L.R. *Environ. Health Perspect.* **2007**, *115*, 1670-1676.

31. Apelberg, B.J.; Goldman, L.R.; Calafat, A.M.; Herbstman, J.B.; Kuklenyik, Z.; Heidler, J.; Needham, L.L.; Halden, R.U.; Witter, F.R. *Environ. Sci. Technol.* **2007**, *41*, 3891-3897.

32. Grice, M.M.; Alexander, B.H.; Hoffbeck, R.; Kampa, D.M. *J. Occup. Environ. Med.* **2007**, *49*, 722-729.

33. Nolan, L.A.; Nolan, J.M.; Shofer, F.S.; Rodway, N.V.; Emmett, E.A. *Reprod. Toxicol.* **2010**, *29*, 147-155.

34. Fei, C.; McLaughlin, J.K.; Tarone, R.E.; Olsen, J. *Environ. Health Perspect.* **2007**, *115*, 1677-1682.

35. Wolf, C.J.; Takacs, M.L.; Schmid, J.E.; Lau, C.; Abbott, B.D. *Toxicol. Sci.* **2008**, *106*, 162-171.

36. Jones, P.D.; Hu, W.; De Coen, W.; Newsted, J.L.; Giesy, J.P. *Environ. Toxicol. Chem.* **2003**, *22*, 2639-2649.

37. Han, X.; Snow, T.A.; Kemper, R.A.; Jepson, G.W. *Chem. Res. Toxicol.* **2003**, *16*, 775-781.

38. Butenhoff, J.; Costa, G.; Elcombe, C.; Farrar, D.; Hansen, K.; Iwai, H.; Jung, R.; Kennedy, G., Jr.; Lieder, P.; Olsen, G.; Thomford, P. *Toxicol. Sci.* **2002**, *69*, 244-257.

39. Lau, C.; Thibodeaux, J.R.; Hanson, R.G.; Rogers, J.M.; Grey, B.E.; Stanton, M.E.; Butenhoff, J.L.; Stevenson, L.A. *Toxicol. Sci.* **2003**, *74*, 382-392.

40. Thibodeaux, J.R.; Hanson, R.G.; Rogers, J.M.; Grey, B.E.; Barbee, B.D.; Richards, J.H.; Butenhoff, J.L.; Stevenson, L.A.; Lau, C. *Toxicol. Sci.* **2003**, *74*, 369-381.

41. Melzer, D.; Rice, N.; Depledge, M.H.; Henley, W.E.; Galloway, T.S. *Environ. Health Perspect.* **2010**, *118*, 686-692.

42. Bloom, M.S.; Kannan, K.; Spliethoff, H.M.; Tao, L.; Aldous, K.M.; Vena, J.E. *Physiol. Behav.* **2010**, *99*, 240-245.

43. Rayne, S.; Forest, K.; Friesen, K.J. *J. Environ. Sci. Health. A.* **2008**, *43*, 1391-1401.

44. Langlois, I.; Oehme, M. *Rapid Commun. Mass Spectrom.* **2006**, *20*, 844-850.

45. Benskin, J.P.; Bataineh, M.; Martin, J.W. *Anal. Chem.* **2007**, *79*, 6455-6464.

46. Lehmler, H.J. *Chemosphere.* **2005**, *58*, 1471-1496.

47. Paul, A.G.; Jones, K.C.; Sweetman, A.J. *Environ. Sci. Technol.* **2009**, *43*, 386-386.

48. Prevedouros, K.; Cousins, I.T.; Buck, R.C.; Korzeniowski, S.H. *Environ. Sci. Technol.* **2006**, *40*, 32-44.

49. Parsons, J.R.; Sáez, M.; Dolfing, J.; de Voogt, P. *Rev. Environ. Contam. Toxicol.* **2008**, *196*, 53-71.

50. Kissa, E. In *Fluorinated Surfactants and Repellents, 2nd ed*; Marcel Dekker: NewYork, **2005**.

51. De Silva, A.O.; Mabury, S.A. *Environ. Sci. Technol.* **2004**, *38*, 6538-6545.

52. De Silva, A.O.; Mabury, S.A. *Environ. Sci. Technol.* **2006**, *40*, 2903-2909.

53. Savu, P.M. In *Kirk-Othmer Encyclopedia of Chemical Technology*; John Wiley & Sons: New Jersey, **1994**.

54. Balague, J.; Ameduri, B.; Boutevin, B.; Caporiccio, G. *J. Fluorine Chem.* **1995**, *70*, 215-218.

55. Millauer, H. United States Patent No. 3,829,512. **1974**.

56. Katsushima, A.; Hisamoto, I.; Nagai, M. United States Patent No. 3,525,758. **1970**.

57. Appel, A.G.; Abd-Elghafar, S.F. *J. Econ. Entomol.* **1990**, *83*, 1409-1414.

58. 3M Co. U.S. Environmental Protection Agency public docket AR226-0550: Fluorochemical use, distribution and release overview. U.S. Environmental Protection Agency, Office of Pollution Prevention and Toxic Substances, Washington, DC, **1999**.

59. Dinglasan-Panlilio, M.J.; Mabury, S.A. *Environ. Sci. Technol.* **2006**, *40*, 1447-1453.

60. Simons, J.H. *J. Electrochem. Soc.* **1949**, *95*, 47-12.

61. Reagen, W.K.; Lindstrom, K.R.; Jacoby, C.B.; Purcell R.G.; Kestner T.A.; Payfer R.M.; Miller, J.W.; Platform presentation at Society of Environmental Toxicology and Chemistry 28th North American Meeting, Milwaukee, WI, USA, November 11–15, **2007**.

62. Loveless, S.E.; Finlay, C.; Everds, N.E.; Frame, S.R.; Gillies, P.J.; O'Connor, J.C.; Powley, C.R.; Kennedy, G.L. *Toxicology.* **2006**, *220*, 203-217.

63. Kestner, T. U.S. Environmental Protection Agency public docket AR226-0564: Fluorochemical isomer distribution by ^{19}F-NMR spectroscopy. U.S. Environmental Protection Agency, Office of Pollution Prevention and Toxic Substances, Washington, DC, **1997**.

64. Arsenault, G.; Chittim, B.; Gu, J.; McAlees, A.; McCrindle, R.; Robertson, V. *Chemosphere.* **2008**, *73*, S53-59.

65. Wellington Laboratories. Certificate of analysis/documentation for T-PFOS. Wellington Laboratories: Guelph, ON, Canada, **2005**.

66. Wellington Laboratories. Certificate of analysis/documentation for individual PFOS/PFOA isomers. Wellington Laboratories: Guelph, ON, Canada, **2008**.

67. Vyas, S.M.; Kania-Korwel, I.; Lehmler, H.J. *J. Environ. Sci. Health. A.* **2007**, *42*, 249-255.

68. White, S.S.; Kato, K.; Jia, L.T.; Basden, B.J.; Calafat, A.M.; Hines, E.P.; Stanko, J.P.; Wolf, C.J.; Abbott, B.D.; Fenton, S.E. *Reprod. Toxicol.* **2009**.

69. OECD. Document ENV/JM/RD(2002)17/FINAL: Hazard Assessment of PFOS. Organisation for Economic Co-operation and Development Environment Directorate, Paris, FR, **2002**.

70. Wendling, L. U.S. Environmental Protection Agency public docket OPPT-2003-0012-0007: Environmental, health and safety measures relating to perfluorooctanoic acid and its salts (PFOA). U.S. Environmental Protection Agency, Office of Pollution Prevention and Toxic Substances, Washington, DC, **2003**.

71. Seacat, A.M.; Thomford, P.J.; Hansen, K.J.; Olsen, G.W.; Case, M.T.; Butenhoff, J.L. *Toxicol. Sci.* **2002**, *68*, 249-264.

72. Butenhoff, J.; Costa, G.; Elcombe, C.; Farrar, D.; Hansen, K.; Iwai, H.; Jung, R.; Kennedy, G., Jr.; Lieder, P.; Olsen, G.; Thomford, P. *Toxicol. Sci.* **2002**, *69*, 244-257.

73. Korkowski, P.; Kestner, T. Chemical characterization of FOSA & PFOSA samples by ^{1}H and ^{19}F NMR Spectroscopy. **1999**.

74. D'Eon, J.; Hurley, M.; Wallington, T.J.; Mabury, S.A. *Environ. Sci. Technol.* **2006**, *40*, 1862-1868.

75. Martin, J.W.; Ellis, D.A.; Mabury, S.A.; Hurley, M.D.; Wallington, T.J. *Environ. Sci. Technol.* **2006**, *40*, 864-872.

76. Plumlee, M.H.; McNeill, K.; Reinhard, M. *Environ. Sci. Technol.* **2009**, *43*, 3662-3668.

77. Tomy, G.T.; Tittlemier, S.A.; Palace, V.P.; Budakowski, W.R.; Braekevelt, E.; Brinkworth, L.; Friesen, K. *Environ. Sci. Technol.* **2004**, *38*, 758-762.

78. Xu, L.; Krenitsky, D.M.; Seacat, A.M.; Butenhoff, J.L.; Anders, M.W. *Chem. Res. Toxicol.* **2004**, *17*, 767-775.

79. Martin, J.W.; Mabury, S.A.; O'Brien, P.J. *Chem.-Biol. Interact.* **2005**, *155*, 165-180.

80. Rhoads, K.R.; Janssen, E.M.; Luthy, R.G.; Criddle, C.S. *Environ. Sci. Technol.* **2008**, *42*, 2873-2878.

81. Ruisheng, Y. 2008. Additional information of production and use of PFOS. Fax from Ministry of Environmental Protection of China.

Stockholm Convention Secretatiat, Geneva, Switzerland. http://chm.pops.int/Portals/0/Repository/addinfo_2008/UNEP-POPS-POPRC-SUB-F08-PFOS-ADIN-CHI.English.pdf

82.   Fluoropolymer Manufacturing, G. *U.S. EPA Administrative Record AR226-1094* **2002**.

83.   Santoro, M.A. Presentation in Workshop on Managing Perfluorinated Chemicals and Transitioning to Safer Alternatives, Geneva, Switzerland, February 12-13, **2009**.

84.   Shelton, K. Presentation in Workshop on Managing Perfluorinated Chemicals and Transitioning to Safer Alternatives, Geneva, Switzerland, February 12-13, **2009**.

85.   Shin-ya, S. Presentation in Workshop on Managing Perfluorinated Chemicals and Transitioning to Safer Alternatives, Geneva, Switzerland, February 12-13, **2009**.

86.   Lieder, P.H.; Chang, S.C.; York, R.G.; Butenhoff, J.L. *Toxicology.* **2009**, *255*, 45-52.

87.   Olsen, G.W.; Chang, S.C.; Noker, P.E.; Gorman, G.S.; Ehresman, D.J.; Lieder, P.H.; Butenhoff, J.L. *Toxicology.* **2009**, *256*, 65-74.

88.   Skutlarek, D.; Exner, M.; Farber, H. *Environ. Sci. Pollut. Res. Int.* **2006**, *13*, 299-307.

89.   Ahrens, L.; Felizeter, S.; Sturm, R.; Xie, Z.; Ebinghaus, R. *Mar. Pollut. Bull.* **2009**, *58*, 1326-1333.

90.   Holzer, J.; Midasch, O.; Rauchfuss, K.; Kraft, M.; Reupert, R.; Angerer, J.; Kleeschulte, P.; Marschall, N.; Wilhelm, M. *Environ. Health Perspect.* **2008**, *116*, 651-657.

91.   Ellis, D.A.; Mabury, S.A.; Martin, J.W.; Muir, D.C. *Nature.* **2001**, *412*, 321-324.

92.   Ellis, D.A.; Martin, J.W.; Muir, D.C.; Mabury, S.A. *The Analyst.* **2003**, *128*, 756-764.

93.   Bastosa, J.K.; Freitasa, L.A.P.; Pagliarussia, R.S.; Merinoc, R.E. *J. Sep. Sci.* **2001**, *24*, 406-404.

94.   Stevenson, L. U.S. Environmental Protection Agency public docket AR-2261150: Comparative analysis of fluorochemicals in human serum samples obtained commercially. U.S. Environmental Protection Agency, Office of Pollution Prevention and Toxic Substances, Washington, DC, **2002**.

95.   Langlois, I.; Berger, U.; Zencak, Z.; Oehme, M. *Rapid Commun. Mass Spectrom.* **2007**, *21*, 3547-3553.

96.   Lv, G.; Wang, L.; Liu, S.; Li, S. *Anal. Sci.* **2009**, *25*, 425-429.

97.   Chu, S.; Letcher, R.J. *Anal. Chem.* **2009**, *81*, 4256-4262.

98. De Silva, A.O.; Stock, N.L.; Bonin, J.; Wong, G.W.Y.; Young, C.; Mabury, S.A. PhD Thesis, Department of Chemistry, University of Toronto, ON, Canada, **2008**.

99. Martin, J.W.; Kannan, K.; Berger, U.; de Voogt, P.; Field, J.; Franklin, J.; Giesy, J.P.; Harner, T.; Muir, D.C.; Scott, B.; Kaiser, M.; Jarnberg, U.; Jones, K.C.; Mabury, S.A.; Schroeder, H.; Simcik, M.; Sottani, C.; van Bavel, B.; Karrman, A.; Lindstrom, G.; van Leeuwen, S. *Environ. Sci. Technol.* **2004**, *38*, 248A-255A.

100. Langlois, I. PhD Thesis, Department of Chemistry, University of Basel, Switzerland, **2006**.

101. Arsenault, G.; Chittim, B.; McAlees, A.; McCrindle, R.; Riddell, N.; Yeo, B. *Chemosphere.* **2008**, *70*, 616-625.

102. Riddell, N.; Arsenault, G.; Benskin, J.P.; Chittim, B.; Martin, J.W.; McAlees, A.; McCrindle, R. *Environ. Sci. Technol.* **2009**, *43*, 7902-7908.

Chapter 2. Simultaneous Characterization of Perfluoroalkyl Carboxylate, Sulfonate, and Sulfonamide Isomers by Liquid Chromatography-Tandem Mass Spectrometry

2.1   Introduction

Perfluorinated acids (PFAs) and their precursors (PFA-precursors) have received increasing scientific attention since 2000 when it was first recognized that PFAs were globally distributed in wildlife[1] and humans.[2] PFA-precursors, chemicals capable of being oxidized to PFAs, may contribute significantly to the environmental and human burden of PFAs through atmospheric reactions,[3-5] biotransformation,[6-8] or perhaps some combination thereof. The concentrations of PFAs in human blood and remote wildlife (i.e., in liver and blood samples) are similar to, or exceed, legacy chlorinated persistent organic pollutants (POPs)[9,10] and their toxicity,[11] persistence, bioaccumulation potential,[12] and long-range transport potential[13] can be considerable, depending on chain length. The most prominent PFA in biological samples, perfluorooctane sulfonate (PFOS), was listed as an "Annex B" persistent organic pollutant in 2009, under the Stockholm Convention, while the OECD and many individual countries are also considering regulations and monitoring programs for PFAs and their precursors. With increasing regulatory, scientific, and public awareness of PFAs comes a need for accurate and precise analytical methods to support the risk assessment

process through environmental (bio-)monitoring, source determination, environmental fate determination, and toxicological studies.

The world's first interlaboratory study for PFAs,[14] in 2005, revealed relatively poor performance of existing high performance liquid chromatography–(tandem) mass spectrometry (HPLC–MS(/MS)) techniques (32–64% RSD and 65–236% RSD for all analytes in human plasma and fish tissue, respectively). The source of the variation between labs likely included systematic biases arising from matrix effects but may also have included the manufacturing source of standards used for quantification. For example, standards may be manufactured as purely linear standards, via telomerization or oligomerization of perfluoroolefines or perfluoroolefin oxides, or uncharacterized technical mixtures containing both linear and branched isomers via electrochemical fluorination. The various manufacturing methods were reviewed previously.[15] The recent availability of linear isotopic internal standards has since assisted tremendously to control matrix effects, but so long as the isomer signature of each PFA (in standards or in samples) is ignored, analytical accuracy will not be achieved and conclusions drawn from years of data collection may be open to criticism. Furthermore, given that each isomer is hypothesized to have different environmental and biological properties,[16] without the appropriate isomer-specific tools many scientific hypotheses will fail to be tested.

Among the prominent environmental PFAs, each may exist as several structural isomers resulting from branching of the perfluorinated chain. Despite this, the most common analytical method used in PFA analysis is

HPLC–MS(/MS) with an alkyl reversed-phase column that permits integration of a single chromatographic peak for each PFA homologue (referred to hereafter as "total PFA" analysis). Given that the various isomers have different ionization efficiencies in electrospray and that each isomer has a distinct fragmentation pattern under MS/MS conditions,[17] unless the standard and the sample have identical isomer compositions, "total PFA" analysis will cause a systematic quantification bias of unknown proportions.[16] Although De Silva et al.[18] developed a derivatization method for isomer-specific perfluorocarboxylate (PFCA) analysis by GC/MS and Langlois and Oehme[17] developed a method for PFOS isomer separation by LC–MS/MS, these have not found widespread use because neither is comprehensive enough to analyze for all PFA or PFA-precursor isomers. Here we build upon the earlier LC–MS work of Langlois and Oehme to develop a comprehensive method to simultaneously separate and detect all PFA and PFA-precursor isomers by a single method using HPLC–MS/MS and a linear perfluorooctyl (PFO) stationary phase. The benefits of the new method are revealed through analysis of human serum.

2.2   Experimental Methods

2.2.1   Nomenclature

Utilizing perfluorooctane sulfonate ($C_8F_{15}SO_3^-$, PFOS) as an example, the following annotations are used herein to represent the structure of each branched isomer based on the relative position of perfluoromethyl substitution. Linear perfluorooctanoate (*n*-PFOS); perfluoromonomethyl isomers (perfluoroisopropyl

(*iso*-PFOS), 5-perfluoromethyl (5*m*-PFOS), 4-perfluoromethyl (4*m*-PFOS), 3-perfluoromethyl (3*m*-PFOS), 2-perfluoromethyl (2*m*-PFOS), 1-perfluoromethyl (1*m*-PFOS)); geminal perfluorodimethyl isomers (*tert*-perfluorobutyl (*tb*-PFOA), 4,4-perfluorodimethyl (4m_2-PFOS), 3,3-perfluorodimethyl (3m_2-PFOS), 2,2-perfluorodimethyl (2m_2-PFOS), and 1,1-perfluorodimethyl (1m_2-PFOS)). It is acknowledged that perfluoromonomethyl PFOS isomers are, by IUPAC nomenclature, perfluoromethyl substituted perfluoroheptanoates, and geminal perfluorodimethyl PFOS isomers are more correctly termed as perfluorodimethyl substituted hexanoates. However, this creates confusion when discussing a homologous class of PFAs; thus, the above terminology is preferred and is adhered to herein.

Branched isomers that could not be structurally assigned were labeled B_x, (where $x = 1, 2, 3$, etc.) in decreasing order of retention time. Unknowns, defined as chromatographic peaks with either (i) one MS/MS transition found in both serum and standards or (ii) more than one MS/MS transition corresponding to a given PFA in serum but absent in standards, were labeled consecutively as U_x, (where $x = 1, 2, 3$,etc.) in decreasing order of retention time. These peaks could not be confirmed as PFA isomers without authentic standards. Finally, interferences, defined as chromatographic peaks definitively ruled out as PFAs by product ion scans, were labeled I_x, (where $x = 1, 2, 3$,etc.) in decreasing order of retention time.

41

2.2.2 Standards and Reagents

HPLC-grade methanol was purchased from Fisher Scientific (Ottawa, ON, Canada). HPLC grade formic acid (50%), ammonium acetate (99%), potassium perfluorohexane sulfonate (PFHxS, >98%), perfluorononanoic acid (PFNA, 97%), perfluorodecanoic acid (PFDA, 98%), perfluoroundecanoic acid (PFUnA, 95%), perfluorododecanoic acid (PFDoA, 95%), perfluoroheptanoic acid (PFHpA, 99%), perfluorotetradecanoic acid (PFTA, 97%), potassium PFOS (98%), and sodium taurodeoxycholic hydrate (95%) were purchased from Sigma-Aldrich (Oakville, ON, Canada). Among these PFA standards, only PFHxS and PFOS were presumed to have been manufactured by electrochemical fluorination based on a high abundance of branched isomers in their chromatograms (e.g., >10% relative abundance). An authentic electrochemically fluorinated PFOA standard was provided by Dupont (Wilmington, DE). Electrochemically fluorinated N-ethyl perfluorooctane sulfonamide (NEtFOSA, 95%) was obtained from Interchim (France). Linear perfluorooctane sulfonamide (FOSA, 98%), isopropyl-PFNA (iso-PFNA), and linear internal standards, N-methyl perfluorooctane sulfonamide (NMeFOSA, linear, >98%), sodium perfluoro-1-[1,2,3,4-$^{13}C_4$]octane sulfonate (^{13}C–PFOS), perfluoro-n-[1,2,3,4,5-$^{13}C_5$]nonanoic acid (^{13}C-PFNA), perfluoro-n-[1,2-$^{13}C_2$]decanoic acid, perfluoro-n-[1,2,3,4-$^{13}C_4$]octanoic acid (^{13}C-PFOA), and perfluoro-n-[1,2-$^{13}C_2$]dodecanoic acid (^{13}C-PFDoA), were purchased from Wellington Labs (Guelph, ON, Canada). FOSA isomers were generated by incubating 100 ppb NEtFOSA isomers, 20 µL human liver microsomes (protein content = 0.4 mg; purchased from BD Gentest, Woburn, MA), and NADPH in a

42

0.01 M potassium phosphate buffer (pH 7.4) over 24 h. Portions of the reaction mixture were removed at several time points, quenched with methanol, centrifuged, and the resulting supernatant was analyzed.

2.2.3 Source and Handling of Human Serum

Ethics approval was obtained from the University of Alberta Health Research Ethics Board to analyze for PFAs and PFA-precursors in pre-existing and anonymized human serum collected from pregnant women in Edmonton in 2006. An equal volume from 14 individual samples were pooled and divided into three 5 mL samples in 15 mL polypropylene centrifuge tubes (Corning, NY) that were frozen (−80 °C) until analysis.

2.2.4 HPLC–MS/MS Conditions

Optimal conditions for isomer separation and linear isomer quantification by HPLC–MS/MS involved 20 μL injections of extract or standard onto a FluoroSep RP Octyl column (3μ 100A, 15 cm × 2.1 mm, ES Industries, West Berlin, NJ). This monomerically bonded perfluorooctyl (PFO) stationary phase consisted of a linear perfluorooctyl chain with a CH$_2$–CH$_2$ spacer group close to the surface of the silica base (Figure 2.1).[19]
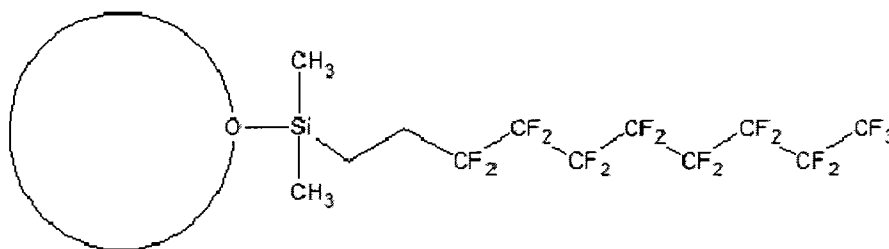
Figure 2.1 General structure of perfluoroctyl stationary phase illustrating the linkage between silica particle and fluoroalkyl chain via a CH$_2$CH$_2$ spacer group.

43

Gradient elution conditions were 200 μL/min, and starting conditions were 50% A (water adjusted to pH 4.0 with ammonium formate)–50% B (100% methanol). Initial conditions were held for 0.3 min, ramped to 64% B by 1.9 min, increased to 66% B by 5.9 min, 70% B by 7.9 min, 78% B by 40 min, and finally to 100% B by 60 min; held until 73 min; returned to initial conditions by 78 min; and the column equilibrated for a further 37 min. Mass spectral data were collected using a hybrid triple-quadrupole linear ion trap mass spectrometer (4000QTRAP, MDS Sciex, Concord, ON, Canada) equipped with an electrospray interface operating in the negative ion mode. Chromatograms were recorded by multiple reaction monitoring (MRM) with between 3 and 13 transitions per analyte (see section on MS/MS Optimization and Tables A-1 to A-11 in Appendix A). For comparison, we also conducted HPLC–MS/MS analysis for "total PFAs" (e.g., by integration of a single peak) using an Agilent Zorbax C8 3.5 μm (2.1 mm × 5 cm) and standard conditions (see Appendix A).

2.2.5 Extraction and Treatment of Samples

Labware was rinsed with HPLC-grade methanol prior to use. Serum samples (5 mL) were added to 6 mL of 0.1 M formic acid containing ^{13}C-PFOS, ^{13}C-PFOA, ^{13}C-PFNA, ^{13}C-PFDA, ^{13}C-PFDoA, and NMeFOSA and processed by solid-phase extraction similar to Kuklenyik et al.,[20] without automation (see Appendix A). Recovery experiments for both "total PFAs" and individual isomers showed that the extraction was quantitative and that isomer profiles were conserved (see Tables A-13 to A-15).

44

2.2.6 Quality Control

To minimize the background signal and inter-run variability of all analytes, an Agilent Eclipse XDB-C18 column was placed directly upstream of the injector to trap the instrumental sources of analyte, as adapted from Flaherty et al.[21] One modification was that a 15 cm column (4.6 mm i.d., 5 μm) was used rather than a drop-in guard cartridge, a necessity due to the increased retention of analytes on PFO (see Appendix A). For serum analysis, procedural blanks (Milli-Q water) were processed identical to samples to monitor contamination during the extraction method (see discussion and Table A-12 in Appendix A). Instrumental blanks (100% methanol) were injected every 3–5 samples to monitor carry-over, and standards were run before and after serum samples to monitor sensitivity drift.

2.3   Results and Discussion

2.3.1   Chromatographic Separations

Standards were used to evaluate the extent of isomer separation for each PFA or PFA-precursor. Only four of the authentic standards (PFOS, PFHxS, PFOA, and NEtFOSA) were known to have been produced by electrochemical fluorination; thus, only these had significant isomer composition. The synthetic route for the other standards was not confirmed but was expected to be through telomerization or oligomerization of perfluoroolefines or perfluoroolefin oxides,[22] but many isomers could be detected in these nevertheless. The linear isomer for each PFA, or PFA-precursor, was always the latest eluting on PFO.

This was presumably a combination of two factors: that the linear isomer is the most hydrophobic, and the *linear* perfluoroalkyl isomer of each analyte should also have the greatest intermolecular attraction to the *linear* PFO stationary phase. The linear isomer was confirmed using authentic linear native and/or linear surrogate standards for PFOS, PFOA, PFNA, PFDA, PFDoA, *N*EtFOSA, and FOSA and could be inferred for all other PFAs since the latest eluting isomer was also the largest peak.

By existing "total PFA" methodologies, it is most common to employ an aqueous mobile phase buffered to neutral pH with 1–10 mM ammonium acetate. Under such conditions on PFO, some isomer separation was achieved, although broad and tailing peaks severely limited the separation of the earliest eluting branched isomers (Figure 2.2A, PFOS shown). To improve peak shapes, we investigated the effect of mobile phase pH on isomer resolution by comparing separations with 5 mM ammonium acetate (pH 6.8) to separations with 5 mM ammonium formate at pH 3.0 and 4.0 (formic acid, pH adjusted with ammonium hydroxide). The low pH ammonium formate buffers were effective at resolving early eluting branched isomers of PFOS and PFOA as a result of decreased peak widths and elimination of tailing (Figure 2.2B, PFOS shown). Furthermore, increased retention of linear and all branched isomers was pronounced for PFOS, PFOA, PFHpA, and PFDoA, with retention times 8–12 min longer at pH 3.0 and 4.0 compared to pH 6.8. Linear PFHxS eluted at nearly identical times at all pHs investigated, and resolution of branched isomers was only moderate, even at lower pH. The remainder of the PFAs had retention times approximately 5 min

46

longer at pH 3.0 or 4.0. No differences were observed between pH 3.0 and 4.0; however, ammonium formate adjusted to pH 4.2 again resulted in poor peak shape and less retention. Therefore, pH 4.0 was selected as the optimal condition for the remainder of this work.
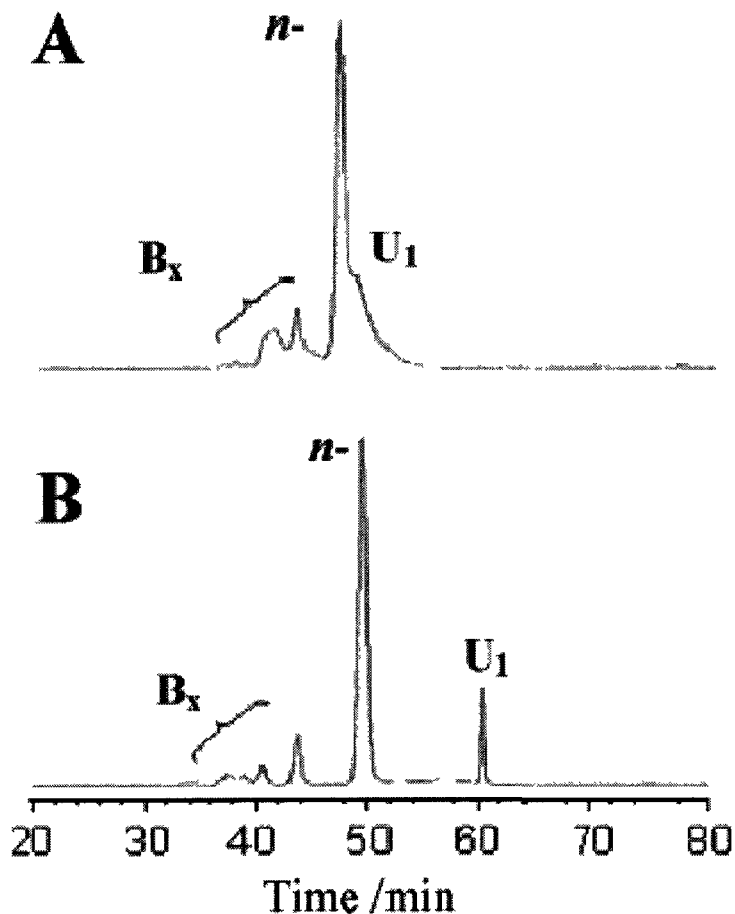
Figure 2.2 LC-MS chromatograms of an ECF PFOS standard (m/z 499) showing the effect of aqueous mobile phase pH on separation of linear (n-) and branched (B_x) isomers: (A) pH 6.8, 5 mM ammonium acetate; (B) pH 3.0 or 4.0, 5 mM ammonium formate. Note the presence of unknown (U_1) at ~50 min (A) and ~60 min (B). This peak was not observed to fragment into PFOS product ions.

47

Conditions on C18 (Agilent Eclipse XDB-C18, 5 µm 4.6 mm × 150 mm) resulted in relatively poor isomer separation, earlier elution, and substantially broader peaks compared to PFO (Appendix A, Figure A-1; PFHxS, PFOA, PFOS, and PFNA shown). Nonetheless, the separations obtained in this work on C18, using the gradient elution program developed on PFO, were similar to other optimized separations published for PFOS isomers by HPLC;[16,17] thus, no further refinement was undertaken. The vast improvement in performance of PFO over C18 is reflected in the increased selectivity (e.g., retention time) of PFOA (55.2 min vs 34.7 min, respectively) as well as the improved resolution for iso-PFOS/5m-PFOS and 5m-PFOS/4m-PFOS (4.2 and 2.0 vs <0.2 and 0.5 on PFO and C18, respectively).

The elution order of PFOS isomers on PFO was not substantially different from what was previously shown on perfluorophenyl by Langlois and Oehme.[17] The elution order on PFO, from latest to earliest, was n-PFOS, iso-PFOS, 5m-PFOS, 4m-PFOS, B₄-PFOS, 3m-PFOS, and on perfluorophenyl was n-PFOS, iso-PFOS, 5m-PFOS, 1m-PFOS, 4m-PFOS, 3m-PFOS. However, the current method for PFOS isomers, using PFO, had some advantages in terms of isomer separation. For example, although peak widths appeared similar by both methods, the 11 PFOS isomers eluted over a ~20 min window on PFO compared to ~7 min for 10 isomers on perfluorophenyl.[17] On the other hand, a perceived disadvantage of the current method was the long run time of 50 min to separate PFOS isomers, whereas Langlois and Oehme[17] achieved their separations in under

30 min. However, the method here was optimized to simultaneously enable the separation of earlier and later eluting analytes; thus, a more rapid optimized method for PFOS isomers may be possible on PFO.

As with alkyl stationary phases, carboxylate and sulfonate PFAs eluted in order of increasing chain length (i.e., C6 earliest, C14 latest) on PFO. However, unlike with alkyl stationary phases, PFOS isomers eluted ~6 min before PFOA despite that PFOS has a lower water solubility than PFOA (0.5 and 3.5 g/L, respectively) and PFOS has a perfluorooctyl chain matching the length of PFO. It is unknown why this occurs but may be due to the nature of the cationic counterion for each or interactions of the sulfonate and carboxylate moieties with PFO. The latest eluting analyte by this method, linear PFTA, had a retention time of 74 min. Admittedly, this is much longer than current methods that avoid isomer separation and we are currently making efforts to reduce this. If the objective is only to profile isomers for PFOS, PFHxS, and PFOA, the run time can be shortened to 55 min.

2.3.2 Structural Identification of Sulfonate Isomers in Standards

Isomer structures of PFOS were elucidated by product ion spectra using the missing "0-series" (*m/z* 130, 180, 230, etc.) technique introduced by Langlois and Oehme[17] and a missing "9-series" technique discussed here. Briefly, the absence of the "0-series" product ion identifies the location of the tertiary carbon. The absence of this fragment occurs due to the stability of the tertiary carbanion

49

which prevents simultaneous breaking of the CF_3- and $CF_3C_xF_{2x}-$ groups, thus leading to an absence of this "0-series" ion.[17] Correspondingly, for each branched isomer, a specific "9-series" fragment (e.g., m/z 119, 169, 219, etc.) cannot be formed, thus its absence should confirm the location of the branching point. For example, for *iso*-PFOS (i.e., $(CF_3)_2(CF_2)_6SO_3^-$) an ion having m/z 119 ($[CF_3CF_2]^-$) cannot form. The expected missing "0-series" and "9-series" product ions for PFOS isomers are stated in Appendix A.

For PFOS, a total of 11 isomers were resolved (Appendix A, Table A-6). *Iso*-PFOS, 5*m*-PFOS, and 4*m*-PFOS were the second, third, and fourth latest eluting isomers, respectively, and were easily identified by their product ions and baseline or near-baseline resolution (Figure 2.3). The earlier eluting isomers were more difficult to identify due to lower concentration and minor coelution; however, we were able to identify 3*m*-PFOS based on missing m/z 230. Isomer B_6 is hypothesized to correspond to 1*m*-PFOS based on the lack of m/z 130 ion and the presence of the distinctive m/z 419 ion;[17] however, the lack of other confirmative transitions precluded further assignment. 2*m*-PFOS was not observed in the standard, as also noted by Langlois and Oehme,[17] nor did we observe it in human serum. Although other m/z 499 molecular ions were resolved in the standard, structural assignments could not be made with certainty; however, some of these are expected to be internal gem-dimethyl isomers due to the high relative abundance of certain "9-series" fragments.

An electrochemically fluorinated standard of PFHxS contained six branched isomers and one unknown having a parent m/z of 399 (Appendix A,

Table A-4). This is the first time separation of PFHxS isomers has been reported. Structural assignment of each isomer was attempted, and the two branched isomers closest to n-PFHxS were hypothesized to be iso-PFHxS (second last eluting) and $3m$-PFHxS (third last eluting) based on missing "0-series" ions. However, these assignments were hampered by apparent incongruity of missing "0-series" and "9-series" fragments. For example, the latest eluting branched isomer, which we hypothesize to be iso-PFHxS due to its late elution and lack of m/z 280 product ion, contained an unexpected product ion at m/z 119 which is impossible for any iso-PFA. The structural assignment of several PFHxS isomers therefore remains uncertain.

2.3.3 Structural Identification of Carboxylate Isomers in Standards

Although some structural information can be obtained for the carboxylate isomers discussed here, unequivocal assignments cannot be made without authentic standards. Enriched isomer fractions would be useful for future structural elucidation as was done for PFOS by Langlois and Oehme.[17] The nine branched PFOA isomers observed in the electrochemical standard may well account for all five monomethyl and four geminal dimethyl branched isomers that are theoretically possible (Appendix A, Table A-5). Structural information was gained from the relative abundance of "9-series" product ions. Only a single minor PFOA isomer (B_8-PFOA) and an unknown (U_1) dissociated to m/z 269 or 319, respectively; therefore, m/z 369, 219, 169, and 119 were primarily used to attempt structural elucidation (Figure 2.4). The isomer eluting immediately prior

51

to *n*-PFOA dissociated to *m/z* 369, 169, and 219, and was tentatively assigned as *iso*-PFOA based on (i) the missing "9-series" fragment, *m/z* 119, and (ii) an abundant product ion at *m/z* 169 corresponding to [(CF$_3$)$_2$CF]$^-$, but this isomer cannot be unequivocally assigned until a pure isopropyl-PFOA standard is available. Further structural elucidation of the branched PFOA isomers was difficult due to the dominant neutral loss of CO$_2$ and no observable neutral loss from the terminal end(s) (i.e., CF$_3$–) of the perfluorinated chain. Therefore, other evidence was drawn upon. First, among the five possible perfluoromethyl isomers, *iso*-PFOA was reported to be the most dominant (~9%) in a different electrochemical standard using NMR, followed by 5*m*-, 4*m*-, and 3*m*-PFOA, the latter three of which were estimated to make up 12.5% total PFOA.[23] Second, by analogy to the elution profile of PFOS isomers in this study, it is assumed that the earlier eluting PFOA isomers are more highly branched. Third, Langlois and Oehme[17] observed that the perfluorinated chain was more readily fragmented at the source when the position of the perfluoromethyl branch moved closer to the sulfonate moiety.[17] Although these branched isomers could not be conclusively identified, it was hypothesized that B$_2$, B$_3$, and B$_4$ correspond to 5*m*-, 4*m*-, and 3*m*-PFOA, respectively.

The method was proven capable of resolving 3 PFHpA isomers (+ 1 unknown), 4 PFNA isomers (+ 2 unknowns), 3 PFDA isomers, 6 PFUnA isomers, 13 PFDoA isomers (+ 6 unknowns), and 7 PFTA isomers. *Iso*-PFNA was confirmed with an authentic standard. The total number of isomers detected here should be considered a lower limit of isomer separation performance by this

method, since these standards did not contain significant branched isomer quantities. These isomers are not characterized in this work, but collision induced dissociation patterns for all PFAs and PFA-precursors are shown in Tables A-1 to A-11 of Appendix A. Some structural information can be obtained using the "9-series" technique, but the low abundance of some ions makes it difficult to determine whether a given "9-series" fragment was not being formed or was simply below the detection limit.
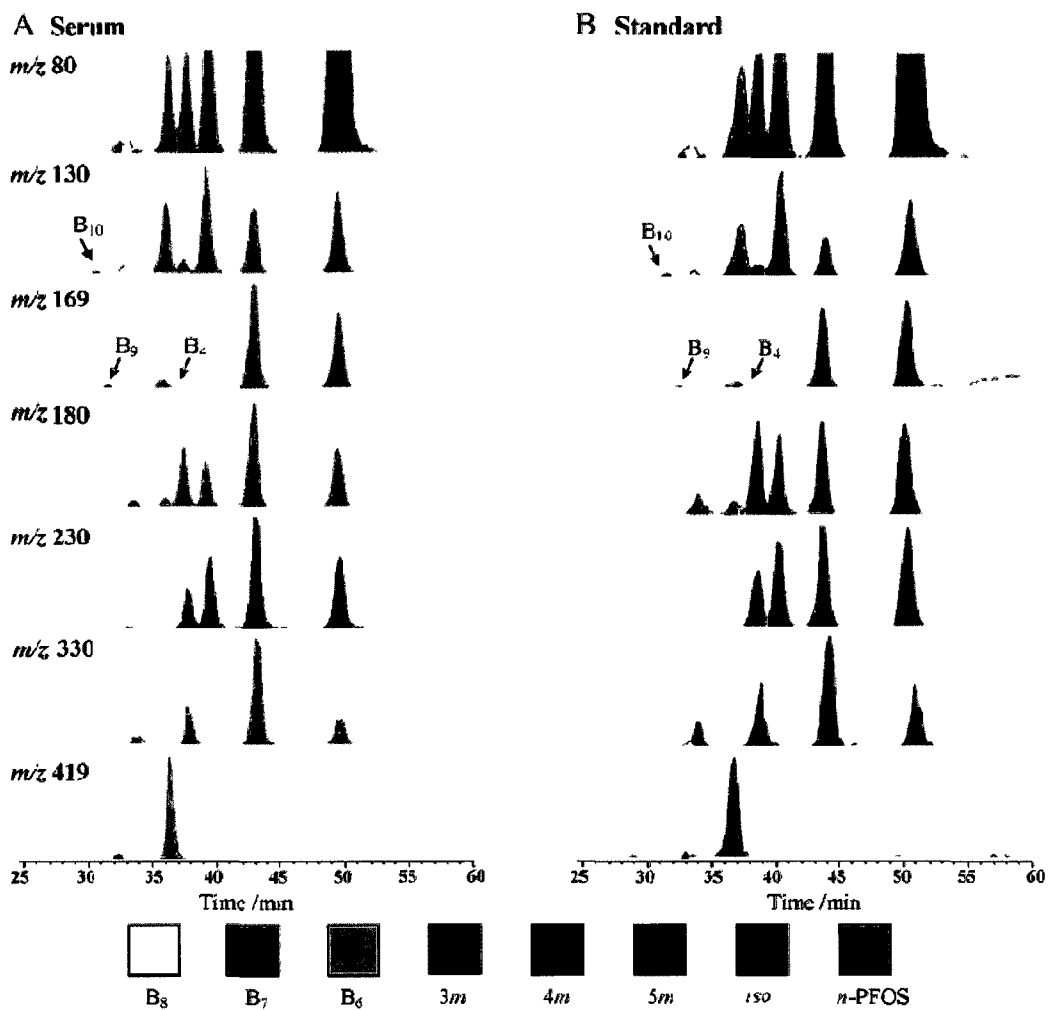
Figure 2.3 Chromatograms of PFOS isomers showing seven product ions, chromatogram set A is from pooled human serum and chromatogram set B is from a 100 ppb technical PFOS standard.
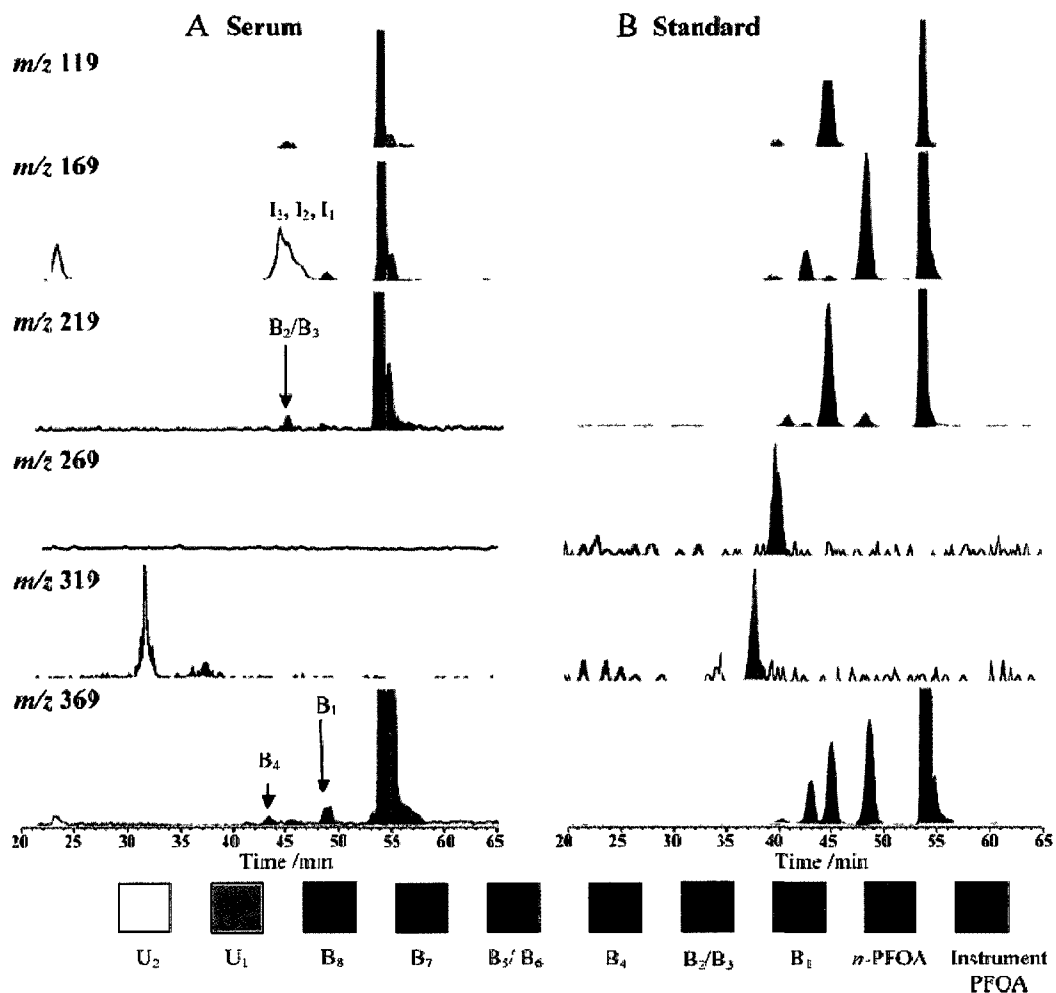
Figure 2.4 Chromatograms of PFOA isomers showing six product ions, chromatogram set A is from pooled human serum and chromatogram set B is from a 100 ppb technical PFOA standard.

2.3.4 Structural Identification of Sulfonamide Isomers in Standards.

Structural elucidation of 15*N*EtFOSA isomers from an electrochemically fluorinated standard was based on "9-series" product ions, while 6 other product ions assisted their resolution: $[C_8F_{12}SO_2NH]^-$, (m/z 402); $[C_6H_3F_{11}NO_2S]^-$, (m/z 362); $[CF_3CH_2]^-$, (m/z 83); $[SO_2H]^-$ (m/z 65), m/z 287, and m/z 126. This is

the first time PFOS-precursor isomer separation has been reported by HPLC. Monitoring of 13 MS/MS transitions allowed for the separation of n-NEtFOSA from 14 branched isomers, among which n-NEtFOSA was confirmed with a linear standard. The peak eluting closest to the linear isomer was hypothesized to correspond to iso-NEtFOSA based on it missing the m/z 119 fragment (Appendix A, Table A-1) but this was not confirmed. The remaining branched isomers could not be structurally identified.

FOSA is often detected in human[24] and wildlife samples;[25-27] thus, it was a priority for us to evaluate the performance of this method with an electrochemical source of this compound. Unfortunately, no such standard was commercially available; however, NEtFOSA has been reported to undergo rapid N-deethylation by cytochrome P450 enzymes to form FOSA, which is in turn metabolized at a much slower rate to PFOS.[7,8] Thus, we generated FOSA isomers via N-deethylation of electrochemical NEtFOSA using human liver microsomes. n-FOSA was identified using an authentic linear standard but structural elucidation of five branched isomers was difficult due to their tendency to produce m/z 78 ions almost exclusively, corresponding to $[SO_2N]^-$. Only two other weak product ions (m/z 169 and 119) could be used to resolve and identify these. The latest eluting branched isomer (B_1) was tentatively assigned as iso-FOSA based on a missing m/z 119 product ion but was not confirmed (Appendix A, Table A-2). Curiously, isomer B_2 was one of the fastest to form and to subsequently disappear, whereas B_1-FOSA was slow to form and was one of the only branched isomers still observable at 24 h (see Appendix A, Figure A-2). Overall, at 10 and 60 min,

the FOSA isomer profile was in stark contrast to that observed in the pooled human serum; while at 24 h the isomer profile was very similar, branched isomers B_1 and B_2 had approximately equal peak areas and were in similar proportion to n-FOSA. These preliminary data are important in that they suggest differences in the biological properties of the isomers, thus, emphasizing the need to analyze for each form separately.

2.3.5 Isomer Profiles in Human Serum

The optimized method was then applied to screening pooled human maternal serum from Edmonton (AB). Pure authentic standards for individual branched isomers (except iso-PFNA) were not available; thus, chromatographic peaks observed in serum had to correspond to chromatographic peaks in the impure standards to be confirmed as an isomer in this work. Four criteria were used: retention time, primary product ion, secondary product ion, and the area ratio between primary and secondary product ions. If one or more of these criteria was not met, the peak was labeled as either an "unknown" (U_x) or an "interference" (I_x) (see Nomenclature section).

Among all PFA isomer profiles in serum, the PFOS isomer profile was the only one that closely resembled the corresponding standard (Figure 2.3). In fact, all 11 isomers present in the standard were identified in human serum in virtually identical proportions. On the basis of the batch-to-batch variability, which can occur during electrochemical fluorination,[22] and the hypothesized pharmacokinetic differences among the isomers,[16] it is very surprising that the

technical standard examined here had such a similar isomer profile to that in humans.

Isomer profiling of PFHxS was initially misleading, as several large peaks in the m/z 399 → 80 and 399 → 99 transitions (later identified as interferences, see Quantification Bias and Identification of Nominal Mass Interferences section) were found to have retention times matching branched PFHxS isomers. As a result, we were forced to rely on less sensitive (albeit interference free) transitions that may have precluded the observation of branched isomers due to increased detection limits. Despite the six PFHxS branched isomers found in standards, we were only capable of confirming one of these (B_1, tentatively *iso*-PFHxS) in human serum. The method's potential for separation of PFHxS isomers in standards suggests it may be useful for isomer profiling of abiotic samples. For example, house dust was associated with elevated concentrations of PFHxS in Ottawa, Canada,[28] and comparison of isomer profiles in dust and blood may reveal exposure sources for small children.

The PFCA concentrations and isomer profiles in Edmonton serum showed similarities to the isomer profiles reported by De Silva et al.[29] for pooled North American human serum (mixed age, gender, blood type) using gas chromatography. The "total PFOA" concentration was reported as 4.4 ppb by De Silva, compared to 4.0 ppb in the present study. In serum from both studies, *n*-PFOA was present at much higher levels relative to branched isomers. De Silva detected four branched PFOA isomers in addition to *n*-PFOA, among which *iso*-PFOA was the most abundant. We also detected up to four branched PFOA

isomers in Edmonton serum: B_1-PFOA (major branched PFOA isomer, tentatively *iso*-PFOA), B_2/B_3, and B_4-PFOA (Figure 2.4). B_4 and B_2/B_3 matched the retention time and product ion patterns observed in the standard. An unknown peak (U_2), not observed in the electrochemical standard, was observed in human serum at ~22 min (earliest eluting of all peaks). This was originally presumed to be an interference, yet it had both primary (*m/z* 169) and secondary (*m/z* 369) product ions that are common to other PFOA isomers, and therefore is likely a PFOA isomer despite its very weak retention (Figure 2.4).

Some of the earliest measurements of "total PFOA" in human blood utilized the *m/z* 169 transition to quantify PFOA.[30] This may be problematic for two reasons. First, moderate sized interference peaks in the *m/z* 169 product ion (I_1, I_2, I_3, Figure 2.4 and Appendix A) may lead to a positive bias. Second, the response of the *m/z* 169 transition for isomers B_2/B_3 was relatively weak in the technical standard (Figure 2.4) but was the second most abundant branched isomer peak based on selected ion monitoring of the parent ion (*m/z* 413, not shown). The *m/z* 369 transition chromatogram had a similar response profile compared to selected ion monitoring of *m/z* 413, and in samples analyzed here, chromatograms did not contain any interference for *m/z* 369. It is therefore recommended that in the absence of isomer separation, the *m/z* 369 transition be used for "total PFOA" quantification.

The linear isomer of PFNA was dominant in human serum, albeit two branched isomers and two unknown peaks were also observed. *Iso*-PFNA was confirmed using a pure *iso*-PFNA standard and was the most abundant branched

59

isomer. B_3-PFNA eluted at 56.2 min and was quite large but was also found in procedural blanks and thus was not detected. PFNA unknowns (U_1 and U_2), and an additional minor isomer (B_2-PFNA), were observed in human serum and not in blanks. Similarly, De Silva detected two branched PFNA isomers, in addition to n-PFNA, which accounted for 1.6% of total PFNA, with iso-PFNA again being present in the highest amounts among branched PFNA isomers.

Branched and linear PFHpA isomers were generally not above blanks; the linear isomer coming from our injector and the branched isomers (B_1 and B_2) and unknown (U_1) attributed to the extraction procedure. For PFDA and PFUnA, the linear isomers and two very minor branched isomers (B_1-PFDA and B_1-PFUnA) were observed in human serum, while for PFDoA and PFTA, only the respective linear isomers were observed in serum. These data agree with those of De Silva,[29] who did not detect any branched isomers of PFDA and one minor branched PFUnA isomer (2.3%) in one sample. Of the sulfonamides, only FOSA was observed in human serum by this new method, of which B_2-FOSA, B_1-FOSA, and n-FOSA were observed, the latter being dominant.

2.3.6 Quantification Bias and Identification of Nominal Mass Interferences

PFAs have been detected globally in human blood, with PFOS generally being the most prevalent compound followed by PFOA and longer chained PFCAs.[12] For comparison to existing data, we quantified "total PFA" concentrations in the pooled maternal sample from Edmonton using a nonisomer separation method and standard conditions. Both primary and secondary product

ions were used to confirm that a single transition was not over-reporting, which has been a problem in the past for the m/z 80 product ion of PFOS in biological samples,[1,30-32] including in human serum.[33] In this work, a quantification bias was assumed when the concentration obtained using the primary transition was >5% different than the secondary transition. The most abundant "total PFAs" were PFOS > PFOA > PFNA > PFHxS (9.1 ± 0.9, 4.0 ± 0.9, 1.5 ± 0.5, and 1.2 ± 0.3 ppb, respectively), with the remainder of PFAs below 1 ppb: PFUnA, 0.8 ppb (±0.3); PFDA, 0.7 ppb (±0.4); PFDoA, 0.4 ppb (±0.2); FOSA, 0.2 ppb (±0.1). Among these, only PFOS and PFHxS showed an apparent quantification bias between primary and secondary transitions. "Total PFOS" determined by monitoring m/z 499 → 99 resulted in 9.1 ppb, whereas using m/z 499 → 80, the concentration was 15.1 ppb. For "total PFHxS", the m/z 399 → 99 transition resulted in a concentration of 27.9 ppb, whereas the m/z 399 → 80 transition resulted in a concentration of 6.4 ppb. We therefore examined the isomer profile of PFOS and PFHxS on PFO to determine whether the bias in "total PFA" analysis may originate from either (i) coeluting branched isomers that fragment to a greater extent in one of the transitions or rather (ii) coeluting mass interferences.

In the electrochemical PFOS standard, *n*-PFOS accounted for ~76% of total PFOS, while in serum, *n*-PFOS accounted for ~80% of total PFOS. Furthermore, the branched isomer profiles were nearly identical among the standard and serum; thus, we concluded that the "total PFOS" analytical bias was not a result of isomer profile differences. Within the elution range of all PFOS isomers on PFO, no interferences were evident. In fact, the ratio of every primary

to secondary MS/MS transition for each isomer in serum matched the standard to within 1–2%. For example, quantifying the linear isomer by both m/z 99 and m/z 80 product ions resulted in a concentration of 7.3 ppb in both instances. However, in the serum m/z 499 → 80 MRM chromatogram (Figure 2.5A), a broad peak was present that was clearly separated from all isomers. Enhanced product ion scans identified this peak as isomers of taurodeoxycholate; confirmed with an authentic standard (Figure 2.5A and discussion in Appendix A). These endogenous surfactants are common to a wide range of animal species and are presumably coextracted with PFAs due to their similar physical properties.[34,35] An additional interference was observed to elute after n-PFOS in an ECF standard (see Appendix A); therefore, all interferences were simultaneously removed by performing isomer separation. A secondary benefit was that the more sensitive m/z 499 → 80 transition could then be used to monitor PFOS, and for the linear isomer this improved detection limits over 20-fold (0.8 pg versus 20 pg using m/z 80 and 99, respectively).
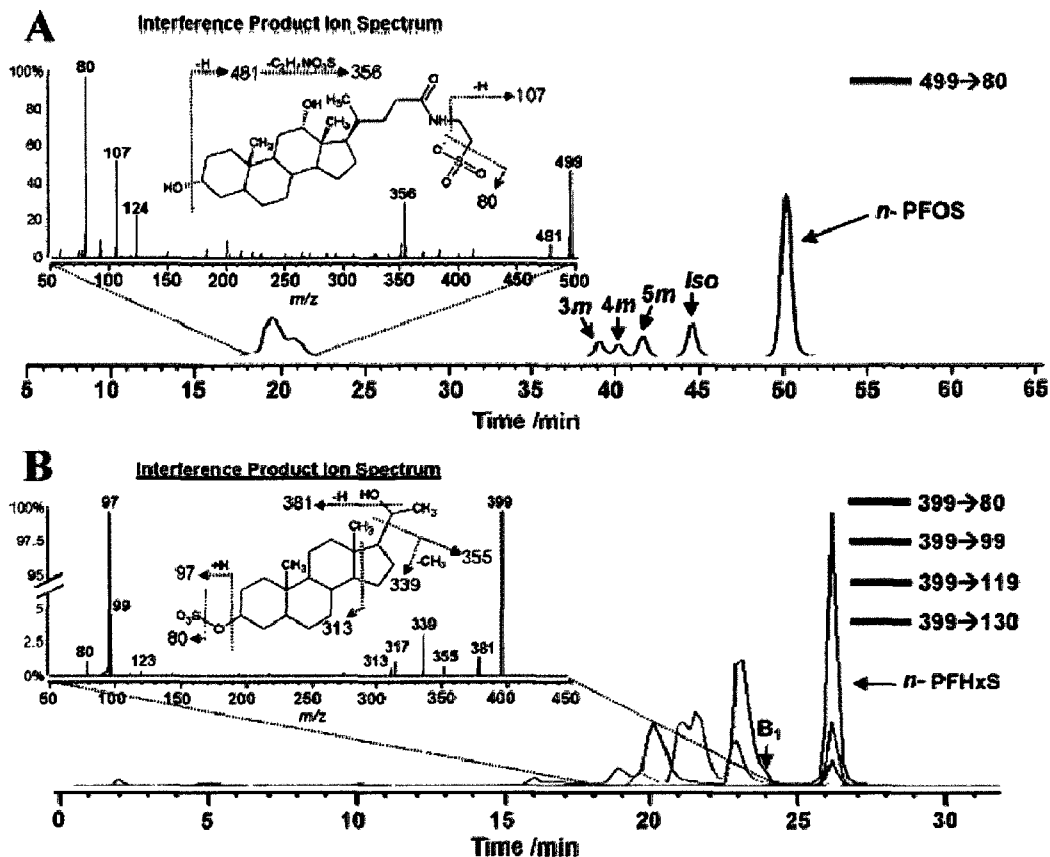
Figure 2.5 Chromatograms of (A) PFOS in human serum showing interference which causes over-reporting using the m/z 499 → 80 transition and (B)PFHxS in human serum showing the presence of interferences in the m/z 399 → 99,80 transitions and their absence in m/z 119 and m/z 130 product ions. Enhanced product ion spectra are shown as inserts in A and B and identified as (A) isomers of taurodeoxycholic acid and (B) isomers of 5-pregnan-3,20-diol-3-sulfate (m/z 80 interference, structure shown) and isomers of ^{34}S-3-hydroxy-5-pregnan-20-one sulfate (m/z 99 interference, structure not shown).

An important outcome of these efforts was that, for these particular serum samples, the "total PFOS" quantification, without isomer separation, based on the m/z 499 → 99 transition (9.1 ppb) is a reasonably accurate approximation of the sum concentration for all PFOS isomers. As noted, the interference-free quantification of n-PFOS, by isomer separation, resulted in a concentration of 7.3

ppb, and because the profile of PFOS isomers in blood is so similar to the standard, it is reasonable to assume that the remaining branched isomers constitute 20% of the total (or another 1.8 ppb) to result in a total PFOS concentration of 9.1 ppb, exactly the same as determined by the nonseparation method. This is perhaps very fortunate, and unless the standard is indeed very similar to the sample being analyzed, the accuracy of traditional analytical methods should not be taken for granted without isomer profile information.

To investigate the bias associated with PFHxS quantification, we reanalyzed the serum extracts without isomer separation using selective ion monitoring (m/z 399) and 9 different product ions by MS/MS. Selective ion monitoring of four out of nine product ions resulted in high and inconsistent PFHxS concentrations in the order m/z 399 > 99 > 80 > 69 ≈ 169 (68.2, 27.9, 6.4, 6.3 ppb, respectively). The remainder of the product ions (m/z 119, 130, 180, 219, and 280) consistently reported a PFHxS concentration of ~1 ppb, with m/z 399 → 119 being the most sensitive ion that did not cause apparent over-reporting. Unfortunately, although monitoring these minor product ions effectively removes any interferences without isomer separation, it cannot compensate for any related ion suppression and it also raises the limit of detection substantially from 0.4 to 3.1 pg using m/z 80 and 119 product ions, respectively.

In an effort to identify the PFHxS interferences, enhanced product ion scans were compared to published spectra to identify them as isomers of 5-pregnan-3,20-diol-3-sulfate (source of m/z 399 → 80, Figure 2.5B inset) and minor contributions from [34]S-3-hydroxy-5-pregnan-20-one sulfate (4.1% natural

isotope, source of m/z 399 → 99 [HO^{34}SO$_3$]$^-$). Detailed mass spectral studies on these steroid sulfates has been carried out by Griffiths et al.,[36] and our own fragmentation assignments can be found in Appendix A. These steroid sulfates exist as multiple isomers and can be found in a wide range of mammalian and non-mammalian vertebrates.[36,37] Concentrations in humans are affected by external stimulus such as stress or sex stimulus and tend to increase during pregnancy.[37]

Issues with the analysis of PFHxS were reported in the most recent worldwide interlaboratory study on PFCs in human serum.[38] In serum A of the interlab samples, out of all PFAs the variability was highest for PFHxS (108% RSD), suggesting that these interferences are likely present in other blood samples. Indeed our analysis of both the interlaboratory and Edmonton serum samples using a nonisomer separation method found that PFHxS concentrations are overpredicted by 10–20-fold using m/z 399 → 99 or m/z 399 → 80 transitions. To our knowledge, all published biomonitoring data for PFHxS have used these problematic transitions. Therefore, we highly advise that future monitoring of PFHxS in human blood employs an isomer separation method, such as this one, which also removes the coeluting interferences from linear PFHxS. In the absence of an isomer separation method, use of the minor transitions (particularly m/z 119) is suggested for quantitative human serum analysis. Some analytical bias of unknown proportion, however, will remain so long as the isomer profile of the standard and sample are different. From results in Edmonton, a linear standard

may be the most appropriate standard for "total PFHxS" analysis in humans since very few isomers could be detected.

2.4 Conclusions

The method presented here adds to and improves upon the De Silva[29] and Langlois and Oehme[17] methods by separating all major sulfonate and carboxylate isomers in a single injection. For the first time, PFOSAs, PFCAs, and PFHxS isomers were separated by HPLC–MS/MS. The new method has the added advantage of removing mass interferences which can otherwise lead to an over-reporting of PFOS and PFHxS concentrations and decreased sensitivity when using "total isomer" quantification methods. In absence of analytical isomer separations we have provided mass spectrometry strategies to minimize quantification biases, and here we further suggest that sample preparation strategies using fluorous silica[39] or hexafluoropropanol[40] should also be considered. Our preliminary results point to differences in biological properties among individual isomers, and this method provides a tool to test hypotheses on PFA isomer behavior and exposure sources.

2.5 Acknowledgment

2.6   References

1.   Giesy, J.P.; Kannan, K. *Environ. Sci. Technol.* **2001**, *35*, 1339-1342.

2.   Kannan, K.; Corsolini, S.; Falandysz, J.; Fillmann, G.; Kumar, K.S.; Loganathan, B.G.; Mohd, M.A.; Olivero, J.; Van Wouwe, N.; Yang, J.H.; Aldoust, K.M. *Environ. Sci. Technol.* **2004**, *38*, 4489-4495.

3.   Martin, J.W.; Ellis, D.A.; Mabury, S.A.; Hurley, M.D.; Wallington, T.J. *Environ. Sci. Technol.* **2006**, *40*, 864-872.

4.   Ellis, D.A.; Martin, J.W.; De Silva, A.O.; Mabury, S.A.; Hurley, M.D.; Andersen, M.P.S.; Wallington, T.J. *Environ. Sci. Technol.* **2004**, *38*, 3316-3315.

5.   D'Eon, J.; Hurley, M.; Wallington, T.J.; Mabury, S.A. *Environ. Sci. Technol.* **2006**, *40*, 1862-1868.

6.   Martin, J.W.; Mabury, S.A.; O'Brien, P.J. *Chem.-Biol. Interact.* **2005**, *155*, 165-180.

7.   Tomy, G.T.; Tittlemier, S.A.; Palace, V.P.; Budakowski, W.R.; Braekevelt, E.; Brinkworth, L.; Friesen, K. *Environ. Sci. Technol.* **2004**, *38*, 758-762.

8.   Xu, L.; Krenitsky, D.M.; Seacat, A.M.; Butenhoff, J.L.; Anders, M.W. *Chem. Res. Toxicol.* **2004**, *17*, 767-775.

9.   Center for Disease Control (CDC). Third National Report on Human Exposure to Environmental Chemicals; NCEH Pub. No. 05-0570; Department of Health and Human Services, Centers for Disease Control and Prevention, National Center for Environmental Health, Division of Laboratory Sciences, U.S. Government Printing Office: Washington, DC, **2005**.

10. Calafat, A.M.; Needham, L.L.; Kuklenyik, Z.; Reidy, J.A.; Tully, J.S.; Aguilar-Villalobos, M.; Naeher, L.P. *Chemosphere.* **2006**, *63*, 490-496.

11. Lau, C.; Anitole, K.; Hodes, C.; Lai, D.; Pfahles-Hutchens, A.; Seed, J. *Toxicol. Sci.* **2007**, *99*, 366-394.

12. Houde, M.; Martin, J.W.; Letcher, R.J.; Solomon, K.R.; Muir, D.C. *Environ. Sci. Technol.* **2006**, *40*, 3463-3473.

13. Wallington, T.J.; Hurley, M.D.; Xia, J.; Wuebbles, D.J.; Sillman, S.; Ito, A.; Penner, J.E.; Ellis, D.A.; Martin, J.; Mabury, S.A.; Nielsen, O.J.; Sulbaek Andersen, M.P. *Environ. Sci. Technol.* **2006**, *40*, 924-930.

14. van Leeuwen, S.P.; Karrman, A.; van Bavel, B.; de Boer, J.; Lindstrom, G. *Environ. Sci. Technol.* **2006**, *40*, 7854-7860.

15. Lehmler, H.J. *Chemosphere.* **2005**, *58*, 1471-1496.

16. Martin, J.W.; Kannan, K.; Berger, U.; de Voogt, P.; Field, J.; Franklin, J.; Giesy, J.P.; Harner, T.; Muir, D.C.; Scott, B.; Kaiser, M.; Jarnberg, U.; Jones, K.C.; Mabury, S.A.; Schroeder, H.; Simcik, M.; Sottani, C.; van Bavel, B.; Karrman, A.; Lindstrom, G.; van Leeuwen, S. *Environ. Sci. Technol.* **2004**, *38*, 248A-255A.

17. Langlois, I.; Oehme, M. *Rapid Commun. Mass Spectrom.* **2006**, *20*, 844-850.

18. De Silva, A.O.; Mabury, S.A. *Environ. Sci. Technol.* **2004**, *38*, 6538-6545.

19. Przybyciel, M. *LC/GC.* **2005**, *June 1*, 7 pages.

20. Kuklenyik, Z.; Reich, J.A.; Tully, J.S.; Needham, L.L.; Calafat, A.M. *Environ. Sci. Technol.* **2004**, *38*, 3698-3704.

21. Flaherty, J.M.; Connolly, P.D.; Decker, E.R.; Kennedy, S.M.; Ellefson, M.E.; Reagen, W.K.; Szostek, B. *J. Chrom. B.* **2005**, *819*, 329-338.

22. Lewandowski, G.; Meissner, E.; Milchert, E. *J. Haz. Mat.* **2006**, *136*, 385-391.

23. Stevenson, L. U.S. Environmental Protection Agency public docket AR-2261150: Comparative analysis of fluorochemicals in human serum samples obtained commercially. U.S. Environmental Protection Agency, Office of Pollution Prevention and Toxic Substances, Washington, DC, **2002**.

24. Karrman, A.; Mueller, J.F.; van Bavel, B.; Harden, F.; Toms, L.M.; Lindstrom, G. *Environ. Sci. Technol.* **2006**, *40*, 3742-3748.

25. Martin, J.W.; Whittle, D.M.; Muir, D.C.; Mabury, S.A. *Environ. Sci. Technol.* **2004**, *38*, 5379-5385.

26. Smithwick, M.; Mabury, S.A.; Solomon, K.R.; Sonne, C.; Martin, J.W.; Born, E.W.; Dietz, R.; Derocher, A.E.; Letcher, R.J.; Evans, T.J.; Gabrielsen, G.W.; Nagy, J.; Stirling, I.; Taylor, M.K.; Muir, D.C. *Environ. Sci. Technol.* **2005**, *39*, 5517-5523.

27. Tomy, G.T.; Budakowski, W.; Halldorson, T.; Helm, P.A.; Stern, G.A.; Friesen, K.; Pepper, K.; Tittlemier, S.A.; Fisk, A.T. *Environ. Sci. Technol.* **2004**, *38*, 6475-6481.

28. Kubwabo, C.; Stewart, B.; Zhu, J.; Marro, L. *J. Environ. Mon.* **2005**, *7*, 1074-1078.

29. De Silva, A.O.; Mabury, S.A. *Environ. Sci. Technol.* **2006**, *40*, 2903-2909.

30. Hansen, K.J.; Clemen, L.A.; Ellefson, M.E.; Johnson, H.O. *Environ. Sci. Technol.* **2001**, *35*, 766-770.

31. Kannan, K.; Koistinen, J.; Beckmen, K.; Evans, T.; Gorzelany, J.F.; Hansen, K.J.; Jones, P.D.; Helle, E.; Nyman, M.; Giesy, J.P. *Environ. Sci. Technol.* **2001**, *35*, 1593-1598.

32. Kannan, K.; Franson, J.C.; Bowerman, W.W.; Hansen, K.J.; Jones, P.D.; Giesy, J.P. *Environ. Sci. Technol.* **2001**, *35*, 3065-3070.

33. Kubwabo, C.; Vais, N.; Benoit, F.M. *J. Environ. Mon.* **2004**, *6*, 540-545.

34. Anderson, I.G.; Haslewood, G.A.D.; Wootton, I.D.P. *Biochem. J.* **1957**, *67*, 323-328.

35. Alil, S.S.; Farhatl, H.; Elliott, W.H. *J. Lipid Res.* **1976**, *17*, 21-24.

36. Griffiths, W.J.; Liu, S.Y.; Yang, Y.; Purdy, R.H.; Sjovall, J. *Rapid Commun. Mass Spectrom.* **1999**, *13*, 1595-1610.

37. Parizek, A.; Hill, M.; Kancheva, R. *J. Clin. Endocrinol. Metab* **2005**, *90*, 395-403.

38. Lindström, G.; van Leeuwen, S. 2nd Worldwide InterlaboratoryStudy on PFCs - Human Serum. Intercal Sweden, Södra Dylta, Sweden **2006**.

39. Simcik, M.F.; Dorweiler, K.J. *Environ. Sci. Technol.* **2005**, *39*, 8678-8683.

40.   Butt, C.M.; Muir, D.C.; Stirling, I.; Kwan, M.; Mabury, S.A. *Environ. Sci. Technol.* **2007**, *41*, 42-49.

Chapter 3. Disposition of Perfluorinated Acid Isomers in Sprague-Dawley Rats Following a Single Dose

3.1   Introduction

Perfluorinated acids (PFAs) are now widespread contaminants of the global environment and have been detected in humans[1,2] and remote arctic wildlife[3,4]. These chemicals and their precursors (PFA-precursors) are unique in their ability to repel both oil and water and thus were used ubiquitously since the 1950s in various consumer products and for industrial surfactant and surface treatment applications. Two of the most prominent environmental PFAs, perfluorooctane sulfonate ($C_8F_{17}SO_3^-$, PFOS) and perfluorooctanoic acid ($C_7F_{15}COOH$, PFOA), have both been identified as developmental toxicants in animal models[5,6], and the latter is carcinogenic to lab rats[7]. The human and ecological risks associated with current exposure levels are not well defined, but PFAs are persistent in the environment[8,9], and those having chain lengths greater than seven carbons are bioaccumulative in wildlife[10-12]. Furthermore, PFOS and PFOA are very slowly eliminated from human blood (half-lives ~5.4 and 3.8 years, respectively)[13]. Historically, PFA production occurred by two processes: electrochemical fluorination (ECF), which yielded an impure mixture of branched

isomers and chain-length homologs, or telomerization, which yielded a relatively isomerically pure mixture of chain-length homologs (typically linear and even carbon chain lengths). Although the ECF manufacturing process was largely phased out in North America in 2002[14], major production of PFOA, longer perfluorocarboxylates, and various PFA-precursors continues today by telomerization[15]. Currently there is much debate over the global sources of PFAs, whether from ECF-based (historical, phased out in 2002) or telomerization-based (current and historical) manufacturing. One hypothesis is that the source(s) of exposure may be determined using the isomer profile in biological samples: A dominant linear signature would suggest exposure to a telomere source, whereas the presence of abundant branched isomers would suggest exposure to an ECF source[16,17]. While no evidence currently exists to support the fractionation of PFA isomers in environmental media (i.e., abiotic environments), this requires further investigation. Nonetheless, the significance of isomer signatures in biological samples remains tentative because it is unclear to what extent the various PFA isomers may be accumulated preferentially in exposed organisms. Recent advances in analytical methodology have allowed the characterization of PFA and PFA-precursor isomer patterns in humans and the environment. Perfluorooctanoic acid isomer patterns in humans[17,18], polar bears[16], and other arctic wildlife[19] are primarily (>98%) linear. In humans exposed occupationally, a predominantly linear PFOA signature was observed in serum despite the fact that exposure was likely from an ECF source[13]. Comparatively, *n*-PFOS accounts for 50 to 96% of total PFOS in humans and wildlife[18-20]. Although differences in isomer profile

74

may be attributable to the various production methods (telomer or ECF) or manufacturer[21], the historical inter-lot variability for 3M ECF PFOS was minimal, with a consistent isomer composition of 70% linear (standard deviation [SD] 1.1%) and 30% branched (SD 0.8%) in eight production lots over 10 years[22]. Likewise, 3M ECF PFOA had a consistent isomer composition of 78% linear (SD 1.2%) and 22% branched (SD 1.2%) in 18 production lots over a 20 year period, as determined by 19F nuclear magnetic resonance (NMR)[22]. Given that the length of the perfluorinated chain is known to influence PFA homolog bioaccumulation potential[8,9] and rodent toxicokinetics[23,24], we hypothesized that the three dimensional structure of the perfluorinated chain may also play a role in the relative toxicokinetics of various branched PFA isomers. In fact, recent rodent data[25] found some evidence that branched isomers were absorbed to a lesser extent than the linear isomer at a high dose; however, the effect was not as apparent at lower dose. Another justification for isomer specific PFA studies is that the isomers may have different toxicological profiles[26]. Furthermore, practical problems with non-isomer-specific data are that the various isomers respond differently in the mass spectrometry (MS) electrospray source[27] and total PFA analytical methods (no isomer separation) are subject to nominal mass co-elution interferences[18], both of which can result in significant analytical bias. The objective of the present study was to assess whether PFA isomer discrimination occurs *in vivo* by conducting an isomer-specific uptake, tissue distribution, and elimination study following a single low oral dose of a PFA isomer mixture. The

findings are compared to a companion subchronic feeding study with the same isomeric mixture[28], and implications for source tracking are discussed.

3.2   Materials and Methods

3.2.1   Nomenclature

In general, the structure of any given perfluorinated substance homolog may be a normal chain (linear) or a perfluoromonomethyl- or perfluorodimethyl-branched isomer (Appendix B, Figure B1). Each branched isomer was labelled arbitrarily as B_x, (where $x = 1, 2, 3$, etc., in order of increasing relative retention time from the linear isomer), except when the structure could be confirmed by authentic standards, in which case the nomenclature system employed previously[16-18] was adopted for the present study. Briefly, using PFOS as an example, the following annotations are used herein to represent the structure of each branched isomer based on the carbon position of perfluoromethyl substitution: linear   perfluorooctanesulfonate   (n-PFOS);   various perfluoromonomethyl isomers, perfluoroisopropyl (iso-PFOS), 5-perfluoromethyl (5m-PFOS), 4-perfluoromethyl (4m-PFOS), 3-perfluoromethyl (3m-PFOS), 2-perfluoromethyl (2m-PFOS), 1-perfluoromethyl (1m-PFOS); various geminal perfluorodimethyl isomers, tert perfluorobutyl (tb-PFOS), 4,4-perfluorodimethyl (4,4m2-PFOS), 3,3-perfluorodimethyl (3,3m2-PFOS), 2,2-perfluorodimethyl (2,2m2-PFOS), 1,1-perfluorodimethyl (1,1m2-PFOS).

3.2.2 Standards and Reagents

High-performance liquid chromatography (HPLC)-grade methanol and HPLC-grade methyl-*tert*-butyl ether (MTBE) were purchased from Fisher Scientific (Ottawa, ON, Canada),and HPLC-grade formic acid (50%), potassium perfluorohexane sulfonate (PFHxS, >98%), and perfluorononanoic acid (PFNA, 97%) were purchased from Sigma-Aldrich (Oakville, ON, Canada). Electrochemically fluorinated PFOS (lot 217) and PFOA (lot 332) standards were provided by 3M (St. Paul, MN, USA). Isopropyl-PFNA (*iso*-PFNA) and *n*-isomer internal standards of sodium perfluoro-1-[1,2,3,4-$^{13}C_4$]octane sulfonate (M + 4, ^{13}C-PFOS), perfluoro-*n*-[1,2,3,4,5-$^{13}C_5$]nonanoic acid (M + 5, ^{13}C-PFNA), perfluoro-*n*-[1,2,3,4-$^{13}C_4$]octanoic acid (M + 4, ^{13}C-PFOA) were obtained from Wellington Labs (Guelph, ON, Canada). Isolated and characterized standards of *iso*-, *5m*-, *4m*-, *3m*-, *1m*-, *4,4m$_2$*-, and *tb*-PFOS as well as *iso*-, *5m*-, *4m*-, *3m*-, *4,4m$_2$*-, and *tb*-PFOA were also acquired from Wellington Labs. A standard of *5,3m$_2$*- and *5,4m$_2$*-PFOA was also obtained as a mixture (3:5 ratio based on NMR).

3.2.3 Animal Husbandry and Treatment

The present study was approved by the University of Alberta Animal Policy and Welfare Committee. Male Sprague-Dawley (S-D) rats were obtained from Biosciences Animal Service (University of Alberta, Edmonton, AB, Canada). All rats were housed individually at a temperature (20–22°C) and

humidity controlled environment and were maintained on a 12-h light:dark cycle. Before and throughout the test period, standard rodent food and tap water were available ad libitum. Clean cages and environmental enrichment of polyvinyl chloride tubing and paper towel were provided on a daily basis. Prior to being tested, rats were evaluated by observation of body weight during three weeks of acclimatization. During this time, the rats were also familiarized with the restraining device and metabolic cages to minimize stress during the testing period. At routine time points over the course of the experiment, rats were placed in cylindrical polycarbonate metabolic cages with mesh bottoms (30 cm x 22 cm) for less than 24 h to obtain urine samples free from fecal contamination. Prior to each use, metabolic cages were rinsed with methanol, soap and tap water, and reverse-osmosis water and then air dried. Nine male S-D rats were randomly divided into control ($n = 2$) and treated ($n = 7$) groups. Three of the treated rats and a single control (group 1) were placed into metabolic cages initially for collection of urine and feces and then killed on day 3 to assess uptake into tissues. The other four treated rats and a single control (group 2) were followed for 38 d by intermittent tail-vein sampling and intermittent urine and feces collection in metabolic cages. On day 38, all rats were killed, and tissues were collected.

3.2.4 Test Material Administration

At the time of dosing, rats appeared healthy and weighed an average of 429 g (402–449 g). Individual dose volumes containing PFOS, PFOA, PFNA, and

PFHxS in reverse-osmosis water were adjusted to body weight measured prior to dosing; thus each animal received 1.4 to 1.5 ml of a dose by oral gavage. Control rats were administered reverse-osmosis water only. The average administered dose was 400 µg/kg PFOS (270 µg/kg n-PFOS), 500 µg/kg PFOA (400 µg/kg n-PFOA), and 390 µg/kg PFNA (200 µg/kg n-PFNA and 190 µg/kg iso-PFNA). The PFHxS isomers were present as impurities in the PFOS standard, and the resulting dose was 30 µg/kg, an order of magnitude lower than that for the other test substances. The identical standards of electrochemical PFOS, PFOA, and iso-PFNA were also used in Part 2 of the present study[28]. On the basis of a previously reported ^{19}F NMR analysis, the isomer composition of electrochemical PFOS manufactured by 3M was 70 to 75% n-PFOS, 9 to 11% iso-PFOS, 14.2 to 18.6 % xm-PFOS (where x = 1–5), 0.15 to 1.2% x, ym_2-PFOS (where x, y = 1–4), and 0.2% tb-PFOS[22,29,30]. By both ^{19}F and ^{1}H NMR, PFOA manufactured by 3M consisted of 78% n-PFOA, 12.5% xm-PFOA (where x = 3–5), 9% iso-PFOA, 0.1% x,xm_2-PFOA (x = 2–4), 0.2% tb-PFOA branched isomers, and 0.1% $2m$-PFOA[22]. Several considerations were made in selecting the dose level because Loveless et al.[25] recently demonstrated that n-PFOA was preferentially absorbed relative to branched isomers with increasing dose in both rats and mice, and other authors have shown dose-dependent toxicokinetics for PFAs[31]. The administered dose had to be high enough to result in blood concentrations that would be quantifiable over 38 d but conversely be below any known toxicological threshold (less than no-observed-effect level [NOEL]) and otherwise as low as possible to avoid saturating uptake, distribution, or elimination pathways. There were no

NOEL values from low single-dose studies with which to compare; thus we relied on subchronic repeated dosing data as a conservative estimate. Perkins et al.[32] determined a 13-week dietary NOEL of 1,000 µg/kg/d for PFOA in male S-D rats, and Seacat et al.[33] determined a 14-week dietary NOEL of 370 µg/kg/d for PFOS in male S-D rats. More recently, Loveless et al.[25] conducted a 14-d oral PFOA toxicity experiment on male S-D rats and determined the lowest observed effect level to be their lowest dose (300 µg/kg/d), which is lower than the NOEL established by Perkins et al.[32]. We therefore felt confident that a single dose of 500 µg/kg for each PFA would be well below any threshold, even considering the potential for additive effects in this mixture.

3.2.5 Body Weight and Liver Somatic Index

No adverse effects were expected, but animals were closely monitored for clinical signs of toxicity, including decreases in body weight and food consumption throughout the study. Liver somatic index was also determined at the time of death (Appendix B, Table B1).

3.2.6 Collection and Treatment of Samples

Urine samples collected in 250-ml polycarbonate beakers inside the metabolic cages were transferred to 50- or 15-ml polypropylene centrifuge tubes (Corning, New York, NY, USA). Feces samples were manually collected from conventional and metabolic cages using tweezers and stored in 50 or 15 ml

polypropylene centrifuge tubes. For tracking blood elimination kinetics, small volumes of blood (1% of total circulating blood per 24 h) were collected from rats by placing them in a restraining device and drawing a sample through the lateral tail vein with a 1-ml plastic syringe and a 1.27-cm, 26-gauge needle (BD Biosciences, Mississauga, ON, Canada). Blood was immediately ejected into a pre-weighed 15-ml Vacutainer® tube (BD Biosciences) coated with lithium heparin. Large volumes of blood were collected by cardiac puncture, after euthanizing with CO_2, using 10-ml plastic syringes equipped with 1.27-cm, 18-gauge needles. Blood sampling time points are shown in Appendix B, Figures B2 to B5. Tissues were also collected at this time in 15 or 50 ml polypropylene centrifuge tubes. All samples were stored at less than -20°C prior to analysis.

3.2.7 PFA Extraction Procedures

All samples were extracted using an established ion-pairing method[34]. The effectiveness of this method for the extraction of individual isomers of PFOS, PFOA, and PFNA was determined through extraction efficiency and spike/recovery experiments. For small-volume tail-vein blood samples, extractions were performed directly in the Vacutainer tubes (BD Biosciences) used for collection, whereas for large-volume blood and urine samples 1 ml was transferred to a 15-ml polypropylene centrifuge tube. For tissues and feces, reverse-osmosis water was added to 1 g (5:1 ratio), the sample was homogenized using a Tissue-Tearor® (BioSpec Products, Bartlesville, OK, USA), and 1 ml of

the resulting homogenate was transferred to a centrifuge tube. All samples were spiked with 10 μl of an internal standard mixture in methanol containing 10 ng each of ^{13}C-PFOS, ^{13}C-PFOA, and ^{13}C-PFNA. Then 1 ml of 0.5 M tetrabutyl ammonium hydrogen sulphate (adjusted to pH 10 with NaOH) and 2 ml of 0.25 M carbonate buffer were added, and the resulting solution was mixed by shaking for 5 min. For extraction, 5 ml of MTBE was added to each tube, the tube was shaken vigorously by hand for 10 min and centrifuged at 2,600 g for 5 min, and the organic phase transferred to a clean 15-ml centrifuge tube. The extraction was repeated twice more, and all supernatants were combined. The solvent extract was reduced to near dryness using a gentle flow of nitrogen and allowed to air-dry at which point the extract was reconstituted in 0.5 ml of methanol, vortexed, and centrifuged again at 2,600 g for 5 min. A portion of the supernatant (450 μl) was transferred to a polypropylene microvial and sealed with a polyethylene cap for instrumental analysis. On the basis of previous findings suggesting that PFAs are not substrates for glucuronidation[35] urine was not subjected to hydrolysis.

3.2.8 Instrumental Analysis of Samples and Gavage Solution

Samples of the gavage solution were measured by HPLCMS/MS using a total PFA quantification method [18]. Briefly, 10 μl of sample was injected onto an Agilent (Mississauga, ON, Canada) Zorbax C_8 3.5-μm (2.1 mm x 5 cm) column equipped with an Agilent Eclipse C_8 guard column (4.6 mm x 12.5 mm) using a gradient elution program with 5 mM ammonium acetate and 100% methanol at a

flow rate of 180 µl/min. The elution program was set initially at 20% methanol, followed immediately by a 1 min linear ramp to 70% methanol, then to 100% by 12.5 min. The column was held at 100% methanol for 7.5 min, returned to initial conditions by 21 min, and allowed to equilibrate for 20 min prior to the next run. Mass spectral data were collected using the same instrumentation as in isomer-specific profiling, as described in the next paragraph, except that only two MS/MS transitions were monitored for each analyte. Isomer profiling and quantification of n-PFOS, n-PFOA, n-PFNA, and iso-PFNA (to which pure standards were available) in samples and gavage solution were achieved using a previously developed HPLC-MS/MS isomer separation method[18] using an Agilent 1100 high-performance liquid chromatograph and a FluoroSep RP Octyl column (3µ, 100A, 15cm x 2.1mm, ES Industries, West Berlin, NJ, USA). The method was shortened to 90 min for the four PFAs examined, and smaller injection volumes (10 µl) were used to minimize column deterioration. Gradient elution conditions were 200 µl/min, and starting conditions were 50% A (water adjusted to pH 4.0 with ammonium formate):50% B (100% methanol). Initial conditions were held for 0.3 min, ramped to 64% B by 1.9 min, increased to 66% B by 5.9 min, 70% B by 7.9 min,78% B by 40 min, 88% B by 42 min, 100% B by 55 min, returning to initial conditions by 60 min and allowing 30 min for equilibration. Mass spectral data were collected using a hybrid triple-quadrupole linear ion trap mass spectrometer (4000 Q TRAP®, MDS Sciex, Concord, ON, Canada) equipped with an electrospray interface operating in negative mode. Chromatograms were recorded by multiple reaction monitoring.

83

3.2.9 Statistical Analysis of Isomer Disposition

A major objective was to compare the blood elimination kinetics among all isomers of each PFA. Group 1 rats were moved because too few time points were available to include in the statistical analysis; thus all blood kinetics are based on group 2 rats, which were monitored for 38 d (four animals). Tail-vein blood concentrations were corrected for growth dilution by determining the percent increase in body weight at each sampling interval, relative to $t = 0$, after fitting growth data to the exponential rate equation: body weight $= a \cdot \exp(g \cdot t)$, where a was a constant, g was the growth rate, and t was time. To determine if statistical differences existed among the isomer depuration rate constants for each PFA ($\alpha = 0.05$), we modeled the relationship between time and natural log (ln)concentration using PROC MIXED (SAS®, version 9.1; SAS Institute, Cary, NC, USA), allowing intercepts and slopes to vary by rat. We used Akaike information criterion values to determine the most appropriate covariance structure for the variance–covariance G matrix and used Kenward-Roger adjusted degrees of freedom. To test the overall null hypothesis that all isomer depuration rate constants for one PFA were equal, we created interaction terms between the indicator variable for each isomer and time and tested contrasts to determine if the interactions were significantly different from zero. For PFOS, PFOA, and PFNA, random effects were included in the models; however, for PFHxS the variance estimates for the random effects of the intercepts and slopes were equal to zero, and the model fit was improved upon removing them; therefore, the final model for PFHxS did not include random effects. To test for significant differences

between individual isomers of each PFA, we constructed *post-hoc* pairwise comparisons. We adjusted the significance level using the Bonferroni correction, which accounts for the number of pairwise comparisons made; therefore, the significance levels were as follows: PFNA, $\alpha = 0.05$; PFOS, $\alpha = 0.0011$; PFOA, $\alpha = 0.0014$; PFHxS, $\alpha = 0.017$.With the exception of *n*-PFOS, *n*-PFOA, *iso*-PFNA, and *n*-PFNA, pure authentic standards of the isomers were not available at the onset of the present work; thus to facilitate a comparison of oral absorption and elimination efficiencies among the various isomers, we calculated relative uptake and elimination coefficients for each isomer. In the present study, the relative extent of oral absorption was defined by comparing the isomer profile in the gavage dose solution to the isomer profile in day 1 blood and by normalizing each to the response of the linear isomer. Specifically, the uptake coefficient (C_u) was calculated by dividing the response of a given branched isomer (B_x), relative to the *n*-isomer in day 1 blood by the corresponding relative response in the gavage dose (Eqn. 1).

$$C_u = \frac{B_{x(\text{blood})}/n_{(\text{blood})}}{B_{x(\text{dose})}/n_{(\text{dose})}} \qquad (1)$$

The resulting coefficients are arbitrary numbers but can be compared in relative terms. Thus, $C_u > 1$ implies preferential uptake of a given branched isomer relative to the *n*-isomer on day 1, and vice versa. To gauge the relative extent of

85

elimination in urine, an elimination coefficient ($C_{e\text{-}urine}$) was calculated using day 3 blood and day 3 urine (Eqn. 2).

$$C_{e\text{-}urine} = \frac{B_{x(urine)}/n_{(urine)}}{B_{x(blood)}/n_{(blood)}} \qquad (2)$$

Thus, $C_{e\text{-}urine} > 1$ implies enrichment of a branched isomer in urine relative to the n-isomer on day 3, whereas $C_{e\text{-}urine} < 1$ implies enrichment of the linear isomer. Similarly, to gauge the relative extent of elimination in feces, an elimination coefficient ($C_{e\text{-}feces}$) was also calculated from day 3 blood and day 3 feces data (Eqn. 3).

$$C_{e\text{-}feces} = \frac{B_{x(feces)}/n_{(feces)}}{B_{x(blood)}/n_{(blood)}} \qquad (3)$$

To examine relative tissue distribution, the isomer profiles in tissues were reported as a percent of total response relative to the corresponding n-isomer. Because the MS/MS transitions chosen for each isomer were arbitrary yet consistent from tissue to tissue, the profiles were not an indication of absolute quantity but enabled a relative comparison of one tissue to the next and examination of how the profiles changed over time. The concentrations of n-PFOS, n-PFOA, *iso*-PFNA, and n-PFNA were determined using the available authentic standards. To examine for potential pseudo elimination pathways,

apparent tissue half-lives were also estimated based on two time points (day 3 and day 38, $n = 6$) using Microsoft Excel™ (Redmond, WA, USA) linear regression; we could not confirm that the data fit a first-order loss model.

3.2.10 Analytical Quality Control

For spike/recovery experiments, 100 ng of each test substance was spiked into 0.1 or 1 ml of control blood or 1 ml of tissue, urine, or feces homogenate, and the solution was vortexed and allowed to equilibrate overnight. The samples were then extracted and quantified using the previously described methods, and internal-standard-corrected recovery was calculated relative to a standard spiked directly into methanol. Extraction efficiency experiments were conducted with blood, urine, feces, or tissues from a dosed rat using the previously described extraction method but with one additional step. After the third extraction, a fourth aliquot of MTBE was added to the homogenate and extracted once more. This final extract was analyzed separately to examine for any residual isomer signal, and extraction efficiency was calculated as a percent of the total response in this and the first three combined extracts.

3.3 Results and Discussion

3.3.1 Analytical Quality Control

Isomer patterns were generally conserved among the various spiked blood, tissue, urine, and feces matrices, and recoveries were acceptable (Appendix B,

Table B2). The lowest recoveries were observed for PFHxS isomers in brain (37–50%), fat, (38–50%) intestine (24–30%), and heart (15–19%); however, the recovery values were fairly consistent among each PFHxS isomer; thus the relative isomer profile was largely unaltered. PFOS was also difficult to recover from these few tissues, but recovery values were again consistent among each PFOS isomer, and thus the relative isomer profile was largely unaltered. Recoveries for PFOA and PFNA were good for all isomers in all matrices. Examination of the fourth MTBE extract (extraction efficiency experiments, Appendix B, Table B2) showed little or no PFAs; thus extractions were quantitative. In control rats, n-PFOA (1 ng/ml) and PFOS isomers (n-PFOS at 2 ng/ml) were detectable in 1 ml terminal blood samples, whereas PFNA and branched PFOA isomers were absent in control blood throughout the experiment. The n-PFHxS was also present in the blood of controls, albeit three orders of magnitude lower than that in treated animals on day 3. These concentrations were over two orders of magnitude lower than those in control rats from a previous study[25]. In control rat livers, n-PFNA (20 ng/g) and PFOS isomers (n-PFOS at 70 ng/g) were the only PFAs detected. These concentrations seemed relatively high, and it is unclear what the source(s) of exposure are; however, these are two orders of magnitude lower than those in dosed animals on day 38. De Silva et al[28] identified a small amount of PFA contamination in control feed, and while this may be a source of exposure for control rats, we did not investigate feed concentrations in the present study. No PFAs were detected in urine or feces of control animals.

3.3.2 Disposition of PFOA Isomers

An average administered dose of 500 µg/kg PFOA (400 µg/kg n-PFOA) resulted in a mean blood concentration of 1.1 µg/ml n-PFOA at 24 h. Visual inspection of isomer profiles (Figure 3.1) suggested preferential uptake of n-PFOA in the blood, and this was supported by C_u values (Table 3.1) below 1 for most branched PFOA isomers (range 0.43 ± 0.07 to 0.88 ± 0.03 for tb- and $3m$-PFOA, respectively) with the exception of B$_8$-PFOA (1.96 ± 0.76, tentatively assigned as 3,3m_2-PFOA based on its unique m/z 319 product ion (Appendix B, Figure B6). Although elimination prior to the first sampling point may have somewhat influenced the uptake profiles of short-lived isomers such as 4,4m_2-PFOA ($t_{1/2}$ = 1.28 d, C_u= 0.74 ± 0.21), there was no consistent trend between C_u and k_d (Appendix B, Figure B7); thus the 24-h blood isomer profiles were primarily indicative of uptake. In general, uptake profiles were similar between group 1 and 2 rats with the exception of a single rat from group 1 that absorbed branched PFOA and PFOS isomers to a much greater extent than all other animals. It is unclear what factor(s) may have contributed to this, particularly because it was not observed for PFNA or PFHxS in the same animal.
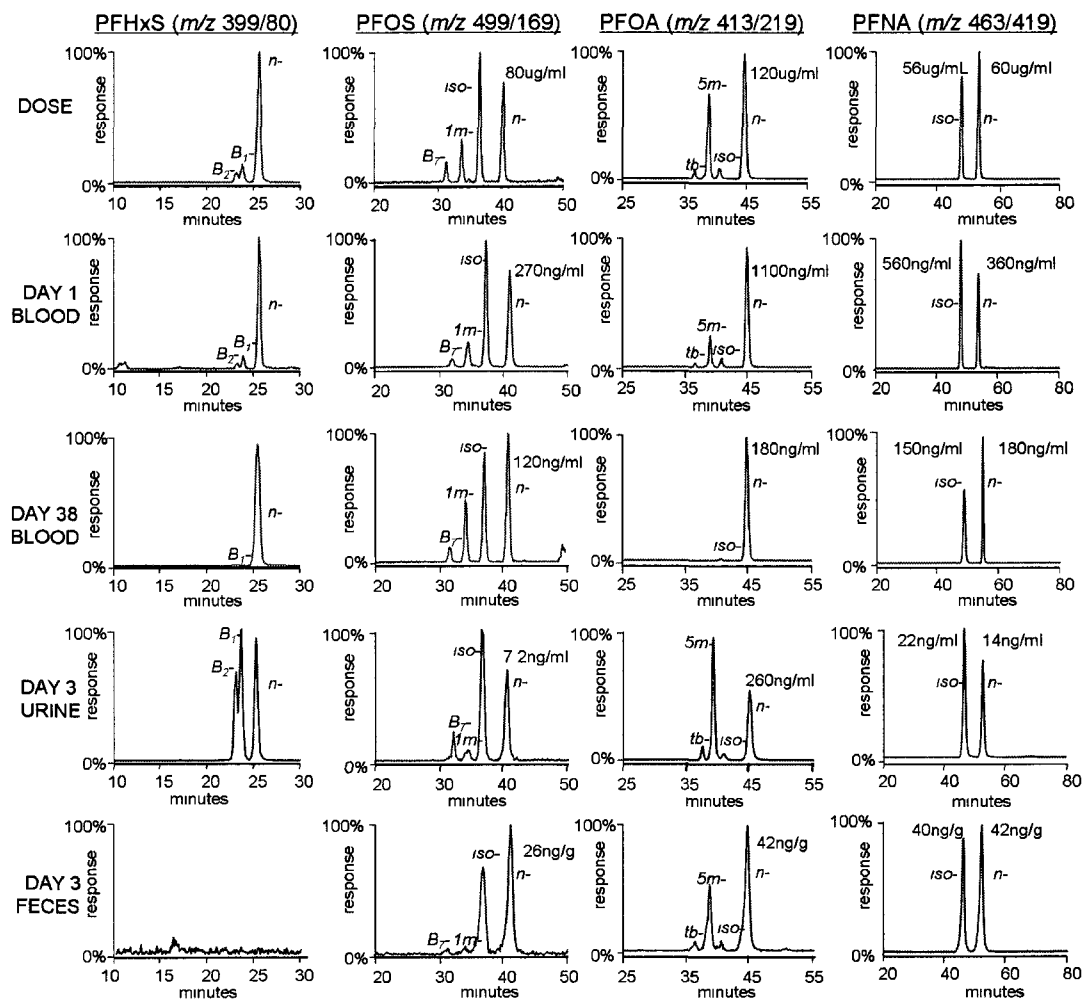
Figure 3.1 Representative chromatograms showing isomer profile in the dose (top row), day 1 blood (second row), day 38 blood (third row), urine (fourth row) and feces (bottom row) for perfluorohexane sulfonate (PFHxS) (*m/z* 399/80, far left), perfluorooctane sulfonate (PFOS) (*m/z* 499/169, middle left), perfluorooctanoic acid (PFOA) (*m/z* 413/219, middle right), perfluorononanoic acid (PFNA) (*m/z* 463/419, far right). Chromatogram response was normalized to the largest peak, and values shown represent the concentration of linear isomer (ng/ml for dose, blood, urine and ng/g for feces). Not every isomer could be shown in each chromatogram.

Table 3.1. Dose-day 1 blood uptake coefficient (C_u), blood depuration rate constants (k_d), blood depuration half-lives $(t_{1/2})$, day 3 blood-urine elimination coefficient $(C_{e\text{-}urine})$, and day 3 blood-feces elimination coefficient $(C_{e\text{-}feces})$ for perfluorohexane sulfonate (PFHxS) perfluorooctane sulfonate (PFOS), and perfluorooctanoic acid (PFOA). For each perfluorinated acid (PFA), error represents ± standard error about the mean (SE), with the exception of depuration coefficient, where 95% confidence intervals (CI) are shown

PFA Isomer (product ion)	C_u ±SE	$-k_d \times 10^{-3}$ (d⁻¹) (95% CI)	$t_{1/2}$ (d)	$C_{e\text{-}urine}$ ±SE	$C_{e\text{-}feces}$ ±SE
PFHxS					
n (99)	1.00	43.0 (22.0-63.0)	15.9	1.00	-
B_1 (169)	0.70 ± 0.04	98.0 (46.0-142)	7.10	13.2 ± 0.54	-
B_2 (99)	0.75 ± 0.05	190 (121-253)	3.60	17.9 ± 2.33	-
PFOS					
n (80)	1.00	20.6 (1.78-39.4)	33.7	1.00	1.00
iso (80)	1.26 ± 0.08	29.6 (10.8-48.3)	23.4	1.71 ± 0.23	0.85 ± 0.11
$5m$ (130)	1.92 ± 0.08	28.4 (9.92-46.8)	24.4	1.66 ± 0.20	0.45 ± 0.10
$4m$ (330)	0.71 ± 0.10	30.0 (9.41-50.5)	23.1	3.95 ± 0.61	-
$3m$ (130)	0.77 ± 0.37	20.5 (0.16-41.1)	33.8	3.74 ± 0.33	-
$1m$ (419)	5.93 ± 1.84	6.8 (11.9-25.6)	102	0.14 ± 0.02	-
tb (130)	0.24 ± 0.07	35.3 (7.96-62.6)	19.6	6.76 ± 3.47	-
B_7 (169)	4.80 ± 1.54	45.0 (17.9-72.0)	15.4	1.14 ± 0.40	-
B_8 (130)	2.23 ± 0.59	61.6 (37.4-85.8)	11.3	11.7 ± 4.07	-
B_9 (419)	17.5 ± 6.04	62.7 (32.1-93.2)	11.1	-	-
PFOA					
n (369)	1.00	51.9 (7.99-95.8)	13.4	1.00	1.00
iso (369)	0.88 ± 0.02	85.9 (41.7-129)	8.11	1.35 ± 0.27	0.85 ± 0.20
$4m$ (119)	0.51 ± 0.05	160 (117-204)	4.32	4.48 ± 1.04	2.71 ± 0.71
$5m$ (219)	0.64 ± 0.04	176 (125-227)	3.95	7.52 ± 2.00	1.91 ± 0.27
$3m$ (169)	0.88 ± 0.03	111 (67.3-154)	6.26	2.51 ± 0.51	1.09 ± 0.14
tb (219)	0.43 ± 0.07	309 (196-420)	2.25	15.2 ± 6.02	7.46 ± 4.39
$5,3 / 5,4m_2$ (169)	0.60 ± 0.13	387 (248-527)	1.79	13.9 ± 6.04	5.50 ± 1.74
$4,4m_2$ (269)	0.74 ± 0.21	542 (238-1320)	1.28	26.9 ± 14.1	-
B_8 (319)	1.96 ± 0.76	76.2 (32.4-120)	9.10	0.69 ± 0.30	-

Plots of PFOA isomer depuration from blood (Appendix B, Figure B2) and blood isomer profiles on day 1 and 38 (Figure 3.1) show clear differences in the elimination of PFOA isomers. This is supported by statistical analysis indicating a significant difference among the isomer-specific k_d's overall ($p<0.0001$), and pairwise analysis indicated where these differences lay (Appendix B, Figure B8). Linear PFOA was the most persistent of the PFOA isomers, with a depuration rate constant of -51.9 x 10^{-3} d^{-1}, corresponding to a half-life of 13.4 d. These values were statistically different from all branched PFOA isomers with the exception of *iso*-, 4,4m_2- and B_8-PFOA (Appendix B, Figure B8). With the exception of 3*m*-PFOA ($t_{1/2}$= 6.26 d) and B_8-PFOA ($t_{1/2}$ = 9.10 d), longer blood half-lives were correlated with decreasing elution time on the perfluorooctyl HPLC column (r^2=0.98, Figure 3.2), ranging from 1.28 d (4,4m_2) to 8.11 d (*iso*-PFOA). This finding suggested that the extent of intermolecular interaction with the linear perfluorooctyl stationary phase, and hence degree of branching and branching location, was correlated with biological persistence. Comparatively, in Part 2 of the present study[28], the blood depuration half-life for *n*-PFOA was 9.1 d, with other identified isomers ranging from 2.7 (PFOA-7) to 6.3 d (*iso*-PFOA). Curiously, in Part 2[28] two minor unidentified PFOA isomers had half-lives longer than that of the linear isomer (PFOA-6, 21.2 d, and PFOA-8,16.0 d); however, these were presumably not detectable by HPLC-MS/MS in the current work.
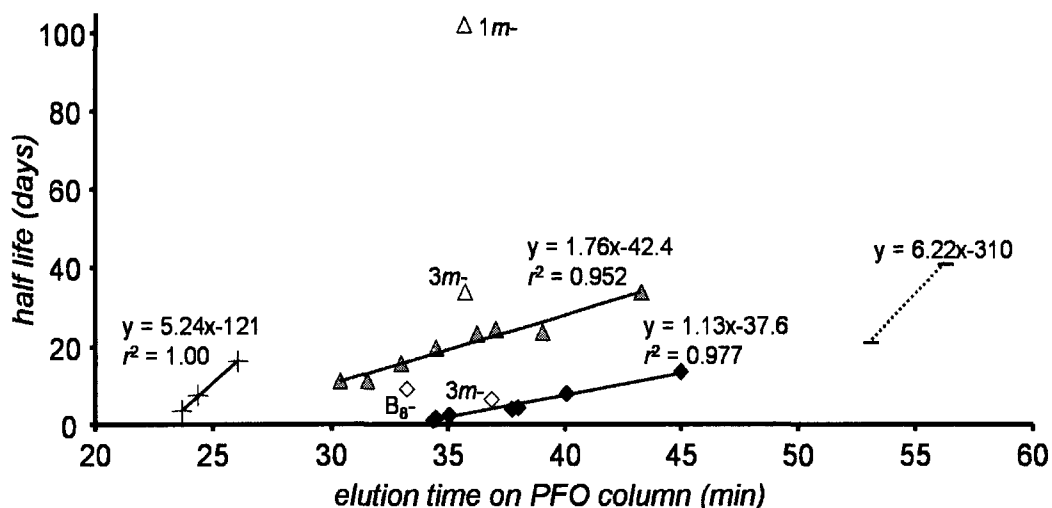
Figure 3.2 Association between half-life (d) versus elution time on the perfluorooctyl column (min) for perfluorohexane sulfonate, (PFHxS, +), perfluorooctane sulfonate (PFOS, ▲), perfluorooctanoic acid (PFOA, ♦) and perfluorononanoic acid (PFNA, -). For PFOS and PFOA, two outliers were removed (hollow triangles and diamonds, respectively). Excellent correlation was observed between elution time, and blood elimination half-life.

The anomalous elution order and half-life behavior of B_8-PFOA and $3m$-PFOA (Figure 3.2), compared to those of other PFOA isomers, are similar to those observed for PFOS, whereby $1m$-PFOS and $3m$-PFOS did not fit the trend of decreasing half-life with decreasing elution time and also had a large spread in 95% confidence intervals compared to other PFOS isomers. It is reasonable to hypothesize that perfluoromethyl groups immediately adjacent (alpha) to the SO_3^- group may act sterically to influence biological handling, for example by shielding the hydrophilic end of the molecule. However, it is unclear why branching at the β-position of PFOA ($3m$-PFOA) and γ-position of PFOS ($3m$-PFOS) increased persistence for both these PFAs.

The half-life of *n*-PFOA (13.4 d) in the present work was very similar to that determined by Vanden Heuvel et al.[36] (15 d) for male rats following intraperitoneal (i.p.) administration and longer than that reported in Ohmori et al.[23] (5.6d) for male rats following intravascular (i.v.) administration. It is unclear what contributed to the short half-life in the latter study. While route of administration may have affected the relative extent of absorption, it is unclear how this contributes to differences in half life once the dose has reached systemic circulation. Dosing concentration may also have played a role to some extent, but this requires further investigation.

The tissue PFOA isomer profile for treated animals was fairly consistent, with the linear isomer being dominant in all samples at all times. Total PFOA concentrations in tissues (Figure 3.3) decreased in the following order: liver > blood > kidneys > lungs > heart > testes > spleen > fat > intestines > muscle > brain. This was consistent with the tissue distribution in S-D rats reported by Vanden Heuvel et al.[36] in which PFOA concentrations decreased in the order: liver > plasma > kidney > lung > erythrocytes > skin > spleen > bone marrow > subcutaneous fat > muscle > brain > abdominal fat. Tissue half-lives were either similar to or less than those calculated for blood (Appendix B, Table B3), suggesting that there was no significant pseudo-elimination of isomers into deep-storage tissue compartments. This result is consistent with the findings of Vanden Heuvel et al., who also observed no difference for PFOA elimination from blood or tissues [36].
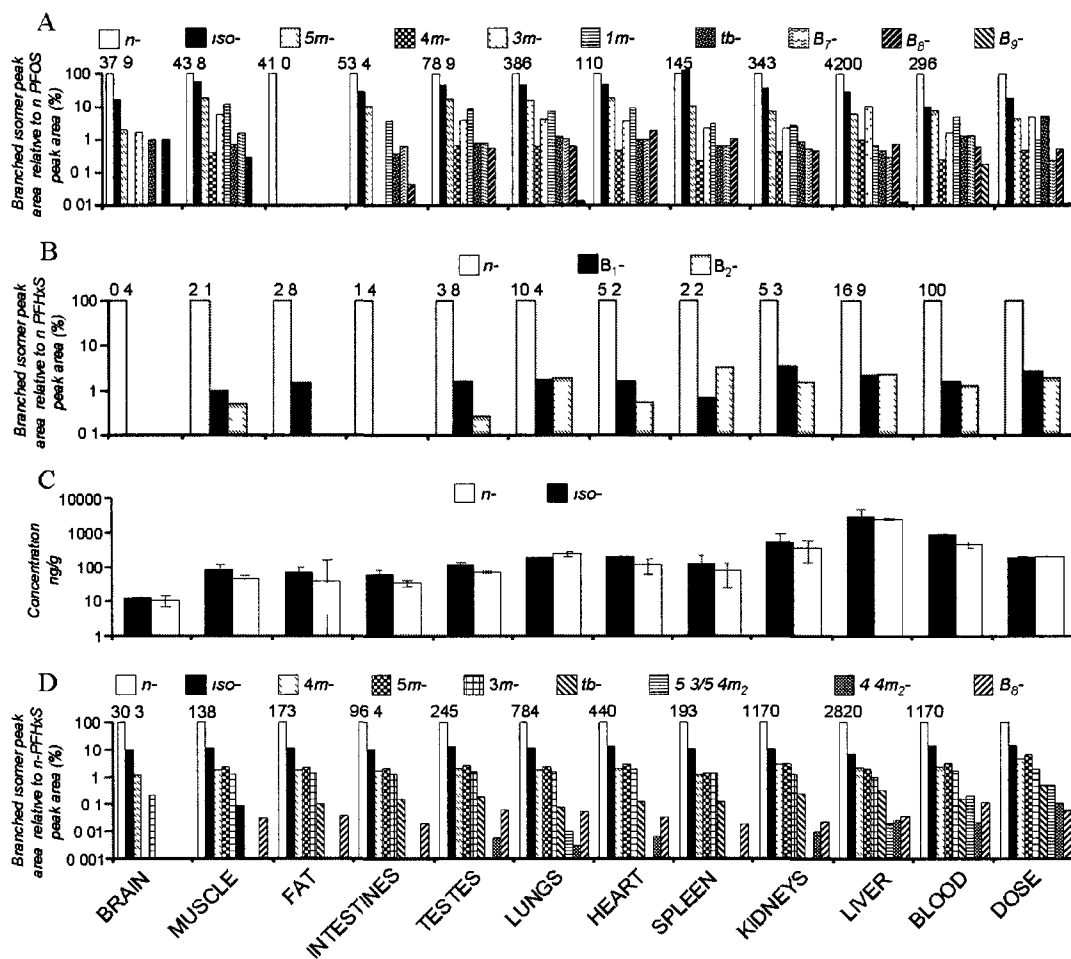
Figure 3.3 Day 3 tissue distribution (n=3) for (A) perfluorooctane sulfonate (PFOS), (B) perfluorohexane sulfonate (PFHxS), (C) perfluorononanoic acid (PFNA), and (D) perfluorooctanoic acid (PFOA). Y-axis were normalized to the response of the n-isomer (PFOS, PFHxS, PFOA), with the exception of PFNA in which concentrations (ng/ml) are given. Values shown represent the concentration (ng/ml) of n-isomer (PFOS, PFOA) or % response relative to the n-isomer in day 3 blood (PFHxS). Error bars for PFNA represent ± standard error about the mean.

Because isomer half lives in tissues were consistently less than in blood, the PFOA isomer profiles in urine and feces must have represented the dominant pathways of elimination from blood. Throughout the experiment, the mean concentration of n-PFOA in feces of dosed rats (28 ± 9 ng/g, day 3) was consistently less than in urine (265 ± 60 ng/ml, day 3). Using an estimated

excretion rate of 23 ml urine/d and 12 g feces/d, based on the average mass of samples collected in the present study, these concentrations represent daily elimination of 340 ng n-PFOA in feces and 6,200 ng n-PFOA in the urine for day 3; that is, approximately 95% of all excreted n-PFOA occurred via urine on day 3. Throughout the elimination period, 91 to 96% of daily excreted n-PFOA was in the urine with the exception of the first 24 h, in which only 65% of excreted n-PFOA was in urine. It is most likely that the increased concentrations in the feces in the first 24 h represented the non-absorbed fraction of the gavage dose. The observation of preferential excretion of PFOA in urine is consistent with previous studies which have shown urine to be the primary route of elimination of PFOA in male rats[24].

Isomer profiles in urine were examined to further determine whether a correlation could be observed with blood depuration half lives. With the exception of B_8 (tentatively 3,3m_2)-PFOA, all branched PFOA isomers were preferentially excreted relative to n-PFOA ($C_{e\text{-}urine} > 1$, Table 3.1), and a strong correlation ($r^2=0.97$) was observed between increasing $C_{e\text{-}urine}$ and decreasing blood depuration rate constants (Figure 3.4), indicating that this was not only the dominant pathway, but that it was a pathway controlling isomer specific elimination. No apparent correlation existed between C_u and $C_{e\text{-}urine}$ (Appendix B, Figure B9), suggesting that isomer-specific uptake and elimination operated under separate mechanisms.
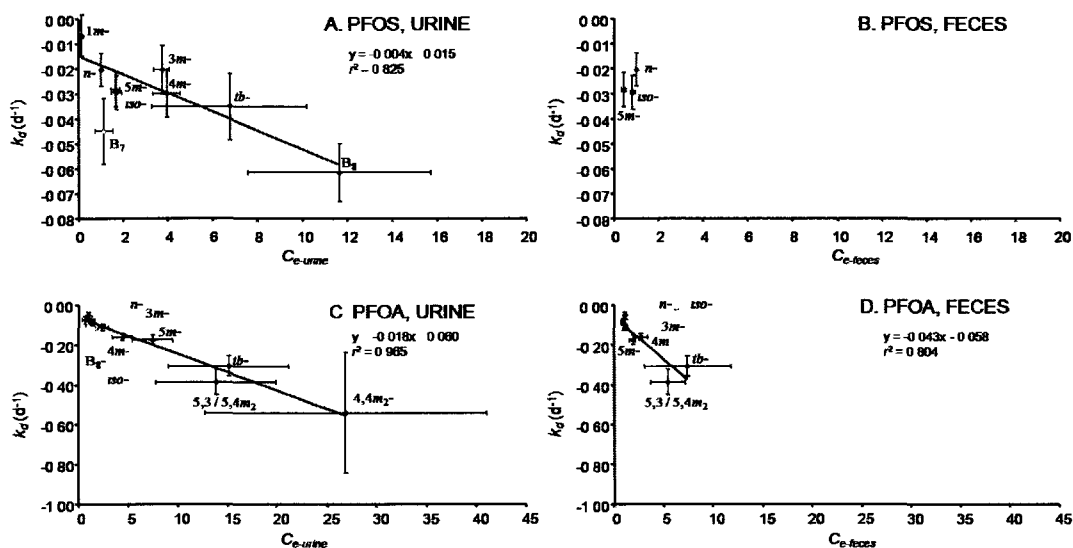
Figure 3.4 Blood depuration coefficient (k_d, d^{-1}) versus day 3 blood-urine elimination coefficient ($C_{e\text{-}urine}$) for (A) perfluorooctane sulfonate (PFOS) and (C) perfluorooctanoic acid (PFOA); and k_d (d^{-1}) versus day 3 blood-feces elimination coefficient ($C_{e\text{-}feces}$) for (B) PFOS and (D) PFOA.

The mechanism of PFOA urinary elimination was hypothesized to be mediated in part by the renal organic anion transporter system, including organic anion transporter polypeptide1 (OATP1) and organic anion transporter 3 (OAT3) [37]. However, it is not clear whether individual branched PFOA isomers have differential affinities to these transporters or whether some branched isomers have lower affinities for serum proteins, thereby possibly allowing branched PFOA to more efficiently undergo glomerular filtration and thus be eliminated more rapidly. We are currently investigating the abilities of PFOA isomers to differentially bind to transporters and serum proteins.

In feces, $4,4m_2$- and B_8 (tentatively $3,3m_2$)-PFOA were not observed, tb-PFOA was observed only until day 3, $5m$- and $3m$-PFOA were observed only

until day 5, and 4*m*-PFOA was observed only until day 10, whereas *iso*- and *n*-PFOA were observed throughout the 38-d elimination period. As in urine, PFOA isomer profiles in feces on day 3 were enriched in branched isomers, relative to *n*-PFOA, as reflected by $C_{e\text{-}feces} > 1$ for most branched isomers. When $C_{e\text{-}feces}$ values were plotted versus blood depuration rate constants (Figure 3.4), a correlation (r^2 = 0.80) was observed whereby smaller k_d values corresponded to increased $C_{e\text{-}feces}$ values, albeit to a lesser extent than in urine and with the exception that *iso*-PFOA had a $C_{e\text{-}feces}$ value below one.

3.3.3 Disposition of PFNA Isomers

For PFNA, pairwise analysis indicated that there was a significant difference between isomer-specific k_d's ($p=0.0025$) of the linear and isopropyl isomers. The PFNA isomer profiles in the dose and in blood (Figure 3.1) and plots of depuration in blood (Appendix B, Figure B-3) suggested both preferential uptake and elimination of *iso*-PFNA. Indeed, treated rats received nearly equal doses of *n*-PFNA (200 µg/kg body wt) and *iso*-PFNA (190 µg/kg body wt) by gavage, yet after 24 h the average concentration of PFNA in blood of all treated animals ($n=7$) was 350 ng/ml *n*-PFNA and 570 ng/ml *iso*-PFNA (Table 3.2). The half-life of *n*-PFNA determined here (40.6 d) was shorter than in Part 2 of the present study (47.5 d)[28] but larger than that determined by Ohmori et al.[23] (29.5 d) in male Wistar rats following i.v. administration at a much higher dose (22.5 mg/kg). Both dosing level and route of administration may play a role in explaining these differences. The half-life of *iso*-PFNA determined here (20.7 d)

was also shorter than that observed in the subchronic dosing experiment ($t_{1/2}$ = 32.1 d)[28]. It is possible that as the internal dose decreased preferential elimination of *iso*-PFNA was enhanced. The preferential uptake and elimination of *iso*-PFNA observed here can also explain the results of the subchronic dosing experiment[28], in which PFNA isomers had approximately equal blood concentrations (~1.5μg/ml) after 72 d of dosing in the feed, despite the fact that *iso*-PFNA was eliminated faster than *n*-PFNA. Thus, any preferential elimination of *iso*-PFNA occurring over the uptake period in the subchronic dosing experiment was offset by its preferential absorption.

With the exception of lungs, which were slightly enriched in *n*-PFNA (albeit non statistically significant), tissues showed either equivalent or isopropyl-dominant PFNA profiles on day 3 (Figure 3.3). Maximum concentrations were found in the liver (2,300 ng/g and 2,700 ng/g for *n*-PFNA and *iso*-PFNA, respectively) followed by kidney > lungs > heart > spleen > testes > muscle > fat > intestines > brain. Isopropyl- and *n*-PFNA followed the same relative order of decreasing concentration in tissues with the exception that heart had a higher concentration of *iso*-PFNA than lung. Depuration rates from tissues (Appendix B, Table B3) were consistently faster than those from blood for *n*-PFNA, suggesting that pseudo-elimination to tissues was not occurring. Similarly, depuration rates from tissues (Appendix B, Table B3) for *iso*-PFNA were approximately the same or faster than those from the blood for *iso*-PFNA, with the exception of lungs, where in elimination was significantly slower compared to blood. Presumably as a result of the more rapid elimination of *iso*-PFNA from blood, the isomer profile in

tissues slowly shifted toward a dominant linear signature. For example, on day 3 the percent compositions of *iso*-PFNA were 54 and 60% of total PFNA in liver and kidneys, respectively, whereas on day 38 the composition had shifted to 35 and 44% *iso*-PFNA, respectively. In the subchronic dosing experiment [28], PFNA isomer profiles in liver and kidney after 35 d of exposure were also *n* dominant, suggesting that preferential elimination of *iso*- PFNA from tissues (rather than its preferential absorption) plays a greater role in determining isomer patterns at steady state.

Unlike PFOA and PFHxS, which were eliminated primarily in the urine, urinary PFNA accounted for only 32 and 35% of the average total daily excreted *n*-PFNA and *iso*-PFNA, respectively, throughout the entire elimination period, with the remainder in feces. Consistent with its shorter blood half-life, *iso*-PFNA was enriched in both the urine (63 ± 1% of total PFNA) and feces (57 ± 3% of total PFNA) throughout the elimination period with the exception of on days 3 and 4 during which ratios were approximately equal in feces. The observation of preferential PFNA elimination in feces is consistent with previous findings following i.p. administration of a 20 mg/kg dose [24]. Interestingly, plots of ln urinary PFNA concentration versus time showed a linear and equivalent rate of decrease for both *n*-PFNA (slope = -0.03, r^2 = 0.79) and *iso*-PFNA (slope = -0.03, r^2 = 0.79), while no trend was apparent in the feces (*n*-PFNA slope= 0.015 r^2 = 0.28, *iso*-PFNA slope= 0.001 r^2 = 0.0002). Despite the change of the PFNA isomer profile in blood, liver, and kidney over time, the percent isomer composition in urine and feces stayed constant throughout the entire elimination

period (Appendix B, Figure B10). This was a curious finding that we cannot explain, but it suggests that as the body burden of PFNA decreases *iso*-PFNA may have been increasingly excreted in urine relative to *n*-PFNA. Nonetheless, the results clearly demonstrate the preferential elimination of *iso*-PFNA in urine and feces at all time points and can thus explain the relative depletion of *iso*-PFNA in all rat tissue and blood samples.

Table 3.2. Mean % isomer composition of perfluorononanoic acid (PFNA) in dose, day 1 blood, and urine and feces over the course of elimination. Blood depuration rate constants (k_d) and blood depuration half-lives ($t_{1/2}$), are also shown. Error represents ± standard error about the mean (SE), with the exception of depuration coefficient, where 95% confidence intervals (CIs) are shown.

PFNA Isomer (product ion)	Dose	Day 1 Blood Composition ±SE	Urine Composition (Days 1-38) ± SE	Feces Composition (Days 1-38) ± SE	$-k_d \times 10^{-3}$ (d^{-1}) (95% CI)	$t_{1/2}$ (d)
n (219)	51%	38.8% ± 0.98	37% ± 1.0	43% ± 3.0	17 (10.5 - 23.6)	40.6
iso (219)	49%	61.2% ± 0.98	63% ± 1.0	57% ± 3.0	33 (25.4 - 41.6)	20.7

3.3.4 Disposition of PFOS Isomers

Visual comparison of dose and blood PFOS isomer profiles (Figure 3.1) and plots of average depuration from blood (Appendix B, Figure B4) suggested that both isomer-specific uptake and elimination were occurring, albeit the effect was more subtle than that for the other PFAs examined. The average PFOS dose of 400 µg/kg (270 µg/kg *n*-PFOS) resulted in an average blood concentration of 270 ng/ml (*n* = 7) *n*-PFOS at 24 h. Three isomers (4*m*-, 3*m*-, and *tb*-PFOS) had C_u

values below 1 (Table 3.1), and the remainder ranged from 1.26 (*iso*-PFOS) to 17.5 (B_9-PFOS). Because the shortest isomer half-life was longer than 11 d (B_9-PFOS), elimination prior to the first sampling point did not likely have a measurable effect on C_u values, and no correlation was observed between C_u and k_d (Appendix B, Figure B7).

For PFOS, there was a significant difference among the isomer-specific k_d's overall (p <0.0001), and pairwise analysis indicated where the differences lay: 1m-PFOS was significantly different from both *iso*- and B_8-PFOS, whereas n-PFOS was statistically different from B8-PFOS (Appendix B, Figure B11). The relatively wide 95% confidence intervals may be explained by the fact that less than two half-lives were achieved over the course of this experiment for most PFOS isomers, whereas 2.8 to 29 half-lives were achieved for isomers of PFOA. Blood depuration half-lives (Table 3.1) decreased with decreasing retention time on our PFO stationary phase (r^2=0.95, Figure 3.2), ranging from 33.7 d (n-PFOS, latest eluting isomer) to 11.1 d (B_9-PFOS, earliest eluting isomer). The exceptions to this trend were for 1m-PFOS and 3m-PFOS, which were the only PFOS isomers to have half-lives longer than that of n-PFOS (102 and 33.8 d, respectively, albeit not statistically significant; see Appendix B, Figure B11), despite eluting prior to n-PFOS. This result was consistent with the subchronic dosing study [28], in which 3m-PFOS and 1m-PFOS had half-lives that did not fit the general trend of decreasing half-life with decreasing elution time. Interestingly, when the perfluoromethyl branching position was plotted versus half-life (Appendix B, Figure B12), a profound effect of the α-perfluoromethyl

branch was observed whereby branching toward the sulfonate end of the molecule resulted in an elevated half-life.

Other evidence for PFOS isomer discrimination existed. For example, visual inspection of Figure 3.1 clearly shows enrichment of branched PFOS isomers in urine, suggesting their preferential elimination by this route. We propose that a longer study design may have led to more obvious alterations to the blood profile because, with the exception of $1m$-PFOS and B_9-PFOS, all PFOS isomers were excreted more efficiently than n-PFOS ($C_{e\text{-}urine} > 1$) (Table 3.1). When $C_{e\text{-}urine}$ values were plotted versus blood depuration rate constant, a general correlation was observed ($r^2 = 0.83$) whereby an increase in half-life corresponded to a decrease in $C_{e\text{-}urine}$ (Figure 3.4), suggesting that the preferential depuration of PFOS isomers from blood could be explained, at least in part, by preferential elimination in the urine. In contrast, feces did not show enrichment of branched isomers, relative to n-PFOS, at any time. This is despite the fact that fecal elimination was a significant route of PFOS elimination as shown by a single i.v. dosing study whereby feces accounted for 33% of total eliminated PFOS after 36 d[38]. The feces elimination coefficient ($C_{e\text{-}feces}$) could only be calculated for $5m$- and iso-PFOS (remaining branched PFOS was below limits of detection in feces), and these were both less than one (Figure 3.4). Due to the absence of other branched PFOS isomers in feces, it can be assumed that the remaining isomers had $C_{e\text{-}feces} < 1$.

We also examined the apparent tissue depuration half-lives to determine if certain tissues may have acted as pseudo-elimination reservoirs for blood-borne

PFOS isomers. These results should be interpreted cautiously, since half lives were calculated from only two time points (days 3 and 38). For most tissues, depuration half-lives were less than those in blood (Appendix B, Table B3). However, in liver, all PFOS isomer half-lives were between a factor of 1.8 (n-PFOS)and 3.8 (B_7-PFOS) longer than those in blood and did not show the same trend as blood, wherein branched isomers had shorter half-lives compared to those of the linear isomer, albeit most were not statistically different. The α-perfluoromethyl branch PFOS isomer ($1m$-PFOS), which had the longest half-life in blood, had no measurable elimination from the liver at all. In general, liver depuration half-lives for branched PFOS isomers were longer than those for n-PFOS (with the exception of tb-, B_8-, and B_9-PFOS). While it is unclear whether this is an artefact of the limited number of time points used in calculating tissue half lives, interestingly, the shorter half-life of n-PFOS in liver, relative to branched isomers, fits well with what was observed in feces: preferential elimination of the linear isomer. Although further work is necessary to fully elucidate the handling of PFOS isomers by the liver and its effect on blood depuration half-life, one possible explanation is that two opposing mechanisms were occurring simultaneously: Preferential elimination of branched PFOS isomers from peripheral tissues and blood to the urine (presumably with some redistribution to the liver) and preferential elimination of n-PFOS from the liver to the feces via bile.

The concentration of PFOS isomers in tissues (Figure 3.3) decreased in the order liver > lung > kidneys > blood > spleen> heart > testes > intestines > muscle

104

> brain > fat. With the exception of lung, which contained the second highest concentrations of PFOS isomers next to liver, the PFOS tissue distribution was consistent with that of Johnson et al.[38] in which PFOS concentrations decreased in the order liver > plasma > kidney > lung > spleen > bone marrow > red blood cells > adrenals > testes > skin > muscle > subcutaneous fat > eye. The elevated concentration of PFOS isomers in lung is interesting given that previous reports identified this organ as a target for toxicological effects in neonate rats [39].

3.3.5 Disposition of PFHxS

Residual PFHxS, an impurity in the electrochemical PFOS standard used here, was administered at a concentration of 30 µg/kg, as calculated using the total PFA method. Although we lacked pure standards for PFHxS isomers, the linear isomer (assumed to be the latest eluting and largest peak) and two branched isomers were tracked over the course of the elimination period by relative response to the ^{13}C-PFOS internal standard. Other minor PFHxS isomers in the dose could not be detected a few days post administration, and thus their kinetics could not be calculated accurately. The profile of PFHxS in day 1 blood was somewhat different than the dose (Figure 3.1), with isomers B_1 and B_2 having uptake coefficients of 0.70 and 0.75, respectively (Table 3.1). Considering that the shortest PFHxS half-life was 3.5 d (B_2-PFHxS), elimination prior to the first sampling point was not likely to have had a significant effect on the C_u values, as confirmed by a plot of C_u versus k_d, that did not reveal a trend (Appendix B,

Figure B7). Thus the calculated difference can be attributed primarily to preferential absorption of the linear isomer.

Plots of average depuration of PFHxS isomers from blood (Appendix B, Figure B5) and visual comparison of dose and blood PFHxS isomer profiles (Figure 3.1) suggested preferential elimination of branched PFHxS isomers. Indeed, for PFHxS, we observed a significant difference among the isomer-specific k_d's overall ($p<0.0001$), and pairwise analysis indicated that each isomer-specific k_d was statistically different from one another. Linear PFHxS had a blood depuration half life of 15.9 d, whereas B_1- and B_2-PFHxS had half-lives of 6.9 and 3.5 d, respectively. As was the case for PFOS, PFOA, and PFNA, an excellent correlation was observed between elimination half-life and elution time on the PFO column ($r^2=1.0$, Figure 3.2). PFHxS was not observed in feces; thus urine was examined to determine whether renal elimination could explain the preferential elimination of branched PFHxS isomers from blood. The isomer profile in day 3 urine clearly showed enrichment of branched isomers relative to day 3 blood (Figure 3.1), and the resulting correlation ($r^2 = 0.84$) between decreasing k_d with increasing $C_{e-urine}$ (Appendix B, Figure B13) supports the preferential elimination of branched isomers by this route.

The tissue concentrations of PFHxS (Figure 3.3) decreased in the order: liver > lungs > heart > kidneys > testes > spleen > muscle > intestines > brain > fat. Branched PFHxS isomers were eliminated quickly from all tissues, such that only n-PFHxS was detectable in tissues on day 38. Tissue half-lives calculated for the linear isomer were similar to that in blood for all tissues except for liver,

where the depuration half-life was over three times longer than that in blood (51.8 and 16.6d for liver and blood, respectively). Interestingly, the depuration half-life of n-PFHxS in liver was similar to that of n-PFOS in the liver (51.1 d). These data may help to explain why, in human studies, PFHxS had a significantly longer half-life than PFOS and PFOA in occupationally exposed humans[13].

3.4 Conclusions

Here we have shown that branching of the perfluoroalkyl chain has a profound effect on the toxicokinetics of perfluorinated acids in male rats administered a single low dose. With few exceptions, branching decreased the blood depuration half-life, increased the rate of excretion of PFOS, PFOA, PFNA, and PFHxS, or both. On the basis of global statistical analysis (PROC MIXED), blood isomer depuration rate constants from each of the perfluorinated acids were identified as having significant differences, and using pairwise analysis, we determined exactly where these differences lay. Furthermore, the biological significance of the statistical results was demonstrated by qualitative changes in the blood isomer profiles over time and consistent associations between blood depuration kinetics and excretion coefficients.

Despite these significant findings, some caution is warranted in interpretation and extrapolation of these data to other organisms. First, blood-borne concentrations from the present study are over an order of magnitude larger than those observed in non-occupationally exposed humans and many other

wildlife species, albeit PFOS concentrations were similar to those found in plasma of glaucous gulls[4] and marine mammals[3], and PFNA concentrations were similar to those found in the liver of polar bears[40]. Although no evidence thus far has demonstrated equal biological handling of PFA isomers in controlled experiments, one cannot rule out that species, sex, and dose may result in different relative kinetics than those determined here. In fact, results for PFNA suggested that differential elimination may be enhanced at a lower dose. In conclusion, we suggest that, in the absence of data demonstrating that isomers are pharmacologically equivalent in a specific species, that it be assumed that isomer patterns in biota are not entirely reflective of isomer patterns in the surrounding abiotic environment.

The blood and tissue isomer profiles resulting from the single oral dose used here are not expected to accurately predict the steady-state isomer profiles under a realistic chronic (repeated or continuous dose) exposure scenario. Part 2 of the present research[28] addresses this by measuring isomer profiles in a subchronic feeding study.

3.5   Acknowledgments

3.6   References

1.   Calafat, A.M.; Needham, L.L.; Kuklenyik, Z.; Reidy, J.A.; Tully, J.S.; Aguilar-Villalobos, M.; Naeher, L.P. *Chemosphere.* **2006**, *63*, 490-496.

2.   Karrman, A.; Mueller, J.F.; van Bavel, B.; Harden, F.; Toms, L.M.; Lindstrom, G. *Environ. Sci. Technol.* **2006**, *40*, 3742-3748.

3.   Martin, J.W.; Smithwick, M.M.; Braune, B.M.; Hoekstra, P.F.; Muir, D.C.; Mabury, S.A. *Environ. Sci. Technol.* **2004**, *38*, 373-380.

4.   Verreault, J.; Houde, M.; Gabrielsen, G.W.; Berger, U.; Haukas, M.; Letcher, R.J.; Muir, D.C. *Environ. Sci. Technol.* **2005**, *39*, 7439-7445.

5.   Luebker, D.J.; York, R.G.; Hansen, K.J.; Moore, J.A.; Butenhoff, J.L. *Toxicology.* **2005**, *215*, 149-169.

6.   Case, M.T.; York, R.G.; Christian, M.S. *Int. J. Toxicol.* **2001**, *20*, 101-109.

7.   Kennedy, G.L., Jr.; Butenhoff, J.L.; Olsen, G.W.; O'Connor, J.C.; Seacat, A.M.; Perkins, R.G.; Biegel, L.B.; Murphy, S.R.; Farrar, D.G. *Crt. Rev. Toxicol.* **2004**, *34*, 351-384.

8.   Martin, J.W.; Mabury, S.A.; Solomon, K.R.; Muir, D.C. *Environ. Toxicol. Chem.* **2003**, *22*, 196-204.

9.   Martin, J.W.; Mabury, S.A.; Solomon, K.R.; Muir, D.C. *Environ. Toxicol. Chem.* **2003**, *22*, 189-195.

10. Tomy, G.T.; Budakowski, W.; Halldorson, T.; Helm, P.A.; Stern, G.A.; Friesen, K.; Pepper, K.; Tittlemier, S.A.; Fisk, A.T. *Environ. Sci. Technol.* **2004**, *38*, 6475-6481.

11. Martin, J.W.; Whittle, D.M.; Muir, D.C.; Mabury, S.A. *Environ. Sci. Technol.* **2004**, *38*, 5379-5385.

12. Houde, M.; Martin, J.W.; Letcher, R.J.; Solomon, K.R.; Muir, D.C. *Environ. Sci. Technol.* **2006**, *40*, 3463-3473.

13. Olsen, G.W.; Burris, J.M.; Ehresman, D.J.; Froehlich, J.W.; Seacat, A.M.; Butenhoff, J.L.; Zobel, L.R. *Environ. Health Perspect.* **2007**, *115*, 1298-1305.

14. Olsen, G.W.; Church, T.R.; Miller, J.P.; Burris, J.M.; Hansen, K.J.; Lundberg, J.K.; Armitage, J.B.; Herron, R.M.; Medhdizadehkashi, Z.; Nobiletti, J.B.; O'Neill, E.M.; Mandel, J.H.; Zobel, L.R. *Environ. Health Perspect.* **2003**, *111*, 1892-1901.

15.   Dupont global PFOA strategy. United States Environmental Protection Agency Public Docket, AR226-1914. United States Environmental Protection Agency, Washington, DC, **2005**.

16.   De Silva, A.O.; Mabury, S.A. *Environ. Sci. Technol.* **2004**, *38*, 6538-6545.

17.   De Silva, A.O.; Mabury, S.A. *Environ. Sci. Technol.* **2006**, *40*, 2903-2909.

18.   Benskin, J.P.; Bataineh, M.; Martin, J.W. *Anal. Chem.* **2007**, *79*, 6455-6464.

19.   Powley, C.R.; George, S.W.; Russell, M.H.; Hoke, R.A.; Buck, R.C. *Chemosphere.* **2008**, *70*, 664-668.

20.   Karrman, A.; Langlois, I.; van Bavel, B.; Lindstrom, G.; Oehme, M. *Environ. Int.* **2007**, *33*, 782-788.

21.   Vyas, S.M.; Kania-Korwel, I.; Lehmler, H.J. *J. Environ. Sci. Health. A.* **2007**, *42*, 249-255.

22.   Reagen, W.K.; Lindstrom, K.R.; Jacoby, C.B.; Purcell R.G.; Kestner T.A.; Payfer R.M.; Miller, J.W.; Platform presentation at Society of Environmental Toxicology and Chemistry 28th North American Meeting, Milwaukee, WI, USA, November 11–15, 2007.

23.   Ohmori, K.; Kudo, N.; Katayama, K.; Kawashima, Y. *Toxicology.* **2003**, *184*, 135-140.

24. Kudo, N.; Suzuki, E.; Katakura, M.; Ohmori, K.; Noshiro, R.; Kawashima, Y. *Chem.-Biol. Interact.* **2001**, *134*, 203-216.

25. Loveless, S.E.; Finlay, C.; Everds, N.E.; Frame, S.R.; Gillies, P.J.; O'Connor, J.C.; Powley, C.R.; Kennedy, G.L. *Toxicology.* **2006**, *220*, 203-217.

26. Martin, J.W.; Kannan, K.; Berger, U.; de Voogt, P.; Field, J.; Franklin, J.; Giesy, J.P.; Harner, T.; Muir, D.C.; Scott, B.; Kaiser, M.; Jarnberg, U.; Jones, K.C.; Mabury, S.A.; Schroeder, H.; Simcik, M.; Sottani, C.; van Bavel, B.; Karrman, A.; Lindstrom, G.; van Leeuwen, S. *Environ. Sci. Technol.* **2004**, *38*, 248A-255A.

27. Langlois, I.; Oehme, M. *Rapid Commun. Mass Spectrom.* **2006**, *20*, 844-850.

28. De Silva, A.O.; Benskin, J.P.; Martin, L.J.; Arsenault, G.; McCrindle, R.; Riddell, N.; Martin, J.W.; Mabury, S.A. *Environ. Toxicol. Chem.* **2009**, *28*, 555-512.

29. Kestner, T. U.S. Environmental Protection Agency public docket AR226-0564: Fluorochemical isomer distribution by ^{19}F-NMR spectroscopy. U.S. Environmental Protection Agency, Office of Pollution Prevention and Toxic Substances, Washington, DC, **1997**.

30. Arsenault, G.; Chittim, B.; McAlees, A.; McCrindle, R.; Riddell, N.; Yeo, B. *Chemosphere.* **2008**, *70*, 616-625.

31. Yoo, H.; Guruge, K.S.; Yamanaka, N.; Sato, C.; Mikami, O.; Miyazaki, S.; Yamashita, N.; Giesy, J.P. *Ecotoxicol. Environ. Safety.* **2007**.

32. Perkins, R.G.; Butenhoff, J.L.; Kennedy, G.L., Jr.; Palazzolo, M.J. *Drug Chem. Toxicol.* **2004**, *27*, 361-378.

33. Seacat, A.M.; Thomford, P.J.; Hansen, K.J.; Clemen, L.A.; Eldridge, S.R.; Elcombe, C.R.; Butenhoff, J.L. *Toxicology.* **2003**, *183*, 117-131.

34. Hansen, K.J.; Clemen, L.A.; Ellefson, M.E.; Johnson, H.O. *Environ. Sci. Technol.* **2001**, *35*, 766-770.

35. Kemper, R.A. U.S. Environmental Protection Agency public docket *AR226-1499.* U.S. Environmental Protection Agency, Office of Pollution Prevention and Toxic Substances, Washington, DC, **2003**.

36. Vanden Heuvel, J.P.; Kuslikis, B.I.; Van Rafelghem, M.J.; Peterson, R.E. *J. Biochem. Toxicol.* **1991**, *6*, 83-92.

37. Katakura, M.; Kudo, N.; Tsuda, T.; Hibino, Y.; Mitsumoto, A.; Kawashima, Y. *J. Health Sci.* **2007**, *53*, 77-76.

38. Johnson, J.D.; Gibson, S.J.; Ober, R.E. U.S. Environmental Protection Agency public docket *8EHQ-1180-00374.* U.S. Environmental Protection

Agency, Office of Pollution Prevention and Toxic Substances, Washington, DC, **1979**.

39. Grasty, R.C.; Bjork, J.A.; Wallace, K.B.; Wolf, D.C.; Lau, C.S.; Rogers, J.M. *Birth Defects Res. B. Dev. Reprod. Toxicol.* **2005**, *74*, 405-416.

40. Smithwick, M.; Mabury, S.A.; Solomon, K.R.; Sonne, C.; Martin, J.W.; Born, E.W.; Dietz, R.; Derocher, A.E.; Letcher, R.J.; Evans, T.J.; Gabrielsen, G.W.; Nagy, J.; Stirling, I.; Taylor, M.K.; Muir, D.C. *Environ. Sci. Technol.* **2005**, *39*, 5517-5523.

Chapter 4. Isomer-specific biotransformation rates of a perfluorooctane sulfonate (PFOS)-precursor by cytochrome P450 isozymes and human liver microsomes.

4.1   Introduction

Perfluorinated acids (PFAs) are an environmental health concern due to their global distribution in wildlife[1] and humans[2-4], and substantial chain length-dependent bioaccumulation potential in wildlife[5]. In humans, perfluorooctane sulfonate ($C_8F_{17}SO_3^-$, PFOS) and perfluorooctanoate ($C_7F_{15}COO^-$, PFOA) half-lives are 5.4 and 3.8 yrs, respectively[6]. While the toxicological relevance of PFA concentrations in humans or wildlife are not currently understood, significant developmental toxicity[7,8] and carcinogenicity[9] in laboratory animals has made it a priority to determine whether these effects are paralleled in humans.

The presence of PFOS and PFOA in the environment may either be attributed to direct release[10,11] or the release of PFA-precursors which can eventually degrade to PFAs through atmospheric oxidation[12-14] or biotransformation[15,16]. PFOS-precursors consist primarily of N-alkyl substituted perfluorooctanesulfonamides, which were manufactured for surfactants or incorporated into surface treatment polymers for paper, textile, and carpet protection[17,18]. The historical synthesis of PFOS and its precursors by electrochemical fluorination (ECF) resulted in a mixture of branched and linear perfluoroalkyl isomers in the final commercial products. Despite the fact that

115

PFOS and other ECF-based fluorochemicals were largely phased out of production by their primary manufacturer in 2001, PFOS-precursors are still detectable in the atmosphere[19], indoor air, and dust[20], and PFOS is still the major PFA in human blood[3,6]. Furthermore, a recent model[21] has demonstrated that for high exposure scenarios, humans can receive a substantial proportion of PFOS from precursors. Much less is known about the importance of PFOS-precursor exposure to wildlife. Nonetheless, human and wildlife biomonitoring has consistently shown the widespread occurrence of perfluorooctane sulfonamide ($C_8F_{17}SO_2NH_2$, FOSA), which can be biotransformed to PFOS[15,22] (Figure C-1, Appendix C); thus, the importance of PFOS-precursor metabolism to current body-burdens remains an important question.

Interestingly, the isomer patterns of PFOS in humans can range from ~ 20–50% branched-chain (Appendix C, Table C-1)[23-26]. This is inconsistent with the relative amounts of branched isomers in all PFOS manufactured by the 3M Co., which were always very close to 30% (stdev 1.1%)[27]. Of the 89 possible PFOS isomer structures[28], ~11 isomers (consisting of linear, monomethyl branched, and dimethyl branched-chains) appear to make up the majority of isomer content in environmental samples and commercial products[24,27,29-32]. Benskin et al.[33] (Chapter 3) and De Silva et al.[34] demonstrated that most branched PFOS isomers are eliminated preferentially in rats; thus, with current data it is difficult to explain why branched PFOS isomers are often enriched in humans. One possibility is enriched branched isomer profiles in current and historical non-3M manufactured PFOS and PFOS-precursors manufactured in other countries.

For example, recent documents submitted to the United Nations Environment Program (UNEP), for review under the International Stockholm Convention on persistent organic pollutants, show that China has continued to expand production and export of PFOS related products since the 2002 phase-out by the 3M Co.[35]. However, while these products remain largely uncharacterized, a preliminary survey of PFOS isomer patterns in ocean water from the Atlantic and Coastal Asia showed a general consistency with isomer patterns known to be present in 3M ECF PFOS[36].

We hypothesized that isomer-specific rates of PFOS-precursor biotransformation may explain the common observation of enriched PFOS isomer profiles in humans (i.e., branched PFOS precursors may metabolize more quickly than the linear isomer); and consequently, that enriched branched PFOS isomer profiles in humans may be a useful tool for tracking sources of PFOS exposure (i.e., direct versus indirect). To test this hypothesis, we employed sensitive isomer-specific analytical methods to examine the effect that perfluoroalkyl chain geometry could have on *in vitro* biotransformation rates of a model PFOS-precursor. Both human liver microsomes and pure human cytochrome P450 (CYP) isozymes were employed.

4.2 Experimental Methods

4.2.1 Nomenclature

In general, the structure of any given perfluorinated substance may be a normal chain (i.e. linear) or a mono- or diperfluoromethyl-branched isomer. For GC analysis of N-ethylperfluorooctane sulfonamide ($C_8F_{17}SO_2NHC_2H_5$, NEtFOSA), isomers were arbitrarily labeled as 1–6 in order of increasing retention time. Isomer 4 was confirmed as n-NEtFOSA based on comparison to an authentic linear standard. In this work we have also distinguished between linear NEtFOSA present in the technical mixture as n_{mix}-NEtFOSA, whereas that of the pure linear isomer standard will be referred to as n_{pure}-NEtFOSA. For HPLC analysis, each branched isomer was arbitrarily labeled as B_x, (where x = 1, 2, 3, etc.) in order of increasing retention time, except when the structure could be confirmed by authentic standards, in which case the nomenclature system employed previously (23) was adopted.

4.2.2 Standards and Reagents

HPLC-grade methanol and methyl *tert*-butyl ether (MTBE) were purchased from Fisher Scientific (Ottawa, ON, Canada). HPLC-grade formic acid (50%) and potassium PFOS (98%) were purchased from Sigma-Aldrich (Oakville, ON, Canada). Linear FOSA (>98%), linear NEtFOSA (n_{pure}-NEtFOSA, >98%) and the linear internal standards N-methyl perfluorooctane sulfonamide ($C_8F_{17}SO_2NHCH_3$, N-MeFOSA, >98%), sodium perfluoro-1-[1,2,3,4-$^{13}C_4$]octane sulfonate (^{13}C-PFOS), were purchased from Wellington Laboratories (Guelph,

ON, Canada). ECF FOSA and ECF PFOA were provided by the 3M Co. (St. Paul, MN). A technical grade mixture of NEtFOSA isomers (95%) was obtained from Interchim (France). Substantial effort was spent on determining optimum conditions for both storing and incubating NEtFOSA, and these details are stated in Appendix C. Stock chemical standards of NEtFOSA were made up in HPLC grade methanol in glass volumetric flasks. These were refrigerated prior to use and tested routinely for possible changes in isomer profile and/or total concentration. CYP isozymes, human liver microsomes, and NADPH regeneration solutions were purchased from Gentest (Woburn, Mass.).

4.2.3 Incubation Conditions

Incubations were conducted in polystyrene tubes containing substrates (1 µL spiked in methanol), buffer, and CYP isozymes or microsomes. These were premixed for 5 min and reactions initiated by adding pre-mixed NADPH regenerating solution (final concentrations of 1.6 mM NADP+, 3.3 mM glucose-6-phosphate, 0.4 U/mL glucose-6-phosphate dehydrogenase, and 3.3 mM magnesium chloride) for a total reaction volume of 1 mL. Molar concentrations of reagents and substrates used with individual CYPs and microsomes are stated below. All incubations were conducted by gently shaking the reaction mixtures in an incubator at 37°C. Nonspecific binding loss, abiotic transformation, or adsorption to container walls were controlled by incubating P450 reductase + Cytochrome b_5 insect cell controls (containing equivalent protein concentration but devoid of human P450) with substrate (95 and 380 nM NEtFOSA for

CYP2C19, and 9.5 and 190 nM NEtFOSA for CYP2C9 in 1 mL total incubation volume) using the same buffer and incubation conditions as used for the respective CYP isozymes. Aliquants removed from these reaction mixtures were monitored for any time-dependent decrease in isomer response (i.e., peak area). Blank incubations for experiments involving human liver microsomes (9.5 and 380 nM NEtFOSA) were conducted by (i) heat-treating the microsomes at 100 °C for 5 min in a water bath to render them inactive, and then incubating the inactive microsomes with substrate under regular conditions to monitor depletion, and (ii) incubating active microsomes with substrate under regular conditions but without NADPH regenerating solution.

4.2.4 CYP2C9

All 2C9 experiments were carried out in 1 mL of pH 7.4 100 mM Tris buffer containing 25 pmol of CYP isozyme (107.5 µg protein), cytochrome c reductase, Cytochrome b_5 (38 pmol), and NADPH. According to the suppliers, diclofenac 4'-hydroxylase activity was 20 pmol product/(min·pmol P450) and cytochrome c reductase activity was 280 nmol /(min·mg protein). For kinetic experiments by solid phase microextraction-gas chromatography-electron capture detection (SPME-GC-ECD), incubations ($n = 4$ replicates) were conducted at 190, 95, 47, 19, and 9.5 nM technical NEtFOSA (i.e., an isomer mixture) and at 95, 47, 28, and 9.5 nM n_{pure}-NEtFOSA ($n = 3$ replicates). A total of 3–6 aliquants were removed over 12 min, with the aliquant volumes ranging from 150 µL (six aliquants per experiment) to 300 µL (three aliquants per experiment). The number

and volume of samples taken was varied to enable work at low substrate concentrations. For example, isomers in the 190 nM incubation were readily observed over 12 min when 150 μL aliquants were removed at 0, 2, 4, 6, 8, and 12 min intervals. However, when incubating with 9.5 nM technical NEtFOSA, the isomers were difficult to observe after 2 min as they approached limits of detection. Therefore, sample aliquants increased to 300 μL at 0.5, 1, and 2 min. In addition, for the 9.5 nM incubations, $t = 0$ samples were obtained in separate experiments by adding 60 μL of water to the mixture rather than NADPH, and then removing 300 μL of this reaction mixture, resulting in a 4-point substrate depletion curve. For HPLC tandem mass spectrometry (LC-MS/MS) product experiments, incubations were conducted at 190 nM NEtFOSA using the same conditions as above and aliquots were removed over 10 min.

4.2.5 CYP2C19

All 2C19 experiments were carried out in 1 mL of pH 7.4 100 mM phosphate buffer containing 25 pmol of CYP2C19 isozyme (82.5 μg protein), cytochrome c reductase, Cytochrome b_5 (30 pmol) and NADPH. According to the suppliers, (S)-mephenytoin 4'-hydroxylase activity was 23 pmol product/(min·pmol P450) and cytochrome c reductase activity was 1700 nmol /(min·mg protein). For kinetic experiments by SPME-GC-ECD, incubations were conducted at 380, 190, and 95 nM technical NEtFOSA ($n = 3 - 4$ replicates) and at 95 and 47 nM n_{pure}-NEtFOSA ($n = 3$ replicates). A total of 3–6 aliquants were removed at time points between 0 and 5 min, and aliquant volumes ranged from

150 μL (6 aliquants per experiment) to 300 μL (3 aliquants per experiment). As in the 2C9 incubations, a $t = 0$ sample for the 3 aliquant experiments was obtained in separate experiments by adding 60 μL of buffer to the mixture rather than NADPH, and then removing 300 μL of this reaction mixture to give a 4-point substrate depletion curve. For LC-MS/MS product experiments, incubations were conducted at 380 nM NEtFOSA using the same conditions as above and aliquots were removed over 10 min.

4.2.6   Human Liver Microsomes

Pooled human liver microsomes were obtained from Gentest. According to the suppliers, the activities of CYP2C9 and CYP2C19 were 3000 pmol/(mg protein·min) and 67 pmol/(mg protein·min) using diclofenac 4′-hydroxylase and (S)-mephenytoin 4′-hydroxylase assays, respectively. All microsomal experiments were carried out in 1 mL of pH 7.4 100 mM phosphate buffer with a protein concentration of 0.5 mg/mL. Incubations were conducted at 9.5 and 380 nM NEtFOSA ($n = 3$ replicates) in the same manner as those conducted with CYP2C9 and CYP 2C19.

4.2.7   Extraction and Treatment of Samples

For analysis by SPME-GC-ECD, aliquants of the incubation mixture were removed and the reaction was terminated with ice-cold MTBE containing internal standard and 15 μL of formic acid, followed by vortexing for 1 min. The reaction mixture was extracted three times with 500 μL of MTBE and transferred directly to an amber glass microvial. The extracts were evaporated under a gentle stream

122

of nitrogen and taken to dryness in ambient air prior to analysis. Once dry, a stir bar on which the Teflon coating was removed (necessary to prevent adsorption of perfluoroalkyl analytes) and 1.5 mL of pH 9.0 Tris/EDTA buffer were added and the vials were capped. Liquid SPME was conducted using a manual SPME device equipped with a 100 µm polydimethyl siloxane fiber (PDMS; Supelco) which was allowed to adsorb with stirring for 40 min. The optimum conditions for SPME were 40 min adsorption at pH 9.0 with no adjustments to the ionic strength (Appendix C, Figure C-2). For analysis conducted by HPLC-MS/MS, reactions were terminated with ice-cold methanol containing internal standards, centrifuged, and the resulting supernatant injected onto the HPLC. Spike/recovery experiments were also performed to ensure (i) that the isomer profile was conserved throughout the extraction procedure, and (ii) quantitative extraction of analytes.

4.2.8 SPME-GC-ECD Analysis

The Teflon-coated stir bar used during SPME adsorption was problematic because it selectively adsorbed n-NEtFOSA, causing a bias to the isomer profiles. This was overcome by manually removing the fluoropolymer coating. The glass SPME microvial was also problematic because NEtFOSA adsorbed to the walls in aqueous solution, but this effect was negligible when the buffer pH was increased, presumably due to formation of the conjugate base. Following adsorption, the SPME fiber was removed from solution and desorbed for 2 min at 250 °C in the injection port of a Varian GC-ECD system. The injector contained a deactivated

glass insert (2 mm i.d.) and was operated in splitless mode at a 1 mL/min of 95% Ar/5% He. A J & W Scientific DB35-MS column (80 m × 0.250 mm, 0.25 μm film thickness) was employed for GC separation using the following temperature program: isothermal at 60 °C for 2 min, increased to 75 at 20 °C /min, and increased to 93 at 0.5 °C /min. The column was then held for 3 min followed by an increase at 30 °C/min to 200 °C, held for 10 min, and finally returned to initial conditions. The detector was held constant at 260 °C. Isomer-specific depletion relative to the internal standard, NMeFOSA (added prior to extraction), was monitored using peak height which is generally more accurate than peak areas when baseline resolution cannot be fully achieved[37]. The effective limit of detection for the most minor branched isomer was approximately 4 pM total NEtFOSA by SPME-GC-ECD.

Peaks observed by ECD were confirmed as NEtFOSA isomers by matching their retention times to GC-MS chromatograms in negative chemical ionization (NCI), positive chemical ionization (PCI) and electron impact ionization (EI) modes. Ions of m/z 400 ($C_8F_{16}^-$, NCI), m/z 528 ($[C_8F_{17}SO_2NC_2H_7]^+$, PCI) and m/z 108 ($[SO_2NC_2H_6]^-$, EI) confirmed the identity of the NEtFOSA peaks routinely monitored by ECD.

4.2.9 HPLC-MS/MS Analysis

Isozyme and microsomal biotransformation products were monitored using a FluoroSep RP Octyl HPLC Column (3 μm 100A 15 cm × 2.1 mm, ES Industries, West Berlin, NJ) and tandem-mass spectrometry using an established

124

method [24]. Multiple product ions of PFOS, PFOA, NEtFOSA, and FOSA (Appendix C, Table C-2) were monitored over the time course of the reaction (up to 24 h for microsomal experiments).

4.2.10 Kinetic and Statistical Analysis

To validate our experimental approach, arbitrary data sets for a system containing two competing substrates were modeled to an appropriate mass action equation using GraphPad Prism 5.0 (GraphPad Software, San Diego, CA). Details of this experiment are given in the Validation of Experimental Approach section of Appendix C.

For CYP isozyme and microsomal experiments, isomer-specific first order rate constants were obtained from the slope of natural log (ln) relative response versus time curves, plotted using Microsoft Excel (examples shown in Appendix C, Figures C-3, C-4, and C-5). Isomer rate constants were tested for statistical differences ($\alpha = 0.05$) using SigmaStat (SigmaStat Software Inc., San Jose, CA) by one-way ANOVA. When the ANOVA was significant, subsequent pairwise comparisons were carried out among all isomers using Tukey's Honestly Significant Difference test.

4.3 Results and Discussion

4.3.1 Description and Validation of Experimental Approach

The objective of this proof-of-principle study was to determine whether there can be significant discrimination among the biotransformation rates of

PFOS-precursor isomers. Ideally, this would be accomplished by incubating pure individual isomers in separate experiments and measuring their kinetic parameters, but pure branched isomer standards are not currently available. Thus, an assay was developed that could produce valid results for a mixture of isomers incubated together. A single metabolic reaction, N-deethylation of NEtFOSA (Appendix C, Figure C-1), was studied using two P450 isozyme systems (CYP2C9 and CYP2C19) which were previously reported to catalyze the N-dealkylation of similar substrates[15]. Substrate depletion using the "in vitro $t_{1/2}$ approach"[38] was employed rather than monitoring metabolite formation because the latter would likely require a comprehensive GC method for multiple metabolites, many of which are currently difficult to analyze by GC.

The composition of technical NEtFOSA was dominated by the linear isomer (~60%, based on estimation from GC-ECD peak area); thus, it was important that the assay results not be biased due to competitive inhibition among isomers. When substrate concentrations are much lower than the Michaelis constant (K_M), depletion of a substrate should follow first-order decay kinetics[39] and competition among isomers should be negligible. Thus, at low concentration the biotransformation rate constants obtained for each individual isomer in the mixture should not be significantly different than if each isomer had been incubated alone. Although a K_M has not previously been published for the N-deethylation of NEtFOSA, previously published work on the biotransformation of similar chemicals can provide a reasonable estimate. Xu et al.[15] determined a K_M of 21.9 μM for the dealkylation of N-ethyl perfluorooctane sulfonamidoethanol to

126

FOSA catalyzed by 20 pmol of CYP2C19. In the same study, the apparent K_M for the N-deethylation of N-ethyl perfluorooctanesulfonamidoethanol by 30 pmol of CYP2C19 was 11.6 μM. In the present study, we used 25 pmol of P450 and NEtFOSA concentrations of 9.5–380 nM, representing concentrations that are 2–4 orders of magnitude lower than the K_M value(s). This experimental approach was further validated by kinetic modeling; the results of these experiments are described in the Validation of Experimental Approach section of Appendix C.

4.3.2 Human CYP Isozymes

In preliminary experiments, various CYP isozymes (1A2, 2B6, 2D6, 2C9, 2C19, and 3A5) were incubated with NEtFOSA isomers to select only those enzymes with a relatively rapid biotransformation rate for the substrates. Only CYP2C9 and CYP2C19 metabolized this substrate to a measurable extent; as a result, we focused on these two isozymes. This is consistent with the observations of Xu et al.[15] who also found that these isozymes metabolized similar PFOS-precursors.

The highest and lowest substrate concentrations used in our experiments were bound by solubility and detection limits, respectively. The water solubility of NEtFOSA was estimated by Martin et al.[13] as 95 nM; however, we were able to conduct incubations at 380 nM with no apparent precipitation of substrate. The effective limit of detection for the most minor branched isomer was approximately 4 pM total NEtFOSA by SPME-GC-ECD. Insect cell control incubations showed negligible loss of NEtFOSA over time.

127

Visual inspection of chromatograms from the incubation of 190 nM NEtFOSA with CYP2C9 showed rapid disappearance of isomer 5 relative to other NEtFOSA isomers (Figure 4.1), and this was confirmed by statistically significant differences in isomer-specific biotransformation rate constants (Figure 4.2 and Appendix C, Figure C-6), which decreased in the order: isomer 5 » 3 > 2 > 1 > 6 > n. Peaks tentatively corresponding to FOSA isomers (i.e., the N-dealkylation product) appeared in all chromatograms (at a retention time of ~40 min) after the incubation was initiated (Figure 4.1). The relative size of the product isomer peaks also changed with time, perhaps indicative of further isomer-specific biotransformation to secondary products.

To examine the effect that total isomer concentration had on biotransformation rate constants, we performed further incubations at 95, 47, 19, and 9.5 nM technical NEtFOSA with CYP2C9. With the exception of isomer 2, the rate constants of all isomers increased significantly with decreasing concentration (Figure 4.2). Despite this, isomer 5 consistently had the largest rate constant, (Figure 4.2 and Figures C-6, C-7), while the rank order of the remaining isomer rate constants remained fairly consistent between the highest (190 nM) and lowest (9.5 nM) concentrations. Also of importance was that the rate constants measured for any particular isomer at the two lowest concentrations (i.e., 9.5 and 19 nM) were not statistically different (Figure 4.2) despite the fact that differences were still observed *between* isomers (Appendix C, Figure C-6). This suggests that there was negligible competition among isomers at these low concentrations (i.e.,

[S] $\ll K_M$), and hence these results should be similar to results obtained had each isomer been tested individually.

To investigate the effect of competitors further, we incubated n_{pure}-NEtFOSA at several concentrations (95, 47, 28, 9.5 nM) and compared the rate constants to those of n_{mix}-NEtFOSA (the linear isomer present in the technical mixture) in incubations with CYP2C9. Rate constants with n_{pure}-NEtFOSA increased significantly with decreasing concentration, but were consistently larger than those obtained for n_{mix}-NEtFOSA down to 28 nM. At this concentration, the rate constants were not statistically different from those obtained at lower concentrations (Appendix C, Figure C-8). These data suggest that at low concentrations, metabolism of n_{mix}-NEtFOSA is unaffected by the presence of other mixture components.

As with CYP2C9, incubations of technical NEtFOSA at 380 nM with 25 pmol CYP2C19 also showed statistically significant differences between rate constants of several isomers (Appendix C, Figure C-9), but with a remarkably different relative change in the isomer profile over time (Appendix C, Figure C-10). Elimination rate constants at 380 nM decreased in the order $2 > 3 > 5 > 1 \gg 6 > n$ (Figures C-9, C-11). When the concentration of NEtFOSA was decreased from 380 to 190 nM, the rate constants of isomers 2, 6, and n-NEtFOSA increased significantly (Appendix C, Figure C-11). A further decrease in concentration to 95 nM (Appendix C, Figure C-12) resulted in a statistically significant increase in rate constants for isomers 3 and 6. Despite these changes, the relative rank order of individual isomer rate constants was similar between the highest (380 nM) and

lowest (95 nM) concentrations. FOSA isomers were also observed from the N-deethylation of NEtFOSA by CYP2C19, but the profiles were different than with CYP2C9. Also notable was that at the lowest concentrations the biotransformation kinetics of n-NEtFOSA were similar, whether the substrate was present in a mixture of isomers or in its pure form (Appendix C, Figure C-13).
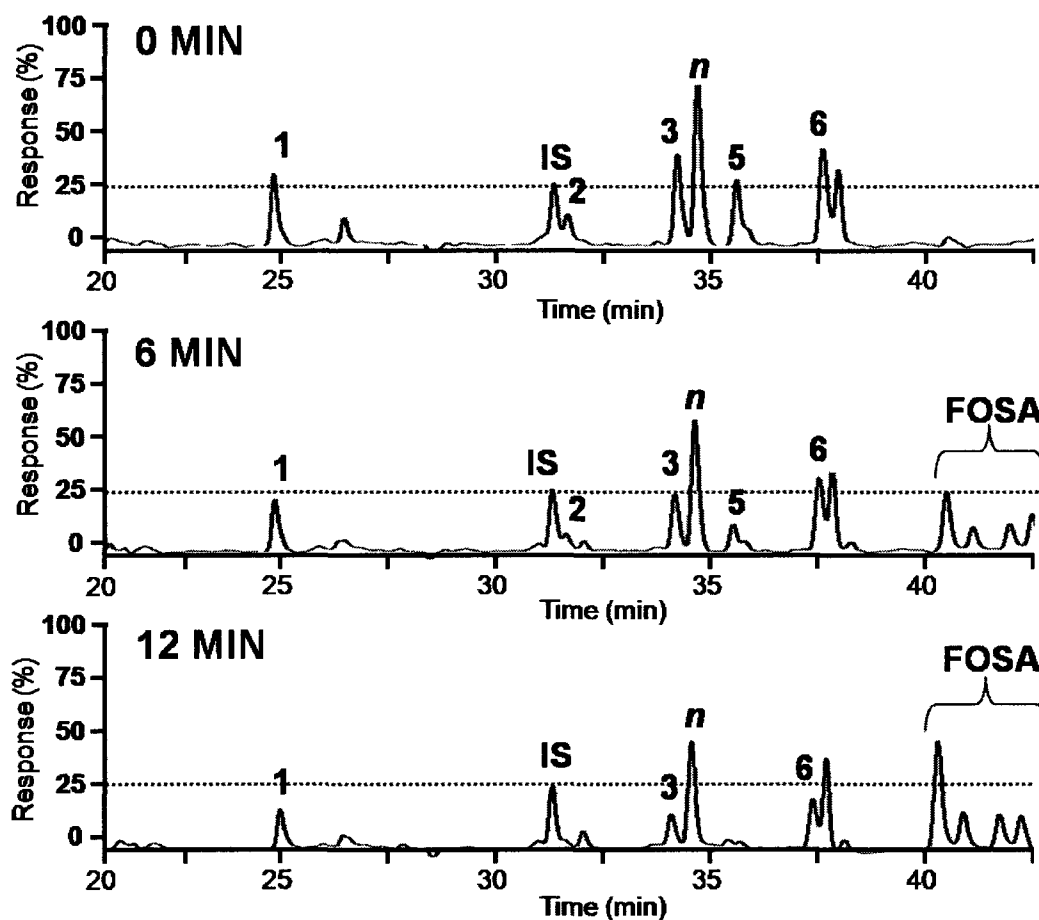
Figure 4.1 Representative SPME-GC-ECD chromatograms showing isomer specific biotransformation of 190 nM NEtFOSA (100 ng in 1 mL total volume,n = 4 replicates) by CYP2C9. Individual isomer response is relative to the internal standard peak (IS), set arbitrarily at 25% (dotted line). Note rapid disappearance of isomer 5 and changes in FOSA isomer profile on right side of chromatogram.
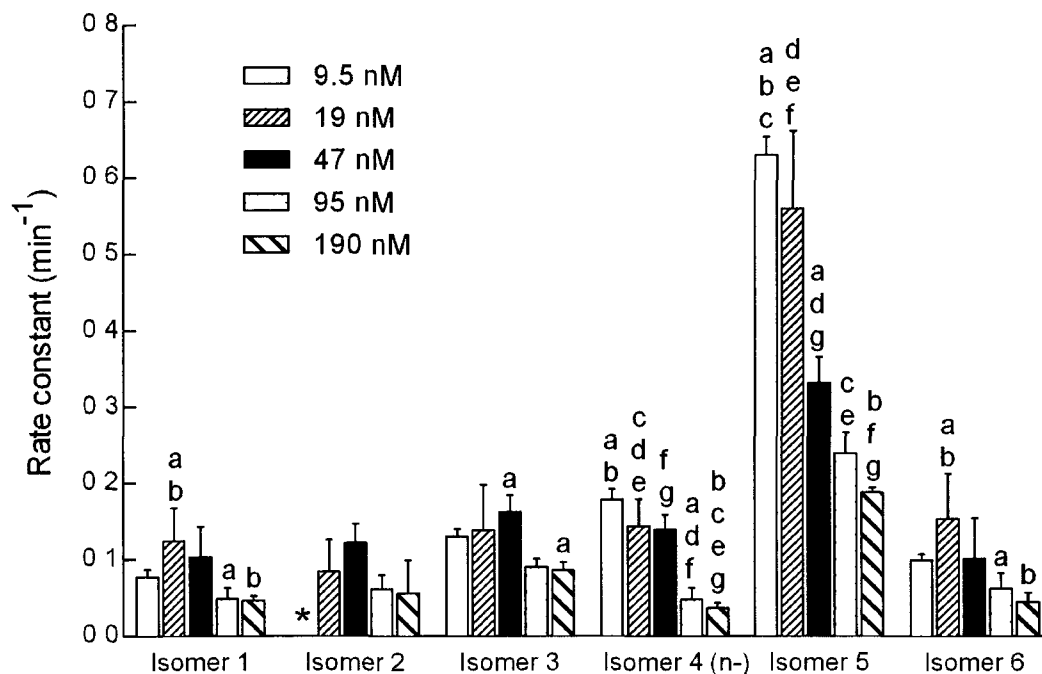
Figure 4.2 Average rate constants ($n = 4$ replicates per concentration) for the biotransformation of 9.5, 19, 47, 95, 190 nM NEtFOSA (5, 10, 25, 50, and 100 ng of NEtFOSA incubated in 1 mL total volume) by CYP2C9. Isomer 5 had the highest rate constant at all concentrations. Error bars represent ±1 standard deviation about the mean. Identical letters represent significant ($\alpha = 0.05$) difference between rate constants obtained for a given isomer. For example, for isomer 1, "a" indicates a significant difference between rate constants at 19 and 95 nM NEtFOSA. A rate constant for isomer 2 could not be calculated at 9.5 nM due to detection limits (denoted by *).

4.3.3 Human Microsomes

The isozyme results cannot be extrapolated directly to the *in vivo* situation where clearance of individual isomers may result from metabolism by multiple CYP isozymes, as well as conjugation and isomer-specific transport processes. Instead, human liver microsomes were used to mirror one aspect of the *in vivo* situation due to their ease of use and a full complement of P450s expressed at levels typical of the human liver. Chromatograms showing the consumption of

380 nM NEtFOSA by human liver microsomes were suggestive of isomer-specific discrimination (Appendix C, Figure C-14) and this was confirmed by statistically different rate constants (Appendix C, Figures C-15 and C-16). As observed for CYP2C9, the disappearance of isomers 3 and 5 in human microsomes was rapid compared to other NEtFOSA isomers. This is not surprising, as the protein concentration of CYP2C9 is much higher than CYP2C19 in microsomes according to the suppliers. Therefore, despite the fact that turnover of NEtFOSA by CYP2C19 in isozymes is much faster than 2C9, the predominant activity in microsomes is likely 2C9, resulting in a similar rank order of isomer rate constants to those generated in CYP2C9 isozyme experiments.

4.3.4 Confirmation by HPLC-MS/MS

The isomer-specific biotransformation demonstrated by GC-ECD was validated qualitatively by LC-MS/MS. The focus of these experiments was not to corroborate the kinetic data (which is difficult, due to different chromatographic elution orders between GC and LC), but rather, to confirm that the isomer profile of technical NEtFOSA changed over time as it was consumed. Furthermore, the use of LC-MS/MS had the added benefit of allowing us to confirm the formation of FOSA as a metabolite, and potentially PFOS. Using an API 4000QTRAP, limits of detection (LODs) for NEtFOSA isomers ranged from 17 fmol total NEtFOSA for the most minor branched isomer, to 1.3 fmol total NEtFOSA for n-NEtFOSA. Likewise, PFOS detection limits ranged from 0.2 fmol of total PFOS (detection of n-PFOS) to 4.2 fmol total PFOS (detection of dimethyl branched

isomers) while LODs of FOSA isomers ranged from 2 fmol total FOSA (detection of n-FOSA) to 70 fmol total FOSA (detection of most minor branched isomer). When using an API 5000, isomer detection limits for all PFAs were improved by ~10-fold.

LC-MS/MS analysis of 2C9, 2C19, and human liver microsome incubation supernatants showed separation of n-NEtFOSA from five major branched NEtFOSA isomer peaks, which partially coeluted but which could be resolved using unique MS/MS transitions (see Figure 4.3 and Appendix C, Table C-2, Figures C-17 and C-18). These major branched NEtFOSA isomers were, in turn, baseline separated from five earlier eluting minor branched NEtFOSA isomers. Based on analogy to the elution pattern of electrochemical PFOS isomer mixtures, it is reasonable to assume that the five major isomers observed in GC-ECD and HPLC-MS/MS chromatograms corresponded to the monoperfluoromethyl substituted isomers, and that the minor NEtFOSA isomers observed by HPLC-MS/MS corresponded to diperfluoromethyl substituted isomers. Further identification was not possible without authentic standards. While phase II metabolism via N-glucuronidation of perfluorooctane sulfonamides has been demonstrated by other authors[40], UDPGA cofactors were not added to our incubations, thus glucuronidation was not expected. However, other biotransformation pathways may be possible; consequently, we cannot rule out the formation of products other than PFOS and FOSA in our microsomal experiments.

Using HPLC-MS/MS, the consumption of technical NEtFOSA by CYP2C9 and CYP2C19 again appeared to be isomer-specific (Figures C-17 and C-18) at concentrations of 190 and 380 nM, respectively. As was observed when monitored by SPME-GC-ECD, the relative disappearance of individual NEtFOSA isomers varied depending on whether the reaction was catalyzed by CYP2C9 or CYP2C19. Although we monitored for the formation of PFOS and PFOA in the isozyme experiments, only FOSA was observed. It was interesting that only two major and three very minor branched FOSA isomers were observed by HPLC-MS/MS, despite the observation of at least five large product peaks by SPME-GC-ECD. FOSA readily produces m/z 78 product ion ($[SO_2N]^-$) in MS/MS but it tends to be recalcitrant to form perfluoroalkyl ions which are very useful for identifying and resolving the various PFOS isomers. While it is possible that some coelution of multiple branched FOSA isomers occurred within the three major peaks observed by HPLC-MS/MS, it is difficult to conceive how the LC method could resolve up to 11 PFOS and NEtFOSA isomers, but only 6 FOSA isomers considering the structural similarities[23]. As an alternative explanation, it is known that some isomers of PFOS undergo in-source fragmentation by electrospray and it is possible that this may occur more so for FOSA under our MS conditions. Further studies on electrospray ionization efficiency of FOSA isomers are suggested, as such phenomena may contribute to quantification errors and limit source identification by isomer profiling. Considering that FOSA is readily observed in the environment, and that it was only produced by electrochemical fluorination, it is also surprising that so few isomers are observed in human

134

serum, as reported by Benskin et al.[24] (Chapter 2). It is possible that these isomers are simply not observable in environmental samples due to their poor electrospray efficiency, or poor fragmentation by collision-induced-dissociation processes of commercial MS/MS instruments.

In microsomes, NEtFOSA biotransformation appeared to be isomer-specific at substrate concentrations of 9.5 and 380 nM (Figure 4.3). Blank incubations showed negligible loss of NEtFOSA or formation of FOSA over time. While secondary products were monitored (e.g., PFOS, PFOA), these were not observed above blank levels. FOSA is widely acknowledged to be a metabolic precursor of PFOS, and while we examined this reaction using an ECF FOSA standard and microsomes, PFOS was not observed as a product. This is consistent with the findings of Xu et al. [15], in which FOSA was not observed to yield PFOS in microsomal, cytosolic, and 9000 g supernatant fractions; but did yield PFOS in rat liver slices at a low rate. While the ratio of branched to linear PFOS isomers formed from precursor metabolism requires further investigation *in vivo*, it is conceivable that under environmental exposure conditions, in which uptake, biotransformation, and elimination mechanisms occur simultaneously, that unique PFOS and FOSA isomer patterns could be produced following repeated exposure to a PFOS-precursor. This requires further validation, but may be a useful tool for estimating how much human or wildlife PFOS exposure is due to biotransformation of precursor compounds.
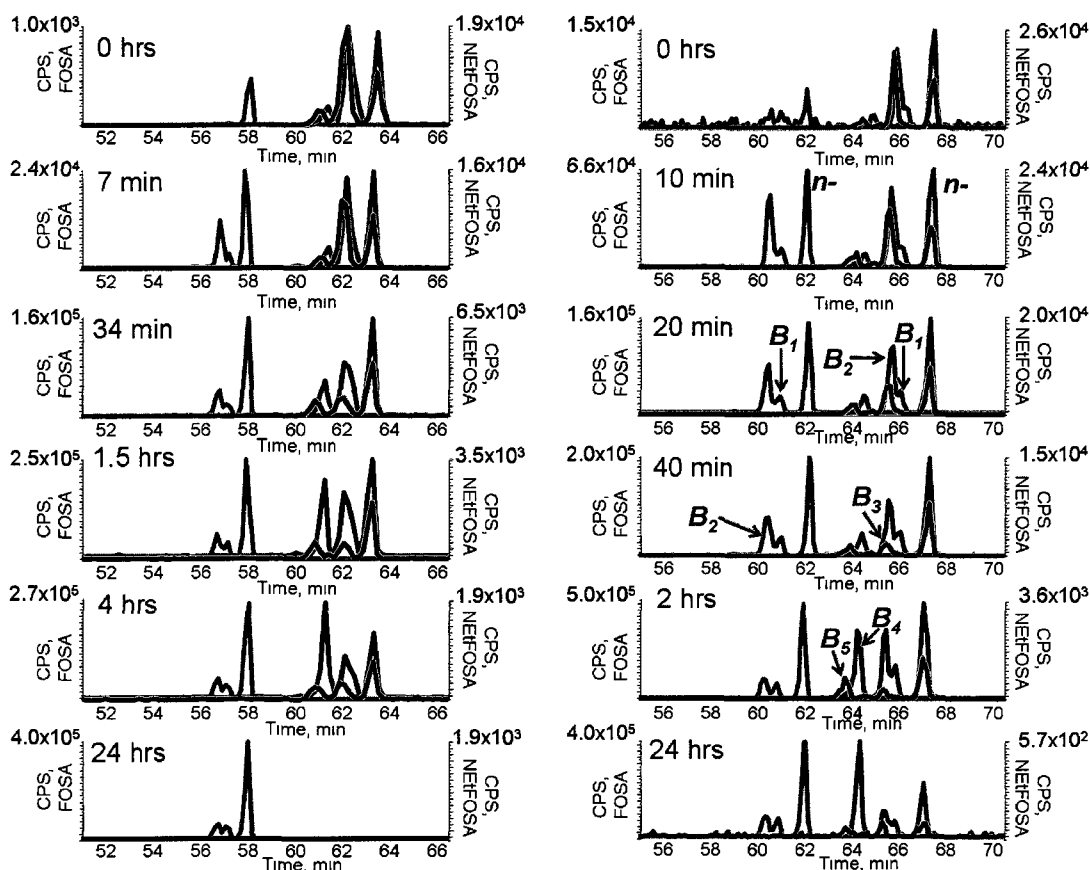
Figure 4.3 N-deethylation of NEtFOSA (red, m/z 269 and black, m/z 219) to FOSA (green, m/z 78) by human liver micrsomes. Left chromatograms are representative of 380 nM NEtFOSA incubations (200 ng in 1 mL total volume, n = 3 replicates), right chromatograms represent 9.5 nM NEtFOSA incubations (5 ng in 1 mL total volume, n = 3 replicates). 380 nM incubations were examined using an API 4000QTRAP, while 9.5 nM incubations were conducted on an API 5000. Both concentrations showed isomer specific biotransformation of substrate. Note similarities in isomer profiles between 380 nM and 9.5 nM incubations at 10 min/7 min, 40 min/34 min, 2hrs/1.5hrs, and 24hrs/4hrs, respectively.

4.4   Significance of Findings

The combined findings from isozyme incubations, that isomer-specific biotransformation rate constants had significant differences at all concentrations, that the rank orders were substantially different using two different isozymes, and that the rank order was unrelated to relative concentration of each isomer in the

mixture (i.e., *n*-NEtFOSA was never the most rapidly transformed, despite being dominant) are unambiguously indicative of an isomer-specific difference in the biotransformation rates of a model PFOS-precursor. These differences were also borne out when human microsomes were used, pointing to the environmental significance of the findings. For example, in microsomes, branched isomers 3 and 5 were observed to have the largest rate constants, consistent with the results for the reaction catalyzed by CYP2C9. Thus the relative isomer profile of a PFOS precursor will not likely be conserved in its metabolites at steady state. However, it is not yet clear if the magnitude of difference will be useful for tracking sources of PFOS exposure (e.g., direct vs precursor exposure), and an *in vivo* exposure using an environmentally relevant PFOS-precursor is warranted.

4.5 Acknowledgments

4.6   References

1.   Giesy, J.P.; Kannan, K. *Environ. Sci. Technol.* **2001**, *35*, 1339-1342.

2.   Kannan, K.; Corsolini, S.; Falandysz, J.; Fillmann, G.; Kumar, K.S.; Loganathan, B.G.; Mohd, M.A.; Olivero, J.; Van Wouwe, N.; Yang, J.H.; Aldoust, K.M. *Environ. Sci. Technol.* **2004**, *38*, 4489-4495.

3.   Calafat, A.M.; Kuklenyik, Z.; Reidy, J.A.; Caudill, S.P.; Tully, J.S.; Needham, L.L. *Environ. Sci. Technol.* **2007**, *41*, 2237-2242.

4.   Olsen, G.W.; Mair, D.C.; Church, T.R.; Ellefson, M.E.; Reagen, W.K.; Boyd, T.M.; Herron, R.M.; Medhdizadehkashi, Z.; Nobiletti, J.B.; Rios, J.A.; Butenhoff, J.L.; Zobel, L.R. *Environ. Sci. Technol.* **2008**, *42*, 4989-4995.

5.   Conder, J.M.; Hoke, R.A.; De Wolf, W.; Russell, M.H.; Buck, R.C. *Environ. Sci. Technol.* **2008**, *42*, 995-1003.

6.   Olsen, G.W.; Burris, J.M.; Ehresman, D.J.; Froehlich, J.W.; Seacat, A.M.; Butenhoff, J.L.; Zobel, L.R. *Environ. Health Perspect.* **2007**, *115*, 1298-1305.

7.   Lau, C.; Thibodeaux, J.R.; Hanson, R.G.; Rogers, J.M.; Grey, B.E.; Stanton, M.E.; Butenhoff, J.L.; Stevenson, L.A. *Toxicol. Sci.* **2003**, *74*, 382-392.

8.   Abbott, B.D.; Wolf, C.J.; Das, K.P.; Zehr, R.D.; Schmid, J.E.; Lindstrom, A.B.; Strynar, M.J.; Lau, C. *Reprod. Toxicol.* **2008**.

9.   Kennedy, G.L., Jr.; Butenhoff, J.L.; Olsen, G.W.; O'Connor, J.C.; Seacat, A.M.; Perkins, R.G.; Biegel, L.B.; Murphy, S.R.; Farrar, D.G. *Crt. Rev. Toxicol.* **2004**, *34*, 351-384.

10.   Wania, F. *Environ. Sci. Technol.* **2007**, *41*, 4529-4535.

11.   Paul, A.G.; Jones, K.C.; Sweetman, A.J. *Environ. Sci. Technol.* **2009**, *43*, 386-386.

12.   Wallington, T.J.; Hurley, M.D.; Xia, J.; Wuebbles, D.J.; Sillman, S.; Ito, A.; Penner, J.E.; Ellis, D.A.; Martin, J.; Mabury, S.A.; Nielsen, O.J.; Sulbaek Andersen, M.P. *Environ. Sci. Technol.* **2006**, *40*, 924-930.

13.   Martin, J.W.; Ellis, D.A.; Mabury, S.A.; Hurley, M.D.; Wallington, T.J. *Environ. Sci. Technol.* **2006**, *40*, 864-872.

14.   D'Eon, J.; Hurley, M.; Wallington, T.J.; Mabury, S.A. *Environ. Sci. Technol.* **2006**, *40*, 1862-1868.

15.   Xu, L.; Krenitsky, D.M.; Seacat, A.M.; Butenhoff, J.L.; Anders, M.W. *Chem. Res. Toxicol.* **2004**, *17*, 767-775.

16.   Martin, J.W.; Mabury, S.A.; O'Brien, P.J. *Chem.-Biol. Interact.* **2005**, *155*, 165-180.

17. Stadalius, M.; Connolly, P.; L'Empereur, K.; Flaherty, J.M.; Isemura, T.; Kaiser, M.A.; Knaup, W.; Noguchi, M. *J. Chrom. A.* **2006**, *1123*, 10-14.

18. 3M Co. 1999. U.S. Environmental Protection Agency public docket AR226-0550: Fluorochemical use, distribution and release overview. U.S. Environmental Protection Agency, Office of Pollution Prevention and Toxic Substances, Washington, DC.

19. Loewen, M.; Wania, F.; Wang, F.; Tomy, G. *Environ. Sci. Technol.* **2008**, *42*, 2374-2379.

20. Kato, K.; Calafat, A.M.; Needham, L.L. *Environ. Res.* **2009**, *109*, 518-523.

21. Vestergren, R.; Cousins, I.T.; Trudel, D.; Wormuth, M.; Scheringer, M. *Chemosphere.* **2008**, *73*, 1617-1624.

22. Tomy, G.T.; Tittlemier, S.A.; Palace, V.P.; Budakowski, W.R.; Braekevelt, E.; Brinkworth, L.; Friesen, K. *Environ. Sci. Technol.* **2004**, *38*, 758-762.

23. Karrman, A.; Langlois, I.; van Bavel, B.; Lindstrom, G.; Oehme, M. *Environ. Int.* **2007**, *33*, 782-788.

24. Benskin, J.P.; Bataineh, M.; Martin, J.W. *Anal. Chem.* **2007**, *79*, 6455-6464.

25.   Haug, L.S.; Thomsen, C.; Becher, G. *Environ. Sci. Technol.* **2009**, *43*, 2131-2135.

26.   Riddell, N.; Arsenault, G.; Benskin, J.P.; Chittim, B.; Martin, J.W.; McAlees, A.; McCrindle, R. *Environ. Sci. Technol.* **2009**, *43*, 7902-7908.

27.   Reagen, W.K.; Lindstrom, K.R.; Jacoby, C.B.; Purcell R.G.; Kestner T.A.; Payfer R.M.; Miller, J.W.; Platform presentation at Society of Environmental Toxicology and Chemistry 28th North American Meeting, Milwaukee, WI, USA, November 11–15, **2007**.

28.   Rayne, S.; Forest, K.; Friesen, K.J. *J. Environ. Sci. Health. A.* **2008**, *43*, 1391-1401.

29.   Chu, S.; Letcher, R.J. *Anal. Chem.* **2009**, *81*, 4256-4262.

30.   Langlois, I.; Berger, U.; Zencak, Z.; Oehme, M. *Rapid Commun. Mass Spectrom.* **2007**, *21*, 3547-3553.

31.   Arsenault, G.; Chittim, B.; Gu, J.; McAlees, A.; McCrindle, R.; Robertson, V. *Chemosphere.* **2008**, *73*, S53-59.

32.   Arsenault, G.; Chittim, B.; McAlees, A.; McCrindle, R.; Riddell, N.; Yeo, B. *Chemosphere.* **2008**, *70*, 616-625.

33. Benskin, J.P.; De Silva, A.O.; Martin, L.J.; Arsenault, G.; McCrindle, R.; Riddell, N.; Mabury, S.A.; Martin, J.W. *Environ. Toxicol. Chem.* **2009**, *28*, 542-512.

34. De Silva, A.O.; Benskin, J.P.; Martin, L.J.; Arsenault, G.; McCrindle, R.; Riddell, N.; Martin, J.W.; Mabury, S.A. *Environ. Toxicol. Chem.* **2009**, *28*, 555-512.

35. Ruisheng, Y. Additional information of production and use of PFOS. Fax from Ministry of Environmental Protection of China. Stockholm Convention Secretatiat, Geneva, Switzerland, **2008**. http://chm.pops.int/Portals/0/Repository/addinfo_2008/UNEP-POPS-POPRC-SUB-F08-PFOS-ADIN-CHI.English.pdf

36. Benskin, J.P.; Arhens, L.W.Y.; Yamashita, N.; Taniyasu, S.; Lam, P.K.S.; Tomy, G.; Muir, D.C.; Scott, B.; Spencer, C.; Rosenberg, B.; Martin, J.W. Platform presentation at Society of Environmental Toxicology and Chemistry 30th North American Meeting, New Orleans, LA, USA, November 19-23, **2009**.

37. Bicking, M.K.L. *LC/GC Eur.* **2006**, *April 1*, 1-8.

38. Obach, R.S.; Reed-Hagen, A.E. *Drug. Metab. Dispos.* **2002**, *30*, 831-837.

39. Segel, I. *Enzyme Kinetics*; John Wiley and Sons: New York, **1975**.

40.   Xu, L.; Krenitsky, D.M.; Seacat, A.M.; Butenhoff, J.L.; Tephly, T.R.;

Anders, M.W. *Drug. Metab. Dispos.* **2006**, *34*, 1406-1410.

Chapter 5. Perfluorinated Acid Isomer Profiling in Water and Quantitative Assessment of Manufacturing Source

Reproduced with permission from: Benskin J.P.; Yeung L.; Yamashita N.; Taniyasu S.; Lam P.; Martin J.W. Perfluorinated acid isomer profiling in water and quantitative assessment of manufacturing source. *Environ. Sci. Technol.* 2010, *44*, 9049-9054. Copyright 2010 American Chemical Society.

5.1   Introduction

Perfluorinated acids (PFAs) and their precursors (PFA-precursors) have been identified as widespread contaminants of the global environment, including remote arctic wildlife[1]. Of the most commonly detected PFAs in the environment, perfluorooctane sulfonate (PFOS, $C_8F_{17}SO_3^-$) and perfluorooctanoate (PFOA, $C_7F_{15}COO^-$) have displayed significant adverse health effects, including an association with low birth weight in humans (PFOS and PFOA)[2] and carcinogenicity in lab animals[3] (PFOA). Due to the hazard profile associated with these chemicals, PFOS and its precursors were recently listed as Annex B persistent organic pollutants under the International Stockholm Convention Treaty.[4] Despite this initiative, production and application continues in developing countries,[5,6] and PFOS concentrations in humans[7] and wildlife[1] from some areas of the world continue to increase. Identification of the exposure sources is important to mitigate future exposure to these chemicals.

Large scale manufacturing of PFOA has taken place by either electrochemical fluorination (ECF) or telomerization. ECF results in a mixture of

branched and linear PFOA isomers, and was used by the major historical PFOA manufacturer, the 3M Co., from the 1950s until 2002; after which the company voluntarily phased out its perfluorooctyl chemistries. PFOA produced by the 3M Co. reportedly had a consistent composition of 78% linear (stdev 1.2%) and 22% branched (stdev 1.2%) isomers, based on ^{19}F-NMR analysis of 18 production lots over a 20 year period.[8] While the extent of current global ECF PFOA manufacturing is largely unknown, large-scale production of linear PFOA has continued since 2002 by telomerization, a process which retains the structure of the starting telogen (typically linear, but isopropyl geometry also possible)[9]. This is considered the dominant global manufacturing process today for perfluorinated carboxylic acids (PFCAs). Among the important questions pertaining to potential regulation of these chemicals, is to what extent PFCAs in the environment can be attributed to ECF (mostly historical production) versus telomerization (ongoing production). Environmental models have predicted that historical emissions of ECF PFOA and slow global transport in oceans, is the dominant source of PFOA to remote marine foodwebs[10,11]. While PFA concentrations determined by trace analysis of seawater[12-15] (including North Atlantic, Greenland, and Norwegian Seas) have been largely consistent with concentrations predicted using models based on the ocean transport global dissemination pathway[11], this agreement does not rule out the importance of alternative pathways, including the long-range atmospheric transport and oxidation of fluorotelomer alcohols.[16] PFOA isomer profiles in polar bears from Greenland and the Canadian Arctic[17], as well as human blood from North America[18,19], are predominantly linear, suggesting a

145

primarily telomer manufacturing source. However, pharmacokinetics studies[20-22] have demonstrated that branched PFOA isomers are preferentially excreted, relative to linear, making quantitative source assignment impossible in such biological samples. Provided that PFOA isomers are unaffected by abiotic isomer fractionation processes in water,[23] samples from industrialized or remote regions may provide an alternative for tracking regional and global sources of PFAs.

Large-scale manufacturing of PFOS has been exclusively by ECF, no telomerization sources are known. From the 1950s to 2002, the majority of PFOS was produced by the 3M Co, and these products had a consistent composition of 70% linear (stdev 1.1%) and 30% branched (stdev 0.8%) isomers, based on ^{19}F-NMR analysis of 8 production lots over 10 years.[8] Production of higher molecular weight perfluorooctane sulfonylfluoride (POSF, $C_8F_{17}SO_2F$) derivatives, such as N-alkyl substituted perfluorooctyl sulfonamides, also had similar isomer compositions.[24] Since the 2002 phase-out, ECF manufacturing of POSF and its derivatives has continued in developing countries, with production volumes increasing towards pre-2002 levels.[5,6] Elucidating the source(s) of PFOS in remote arctic wildlife is difficult since its environmental occurrence can arise from both direct release and slow transport in oceans, or alternatively, from emission of various sulfonamide precursors, to water or air, that may degrade metabolically[25], or through atmospheric oxidation,[26] to PFOS. Examination of PFOS isomer profiles may provide evidence of minor ECF manufacturing sources (i.e. with different isomer patterns than 3M Co. PFOS), transport mechanisms, or may point to differences in the environmental fate of PFOS isomers.

146

Concentrations of PFAs in water can be orders of magnitude lower than in biological samples,[1,12] thus more sensitive PFA isomer profiling methods are necessary, particularly for remote ocean water. Here we describe a sensitive HPLC-MS/MS method for isomer-specific PFA analysis in water, and its application to quantitative manufacturing source determination in samples from Asia, the Mississippi river (U.S.) and North Sea canal (the Netherlands).

5.2 Experimental Methods

5.2.1 Isomer Nomenclature

PFA and PFA-precursor acronyms and empirical formulae are listed in Appendix D (Appendix D, Table D-1). The isomer nomenclature system used here has been used previously[24] for the limited number of isomers actually present in the commercially manufactured PFA- and PFA-precursor formulations. Using PFOA as an example, linear and perfluoroisopropyl branches are abbreviated as *n*- and *iso*-PFOA, respectively. For the remaining monomethyl branched isomers, *m* refers to a perfluoromethyl branch and the number preceding it indicates the carbon position on which the branch resides. Dimethyl substituted branched isomers are labelled as m_2 and the preceding numbers refer to the location(s) of the CF_3 branching points, when these could be structurally confirmed. In all other cases, dimethyl branched isomers were labelled collectively as *dm*. The same nomenclature system was adopted for perfluoroalkyl sulfonates and carboxylates,

however it should be noted that 1m-PFCAs do not exist, since the carbon in the 1-position corresponds to the carboxylate moiety.

5.2.2 Sampling of Coastal Asian Seawater

Coastal Asian samples were provided as extracts and were collected from sites previously analysed for total PFAs[12,27]. Duplicate sub-surface samples were collected from two separate locations (i.e. 2 x 200 mL samples/location), in Tomakomai Bay, Japan, on December 23, 2003. Triplicate subsurface samples (3 x 500 mL) were collected from a single location in Tokyo Bay, Japan, on June 11, 2008. Duplicate samples (2 x 500 mL each) were collected from two locations in the Sea of Japan (Japan Sea site 1, 37° 59.986'N, 135° 36.022'E; Japan Sea site 2, 41° 20.880'N, 137° 19.949'E), Hangzhou (China), and Shanghai (China) in 2008. Travel and procedural blank extracts were provided for each sampling location.

5.2.3 Sampling of Mississippi River Water

Sub-surface grab samples (4 x 500 mL) were collected in polypropylene bottles from the bank of the Mississippi river (29° 57.391'N, 90° 3.689'W) in New Orleans on November 22, 2009. Blanks (2 x 500 mL MilliQ water) were transported to the sampling site, opened, and exposed to air for the duration of sampling.

5.2.4 Sampling North Sea Canal Water

A 1L water sample was obtained as part of the first worldwide interlaboratory study on perfluorinated compounds.[28] The sample was collected from the North Sea canal (the Netherlands) in January, 2005, and suspended solids were removed by filtering the water through 0.45 μm filter paper. Microbial activity was reduced by lowering the pH to 2, and the water was shipped in 1 L brown, high-density polyethylene bottles.[28] Upon receiving the sample, it was stored at 4°C until extraction. Procedural or travel blanks were not provided; however, a laboratory blank was extracted with this sample.

5.2.5 Standards and Reagents

HPLC-grade methanol and methyl *tert*-butyl ether (MTBE) were purchased from Fisher Scientific (Ottawa, ON, Canada). HPLC-grade formic acid (50%) and potassium PFOS (98%) were purchased from Sigma-Aldrich (Oakville, ON, Canada). A full list of standards utilized at the University of Alberta is shown in Appendix D, Table D-1. Lists of all reagents and standards used for collection of Asian samples can be found in Taniyasu et al.[27] and Yamashita et al.[12] 3M (St. Paul, MN, USA) provided ECF PFOS (Lot # 217) and ECF PFOA (Lot # 332). PFOA and potassium PFOS (K-PFOS) from the Wuhan Defu Economic Development Co., Ltd, (Wuhan, China) and K-PFOS and tetraethyl ammonium PFOS (TEA-PFOS) from Wuhan Jinfu Technology

Development Co., Ltd. (Wuhan, China) were also obtained, but lot numbers or further description of these products were not available.

5.2.6 Extraction and Treatment of Samples

Extraction of water samples utilized Oasis® weak anion exchange (WAX; 6 cc, 150 mg, 30 µm; for Coastal Asian samples) or Oasis® hydrophilic-lipophilic balance (HLB; 6 cc, 200 mg, 30 µm; for Coastal Asian, Mississippi river, and North Sea canal water samples) cartridges, which have been previously shown to give consistent results for the quantification of total PFOS and PFOA[27]. Details can be found in the section on *Extraction and treatment of samples*, in Appendix D.

5.2.7 Instrumental Analysis

Isomer separation and total PFOS quantification by liquid chromatography tandem mass spectrometry was adapted from Benskin et al.[19] (discussed in Chapter 2), and utilized a FluoroSep RP Octyl column (3µm, 100A, 15 cm × 2.1 mm, ES Industries, West Berlin, NJ) and triple-quadrupole mass spectrometer (API 5000Q, MDS Sciex, Concord, ON, Canada) operating in negative ion, multiple reaction monitoring (MRM) mode. Details on this method, as well as instrumental modifications to facilitate large volume injections can be found in the sections on *Instrumental modification* and *Instrumental analysis* in Appendix D.

5.2.8 QA/QC

Procedural and sampling blanks were examined for each location (see sampling sections for details), and PFA concentrations observed in blanks were subtracted from samples in all instances. To validate our extraction and quantification methods for total PFAs, concentrations in the North Sea canal sample were compared to assigned values for this sample provided in van Leeuwen et al.[28]. In addition, isomer-specific spike/recovery and standard addition experiments were conducted to confirm that isomer profiles were conserved during extraction and treatment of samples. For coastal Asian samples, 10 ng of 3M ECF PFOS and PFOA were spiked into 0.5 L of Milli-Q water and extracted using WAX or HLB cartridges, as described previously. For North Sea canal and Mississippi river water, 500 mL water spiked with 200 pg ECF PFOS and PFOA was extracted along with real samples using HLB cartridges. Isomer profiles in spiked water were compared to un-extracted standards of 3M ECF PFOS/PFOA.

The potential influence of matrix-induced suppression or enhancement on isomer profiles was examined by comparing Tokyo Bay and Tomakomai Bay seawater extracts using large volume injections with and without a standard addition spike of ECF PFOS and PFOA. These particular extracts were chosen for standard addition experiments because of their relatively large extract volumes, which allowed us to perform multiple 275 µL injections (i.e. with and without

addition of spike). The isomer profiles in the original sample extracts were subtracted from that of the spiked sample, and the results were compared to the original spike of ECF PFOS and PFOA.

5.2.9 Isomer Specific Method Quantification Limits and '% Branched' Dynamic Range

The potential for large volume injections to improve detection of individual PFOS and PFOA isomers was assessed by comparing isomer specific quantification limits from low (10 µL) and high (275 µL) volume injections. Method quantification limits (MQLs) for isomer-specific PFOS and PFOA MRM transitions were defined as the minimum absolute quantity of total 3M ECF PFOS or PFOA producing a signal to noise ratio of 10 for each isomer in any volume of water, following preconcentration to 300 µL.

We also examined how the apparent percent branched PFOA isomer content changed as the branched isomers approached, and dropped below, detection limits. To do this, we injected quantities of ECF PFOA from 0.7 pg up to 7000 pg and plotted the apparent % branched isomer content (i.e. branched peak area in *m/z* 369 product ion / total peak area in *m/z* 369 product ion) versus concentration. A '% branched' dynamic range was calculated, which we defined as the range of total ECF PFOA injected for which the apparent branched content remained stable.

5.2.10 Isomer Identification and Quantification

Details of isomer separation, identification and quantification by LC-MS/MS can be found in this section of Appendix D, and Figures D-1 and D-2. Briefly, the major PFOS isomers (*n, iso, 5m, 4m, 3m, 1m, dm*) were quantified using a characterized technical standard and isomer-specific quantification, while the linear PFOA isomer and major branched PFOA isomers (sum of *iso, 5m, 4m, 3m*-PFOA) were quantified separately from one another using an *n*-PFOA standard. For all other PFAs, linear standards were used for both linear and "total" (i.e. branched + linear isomer) concentrations.

5.2.11 PFOA Source Assignments

For PFOA, additional calculations were performed to assess the contribution from up to three major manufacturing sources: linear-telomer (i.e. 100% *n*-PFOA), isopropyl-telomer (i.e. 100% *iso*-PFOA), and ECF, (~82% linear/18% branched PFOA, by weight, based on LC-MS analysis and an *n*-PFOA standard). We note that other manufacturing techniques have been used for minor production of branched and linear PFCAs (reviewed in [9,24]), however for the purposes of this work we have assumed contributions from these sources to be negligible.

PFOA isomer profiles, expressed as a ratio of each individual branched isomer relative to the linear isomer, were compared to the corresponding profile of an ECF PFOA standard using one-way analysis of variance (ANOVA, SigmaStat Software Inc., San Jose, CA). When a significant difference was

observed between the isomer profile in the sample versus that of the standard, we performed additional ANOVAs on the ratios of 5*m:iso*, 4*m:iso,* and 3*m:iso*-PFOA to determine whether this was strictly a result of additional contributions of *n*-PFOA (in which case these ratios should not be different from that of the standard), or alternatively, differences in the ratios of individual branched isomers, possibly suggesting other sources, or biotic or abiotic fractionation.

When the ratios of 5*m:iso*, 4*m:iso,* and 3*m:iso*-PFOA were not statistically different from ECF standards, we concluded that the difference in overall isomer profiles were a result of additional contributions strictly from a linear-telomer source. We estimated the magnitude of contribution from both ECF and linear-telomer sources using a 10-point calibration curve of % branched versus % ECF, which we prepared by measuring the branched content in standards spiked with known quantities of 3M ECF PFOA and *n*-PFOA.

Samples with contributions from linear-telomer, isopropyl-telomer (assumed, based on patent literature [29]), and ECF sources were indicated by statistically significant differences in *iso:n*, 5*m:n*, 4*m:n,* and 3*m:n*-PFOA as well as 5*m:iso*, 4*m:iso,* and 3*m:iso*-PFOA, but not 4*m*:5*m* and 3*m:*5*m* ratios, compared to ECF standards. For these samples, the above procedure was utilized, but % branched versus % ECF calibration curves were based only on the sum of 5*m*, 4*m*, and 3*m*-PFOA isomers in the *m/z* 369 product ion. The percent contribution of ECF-derived *iso*-PFOA to the total *iso*-PFOA concentration was estimated by dividing the ratio of *iso*-PFOA : branched isomers (sum of 5*m*, 4*m*, and 3*m*-PFOA) in the sample by the corresponding value from our ECF PFOA reference

standard, multiplied by 100%. The concentration of *iso*-PFOA attributed to ECF is then subtracted from the total *iso*-PFOA concentration to obtain the concentration of *iso*-PFOA attributed to telomer manufacturing.

5.3 Results and Discussion

5.3.1 Analytical Method Development and QA/QC

Isomer spike/recovery (Appendix D, Table D-2) and standard addition experiments (Appendix D, Table D-3), indicated that PFOS and PFOA isomer profiles were unaffected by extraction method or matrix effects. Measured versus interlaboratory assigned values[28] for the North Sea canal extract were in good agreement, further validating our extraction and quantification methods (see *QA/QC* section and Table D-4 in Appendix D).

'Percent branched' dynamic range experiments (Figure 5.1) demonstrated that calculated PFOA branched content remained stable following injections of $\geq$ 2 pg and $\leq$ 2000 pg total PFOA. However, when < 2 pg was injected, some branched isomers were below detection limits in the *m/z* 413/369 transition, and with 0.7 pg of total PFOA injected, only the linear isomer was observable, resulting in the % branched being incorrectly calculated as 0%. To the contrary, following injections of >2000 pg total PFOA, enrichment of branched isomers was observed. In this case, the error arises due to gradual detector saturation by the *n*-isomer, resulting in a biased chromatogram that appears enriched in relative branched isomer content (Figure 5.1). Caution is therefore warranted when

examining branched content (PFOS and PFOA) at low or high concentrations in any sample.

After considering the aforementioned quality control, and the vast improvements in MQLs (up to 2 orders of magnitude smaller when using large volume injections; Appendix D, Table D-5), the utility of large volume injections for real samples was apparent, as demonstrated in the case of low concentration samples (e.g. Japan Sea extracts), whereby branched isomers which were not quantifiable by low volume injection but were clearly observed and quantifiable using large volume injection (Appendix D, Figure D-3).
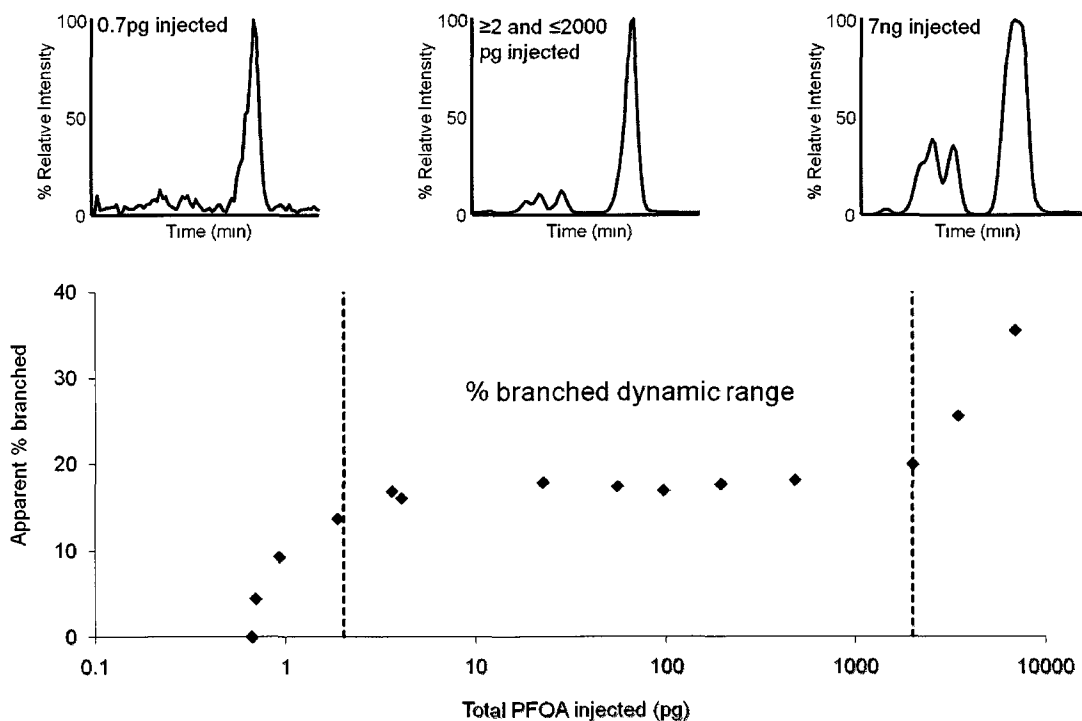
Figure 5.1 The effect on apparent % branched PFOA content (% branched = branched peak area / total peak area) when low, moderate and large quantities of PFOA are injected. When <2pg PFOA is injected, the % of total PFOA attributed to branched isomers is biased low. When quantities of PFOA over 2000 pg are injected, the % branched is biased high.

5.3.2 PFCAs in Coastal Asian Locations

Linear and total (branched+linear) PFA concentrations are given in Table D-4 of Appendix D,. While branched PFOA isomers were detected in all samples from coastal Asia (Figure 5.2) a statistical comparison of isomer profiles revealed significant differences in the branched:n-PFOA isomer ratios (Appendix D, Table D-6) in Tokyo Bay, one location in Tomakomai Bay, and one location in the Japan Sea, compared to 3M ECF PFOA. With the exception of Tokyo Bay, the ratios of $5m{:}iso$, $4m{:}iso$, and $3m{:}iso$-PFOA (Appendix D, Table D-7) were not significantly different than 3M ECF PFOA, indicating that the differences in isomer profile were a result of additional contributions from a linear, presumably telomer, source. For Tokyo Bay, a follow-up statistical analysis of $4m{:}5m$ and $3m{:}5m$ PFOA isomer ratios (Appendix D, Table D-8) revealed no significant differences compared to 3M ECF PFOA, suggesting that the differences in isomer profile were a result of additional contributions from both linear and isopropyl sources. ECF manufacturing accounted for 94, 98, 98, and 100% of total PFOA in Japan Sea site 1, Shanghai, Tomakomai Bay site 1, and Hangzhou, respectively (Appendix D, Table D-9). Total PFOA concentrations at these locations were 4.86, 242, 11.1, and 12.5 ng/L, respectively. Substantially smaller contributions from ECF were observed in Tokyo Bay (33%, 1.76 ng/L total PFOA), Tomakomai Bay site 1 (75% ECF, 14.8 ng/L total PFOA), and Japan Sea site 2 (74% ECF, 2.93ng/L total PFOA). In Tokyo Bay, 14% of total PFOA was attributed to an isopropyl-telomer source.

Tokyo Bay was also unique in that it was the only Asian sample that contained branched isomers of PFCAs greater than C_8. Although these were minor relative to the respective linear isomers, perfluorononanoate (PFNA) had 2 detectable branched isomers, while perfluorodecanoate (PFDA), perfluoroundecanoate (PFUnA) and perfluorododecanoate (PFDoA) each had one detectable branched isomer, confirmed by multiple MRM transitions (Appendix D, Figure D-4). These observations are consistent with analysis of dated sediment cores in Tokyo Bay[30], whereby linear and branched isomers of PFOA, PFNA, PFDA, PFUnA, and PFTrA were observed. Furthermore, the finding of ECF, linear-telomer, and isopropyl-telomer sources is consistent with what is known about regional manufacturing. Small-scale ECF ammonium PFOA manufacturing reportedly took place in Japan from 1947-2002[31], and in 1975 at least one site in Japan began manufacturing it by direct oxidation of perfluorooctyl iodide[31]. Manufacturing of specific branched PFCAs (presumably by telomerization) also reportedly took place in Japan since the mid-1970s,[30] which corroborates the finding of an isopropyl source in this location.

The observation of almost strictly ECF PFOA in Shanghai and Hangzhou (China) (Appendix D, Table D-9) is notable considering the recent increase in large-scale fluorochemical manufacturing in this country, starting in 2003.[5,6] Fluoropolymer manufacturers (which presumably use PFOA as a polymerization aid), are located in southern and eastern China, in particular Hubei, Zhejiang, Fujian, Guangdong and Jiangsu provinces.[7] One source indicated that PFOA is imported by 4 enterprises but not locally manufactured[6], although this requires

158

confirmation. Our analysis of Defu PFOA indicated that it was manufactured by an ECF process, based on the relatively high branched content (~15.1 %), albeit its branched content is slightly less than that in 3M ECF PFOA (~18.0 %). It is unclear if the PFOA obtained from Defu Chemical Co. is representative of all PFOA used in fluoropolymer manufacturing in China, but nevertheless, the differences in branched content (<3%) between these materials is unlikely to be great enough to differentiate them from one another in environmental samples.
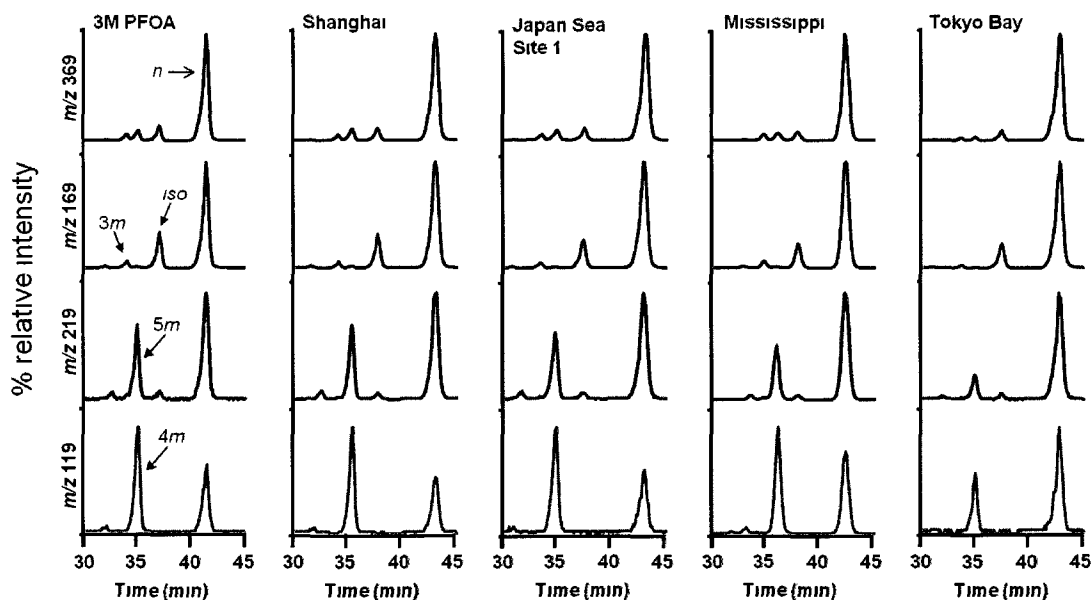
Figure 5.2 PFOA chromatograms in coastal Asian locations and Mississippi river compared to 3M ECF PFOA. Blue tract represents m/z 369; red trace, m/z 169; green, m/z 219, and grey, m/z 119. Note substantial decrease in the signal of 5m-PFOA (m/z 219) and 4m-PFOA (m/z 119) relative to n-PFOA in Tokyo Bay.

159

5.3.3 Perfluoroalkyl Sulfonates and PFOS-Precursors in Coastal Asian Locations

PFOS isomer profiles in coastal Asia appeared similar or slightly enriched in branched isomer content relative to 3M ECF PFOS (Appendix D, Table D-10). Profiles which closely resembled 3M ECF PFOS (72.8% linear) were found in samples from Shanghai (69.3% linear) and Hangzhou (70.8% linear), China. Detailed information on PFOS manufacturing in China is not available, however recent reports indicated that, before 2004, production of perfluorooctane sulfonyl fluoride (POSF)-based products by 15 enterprises was <50 t, but by 2006, this had increased up to 200 t, approximately half of which was exported.[5,6] A total of 66 PFOS-related products have been registered with the Inventory of Existing Chemical Substances in China[6]. Our analysis of three Chinese commercial products from 2 manufacturers revealed all three to be manufactured by an ECF process. n-PFOS accounted for 78.2% of total PFOS in material obtained from the Defu Company, significantly higher than that in 3M ECF PFOS (72.8% linear), Jinfu K-PFOS (69.1% linear), or Jinfu TEA-PFOS (69.2% linear). The relative ratios of individual branched isomers appeared similar between Jinfu (TEA- and K-PFOS) and 3M PFOS, with the exception that *iso* and 5*m*-PFOS were present at slightly higher levels in Defu PFOS, while 3*m*-PFOS was present at slightly lower levels, compared to our 3M ECF PFOS standard. Water samples from Hangzhou and Shanghai, China, were collected in 2008, approximately 5 years after large scale fluorochemical manufacture began in China, and thus it is

conceivable that the isomer patterns measured in these locations represent some average of current and historical ECF manufacturing.

Samples collected at two different locations in Tomakomai Bay contained significantly different n-PFOS content (61.3 vs. 68.6%) and had concentrations nearly two orders of magnitude apart (525 vs. 7.9 ng/L), suggesting at least two different sources of PFOS. The identification of two different sources of PFOS in this location is not surprising, considering that Tomakomai Bay was the site of a local aqueous film-forming foam (AFFF) spill only 3 months prior to sampling.[27] This likely explains the elevated concentrations in Tomakomai Bay site 1, whereas Tomakomai Bay site 2 is likely representative of background levels. However, it is not clear what source might contribute the high percentage of branched isomers here. Further investigation into the isomeric composition of PFOS (and any related precursors) in AFFF foams would be needed to address this. A similar deficiency in n-PFOS was also observed consistently in both Japan Sea samples (60.4 and 61.2% linear at sites 1 and 2, respectively), and to a lesser extent in Tokyo Bay (64.6% linear). A discussion on the possible causes for branched PFOS isomer enrichment is presented in the next section.

PFHxS was detected in most samples, with the exception of Hangzhou and Japan Sea site 2, where PFOS concentrations were also quite low (Appendix D, Table D-4). Elevated PFHxS concentrations in Tomakomai Bay site 1 were consistent with high PFOS concentrations at this location, likely due its presence (as residual or an active component) in AFFF. At least two major branched PFHxS isomers were observed in each sample when n-PFHxS was detected. In

Tomakomai Bay, an additional 3 minor isomers were also observed at both sites. The PFHxS isomer profile in Asian sampling locations was close to that which was observed as residual impurity in the 3M ECF PFOS standard used here.

5.3.4 Mississippi River Water Isomer Profiles

An ECF manufacturing source accounted for 85% of the total PFOA (8.66 ng/L) observed in the Mississippi river water samples, (Appendix D, Table D-9). Considering that a major 3M fluorochemical plant, which utilized ECF PFOA products prior to 2002, is located in St. Paul on the Mississippi River, a high contribution of ECF PFOA is not surprising. The little data that already exists on PFC concentrations in the Mississippi river has focused on the upper Mississippi river basin, where PFC concentrations appear to decrease moving downstream, away from point sources.[32] Interestingly, PFOS concentrations were often greater than PFOA concentrations in the Northern Mississippi river basin, but in the present study, PFOA concentrations were slightly greater than PFOS concentrations, perhaps reflecting the phase-out of 3M PFOS but the ongoing use of PFOA and its telomer precursors.

PFOS in the Mississippi river water samples was enriched in branched isomer content, accounting for 51.9% of total PFOS (7.74 ng/L) compared to 27.2% branched content in our 3M ECF standard (Appendix D, Table D-10). Enrichment of branched PFOS was observed previously in water from Lake Ontario,[33] accounting for 44 – 57% of total PFOS. In that study, sediment was

deficient in branched content (11 − 19%) relative to a technical PFOS standard (23.9% branched), suggesting that *n*-PFOS, being more hydrophobic than branched isomers, may preferentially adsorb to sediments, causing fractionation of the isomer profile, but this requires further validation. Alternatively, low apparent branched content may arise from some branched isomers being below detection limits. Preferential absorption and retention of *n*-PFOS has been observed in rodents[21,22] and fish[34], thus assuming this behaviour is consistent in humans, enrichment of branched PFOS might be expected in waste water treatment plant effluent. Also interesting was the observation of branched FOSA enrichment in the Mississippi, accounting for ~42% of total FOSA, based on quantification with a linear isomer standard (Appendix D, Table D-4). Since PFOS was also enriched, this may suggest that the PFOS and FOSA observed in Mississippi river water may be a result of higher molecular weight precursor biodegradation, or metabolism. Biotransformation of a model PFOS-precursor showed that the branched isomers were metabolized more rapidly[35], which could lead to enrichment of branched FOSA and PFOS. Numerous other possibilities should be considered, including fractionation of the linear isomer to sediment, or boundary layer partitioning.

Minor quantities of branched PFNA and PFUnA were also observed in the Mississippi River, but not to the same extent (relative to the respective linear isomers) as in Tokyo Bay. Others have also observed long chain (i.e. C_9 and greater) PFCA branched isomers in abiotic and biological samples from North America, however their detection is inconsistent.[36,37] The presence of branched

isomers has typically been interpreted as an ECF contribution; however, based on patents describing synthesis of isopropyl PFCAs by telomerization in North America[38], contributions from isopropyl-telomer manufacturing cannot be ruled out. Certainly, our analysis of Tokyo Bay seawater revealed the presence of an isopropyl-telomer source, in addition to ECF and linear-telomer PFOA sources. However, in Mississippi river water, we did not observe a change in the relative ratios of individual branched PFOA isomers, which was the evidence for an isopropyl telomer source in Tokyo Bay. Considering the history of ECF manufacture on the Mississippi river, it is more reasonable that these are a by-product of historical ECF manufacture.

5.3.5 North Sea Canal Water

Of the 18.6 ng/L PFOA present in this sample, 80% was attributed to ECF manufacturing. PFOS isomer profiles were similar to 3M ECF PFOS, with *n*-PFOS accounting for ~66% of total PFOS (18.7 ng/L), sharply contrasting the PFOS isomer profile observed in the Mississippi river. Only 30% of total FOSA (1.4 ng/L) was attributable to branched isomers, which also contrasts the enrichment of branched FOSA observed in the Mississippi river. Branched PFHxS isomer content was similar to what was observed in coastal Asian sampling locations. A single, minor branched isomer of PFNA and PFUnA was also observed, in addition to linear isomers.

5.3.6 Environmental Significance

With the exception of Tokyo Bay, ECF manufacturing is the dominant source of PFOA in the coastal Asian sampling locations, Mississippi river, and North Sea canal water examined here. While for the Mississippi and North Sea canal this is most likely historical ECF, it is not clear whether samples collected in China are a result of current or historical ECF manufacturing. PFOA isomer profiles in Tokyo Bay also contained contributions from three different, presumably local, manufacturing sources, as evidenced by the presence of an isopropyl-telomer source. While we cannot rule out that these isomer profiles have been influenced by abiotic or biological fractionation, the consistent relative ratios of individual branched PFOA isomers, as well as the lack of branched PFOA isomer enrichment (relative to our 3M standard) in *any* sample, suggests little influence of environmental or biological fractionation.

Despite that PFOS was manufactured solely by ECF, there is no clear explanation for the difference in isomer profiles observed in Mississippi river water (48.1% linear) versus coastal Asian locations and the North Sea canal (60 - 70.8% linear). While profiles in China appeared similar to historically manufactured PFOS, we cannot rule out recent local manufacturing of PFOS in this country. Isomer-specific fractionation through biological or abiotic processes may have led to enrichment of branched PFOS content in the Mississippi river and to a minor extent in some coastal Asian samples (in particular, Japan Sea), however it is notable that a deficiency in branched PFOS content was not observed in *any* water sample analyzed here.

Overall, the method reported here addresses the necessary QA/QC considerations and sensitivity to accurately report isomer profiles in low concentration water samples from more remote regions, to which we are currently investigating. These data will ultimately help to test model predictions on the sources and global dissemination pathways of perfluorinated compounds.

5.4   Acknowledgments

5.5   References

1.   Dietz, R.; Bossi, R.; Riget, F.F.; Sonne, C.; Born, E.W. *Environ. Sci. Technol.* **2008**, *42*, 2701-2707.

2. Apelberg, B.J.; Witter, F.R.; Herbstman, J.B.; Calafat, A.M.; Halden, R.U.; Needham, L.L.; Goldman, L.R. *Environ. Health Perspect.* **2007**, *115*, 1670-1676.

3. Lau, C.; Anitole, K.; Hodes, C.; Lai, D.; Pfahles-Hutchens, A.; Seed, J. *Toxicol. Sci.* **2007**, *99*, 366-394.

4. United Nations Environmental Protection Secretariat of the Stockholm Convention on Persistent Organic Pollutants Pollutants. Geneva, Switzerland, **2009**.

5. Wei, Y. Presentation in Workshop on Managing Perfluorinated Chemicals and Transitioning to Safer Alternatives, Geneva, Switzerland, February 12-13, **2009**.

6. Wenya, H. Presentation in Workshop on Managing Perfluorinated Chemicals and Transitioning to Safer Alternatives, Geneva, Switzerland, February 12-13, **2009**.

7. Chen, C.L.; Lu, Y.L.; Zhang, X.; Geng, J.; Wang, T.Y.; Shi, Y.J.; Hu, W.Y.; Li, J. *Chem. Ecol.* **2009**, *25*, 163-177.

8. Reagen, W.K.; Lindstrom, K.R.; Jacoby, C.B.; Purcell R.G.; Kestner T.A.; Payfer R.M.; Miller, J.W.; Platform presentation at Society of Environmental Toxicology and Chemistry 28th North American Meeting, Milwaukee, WI, USA, November 11–15, **2007**.

9.   Kissa, E. *Fluorinated Surfactants and Repellents, 2nd ed*; Marcel Dekker: NewYork, **2005**.

10.   Wania, F. *Environmental science & technology* **2007**, *41*, 4529-4535.

11.   Armitage, J.M.; MacLeod, M.; Cousins, I.T. *Environ.Sci.Technol.* **2009**, 1134-1136.

12.   Yamashita, N.; Kannan, K.; Taniyasu, S.; Horii, Y.; Petrick, G.; Gamo, T. *Mar. Pollut. Bull.* **2005**, *51*, 658-668.

13.   Yamashita, N.; Taniyasu, S.; Petrick, G.; Wei, S.; Gamo, T.; Lam, P.K.; Kannan, K. *Chemosphere.* **2008**, *70*, 1247-1255.

14.   Busch, J.; Ahrens, L.; Xie, Z.; Sturm, R.; Ebinghaus, R. *J. Environ. Monit.* **2010**.

15.   Ahrens, L.; Xie, Z.; Ebinghaus, R. *Chemosphere.* **2010**, *78*, 1011-1016.

16.   Ellis, D.A.; Martin, J.W.; De Silva, A.O.; Mabury, S.A.; Hurley, M.D.; Andersen, M.P.S.; Wallington, T.J. *Environ. Sci. Technol.* **2004**, *38*, 3316-3315.

17.   De Silva, A.O.; Mabury, S.A. *Environ. Sci. Technol.* **2004**, *38*, 6538-6545.

18.   De Silva, A.O.; Mabury, S.A. *Environ. Sci. Technol.* **2006**, *40*, 2903-2909.

19. Benskin, J.P.; Bataineh, M.; Martin, J.W. *Anal. Chem.* **2007**, *79*, 6455-6464.

20. De Silva, A.O.; Tseng, P.J.; Mabury, S.A. *Environ. Toxicol. Chem.* **2008**, *28*, 330-337.

21. Benskin, J.P.; De Silva, A.O.; Martin, L.J.; Arsenault, G.; McCrindle, R.; Riddell, N.; Mabury, S.A.; Martin, J.W. *Environ. Toxicol. Chem.* **2009**, *28*, 542-512.

22. De Silva, A.O.; Benskin, J.P.; Martin, L.J.; Arsenault, G.; McCrindle, R.; Riddell, N.; Martin, J.W.; Mabury, S.A. *Environ. Toxicol. Chem.* **2009**, *28*, 555-512.

23. McMurdo, C.J.; Ellis, D.A.; Webster, E.; Butler, J.; Christensen, R.D.; Reid, L.K. *Environ. Sci. Technol.* **2008**, *42*, 3969-3974.

24. Benskin, J.P.; De Silva, A.O.; Martin, J.W. *Rev. Environ. Contam. Toxicol.* **2010**, 208: 111-160.

25. Xu, L.; Krenitsky, D.M.; Seacat, A.M.; Butenhoff, J.L.; Anders, M.W. *Chem. Res. Toxicol.* **2004**, *17*, 767-775.

26. Armitage, J.M.; Schenker, U.; Scheringer, M.; Martin, J.W.; Macleod, M.; Cousins, I.T. *Environ. Sci. Technol.* **2009**, *43*, 9274-9280.

27. Taniyasu, S.; Kannan, K.; So, M.K.; Gulkowska, A.; Sinclair, E.; Okazawa, T.; Yamashita, N. *J. Chrom. A,* **2005**, *1093*, 89-97.

28. van Leeuwen, S.P.; Karrman, A.; van Bavel, B.; de Boer, J.; Lindstrom, G. *Environ. Sci. Technol.* **2006**, *40*, 7854-7860.

29. Katsushima, A.; Hisamoto, I.; Nagai, M.; Fukui, T.; Kato, T. Japanese Patent No. 0831272 (in Japanese). **1976**.

30. Zushi, Y.; Tamada, M.; Kanai, Y.; Masunaga, S. *Environ. Pollut.* **2010**, *158*, 756-763.

31. Prevedouros, K.; Cousins, I.T.; Buck, R.C.; Korzeniowski, S.H. *Environ. Sci. Technol.* **2006**, *40*, 32-44.

32. Nakayama, S.F.; Strynar, M.J.; Reiner, J.L.; Delinsky, A.D.; Lindstrom, A.B. *Environ. Sci. Technol.* **2010**, *44*, 4103-4109.

33. Houde, M.; Martin, J.W.; Letcher, R.J.; Solomon, K.R.; Muir, D.C. *Environ. Sci. Technol.* **2006**, *40*, 3463-3473.

34. Sharpe, R.L.; Benskin, J.P.; Laarman, A.L.; MacLeod, S.M.; Martin, J.W.; Wong, C.S.; Goss, G.G. *Environ. Toxicol. Chem.* **2010**, *29,* 1957-1966.

35. Benskin, J.P.; Holt, A.; Martin, J.W. *Environ. Sci. Technol.* **2009**, *43*, 8566-8566.

36. Furdui, V.I.; Helm, P.A.; Crozier, P.W.; Lucaciu, C.; Reiner, E.I.; Marvin, C.H.; Whittle, D.M.; Mabury, S.A.; Tomy, G.T. *Environ. Sci. Technol.* **2008**, *42*, 4739-4744.

37. De Silva, A.O.; Muir, D.C.; Mabury, S.A. *Environ. Toxicol.Chem.* **2009**, 28, 1801-1815.

38. Millauer, H. United States Patent No. 3,829,512. **1974**.

Chapter 6. Perfluorinated Acid Isomer Profiles in Water from Remote Locations

In preparation for submission to Environ Sci Technol.

Author list: Benskin, J.P.; Ahrens, L.; Tomy, G.; Muir, D.; Scott, B.; Spencer, C.; Rosenburg, B.; Martin, J.W.

6.1 Introduction

Perfluorinated acids (PFAs) and their precursors (PFA-precursors) have been manufactured for over 60 years for use in various commercial products and processes. These substances can have considerable long range transport[1] and bioaccumulation[2] potentials, and have been identified as widespread contaminants of the global environment, including remote arctic wildlife[3]. Perfluorooctane sulfonate (PFOS, $C_8F_{17}SO_3^-$) and perfluorooctanoate (PFOA, $C_7F_{15}COO^-$) are two of the most commonly detected PFAs in the environment which have displayed significant adverse health effects, including an association with low birth weight in humans (PFOS and PFOA)[4] and carcinogenicity in lab animals[5] (PFOA). Despite increased international concern regarding these chemicals,[6] their production and use continues in developing countries,[7] and PFOS concentrations in humans[8] and wildlife[9] from some parts of the world continue to increase.

Two large-scale manufacturing techniques have been used to produce PFOA, and these can be distinguished by the isomeric purity of the final product. Electrochemical fluorination (ECF) results in a mixture of branched and linear isomers while telomerization typically results in a pure linear product. It is

estimated that the majority (80-90% in 2000, [10]) of global PFOA manufacturing from the 1950s until 2002 was predominantly by ECF by the 3M Co. This product had a consistent isomer composition of 78% linear (stdev 1.2%) and 22% branched (stdev 1.2%), based on analysis of 18 production lots over a 20 year period.[11] The 3M Co. voluntarily phased out ECF manufacture of perfluorooctyl chemistries in 2002, but the extent of current ECF PFOA manufacturing by other companies is largely unknown. Large-scale production of linear PFOA has continued since 2002 by telomerisation, a technique originally patented by DuPont, and used since the 1970s, which retains the structure of the starting telogen (typically linear, but isopropyl geometry also possible) in the final material[12]. Telomerization is considered the dominant global manufacturing process today for perfluorinated carboxylic acids (PFCAs) and fluorotelomer products (i.e. $CF_3(CF_2)_xC_2H_4R$) some of which can degrade to form PFCAs in the environment. The extent to which ECF (mostly historical production) versus telomer (mostly current production) manufacturing contribute to PFOA concentrations in remote marine food webs (today and in the future) has important implications towards regulation of these chemicals. Environmental models have predicted that historical emissions of ECF PFOA and slow global transport in oceans are the dominant source of PFOA in remote regions[10,13-15]. While PFA concentrations determined by trace analysis of seawater[16-19] (including North Atlantic, Greenland, and Norwegian Seas) have been largely consistent with concentrations predicted using models based on the ocean transport global dissemination pathway[14], this agreement does not rule out the importance of

alternative pathways, including the long-range atmospheric transport and oxidation of fluorotelomer alcohols,[20] or possibly PFOA itself, via marine aerosols[21].

Large-scale manufacturing of PFOS and PFOS-precursors (e.g. N-alkyl substituted perfluorooctyl sulfonamides, $C_8F_{17}SO_2NHR$) has been exclusively by ECF. PFOS manufactured by the 3M Co. from the 1950s to 2002 had a consistent isomer composition of 70% linear (stdev 1.1%) and 30% branched (stdev 0.8%), based on analysis of 8 production lots over 10 years.[11] Production of PFOS precursors (e.g. N-alkyl substituted perfluorooctyl sulfonamides) from their starting material, perfluorooctane sulfonylfluoride (POSF, $C_8F_{17}SO_2F$), also reportedly had similar isomer compositions to PFOS itself.[22] Since the 2002 phase-out, minor ECF manufacturing of POSF and its derivatives has continued in developing countries, with production volumes increasing towards pre-2002 levels.[7] Elucidating the source(s) of PFOS in remote arctic wildlife is difficult since its environmental occurrence can arise from multiple sources, including direct release and slow transport in oceans, atmospheric transport of volatile precursors followed by abiotic degradation, or alternatively, atmospheric transport of volatile precursors followed by partitioning and biodegradation.[23] While it is unclear which pathway is the dominant contributor to PFOS concentrations in remote locations, most data appears to support either direct release and slow transport in oceans, or atmospheric transport followed by exposure and biodegradation of precursors. PFOS concentrations in ringed seals[24] and polar bear[9] from Greenland and guillemot eggs[25] from the Baltic Sea have either shown

no decrease or an increase since 2000, consistent with continued exposure from slow, oceanic transport. In contrast, Canadian Arctic Ringed seals[26] and Alaskan Sea otters[27] show a rapid decline in PFOS concentrations consistent with the 2002 phase-out, suggesting fast atmospheric transport followed by exposure and subsequent biodegradation of precursors. Contrary to both routes, PFOS concentrations in Swedish Peregrine Falcon eggs levelled off in the mid 1980s[28], suggesting different routes of exposure for marine and terrestrial biota.

While PFA isomer profiles may provide a tool for elucidating manufacturing source (historical versus current), and/or global transport mechanism(s), biological[29-31] or abiotic[21,32] isomer fractionation processes may need to be considered when interpreting isomer profiles in environmental samples. Nonetheless, a preliminary survey of PFOA isomer profiles in water from source regions revealed branched isomer ratios which were not significantly different from an ECF standard[33] (discussed in Chapter 5), thus PFOA isomer profiles in remote water are expected to be useful for quantitative source assessment. In contrast, PFOS has only been manufactured by ECF; therefore isomer profiles in remote regions may represent a combination of transport pathway and exposure source (i.e. direct versus indirect exposure). The present study examines isomer profiles of PFOA, PFOS, and other PFAs and PFA-precursors in seawater from the Atlantic, Norwegian/North Sea, and Baffin Bay. For PFOA, results are presented as the % contribution of ECF-manufacturing to total PFOA concentrations, or "% ECF", while PFOS isomer data are presented as % branched, on a weight basis.

6.2 Experimental Methods

6.2.1 Isomer Nomenclature

PFA and PFA-precursor acronyms and empirical formulae are listed in Appendix E (Table E-1). The isomer nomenclature system used here has been used previously[33] for the limited number of isomers actually present in the commercially manufactured PFA- and PFA-precursor formulations. Using PFOA as an example, linear and perfluoroisopropyl branches are abbreviated as *n*- and *iso*-PFOA, respectively. For the remaining monomethyl branched isomers, *m* refers to a perfluoromethyl branch and the number preceding it indicates the carbon position on which the branch resides. Dimethyl substituted branched isomers are labelled as m_2 and the preceding numbers refer to the location(s) of the CF_3 branching points, when these could be structurally confirmed. In all other cases, dimethyl branched isomers were simply labelled collectively as *dm*. The same nomenclature system was adopted for perfluoroalkyl sulfonates and carboxylates, however it should be noted that 1*m*-PFCAs do not exist, since the carbon in the 1-position corresponds to the carboxylate moiety.

6.2.2 Atlantic Ocean, North and Norwegian Sea Sampling Campaigns

Surface water samples were collected from the research vessel *Polarstern* (Alfred-Wegener-Institut (AWI), Bremerhaven) from Oct 29 to Nov 22, 2007 (Atlantic samples) and August 14-17, 2007 (North and Norwegian Seas). Sampling locations are shown in Figures 6.1 and 6.2. Two litre water samples were collected in brown glass bottles via a ship intake system at approximately 11

m below the surface, or were dropped under water by a sampler at 2 m or directly at the surface. These samples were provided as extracts and had been previously analyzed for total PFAs, results of which can be found in Ahrens et al 2009[34] and Ahrens et al. 2010[35].
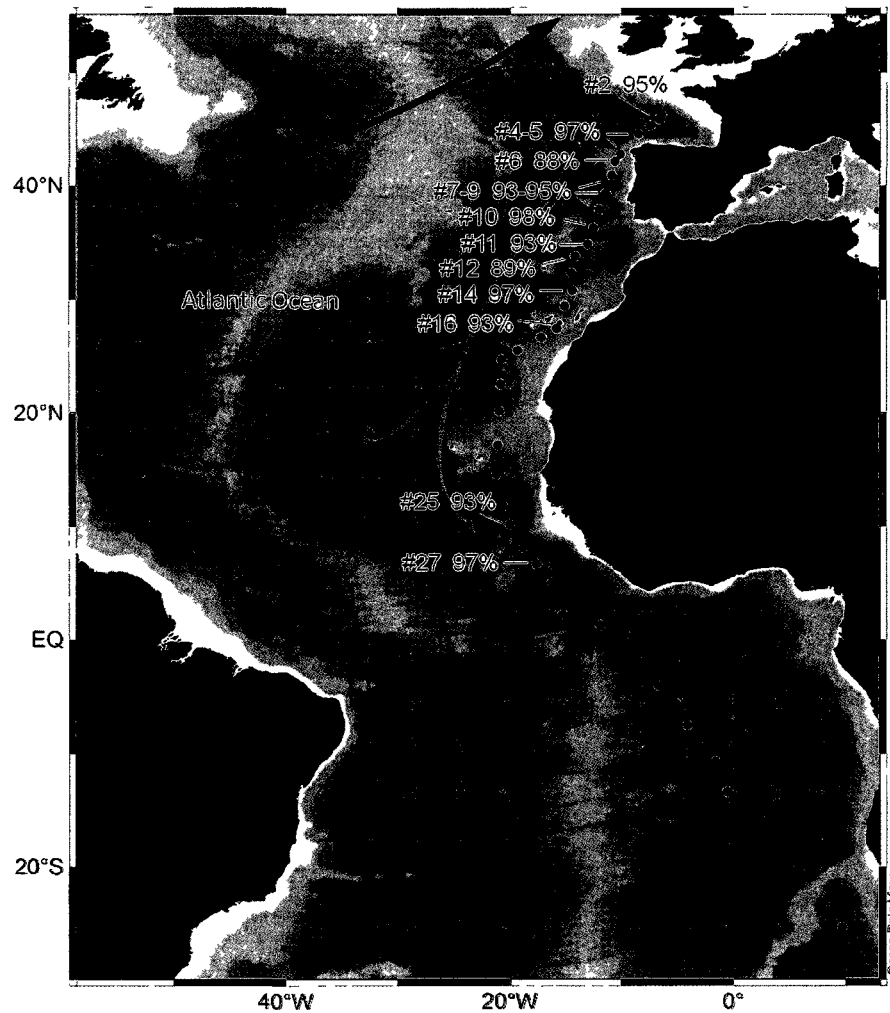
Figure 6.1 Atlantic sampling locations and % ECF PFOA plotted using Ocean Data View[36]. North Atlantic current is shown in orange and Canary current is shown in yellow.
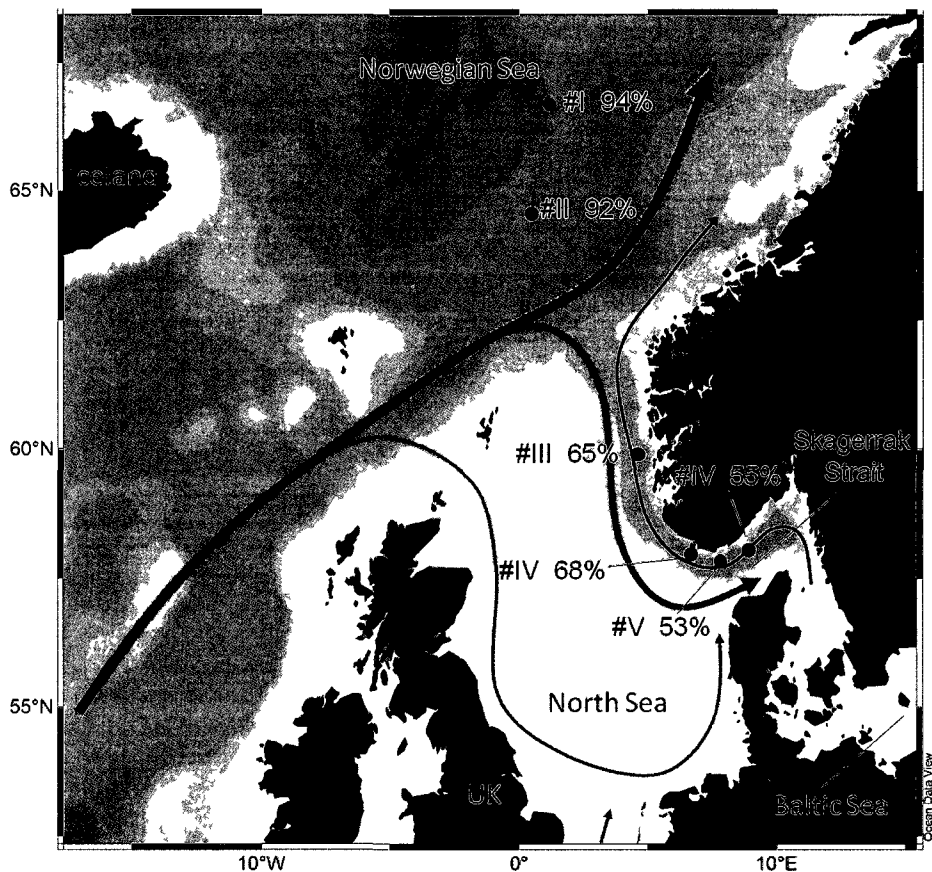
Figure 6.2 Sampling locations, water circulation, and % conbtribution of ECF PFOA to total PFOA in Norwegian and North Sea sampling locations, using plotted using Ocean Data View[36]. Arrows represent general flow of Atlantic water (orange) and Norwegian coastal water (blue), with mixing in Skagerrak Straight[37,38]. Note almost exclusive contribution of ECF source in Norwegian sea, with inreasing contributions of linear-telomer PFOA in the North Sea and in Skaggerak Strait.

Water samples were filtered through a glass fibre filter (GFF, Whatman, ø 47 mm) on the same day of sampling; the water phase was stored at 4°C and the GFF at -20 °C. The water phase and the GFF were spiked with 100 µL IC-mix (10 ng absolute) separately. The filtrate was spiked with the IS and extracted by solid phase extraction (SPE) with Waters Oasis WAX cartridges (150 mg, 6 cm^3, 30 µm). After preconditioning with 5 mL methanol and Millipore water, the cartridge

178

was loaded with a two litre sample at approximately 4 drops sec^{-1}. The cartridge was then washed with 5 mL 0.1% formic acid in Millipore water and dried for 30 min. After loading and drying on the ship, the cartridges were stored at -20 °C and eluted in a clean lab at GKSS Research Centre (Geesthacht, Germany). Perlfuoroalkyl sulfonamides were eluted with 14 mL acetonitrile while perfluoroalkyl sulfonates and carboxylates were eluted with 5 mL 0.1% ammonium hydroxide in methanol. The extract was reduced under nitrogen and then made up to <500 μL with 50:50 MeOH/water. The samples were then shipped to Alberta.

6.2.3 Baffin Bay and Lancaster Sound Sampling Campaign

Spatial and depth samples were collected in Baffin Bay and Lancaster Sound in September, 2008, at sites shown in Figure 6.3. These samples were provided as extracts which were analyzed previously for total PFAs. Extraction of these samples was accomplished as follows: Waters Oasis WAX cartridges (150 mg, 6 cc) were conditioned in a clean room with 4mL 1% ammonium hydroxide/methanol solution, 4 mL methanol and 4 mL SPE cleaned OmniSolv water. The cartridge was then placed in a 50 mL polypropylene tube, sealed with wax film and shipped to the field. Surface water samples (4-5 m depth) were collected in Niskin bottles and transferred immediately into 4 L polypropylene bottles (PPB). A Rosette sampler was used to collect seawater samples at varying depths. Sampled water (1-4 L) was pumped through the SPE cartridges at 5-10 mL/min. Cartridges were then placed into the 50 mL tube and shipped back to

179

Environment Canada laboratories. Prior to elution, cartridges were centrifuged in the travel centrifuge tube for 2 min at 3000 rpm to remove residual water and then rinsed with 4 mL methanol at rate of 1 drop/sec. PFAs were eluted with 6 mL of 0.1% ammonium hydroxide/methanol solution into a 15 mL polypropylene tube. Extracts were reduced in volume to 0.5ml, transferred to microvial, and shipped to Alberta following total PFA analysis.
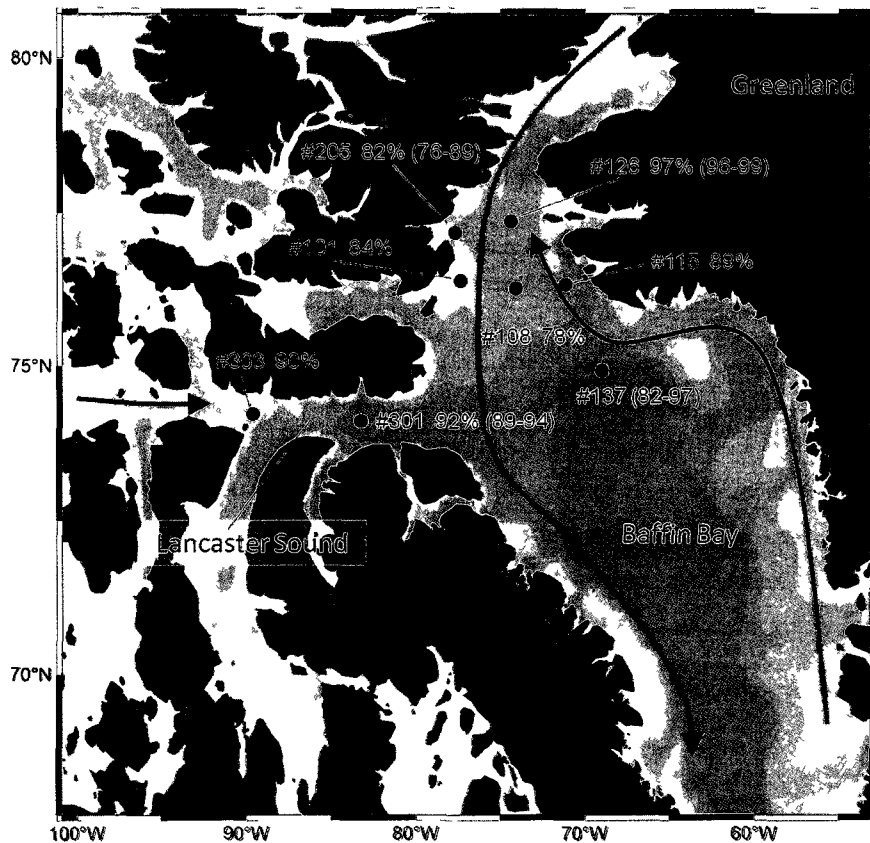
Figure 6.3 Baffin Bay/Lancaster Sounds sampling locations, % contribution of ECF manufacturing source, and regional water circulation, plotted using Ocean Data View[36]. Arrows represent general flow of West Greenland current (blue), Baffin current (orange), and water flowing through Canadian Archipaeligo (red)[39,40]. Stations 101, 108, 115, and 303 were single surface samples. Values shown for stations 126, 137, 205 and 301 are averages of all depths, with the range shown in parentheses.

6.2.4 Instrumental Analysis

Isomer separation and total PFOS quantification by liquid chromatography tandem-mass spectrometry utilized a FluoroSep RP Octyl column ($3\mu m$, 100A, 15 cm × 2.1 mm, ES Industries, West Berlin, NJ) and triple-quadrupole mass spectrometer (API 5000Q, MDS Sciex, Concord, ON, Canada) operating in negative ion, multiple reaction monitoring (MRM) mode. Details of this method have been published previously[33,41] and are discussed in Chapters 2 and 5. Each sample was received as an extract and no manipulation of these extracts were made prior to analysis (including dilution/evaporation). All extracts were provided in 50:50 MeOH: water and total volumes were estimated visually to determine feasible injection volumes. To achieve accurate sensitivity, in all instances the "whole" sample (~92% of estimated total volume) was injected. Injections were typically 100-275μL, but in some instances were as low as 50 μL depending on the volume of extract received.

6.2.5 QA/QC

Procedural and sampling blanks were examined for each location and PFA concentrations observed in blanks were subtracted from samples in all instances. Details of spike/recovery experiments, assessment of matrix effects, % branched dynamic range, and PFA isomer limits of detection can be found elsewhere[33] and are discussed in Chapter 5.

6.2.6 Standards and Reagents

HPLC-grade methanol was purchased from Fisher Scientific (Ottawa, ON, Canada). HPLC-grade formic acid (50%) was purchased from Sigma-Aldrich (Oakville, ON, Canada). A full list of standards utilized at the University of Alberta is shown in Table E-1 of Appendix E.

6.2.7 Isomer Identification and Quantification

Details of isomer separation, identification,n and quantification by LC-MS/MS can be found elsewhere[33] and are discussed in Chapter 5. Briefly, the major PFOS isomers (n, iso, $5m$, $4m$, $3m$, $1m$, $\sum dm$) were quantified using a characterized technical standard (brPFOSK, Wellington Labs, Guelph, ON, Canada) and isomer-specific quantification. For PFOA, an n-PFOA standard was used to quantify both total PFOA (i.e. sum of n, iso, $5m$, $4m$, $3m$-PFOA peaks in m/z 369 product ion) as well as strictly n-PFOA. PFOA isomer ratios were determined by integrating the peak area of each individual PFOA isomer in isomer-specific transitions. For all other PFAs, linear standards were used for determining both linear and "total" (i.e. branched + linear isomer) concentrations.

6.2.8 PFOA Source Assignments

For PFOA, additional calculations were performed to assess the contribution from up to three major manufacturing sources: linear-telomer (i.e. 100% n-PFOA), isopropyl-telomer (i.e. 100% iso-PFOA, assumed, based on patent literature[42,43]), and ECF, (~82% linear/18% branched PFOA, by weight, based on LC-MS analysis and an n-PFOA standard). It is acknowledged that other

manufacturing techniques have been used for minor production of branched and linear PFCAs (reviewed in[44,45]), however for the purposes of this work we have assumed contributions from these sources to be negligible. Details of these calculations, including validation and limitations, can be found elsewhere[33] and are discussed in detail in Chapter 5. Since only a single sample was collected at each sampling site, we assumed the standard deviation of each measurement using the % relative standard deviation of 4 replicate analyses of 3M ECF PFOA at low concentration (<200pg/L).

PFOA isomer profiles (i.e. branched:*n*-PFOA isomer ratios) were compared to the corresponding profile of an ECF PFOA standard using one-way analysis of variance (ANOVA, SigmaStat Software Inc., San Jose, CA). When a significant difference was observed between the isomer profile in the sample versus that of the standard, we performed additional ANOVAs on the ratios of 5*m:iso*, 4*m:iso,* and 3*m:iso*-PFOA to determine whether this was strictly a result of additional contributions of *n*-PFOA (in which case these ratios should not be different from that of the standard), or alternatively, differences in the ratios of individual branched isomers, possibly suggesting other sources, or biotic or abiotic fractionation.

When the ratios of 5*m:iso*, 4*m:iso,* and 3*m:iso*-PFOA were not statistically different from ECF standards, we concluded that any significant differences in overall isomer profiles were a result of additional contributions from a linear-telomer source. We estimated the magnitude of contribution from both ECF and linear-telomer sources using a 10-point calibration curve of % branched PFOA

versus % ECF PFOA (chromatograms shown in Appendix E, Figure E-1), which we prepared by measuring the branched content in standards spiked with known quantities of 3M ECF PFOA and *n*-PFOA.

As discussed in chapter 5, samples with contributions from linear-telomer, isopropyl-telomer, and ECF sources were indicated by statistically significant differences in *iso:n*, *5m:n*, *4m:n*, and *3m:n*-PFOA as well as *5m:iso*, *4m:iso*, and *3m:iso*-PFOA, but not *4m:5m* and *3m:5m* ratios, compared to ECF standards. For these samples, the above procedure was utilized, but % branched versus % ECF calibration curves were based only on the sum of *5m*, *4m*, and *3m*-PFOA isomers in the *m/z* 369 product ion. The percent contribution of ECF-derived *iso*-PFOA to the total *iso*-PFOA concentration was estimated by dividing the ratio of *iso*-PFOA : branched isomers (sum of *5m*, *4m*, and *3m*-PFOA) in the sample by the corresponding value from the ECF PFOA reference standard, multiplied by 100%. The concentration of *iso*-PFOA attributed to ECF is then subtracted from the total *iso*-PFOA concentration to obtain the concentration of *iso*-PFOA attributed to telomer manufacturing.

6.3   Results and Discussion

6.3.1   Atlantic Ocean

Total PFOA concentrations were similar to those reported previously in Ahrens et al.[34] for this sample set (Appendix E, Table E-2). Visual inspection of PFOA isomer chromatograms (Figure 6.4) revealed that ECF manufacturing was responsible for the majority of PFOA (i.e. >89%) in these samples. Nonetheless,

significant differences in individual branched isomer:n PFOA isomer ratios were observed in most samples (Appendix E, Table E-3), and with the exception of samples 1, 3, 6, 16, 19, and 26, these differences were a result of additional contributions (up to 11%) from a linear-telomer PFOA source (indicated by non-significant differences in branched:iso-PFOA ratios, Appendix E, Table E-4). Samples 6 and 16 were found to contain minor contributions (8 and 6%, respectively) of PFOA from a strictly isopropyl source (indicated by significant differences in branched:iso-PFOA ratios but not $3m$:$5m$ and $4m$:$5m$-PFOA ratios, Appendix E, Table E-5). Samples 1, 3, 19, and 26 were slightly enriched in branched content (up to 5.4% more than our ECF PFOA standard), above what would be expected from analytical variability ($P<0.05$). For samples 3 and 26, this difference was simply a deficiency in n-PFOA, with the relative ratios of branched isomers remaining the same as ECF-PFOA. However, for samples, 1 and 19, the relative ratios of branched isomers were significantly ($P<0.05$) different (albeit visually subtle, see chromatogram of sample 1 in Figure 6.4) from the corresponding values in 3M ECF PFOA. Due to this enrichment, we were unable to calculate % ECF values for samples 1, 3, 19, and 26. It is unclear what may have caused this fractionation; 2 of the samples (samples 1 and 3) were both collected in the Bay of Biscay, an area which contained the highest concentrations of PFOA out of all Atlantic sampling sites. Nonetheless, other samples (2 and 4) collected in the Bay of Biscay showed no enrichment. McMurdo et al.[21,32] suggested that fractionation of PFOA isomers could occur at the surface boundary layer, resulting in enrichment of branched content. Presumably, turbulent sea state

185

could enhance this phenomenon; however weather conditions and sea state were not recorded at the time of sampling.

Total PFOS concentrations were generally consistent with those reported previously[34] (Appendix E, Table E-6) and PFOS isomer profiles were either similar, or slightly enriched in branched content compared to 3M ECF PFOS (< 8% difference in branched content; Appendix E, Table E-6). For samples 8, 12, and 14, total branched content may be under-reported by up to a few percent due to the non-detection of 1*m*-PFOS. These profiles are generally consistent with PFOS isomer profiles observed in coastal Asia and the North Sea Canal[33], but contain much less branched content than that observed in the Mississippi river[33]. In comparison, perfluorooctane sulfonamide (FOSA; a known PFOS-precursor) branched content varied from 9-18% (Appendix E, Table E-8), albeit this is based on the sum of 3 branched isomer peaks in the *m/z* 498/78 transition, and is unlikely representative of the true weight % of FOSA isomers. Linear regressions between % branched PFOS, % branched PFOA, and % branched FOSA revealed no significant associations (P<0.05).

We attempted to examine the isomer profile of PFHxS, however *m/z* 99 and 80 product ions contained multiple co-eluting interferences, and the *m/z* 119 ion was not sensitive enough to quantify branched isomers. As a result, only the concentration of the linear isomer (Appendix E, Table E-7) is reported, and we cannot rule-out the presence or absence of branched PFHxS isomers. Examination of longer chain perfluorocarboxylates revealed almost exclusively linear signatures (Appendix E, Table E-7). A tentative branched PFNA isomer was

186

detected intermittently in m/z 169 and 219 product ions, but this was always <1%

of the peak area of the linear isomer and was therefore not quantified. Since this

tentative isomer did not appear to produce a m/z 419 product ion, we ruled it out

as *iso*-PFNA. $3,7m_2$-PFDA was also detected in samples 1 and 2 at concentrations

close to that of the *n*-PFDA, and this was confirmed by an authentic standard (See

Ahrens et al.[34]). This was indeed surprising, as large-scale manufacturing of this

isomer has not been reported in the scientific literature, but nevertheless, it is

commercially available through Alfa Aesar (Windham, NH, USA; previously

Lancaster Synthesis)[34]. Detection of single, branched isomers of long-chain

PFCAs (i.e. >C8) at elevated concentrations is not without precedent. For

example, Furdui et al.[46] detected single branched isomers of PFUnA and PFTrA

in Lake trout from Lake Ontario and suspended sediments from the Niagara river

at elevated levels, and De Silva et al. reported the presence of branched PFNA,

PFDA, PFUnA, and PFDoA isomers in North American environmental samples[47].
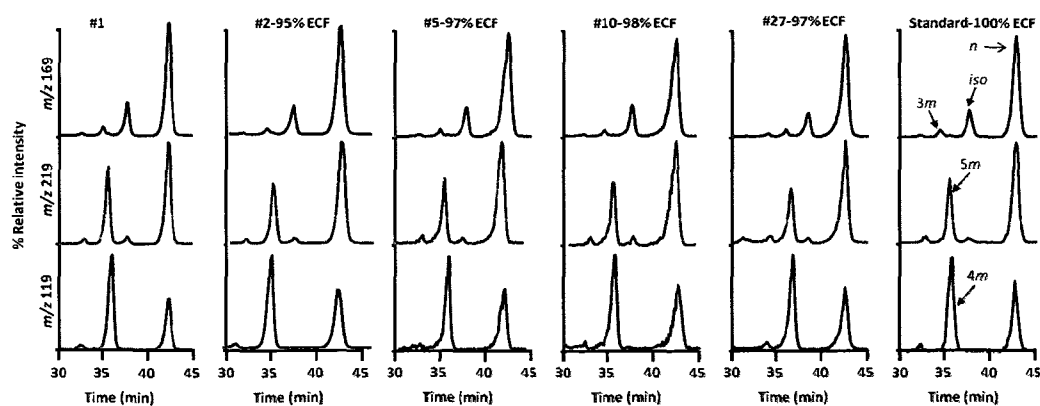
Figure 6.4 PFOA chromatograms from Atlantic sampling sites. Blue traces represent m/z 413/169; red, m/z 413/219; green m/z 413/119. Sample 1 showed a unique profile and thus % ECF was not calculated for this sample. Values shown are sampling site # and % ECF.

6.3.2 Norwegian and North Seas

Total PFOA concentrations in samples III-VI (Appendix E, Table E-2) were in general agreement with the results of Ahrens et al.[35], while concentrations in samples I and II were slightly higher in the present study (92-94 vs ~10 pg). PFOA isomer chromatograms for these locations are shown in Appendix E, Figure E-2, and ECF contributions are shown in Figure 6.2 and in Table E-2, Appendix E. The *3m:n*, *4m:n*, *5m:n*, and *iso:n*-PFOA ratios in all six locations were significantly different from corresponding values in 3M ECF PFOA, and were attributable to additional contributions from a linear-telomer PFOA source. For samples collected in the Norwegian Sea (I and II), this contribution was minor (up to 6% telomer PFOA); however, moving southeast into the North Sea and Skagerrak Strait (between Norway and Denmark), the contribution of *n*-PFOA increased, accounting for 32-35% in samples III and IV and 45-47% in samples V and VI. Samples I and II are influenced predominantly by Atlantic water, via the North Atlantic and Norwegian Atlantic currents. Considering that the Canary Current is also influenced by the North Atlantic current, it is not surprising that both Atlantic and Norwegian Sea samples all showed similar high ECF content; both appear to be influenced by a predominantly ECF signature in the North Atlantic current.

The increase in linear-telomer contribution in samples III-VI, which was accompanied by an increase in the total PFOA concentration, likely arises from elevated concentrations (up to several ng/L) in the Baltic Sea and German coast, as reported previously in Ahrens et al.[35] Approximately 50% of Atlantic water

188

entering the North Sea is mixed with brackish water from the Baltic before it leaves the North Sea as the Norwegian Coastal current. This mixing occurs predominantly in Skagerrak Strait[37,38], where samples V and VI were collected. Considering the relative contributions of Atlantic and Baltic water to this area, and the fact that Atlantic water contains a predominantly ECF PFOA signature, it is reasonable to speculate that water in the Baltic may contain a predominantly linear-telomer PFOA signature. According to Moller et al.[48] and Pistochi et al.,[49] fluoropolymer industries located near the Scheldt (Netherlands), Elbe (Germany), and Rhine (Germany) river basins are important sources of perfluorinated acids to the North Sea, while industries located near the Oder river basin (Germany/Poland) are expected to contribute significantly to PFA concentrations in the Baltic Sea. Further PFOA isomer profiling should be conducted in this region to gain a more comprehensive picture of current use PFOA in this region. In general, it appears that PFOA in the Norwegian Sea is more representative of historical (ECF) PFOA in the North Atlantic current, while concentrations in the North Sea/Baltic appear to be influenced by current manufacture/ use of linear PFOA.

Like PFOA, total PFOS concentrations (Appendix E, Table E-6) also increased as the distance from the sampling location to the Baltic Sea decreased; however this was not accompanied by a change in isomer profile, as was observed for PFOA. PFOS isomer profiles appeared similar or slightly enriched in branched content relative to 3M ECF PFOS (Appendix E, Table E-6), consistent with profiles observed in Atlantic samples. FOSA branched content was also similar to

189

that observed in Atlantic samples, varying from 81-97%; however, linear regressions with longitude, latitude, branched PFOS or branched PFOA revealed no significant correlations (P>0.05). Notably, sample III, which had the highest total FOSA concentration, also contained the least branched content (3.1%). Long chain (i.e. >C_8) PFCA concentrations for North and Norwegian Seas are provided in Table E-8 of Appendix E. Only linear isomers were detected at these sampling sites. PFNA concentrations (44-137 pg/L) were higher than those reported in Ahrens et al. (ND-40 pg/L)[35], for the same extract, but showed the same trend of increasing concentrations from sites I-IV followed by decreasing concentrations to site VI.

6.3.3 Baffin Bay and Lancaster Sound

The spatial distribution of ECF PFOA contributions in Baffin Bay and Lancaster Sound are shown in Figure 6.3 while the change in total PFOA concentration and % ECF with depth are shown in Figure 6.5. At all stations, PFOA concentrations were observed to reach a maximum within 100 m and then generally decreased with increasing depth. The exception to this was station 301, which showed a decrease in total PFOA to 400 m and then a sharp increase at 600 m. Nonetheless, % ECF values generally remained constant with depth at all sampling locations. ECF PFOA accounted for the majority (76-99%) of total PFOA concentrations in all sampling sites; however, linear-telomer contributions were found to be significant in all but 3 samples, one of which was not

statistically different from 3M ECF PFOA (see Tables E-10 and E-11 in Appendix E for branched:*n*- and branched:*iso*-PFOA ratios). The remaining two samples, one of which was collected at 400 m depth (station 301), and the other from the surface of Prince of Wales glacier (station 205) showed unique isomer profiles which could not be explained by additional contributions from linear-telomer or isopropyl-telomer sources. For these samples, % ECF was not calculated.
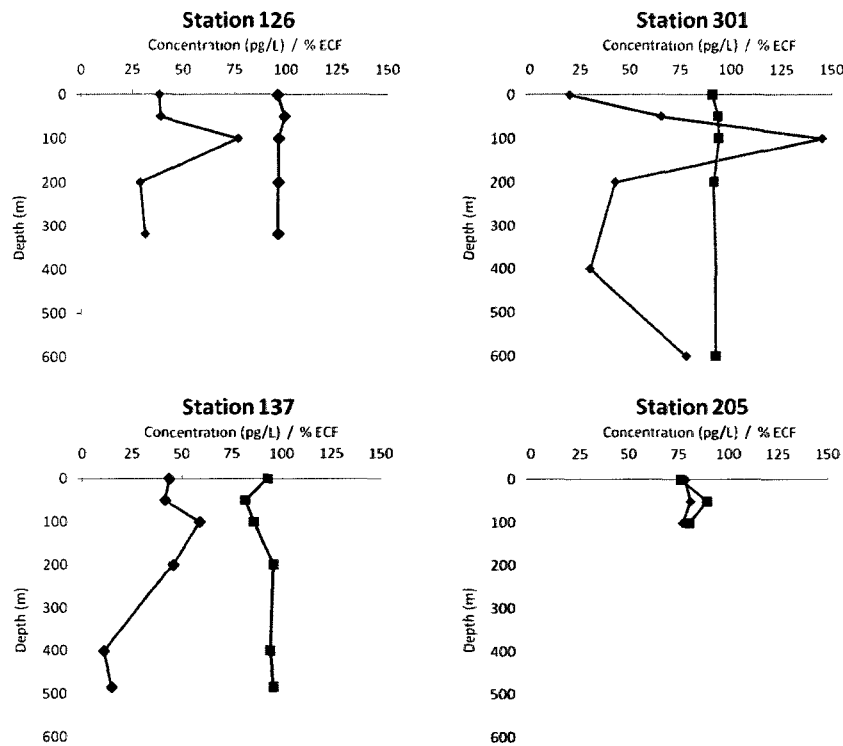
Figure 6.5 % ECF (red line) and total PFOA concentration (pg/L, blue line) versus depth for 4 sampling sites from Baffin Bay/ Lancaster Sound. No signficant differences were observed in % ECF with depth, however concentrations were consistently observed to reach a maximum within 100 m, followed by a general decrease with depth. It is unclear why PFOA concentrations in station 301 spiked at 600 m. The % ECF value at 400 m for station 301 could not be calculated due to a signifcant difference in isomer profile to our 3M ECF PFOA standard.

191

Multiple linear regressions of % ECF versus depth, longitude, latitude, and total PFOA concentration revealed no significant correlations. Nonetheless, examination of regional water circulation revealed a possible explanation for the observed differences in ECF contributions. The North Baffin Bay region is influenced by 2 major water bodies: the relatively cold, south-flowing Baffin current and the warm, north-flowing West Greenland current[39] (Figure 6.3). The mixing of these two waters is complex, but has been investigated previously. Dunlap and Tang[40] conducted a detailed model simulation on mean circulation during the month of September. Average model currents in the upper 350 m provided in this study indicate that Stations 126, 115, and 137 (which all showed similar mean ECF content, between 89-97%) could be influenced by the northerly flowing West Greenland current, while stations 205, 108 and 101 (which showed slightly less mean ECF contributions of 78-84%) could all be influenced by the southerly-flowing Baffin current. Samples 303 and 301 also had consistent ECF content (90 and 92%, respectively) and appear to both be influenced by easterly flowing water from the Canadian Archipelago. Collectively, this may imply that PFOA in the Arctic Ocean could contain higher contributions of telomer PFOA than that of the West Greenland Current and water from the Canadian Archipelago, albeit this requires confirmation.

This is not the first time spatial differences in branched PFOA isomer content have been observed in Arctic regions. De Silva and Mabury[50] reported that polar bears from Ittoqqortoormiit/Scoresby Sound in 1999-2001 showed higher branched PFOA content than bears sampled from south-eastern Hudson

Bay, near Sanikiluaq, Nunavut, in which no branched isomers were detected. While PFOA isomer profiles in polar bears are most likely influenced by isomer-specific pharmacokinetics[29-31], or enrichment of the linear isomer through biomagnification, the fact that the same species contained different PFOA branched content in various regions indicates exposure to two different sources. Further isomer profiling should be conducted along the West Greenland current, Arctic Ocean, and Canadian Archipelago to further investigate these spatial trends.

PFOS isomer profiles were extremely difficult to profile accurately due to a major interference in the m/z 80 product ion which usually co-eluted with branched and/or n-PFOS isomers. Due to the lack of sensitivity of isomer-specific transitions, there were only 3 samples for which we could obtain accurate isomer profiles, and m/z 80 and m/z 130 chromatograms for these samples are provided in Appendix E (Figure E-4). These results should be interpreted cautiously due to the lack of samples which could be accurately profiled. Station 301 (50m) contained a profile similar to that observed in Atlantic samples, with branched content accounting for 36% of total PFOS. In contrast, station 126 (50m) and station 205 (100m) both displayed PFOS isomer profiles which were substantially enriched in branched content (61 and 59%, respectively). Further work is needed to confirm these results.

FOSA was only detectable in 12 samples in Baffin Bay/Lancaster Sound at concentrations of <12 pg/L and always within the upper 200m of the water column. Branched content ranged from 20-39% (Appendix E, Table E-12), which

is higher than that detected in the Atlantic Ocean and North, and Norwegian Seas. This may reflect differences in the extent of degradation of precursors (discussed in Chapter4), but further research is needed to explore this hypothesis. Branched long chain perfluorocarboxylates (C_9-C_{14}) were not detected in any location in Baffin Bay or Lancaster Sound, but due to the low total PFA concentrations in this region, we cannot rule out their presence or absence. In contrast, De Silva et al.[47] detected multiple PFNA isomers in Arctic Lake water, sediments, and Ringed seal liver. In the same study branched isomers of PFDA, PFUnA, and PFDoA were not detected in surface waters of Arctic Lakes, but a single branched isomer (in addition to linear) PFDA, PFUnA, and PFDoA were detected in Arctic lake sediment and wildlife samples. These isomers were presumed to be of isopropyl geometry, and accounted for no more of 12% of total concentrations (based on GC-MS peak area). The authors hypothesised atmospheric transport of iso-11:2 fluorotelomer alcohol as the source of this compound. The absence of branched, long-chain PFCA isomers (C_9-C_{12}) in arctic seawater, may confirm this hypothesis.

6.3.4 Environmental Significance

The extent to which historical versus currently manufactured PFOA contributes to concentrations in remote seawater is of increasing importance as production of fluorochemicals continues in developing countries. A simple estimation based on PFOA concentrations in remote regions (2-200pg/L) and the

total volume of global seawater ($\sim 1 \times 10^{12}$ L), reveals approximately 2600-260000 tonnes of total PFOA in the world's oceans. While the estimated total mass of PFOA produced historically (3200-7200 tonnes[10]) falls within this range, there is considerable variability (2 orders of magnitude) in total estimated mass based on field measurements, making it difficult to quantitatively assess the contributions from historical versus current manufacturing. Certainly, more elaborate models[13-15] predict that historical ECF manufacturing plus slow, oceanic transport is the dominant source of PFOA to remote arctic food webs; however, this does not rule out the importance of other manufacturing sources and/or pathways. Isomer profiling of seawater provides an additional means of validating model predictions on the contribution of historical versus current manufacturing sources to remote regions.

In the present study PFOA isomer profiles in remote regions appear to be predominantly historical, however telomer contributions were significant in both the North Sea and Baffin Bay regions. Future work should involve characterization of PFOA isomer profiles in the Baltic Sea to pinpoint the linear-telomer source in this region. Isomer profiling of the Canadian Archipelago, as well as the Arctic Ocean should also be conducted to confirm our tentative observations of slightly higher telomer contributions from the Baffin current. Finally, PFOA isomer profiling should be conducted along the eastern seaboard of North America to identify potential contributions from current PFOA manufacturing to ocean water isomer profiles in this region.

6.4 Acknowledgments

6.5 References

1. Ellis, D.A.; Martin, J.W.; Mabury, S.A.; Hurley, M.D.; Andersen, M.P.; Wallington, T.J. *Environ. Sci. Technol.* **2003**, *37*, 3816-3820.

2. Houde, M.; Martin, J.W.; Letcher, R.J.; Solomon, K.R.; Muir, D.C. *Environ. Sci. Technol.* **2006**, *40*, 3463-3473.

3. Butt, C.M.; Berger, U.; Bossi, R.; Tomy, G.T. *Sci. Total. Environ.* **2010**.

4. Apelberg, B.J.; Witter, F.R.; Herbstman, J.B.; Calafat, A.M.; Halden, R.U.; Needham, L.L.; Goldman, L.R. *Environ. Health Perspect.* **2007**, *115*, 1670-1676.

5. Lau, C.; Anitole, K.; Hodes, C.; Lai, D.; Pfahles-Hutchens, A.; Seed, J. *Toxicol. Sci.* **2007**, *99*, 366-394.

6. United Nations Environmental Protection Secretariat of the Stockholm Convention on Persistent Organic Pollutants Pollutants. Geneva, Switzerland, **2009**.

7.   Ruisheng, Y. Additional information of production and use of PFOS. Fax from Ministry of Environmental Protection of China. Stockholm Convention Secretariat, Geneva, Switzerland, **2008**. http://chm.pops.int/Portals/0/Repository/addinfo_2008/UNEP-POPS-POPRC-SUB-F08-PFOS-ADIN-CHI.English.pdf

8.   Chen, C.L.; Lu, Y.L.; Zhang, X.; Geng, J.; Wang, T.Y.; Shi, Y.J.; Hu, W.Y.; Li, J. *Chem. Ecol.* **2009**, *25*, 163-177.

9.   Dietz, R.; Bossi, R.; Riget, F.F.; Sonne, C.; Born, E.W. *Environ. Sci. Technol.* **2008**, *42*, 2701-2707.

10.   Prevedouros, K.; Cousins, I.T.; Buck, R.C.; Korzeniowski, S.H. *Environ. Sci. Technol.* **2006**, *40*, 32-44.

11.   Reagen, W.K.; Lindstrom, K.R.; Jacoby, C.B.; Purcell R.G.; Kestner T.A.; Payfer R.M.; Miller, J.W.; Platform presentation at Society of Environmental Toxicology and Chemistry 28th North American Meeting, Milwaukee, WI, USA, November 11–15, **2007**.

12.   Kissa, E. *Fluorinated Surfactants and Repellents, 2nd ed*; Marcel Dekker: NewYork, **2005**.

13.   Armitage, J.; Cousins, I.T.; Buck, R.C.; Prevedouros, K.; Russell, M.H.; MacLeod, M.; Korzeniowski, S.H. *Environ. Sci. Technol.* **2006**, *40*, 6969-6975.

14. Armitage, J.M.; MacLeod, M.; Cousins, I.T. *Environ. Sci. Technol.* **2009**, 1134-1136.

15. Wania, F. *Environ. Sci. Technol.* **2007**, *41*, 4529-4535.

16. Yamashita, N.; Kannan, K.; Taniyasu, S.; Horii, Y.; Petrick, G.; Gamo, T. *Mar. Pollut. Bull.* **2005**, *51*, 658-668.

17. Yamashita, N.; Taniyasu, S.; Petrick, G.; Wei, S.; Gamo, T.; Lam, P.K.; Kannan, K. *Chemosphere.* **2008**, *70*, 1247-1255.

18. Busch, J.; Ahrens, L.; Xie, Z.; Sturm, R.; Ebinghaus, R. *J. Environ. Monit.* **2010**.

19. Ahrens, L.; Xie, Z.; Ebinghaus, R. *Chemosphere.* **2010**, *78*, 1011-1016.

20. Ellis, D.A.; Martin, J.W.; De Silva, A.O.; Mabury, S.A.; Hurley, M.D.; Andersen, M.P.S.; Wallington, T.J. *Environ. Sci. Technol.* **2004**, *38*, 3316-3315.

21. McMurdo, C.J.; Ellis, D.A.; Webster, E.; Butler, J.; Christensen, R.D.; Reid, L.K. *Environ. Sci. Technol.* **2008**, *42*, 3969-3974.

22. Benskin, J.P.; De Silva, A.O.; Martin, J.W. *Rev. Environ. Contam. Toxicol.* **2010**, *208*, 111-160.

23. Armitage, J.M.; Schenker, U.; Scheringer, M.; Martin, J.W.; Macleod, M.; Cousins, I.T. *Environ. Sci. Technol.* **2009**, *43*, 9274-9280.

24. Bossi, R.; Riget, F.F.; Dietz, R. *Environ. Sci. Technol.* **2005**, *39*, 7416-7422.

25. Holmstrom, K.E.; Jarnberg, U.; Bignert, A. *Environ. Sci. Technol.* **2005**, *39*, 80-84.

26. Butt, C.M.; Muir, D.C.; Stirling, I.; Kwan, M.; Mabury, S.A. *Environ. Sci. Technol.* **2007**, *41*, 42-49.

27. Hart, K.; Gill, V.A.; Kannan, K. *Arch. Environ. Contam. Toxicol.* **2009**, *56*, 607-614.

28. Holmstrom, K.E.; Johansson, A.K.; Bignert, A.; Lindberg, P.; Berger, U. *Environ. Sci. Technol.* **2010**, *44*, 4083-4088.

29. De Silva, A.O.; Tseng, P.J.; Mabury, S.A. *Environ. Toxicol. Chem.* **2008**, *28*, 330-337.

30. Benskin, J.P.; De Silva, A.O.; Martin, L.J.; Arsenault, G.; McCrindle, R.; Riddell, N.; Mabury, S.A.; Martin, J.W. *Environ. Toxicol. Chem.* **2009**, *28*, 542-512.

31. De Silva, A.O.; Benskin, J.P.; Martin, L.J.; Arsenault, G.; McCrindle, R.; Riddell, N.; Martin, J.W.; Mabury, S.A. *Environ. Toxicol. Chem.* **2009**, *28*, 555-512.

32. Ellis, D.A.; Webster, E. *Environ. Sci. Technol.* **2009**, *43*, 1234-1231.

33.   Benskin, J.P.; Yeung, L.W.Y.; Yamashita, N.; Taniyasu, S.; Lam, P.K.S.; Martin, J.W. *Environ. Sci. Technol.* **2010**, *44*, 9049-9054.

34.   Ahrens, L.; Barber, J.L.; Xie, Z.; Ebinghaus, R. *Environ. Sci. Technol.* **2009**, *43*, 3122-3127.

35.   Schlitzer, R. Ocean Data View Software, **2010**. http://odv.awi.de

36.   Ahrens, L.; Gerwinski, W.; Theobald, N.; Ebinghaus, R. *Mar. Pollut. Bull.* **2010**, *60*, 255-260.

37.   Winther, N.G.; Johannessen, J.A. *J. Geophys. Res.* **2006**, *111*, 12.

38.   European Environment Agency website. Accessed Aug 18, **2010** from: *http://www.eea.europa.eu/data-and-maps/figures/north-sea-physiography-depth-distribution-and-main-currents*

39.   Melling, H.; Gratton, Y.; Ingram, G. *Atmos.-Ocean.* **2001**, *39*, 301-325.

40.   Dunlap, E.; Tang, C.C.L. *Atmos.-Ocean.* **2006**, *44*, 99-110.

41.   Benskin, J.P.; Bataineh, M.; Martin, J.W. *Anal. Chem.* **2007**, *79*, 6455-6464.

42.   Millauer, H. United States Patent No. 3,829,512. **1974**.

43.   Katsushima, A.; Hisamoto, I.; Nagai, M.; Fukui, T.; Kato, T. Japanese Patent No. 0831272 (in Japanese). **1976**.

44.   Vyas, S.M.; Kania-Korwel, I.; Lehmler, H.J. *J. Environ. Sci. Health. A.* **2007**, *42*, 249-255.

45.   Benskin, J.P.; De Silva, A.O.; Martin, J.W. *Rev. Environ. Contam. Toxicol.* **2010**, *208*, 111-160.

46.   Furdui, V.I.; Helm, P.A.; Crozier, P.W.; Lucaciu, C.; Reiner, E.I.; Marvin, C.H.; Whittle, D.M.; Mabury, S.A.; Tomy, G.T. *Environ. Sci. Technol.* **2008**, *42*, 4739-4744.

47.   De Silva, A.O.; Muir, D.C.; Mabury, S.A. *Environ. Toxicol.Chem.* **2009**.

48.   Moller, A.; Ahrens, L.; Surm, R.; Westerveld, J.; van der Wielen, F.; Ebinghaus, R.; de Voogt, P. *Environ. Pollut.* **2010**.

49.   Pistocchi, A.; Loos, R. *Environ. Sci. Technol.* **2009**, *43*, 9237-9244.

50.   De Silva, A.O.; Mabury, S.A. *Environ. Sci. Technol.* **2004**, *38*, 6538-6545.

Chapter 7. Summary, Conclusions, Future Work

Excerpts of this chapter have been published with kind permission from Springer Science+Business Media: *Rev. Environ. Contam. Toxicol.* Isomer Profiling of Perfluorinated Substances as a Tool for Source Tracking: A Review of Early Findings and Future Applications, 208, 111-160, Benskin, J.P.; De Silva, A.O.; Martin, J.W. Copyright Springer Science+Business Media, LLC 2010.

7.1   Analytical Quantification Bias

Martin et al.[1] provided preliminary evidence that PFOS isomer-specific collision induced dissociation patterns could result in an analytical bias of unknown proportion unless the isomer profile in the sample was identical to the standard used for quantification. This hypothesized bias was quantified recently by Riddell et al.[2], in which individual purified PFOS isomers were used to compare response factors, relative to the linear isomer. These results showed that regardless of the product ion used (m/z 80 or 99), at least one PFOS isomer ($1m$-PFOS monitored using m/z 80, $4,4m_2$- and $4,5m_2$-PFOS monitored using m/z 99) will be completely absent from the chromatogram. Considering that PFOS isomer profiles in biota can vary substantially, total PFOS analysis using m/z 80 or m/z 99 product ions will lead to some inaccuracies, and possibly, incorrect conclusions to various hypotheses. To further examine this, Riddell et al.[2] also quantified 2 human serum pools containing different PFOS isomer profiles (~30-50% branched PFOS isomer content by LC-MS) using a characterized technical

standard (21.1% branched PFOS by ^{19}F NMR) and isomer-specific as well as total

PFOS quantification methods. For sample A, total PFOS quantification resulted in

m/z 80 over-reporting by ~30% compared to *m/z* 99, while quantification of

sample B resulted *m/z* 99 over-reporting by ~17% relative to *m/z* 80. When total

branched PFOS was quantified separately from the linear isomer, the difference in

values obtained from using *m/z* 80 and 99 for total branched isomer quantification

was notably less than for total quantification methods, while consistent values

were obtained for quantification of *n*-PFOS regardless of the product ion used

(*m/z* 80 or 99). In the absence of methods which can quantify isomers

individually, chromatographic separation of linear from 'total branched' PFOS,

followed by their independent quantification with a characterized technical

standard, will provide improvement in the accuracy of total PFOS data.

Researchers should also be aware of a systematic bias that can be

introduced when comparing isomer patterns in environmental samples at trace

concentrations to ECF standards. As the concentration of branched isomers in a

sample approach the detection limit, and disappear from chromatograms, the

contribution of the linear isomer to total PFOA or PFOS may be incorrectly

reported as 100% (See Chapter 5, Figure 5.1). Any survey of isomer profiles

should therefore take care to determine their '% linear dynamic range' – the

concentration above which the isomer profile (or % linear calculation) of a

standard stabilizes. Isomer profiles determined in samples that are below the

concentration of the % linear dynamic range should only be reported with the

necessary uncertainty identified, or flagged, as such. For example, Table 7.1

illustrates the results of Stevenson[3], in which an ECF standard of PFOA at 0.5 ng/mL and 10 ng/mL had % linear values of 81.2 and 74.7, based on LC-MS peak area, respectively, suggesting that % linear dynamic range likely lies somewhere in between these two concentrations. Alternatively, this bias may be diminished by reporting the ratio of each individual detected branched isomer to the *n*-isomer; thus permitting isomer-specific comparisons between studies.

Recently, the authors of several papers have utilized non-isomer specific methods to assess the relative proportion of total branched from linear isomers in samples[4-7]. Although interesting observations have been made from this practise, caution is warranted as it can potentially lead to bias and over-interpretation of data, even when simply comparing peak areas. For example, when branched isomers are not baseline resolved from the linear isomer, it is unclear what contribution co-eluting branched isomers make to the signal of the *n*-isomer, which could potentially result in an overestimation of the true weight percent of the linear isomer in the mixture. Even in isomer-specific methods where near-baseline or baseline resolution is achieved, α-branched PFOS can still elute with *n*-PFOS and therefore contribute to the *m/z* 499/99 signal of this isomer[2]. For the purposes of qualitative assessment of relative branched content between samples, the above bias can be overcome by providing the corresponding branched content for a standard determined in the same manner, albeit this practice can also lead to over interpretation, (see the section on *Perfluoroalkyl Sulfonate and Sulfonamide Isomer Profiles*) because the isomer content in standards supplied by specialty chemical manufacturers are usually not the same as historically manufactured

fluorochemicals. For example, a sample with 30% branched PFOS content may appear enriched in branched isomers when compared to a Fluka standard (20% branched), despite the fact that it is indistinguishable from historically manufactured 3M ECF PFOS (30%). The numerous analytical methods (LC-MS, LC-MS/MS, and GC-MS) as well as different quantification techniques (monitoring single parent ion, single product ion, sum product ion, isomer-specific product ion) used for assessing branched isomer content can also make it difficult to compare branched content between studies. Nevertheless, this can again be overcome by providing the branched content of a characterized technical standard obtained in the same manner as the samples.

Table 7.1 PFOA isomer composition (%) in humans and standards. Values shown are means unless stated otherwise. The presence/absence of dimethyl branches could not be confirmed.

Reference	Sample	n-	iso-	IMM[a]	Other[b]	∑branched	Analysis
Stevenson[3]	10ng/mL 3M ECF PFOA	74 7				25 3	LC-MS/MS (C18, total ion count of m/z 369, 219,169, 119) Branched content determined using relative sum product ions Near baseline separation of branched from linear
	0 5 ng/mL 3M ECF PFOA	81 2				18 8	
	Serum (Bioresource[c] Lot 020821)	99 7				<0 31	
	Serum (Lampire[d] Lot X324B)	84 0				16	
	Serum (Sigma[e] Lot 022K0965)	86 0				14	
	Serum (Golden West[g] G01406042)	99 8				<0 21	
Keller et al[8]	Serum (SRM 1957, eight US States, 2004)	97 9				2 1	LC MS/MS (C18 column, sum of m/z 369, 219, 169 product ions) Branched content determined using relative sum product ions Extent of isomer separation unclear
Olsen et al[9]	3M ECF PFOA	78				22	LC-MS (C18, m/z 413) Branched content determined using relative peak areas Extent of isomer separation unclear
	Serum (Occupationally exposed)	99 (range 94-99 9)				~1 (range 0 1 6 0)	
De Silva and Mabury[10]	3M ECF PFOA	79 6	9 9	9 7	0 77	20 4	GC-MS (RTX-35, m/z 505) Branched content determined using relative peak areas 9 PFOA isomers resolved in standard
	Serum (Sigma[f], Golden West[f])	98	1 5	0 5		2 1 (1 2-3 0)	
Benskin et al[11]	Serum (Pregnant women, Edmonton, Canada, 2006)	>98				<2	LC-MS/MS (PFO, m/z 369) Branched content determined using relative peak areas 8 PFOA isomers resolved in standard

[a]IMM-internal monomethyl branches (5m, 4m, 3m)
[b]Other-unidentified branched isomers
[c]Bioresource – Bioresource Technology Inc , Fort Lauderdale, FL
[d]Lampire – Lampire Biological Laboratories, Pipersville, PA [f]Sigma – Sigma-Aldrich, Milwaukee, WI
[e]Golden West – Golden West Biologicals, Temecula, CA

7.2 Strategies for Isomer Separation by LC-MS/MS

For PFOS, current isomer separation techniques using PFP, PFO, or C_{18} stationary phases can typically and effectively separate dimethyl branched

isomers from internal monomethyl isomers (5*m*, 4*m*, 3*m*), and *iso*-PFOS from the linear isomer. However, separation of individual internal monomethyl branched isomers from each other (5*m*, 4*m*, 3*m*) on these phases often proves challenging when using only the *m/z* 99, 80, or 499 (single MS) ions. Likewise, the α-branch isomer (1*m*-PFOS) tends to co-elute amongst internal monomethyl branches on PFO[11], with the isopropyl branch[12] or somewhere between isopropyl and linear[13] on PFP, or with *n*-PFOS, on C_{18}[2]. Fortunately, these co-eluting PFOS isomers can be resolved using knowledge of isomer-specific collision-induced dissociation[14] in combination with less sensitive, albeit highly specific MS/MS transitions. As shown in Figure 7.1a, the *m/z* 80 product ion provides good separation of *n*, *iso*, monomethyl, and dimethyl isomers on a PFO column, similar to that which has been previously obtained on C_{18}[15] and PFP[13,14] phases. With PFO, resolution of individual monomethyl branches is most easily accomplished using the *m/z* 130 product ion for 3*m* and 5*m* isomers, and *m/z* 330 product ion for 4*m*-PFOS. A similar strategy can be adopted for the resolution of 1*m*-PFOS using *m/z* 419, since this is the only major isomer to produce this ion. Furthermore, 1*m*-PFOS does not produce a *m/z* 80 ion, therefore, provided that this ion is used for quantification of *iso*-PFOS and *n*-PFOS, 1*m*-PFOS should not cause any interference when using PFP or C_{18} phases. Although some minor isomers that are detectable in ECF PFOS standards also produce the *m/z* 419 ion (Figure 7.1a), 1*m*-PFOS is the only isomer that has been detected to date in environmental samples that produces this highly specific product ion. A similar strategy can be employed for PFOA isomers using *m/z* 369, 169, 219, 119 product ions as shown

in Figure 7.1b. Monomethyl PFOA isomers, 5m and 4m-PFOA, elute essentially together but produce distinct m/z 219 (5m) and 119 (4m) ions, respectively, which permits their resolution.
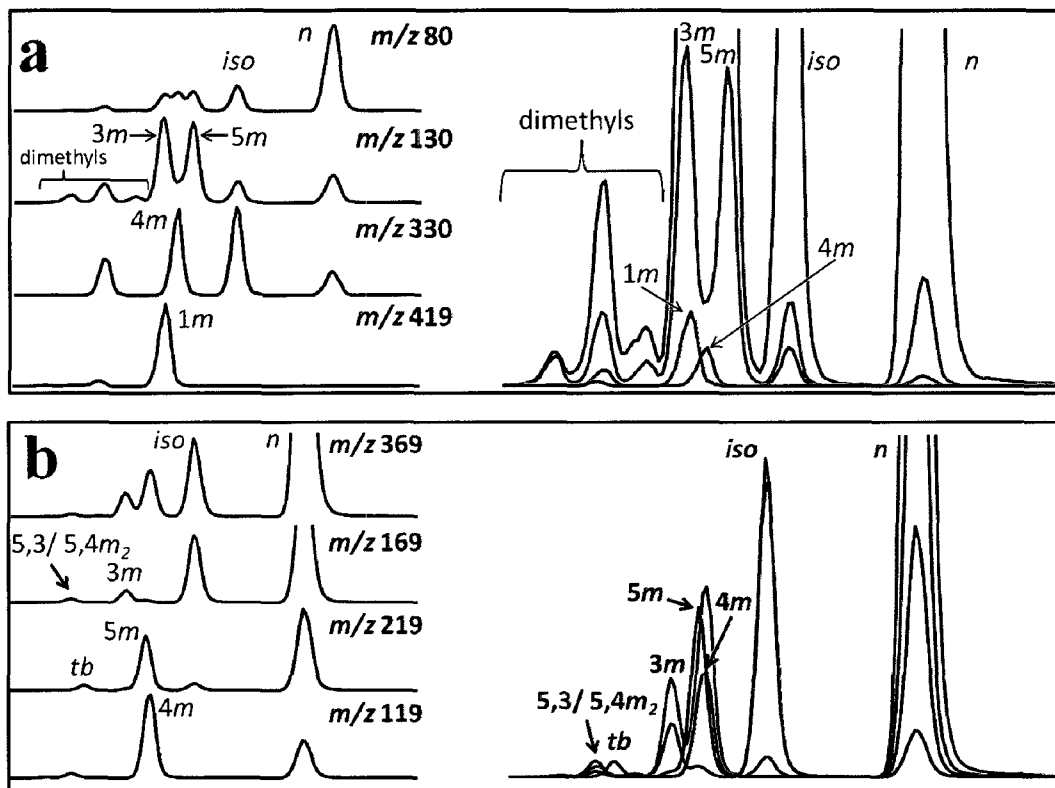
Figure 7.1 a Recommended product ions for PFOS isomer-specific LC-MS/MS analysis: m/z 80 (*red trace*): n, iso; m/z 130 (*green trace*): 5m, 3m, dimethyls; m/z 330 (*blue trace*): 4m; m/z 419: 1m (*black trace*). **b** Recommended product ions for PFOA isomer-specific LC-MS/MS analysis: m/z 369 (*red trace*): n, iso; m/z 169 (*green trace*): 3m, 5,3/5,4m₂; m/z 219 (*blue trace*): 5m, tb; m/z 119 (*black trace*): 4m

7.3 Influence of Physical Chemical Properties on Environmental Fractionation of Perfluoroalkyl Isomers

Among the most intriguing topics in perfluoralkyl research today pertains to the mechanism(s) of long range transport of PFAs to remote regions, such as the Arctic. Much of this discussion, and the associated environmental modelling, relies heavily on accurate knowledge of physical and chemical properties. While one hypothesis suggests atmospheric transport and degradation of volatile PFA-precursors,[16-18] another proposes slow, long range transport of PFAs in ocean water[19-23]. A more recent third hypothesis, presented by McMurdo et al.[24], is that PFOA has a higher pK_a than previously thought and thus atmospheric transport of PFOA (i.e., the protonated form) may occur due to partitioning from marine aerosols, and furthermore that fractionation of branched and linear PFOA isomers may occur because of this process. The authors suggest that, based on the greater surface activity of n-PFOA[25], n-PFOA will become preferentially enriched on surface microlayers. Further fractionation of linear from branched PFOA isomers would then occur during the transfer of PFOA in aerosol droplets to the gas phase due to the (presumably) differing Henry's Law constants and pK_a of all the isomers. From model calculations, pK_a values of close to $0^{26,27}$, 1.3^{28}, 2.8^{29}, and 3.8^{30} have been predicted, while values of $< 1^{31}$, and 1.3^{32} were derived from experimental measurements. In two recent studies, pK_as of ≤ 1.5 and $\geq 3.5^{20,24}$, and 2.8 and 3.8^{33}, were suggested for total branched and linear PFOA, respectively. This was followed by computational model estimations for the pK_as of individual branched isomers of PFOA, which ranged from -0.1 ($5m$ and $4m$-PFOA) to -5.1

209

$(1,1,2,2m_4\text{-PFOA})$, with n-PFOA having a pK_a of -0.2[34]. The lower values for most branched PFOA isomers are based on knowledge that electron withdrawing CF_3 groups stabilize the carboxylate group, thus making most branched isomers stronger acids than the linear isomer. However, the inductive effect of the trifluoromethyl group is diminished as the distance from the carboxyl group increases, and becomes negligible when the separation exceeds four alkyl units [30,35]. Although helicity has also been suggested to influence the pK_a of n-PFOA[30], it is not clear to what extent a *lack* of helicity will influence branched isomer pK_as. Considering branching position alone, the suggestion of a significantly lower pK_a of "total branched" PFOA by Ellis et al.[33] and Armitage et al.[20], requires that the majority of perfluoromethyl branches be situated alpha or beta to the carboxyl group. However, on the basis of monoperfluoromethyl isomers present in ECF PFOA, determined by ^{19}F NMR (See Chapter 1, Table 1.2), only *2m-* and potentially *3m*-PFOA have branching positions that should significantly influence the pK_a (Table 7.2); and the former isomer makes up only a scant 0.1% of 3M ECF PFOA. The quantities of *3m*-PFOA have not been specifically reported, but total internal monomethyl branches (*3m-*, *4m-*, and *5m*-PFOA) constitute 12.6% of 3M ECF PFOA (See Chapter 1, Table 1.2) and *3m*-PFOA is also readily identifiable in standards and in the environment. Thus, the partitioning processes described by McMurdo et al.[24] could possibly be investigated by monitoring for a relative deficiency of *3m*-PFOA in atmospheric samples over oceans or large lakes.

Table 7.2 Isomer composition (wt %) of ECF PFOA and predicted pK_a values

| | Isomer Composition | pK$_a$ | | |
		Rayne et al.[34]	Ellis and Webster[33]	Armitage et al.[20]
n-PFOA	77.6	-0.2	≥3.8	3.5
iso-	9	-0.1		
5m-		-0.1		
4m-	12.6[a]	-0.2	≤2.8[b]	1.5[b]
3m-		-1.3		
2m-	0.1	-1.7		
tb-	0.2	-0.3		

a. Represents sum of *5m*, *4m* and *3m* isomers.
b. Assumed to be average of all branched isomers.

Overall, it is predicted that some enrichment of linear PFOA isomers may occur in the atmosphere as a result of the mechanism described by McMurdo et al.[24]. From a mass balance perspective, we speculate that the converse is unlikely and thus that ocean water PFOA isomer profiles should not be significantly influenced by isomer-specific partitioning to air. Any minor fractionation of isomers to aerosols or the atmosphere, although perhaps important as a global transport pathway, should not influence the bulk PFOA profile in the world's oceans, particularly in mid latitude source regions. Our analyses of PFOA in Eastern Atlantic ocean water has revealed a branched isomer profile (including *3m*-PFOA) which was, in general, not significantly different to that of 3M ECF PFOA[36] (See Chapter 6 and Table 7.3). Although this does not provide evidence *against* fractionation of PFOA isomers to marine aerosols and the atmosphere, it is strong evidence that such processes are unlikely to affect the overall isomer profiles in the world's oceans. Ultimately, more definitive evidence of selective

atmospheric partitioning may be gleaned from PFOA isomer profiling in the atmosphere or in aerosols.

Other interesting differences in the physical/chemical properties of PFOA isomers imparted by perfluoroalkyl branching patterns are reported in the literature. For example, the mere ability to separate isomers by HPLC, or their derivatives by GC, implies differential hydrophobicity and vapour pressures, respectively [11,14,37,38] also attributed a higher branched content in PFOSF, compared to PFOS standards, to selective removal of branched isomers during purification of the potassium salt. This is supported by the preparative-scale isolation of n-PFOS from branched isomers by successive recrystallization in water[15] and carbonate buffer followed by centrifugation[39], demonstrating that branched isomers are more water soluble than the linear chain – consistent with all HPLC elution orders on reversed phase stationary phases. Furthermore, branching has also been observed to decrease melting point[25], and in a separate study, to increase boiling point in perfluoroalkanes[40].

More recently, De Silva et al.[41] built on the work of Gauthier[42] by measuring the n-octanol-water partition coefficients (K_{ow}) for nine isomers of 3M ECF NEtFOSE. The log K_{ow} values were statistically indistinguishable for seven branched isomers, including the isopropyl isomer, with a mean value of 5.41. However, isomer 4 (Figure 7.1a) had a statistically higher K_{ow} of 5.58, and the n-isomer of NEtFOSE had a statistically lower log K_{ow} of 5.33. It is unclear whether the minor differences in these, or other physical and chemical properties are sufficient to cause any significant differential transport or bioaccumulation

potential. Similar studies may be warranted for other ECF chemical products and for other physical properties.

The subtle differences in the physical/chemical properties between branched and linear PFA isomers are also apparent in abiotic degradation studies. For example, Yamamoto et al.[43] observed that three branched PFOS isomers degrade more rapidly than do the linear chain when subjected to UV light in the presence of water or alkaline 2-propanol. Similarly, Ochoa-Herrera et al.[39] demonstrated that branched PFOS isomers could more readily undergo reductive dehalogenation by Ti(III)-citrate, in the presence of a vitamin B12 catalyst. In this study, *iso*- and 5*m*-PFOS were the most labile isomers, followed by 3*m* and 4*m*-, 1*m*-, and finally *n*-PFOS. The authors suggested a decrease in C-C bond strength resulting from perfluorinated chain branching and/or the stabilization of radical intermediates imparted by branched structures as possible explanations for this observation. Ochoa-Herrera et al.[39] also presented isomer-specific Gibbs free energies using *ab initio* calculations to predict the relative stability of the various isomers. The results indicated that after *n*-PFOS, 1*m* and *iso*-PFOS were the most stable, followed by 3*m*, 4*m*, and 5*m*-PFOS. These data contrast those of Rayne et al.[44], in which branched isomers were all found to be more thermodynamically stable than *n*-PFOS; based on gas-phase enthalpies, entropies, and free energies of formation. If municipal or industrial water treatment facilities begin to apply such catalytic reductive or oxidative treatment procedures then some unique isomer profiles may be relevant in local environments.

The stability of perfluorinated radical intermediates may also influence the isomer-specific abiotic oxidation of ECF perfluoroalkyl sulfonamides. These are hypothesized to be a source of branched PFOS and perfluoroalkyl carboxylates (including PFOA) in the environment based on their occurrence in smog chamber studies with volatile precursors in the presence of Cl and OH radicals[45,46] and indirect photolysis experiments with OH radicals[47]. It should be noted that alpha-branched PFOA is unlikely to form from oxidation of alpha branched perfluoroctyl sulfonamides by these processes[46,48]. Thus, while an absence of 2m-PFOA may be indicative of oxidation processes, it is only present at trace levels in 3M ECF PFOA (<0.1 %) and has yet to be detected by current LC-MS methods, perhaps due to its unique collision induced dissociation to m/z 85 (CF_3O^-) and m/z 63 ($[CO_2F]^-$) product ions[49]. Isomer-specific monitoring of PFA atmospheric deposition in remote regions may provide insight into this issue.

7.4   Characterization of Perfluoroalkyl Isomer Profiles in the Environment

7.4.1 PFOA Isomer Profiles

Especially relevant for regulation of fluorochemicals, is the extent of the environmental PFA burden attributed to current-use fluorochemicals versus those whose source has largely been regulated or phased out. Early on, it was hypothesized that this could be assessed by monitoring of isomer profiles in biological samples, since historical (pre-2002 phase-out) releases of ECF fluorochemicals consisted of a mixture of isomers whereas current and historical

manufacture of telomer-derived products has largely been of strictly the linear isomer[10]. However, due to the preferential excretion of branched isomers, it is possible that, at steady state, tissues of organisms exposed exclusively to ECF PFOA could take on isomer profiles that are predominantly linear[49-51]. This evidence from rodents and fish thus raises ambiguity when attempting to ascribe manufacturing source based on PFOA isomer patterns in biological samples.

Notwithstanding, some information may be gained by examining isomer profiles in biological samples. For example, De Silva and Mabury[37] examined PFCA isomer profiles in Arctic polar bear livers, from the south eastern Hudson Bay region of Canada and central eastern Greenland, and found that Greenland bears showed some contribution from an electrochemical source (i.e., minor detectable branched isomers; Table 7.3), whereas Canadian bears had none detectable. Canadian bears had higher total concentrations of PFOA (mean 25 ng/g) compared to Greenland bears (9 ng/g), and thus the absence of branched isomers in Canadian bears cannot be explained by detection limits. Consistent with this observation, there were also no detectable branched PFOA isomers in seals[52] or cod[53] from the western and central Canadian Arctic. The discrepancy among polar bear populations may result from exposure to PFOA from two different sources, or via different transport mechanisms. For example, Greenland Bears may have PFOA isomer signatures similar to what is transported from the Arctic, which appears predominantly electrochemical in origin[36]. Conversely, the strictly linear signature of Canadian polar bears may indicate less exposure to PFAs which have undergone long range transport in oceans, and more exposure to

telomer-derived PFAs which have undergone atmospheric transport, since the atmosphere has been shown to deliver a highly linear profile of PFOA as evidenced by 99% *n*-PFOA in water and 95% *n*-PFOA in sediment from isolated remote Arctic lakes [52].

PFOA isomer profiles in samples (biotic and abiotic) from throughout North America also reveal a predominantly linear signature, albeit a '% linear' dynamic range was not defined in many of these studies, thus the % linear may be positively biased for some samples (see Chapter 5). Furdui et al.[54] observed only *n*-PFOA in isomer profiles in Lake Ontario Lake Trout and suspended sediment. Consistent with this result, in a separate study De Silva et al.[52] observed predominantly *n*-PFOA (95%) in biological samples from Lake Ontario but substantially more branched PFOA isomers in surface water (85-94% linear), supporting the hypothesis of isomer-specific biological discrimination. In samples that contained branched isomers, *n*-, *iso*-, and 5*m*-PFOA were detected in humans, rainwater, Lake Ontario surface water and biota, and dolphins (Table 7.3). Of these, Lake Ontario surface water (87-93% linear PFOA) also contained 4*m*-PFOA, and appeared to have the profile most similar to that of 3M ECF PFOA.

To date, the highest relative quantity of branched PFOA measured in environmental samples is in ocean water from the Atlantic and coastal Asia[36,55] (Table 7.3). In these samples, PFOA isomer profiles were, for the most part, consistent with a 3M ECF PFOA standard. The exception was in samples from Tokyo Bay which appeared to contain significant additional contributions from a linear (presumably telomer) source, but these samples also did not have a

consistent ratio of *iso*-PFOA to other branched PFOA isomers, suggesting a potential additional source of *iso*-PFOA (also presumably telomer). This latter hypothesis is supported by the observation of single branched isomers (assumed to be isopropyl) in addition to linear isomers of PFNA, PFDA, PFUnA, PFDoA, in Tokyo Bay, (absent in all other coastal Asian sampling locations), as well as recent data presented by Zushi et al.[56] in Tokyo Bay sediment cores (see the section on *Perfluorocarboxylate Isomer Profiles other than PFOA*).

In humans, the PFOA isomer signature appears predominantly linear regardless of location, and sex (Table 7.1). Serum from the background population and from occupationally exposed men and pregnant or non-pregnant women in four different studies showed consistently ≤2% total branched PFOA content[8,10,11,57]. Interestingly, the highest relative amount of branched PFOA in human serum is from unpublished data by 3M, in which a number of pooled human serum samples were analyzed by LC-MS/MS and branched content of up to 16% was observed, compared to 25.3% branched in a 10 ng/mL 3M ECF standard (Table 7.3). It should be noted that the apparent elevated quantity of branched isomers in this 3M ECF standard is likely a result of simply summing the responses of *m/z* 119, 169, 219, and 369 product ions, and is therefore not representative of the actual weight % of branched isomers in 3M ECF PFOA, which is acknowledged as ~20% [58].

Table 7.3 PFOA isomer composition (%) in environmental and biological samples and standards. Values shown are means unless stated otherwise. The presence/absence of dimethyl branches could not be confirmed in any study.

Ref.	Sample	n-	iso-	IMM[a]	other[c]	Σ branched	Analysis
Benskin et al [36,55]	3M ECF PFOA	77				23	LC-MS/MS (PFO, m/z 369, 219, 169, 119) Branched content determined using isomer specific product ions 10 PFOA isomers resolved in standard
	Atlantic Ocean (avg 23 locations) from N46° 17 257' W06° 29 386' to N01° 13 523' W11° 57 961'	78				22	
	Water, coastal Asia (avg 4 locations)	77				23	
	Water, Tokyo Bay, Japan	90				10	
De Silva and Mabury [37]	3M ECF PFOA	77			2 1	23	GC-MS (ZB 35, m/z 505) Branched content determined using relative peak areas 7 PFOA isomers resolved in standard
	Polar bear *Ursus maritimus* (Greenland)	95				5 0 (2 8-9 8)	
	Polar bear *Ursus maritimus* (Canada)	100				nd[d]	
De Silva et al [52]	3M ECF PFOA	78				22	GC MS (RTX-35 or ZB-WAX, m/z 505) Branched content determined using relative peak areas 8 PFOA isomers resolved in standard
	Char Lake surface water (Nunavut, Canada)	99	0 69	0 39		1 1	
	Amituk Lake surface water (Nunavut, Canada)	99	0 40	0 25		0 65	
	Lake Ontario surface water (Canada)	85-94	2 8 6 8	3 1 8 5		5 9-15	
	Ontario precipitation (Canada)	96	1 9	1 7		3 7	
	Dolphin plasma *Tursiops truncatus* (USA)	99	0 40	0 30		0 70	
	Lake trout *Salvelinus namaycush* (Lake Ontario, Canada)	95	2 9	2 1		4 9	
	Mysis *Mysis relicta* (Lake Ontario, Canada)	99	0 69	0 40		1 1	
	Diporeia *Diporeia hoyi* (Lake Ontario, Canada)	99	0 79	0 42		1 2	
	Alewife *Alosa pseudoharengus* (Lake Ontario, Canada)	99	0 59	0 50		1 1	
	Sculpin *Cottus cognatus* (Lake Ontario, Canada)	99	0 69	0 40		1 1	
	Smelt *Osmerus mordax* (Lake Ontario, Canada)	99	0 6	0 24		0 83	
	Zooplankton (Lake Ontario, Canada)	98-99	0 99	0 39-0 79		1 4 1 8	
	Ringed seal *Phoca hispida* (Lake Ontario, Canada)	100				nd	
	Lake Ontario sediment (Canada)	97-98	0 98-1 4	0 59-1 5		1 6 2 8	
	Char Lake sediment (Nunavut, Canada)	95	2 9	2 1		4 9	
Furdui et al [54]	Trout *Salvelinus namaycush* (Lake Ontario, Canada)	100				nd	LC-MS/MS (C$_{18}$ column, m/z 369) Branched content determined using relative peak areas Extent of isomer separation unclear
Powley et al [53]	Arctic Cod *Arctogadus glacialis* (Canada)	100				nd	LC-MS/MS (C$_8$ column, m/z 369) Branched content determined using relative peak areas Extent of isomer separation unclear
	Bearded and Ringed Seal *Erignathus barbatus and Phoca hispida* (Canada)	100				nd	

[a] IMM-internal monomethyl branches (5m, 4m, 3m) branched isomers   [a] HS - human serum
[b] DM-dimethyl branches   [b] nd – not detected
[c] Other-unidentified

218

7.4.2   Perfluoroalkyl Sulfonate and Sulfonamide Isomer Profiles

The exclusive production of PFOS and PFOS-precursors by ECF make PFOS isomer signatures a potentially powerful tool for conducting exposure source determination experiments. Unlike PFOA, which has a predominantly linear isomer signature in humans, PFOS isomer profiles vary depending on geographic location and time of sample collection (Table 7.4). For example, in one of the earliest studies of PFOS isomer profiling in humans, contributions of the linear isomer to total PFOS ranged from ~59% (Australia serum and UK plasma), to ~68% (Sweden plasma) compared to a Fluka standard (78%)[12]. At the time, this apparent preferential accumulation of branched PFOS isomers was attributed to pharmacokinetic discrimination, however, this is contrary to what is observed for PFOS isomers in rodents[49,50], where the linear isomer was preferentially retained, albeit non-significantly relative to most branched isomers. Furthermore, PFOS standards manufactured by Sigma Aldrich/Fluka (~80% n-PFOS by ^{19}F NMR; See Chapter 1, Table 1.2) are known today to have lower branched isomer content than 3M ECF PFOS (~70% n-PFOS by ^{19}F NMR, See Chapter 1, Table 1.2), thus a Fluka standard is a non-ideal reference standard, as we indicated earlier, and it is not clear if both these human samples would have been significantly different from 3M ECF PFOS. Nonetheless, the difference between the % linear values found in Australia/ UK, and Sweden implies that some factor, whether it be pharmacokinetic or source, is influencing the isomer profiles in these locations. Furthermore, Haug et al.[6] also reported the apparent enrichment of branched PFOS isomers in a more recent survey of human blood

samples from Norway. In this study, an 11% decrease in the relative proportion of

n-PFOS was observed between 1976 (68% linear) to 2007 (57% linear), albeit the

branched content in a reference standard was not provided. Interestingly, the same

trend of decreasing branched content with time was also observed by Riddell et

al.[2] in human serum standard reference materials (SRMs) collected in 1996 (SRM

1589a) and 2004 (SRM 1957) using isomer-specific quantification. SRM 1589a

was collected across eight States and SRM 1957 was collected from the Great

Lakes region, and it is unclear what geographical location-related factors may

have influenced these profiles. Nonetheless, SRM 1589a (~30% branched) clearly

had lower branched content than did SRM 1957 (~50% branched) and this was

supported by the results of Keller et al.[8], who also found SRM 1957 to contain

elevated branched content (41%), although the branched content for a reference

standard was not provided. Interestingly, a qualitative comparison of branched

PFOS content in human serum (SRM 1957), human milk (SRM 1954), and a

technical standard (unknown supplier) based on peak heights from

chromatograms provided in Keller et al.[8] indicates that the branched content in

human milk may be quite similar to the reference standard and deficient in

branched content relative to human serum (SRM 1957). It is unclear what factors

might be influencing these isomer profiles and further investigation is needed;

still, it is reasonable to hypothesize that the linear isomer, being more lipophilic

(or hydrophobic), might partition to human milk to a greater extent than do

branched isomers.

The results of Haug et al.[59] are generally supported by those of Rylander et al.[5], who also examined human blood samples from Norway collected in 2005 and found a similar contribution of linear isomers; notwithstanding there was a small, albeit significant difference between men (67% linear, range 49-100%) and women (69% linear, range 56-100%), but again, these were not compared to a technical standard, thus it is difficult to say if these are similar to the ~70% linear content in 3M ECF PFOS, or not. Isomer profiles of PFHxS, PFOS, and FOSA have also been examined in the serum of pregnant women from Edmonton, Canada (as detailed in Chapter 2)[11]. Although up to six branched isomers were detected in a PFHxS standard from Fluka, endogenous interferences present in the serum[60] hampered the elucidation of PFHxS isomer profiles, thus only a single branched PFHxS isomer was detected in addition to n-PFHxS. Two branched FOSA isomers were also observed, in addition to n-FOSA. PFOS isomer profiles in human serum were very similar (~80% linear based on quantification using an n-PFOS standard) to a Fluka standard (76%), suggesting that the branched isomer content was substantially lower than that of 3M ECF PFOS. This is generally consistent with recent data by Rylander et al.[4], in which the median contribution of the n-isomer to total PFOS in delivering women from south central Vietnam was 83% (range 17-93%), based on LC-MS/MS analysis; however, it is unclear if all branched isomers were fully resolved from the linear chain, or how this percentage compared to that in a technical standard. Nonetheless, when taken at face value, it is interesting that samples from both of these studies were collected from pregnant or delivering women, and both reported a deficiency in branched

PFOS content relative to studies from Norway[5,6], Australia, and the UK[12], which generally showed enrichment of branched content and did not involve pregnant or delivering women. While it is unknown what factor or combination of factors (e.g., source, pharmacokinetics, etc.) contribute to these differences, one possibility is that pregnancy reduces the body burden of branched isomers in the mother by preferentially transferring branched PFOS to the fetus. At this time this hypothesis remains tentative; however, recent data has shown that branched PFOS isomers can preferentially cross the placental barrier relative to n-PFOS[61]

In contrast to humans, enrichment of branched PFOS in wildlife has not been frequently observed (Table 7.5). Lloyd et al.[62] qualitatively observed enrichment of branched isomers in red deer liver and Whitebait relative to a Fluka PFOS standard, while Powley et al.[53] reported 50% branched PFOS in Cod from the western Canadian arctic, relative to Fluka PFOS (74%). In all other literature to date, PFOS isomer profiles in wildlife appear either similar, or deficient in branched content relative to technical standards. For example, Chu and Letcher[63] observed enrichment of n-PFOS in eggs from herring gull (94.5% n-PFOS) and double-crested cormorant (95.9% n-PFOS) from the Great Lakes, as well as in polar bear samples from the Norwegian arctic (plasma, 82.4 % n-PFOS) and Canadian arctic (liver, 92.4% n-PFOS), compared to a technical standard from Wellington (65% n-PFOS). In these samples, dimethyl branched isomers (3,5m_2, 4,5m_2, tb-, and 4,4m_2-PFOS) were not detectable, which is consistent with the results of Houde et al.[13], who also found an absence of dimethyl branched isomers, and enrichment of n-PFOS in a Lake Ontario foodweb. In this study, the

n-isomer accounted for more than 88% total PFOS in all biological samples, which was similar to that observed in sediment (81 - 89% *n*-PFOS) but contrasted with the composition in Fluka PFOS (77%) and Lake Ontario water (43 - 56% *n*-PFOS), the latter of which was noticeably deficient in *n*-PFOS. Powley et al.[53] reported similar results in bearded and ringed seal from the western Canadian arctic, which were both highly enriched in *n*-PFOS (96%) compared to a Sigma-Aldrich/Fluka standard (76%). Likewise, Senthil Kumar et al. [7], observed 77-89 % *n*-PFOS in a range of aquatic wildlife from Georgia, USA, and Lloyd et al.[62], reported a qualitative deficiency in branched PFOS in Cromer crab and Carp roe, compared to a Fluka standard.

Although the deficiency in branched PFOS observed in most wildlife may be explained by preferential absorption or retention of the linear isomer, as observed to a minor extent in rodents[49,50] and significantly in fish[64] (see section on *Differences in Toxicity and Bioaccumulation of PFA Isomers*), it is also possible that in biological samples where total PFOS concentrations are extremely low, some branched isomers may be below detection limits, resulting in a positive bias in the % of total PFOS attributed to the linear isomer (see Chapter 6 and % linear dynamic range in the section on *Analytical Quantification Bias*). Nevertheless, deficiencies in branched content are still observed in samples containing total PFOS concentrations which are well above isomer detection limits in ECF standards, therefore there is a reasonable degree of confidence in these data.

Interestingly, the positive analytical bias discussed above, and what is known about the pharmacokinetics of PFOS isomers, does not explain the

frequent observation of enriched branched isomer content in humans. One hypothesis is that preferential biotransformation of branched PFOS-precursors (e.g., perfluorooctane sulfonamides) results in an enrichment of branched PFOS. As described in Chapter 4, isomer-specific biotransformation was investigated using mixture incubations of various concentrations of a technical PFOS-precursor (NEtFOSA isomers) with cytochrome P450 isozymes (CYPs) 2C9, 2C19, and human liver microsomes[65]. Isomer-specific biotransformation rate constants were significantly different at all concentrations, and the rank orders of these rate constants were different with two different isozyme systems. Furthermore, when the ECF mixture was incubated with human liver microsomes (containing all of the major CYP isozymes), isomer-specific biotransformation and product formation were also observed. These data cannot be extrapolated directly to predict the extent of isomer-specific PFOS accumulation from precursors in an environmental exposure scenario, whereby constant exposure, biotransformation, and elimination processes will all combine to achieve a steady state. Thus, further *in vivo* experiments are necessary with PFOS precursors. However, based on this early evidence it is reasonable to speculate that preferential biotransformation of branched PFOS-precursor isomers may result in enriched branched PFOS isomer patterns, thereby providing a possible explanation for the high abundance of branched PFOS isomers in some humans and wildlife (Tables 7.4 and 7.5), and a potential biomarker for exposure to precursors. This precursor hypothesis currently remains tentative, however it could be confirmed by measuring non-racemic proportions of PFOS isomer

enantiomers in biological samples, as described in a proof-of-principle study by Wang et al.[66]. In this work, a chiral, α-branched PFOS ($1m$-PFOS) precursor was observed to biotransform enantioselectively when incubated with human liver microsomes. Based on these results, PFOS source exposure in humans and wildlife may be determined by examination of enantiomeric fractions, although a method for separation of PFOS enantiomers requires development before this hypothesis can be tested.

PFOS isomer profiles in coastal Asia and the Atlantic Oceans were also recently examined and found to be very similar or slightly enriched in branched isomers compared to 3M ECF PFOS[36,55]. On the contrary, enrichment of n-PFOS (i.e. >70% linear content), in comparison to 3M ECF PFOS, was never observed in ocean samples. Differential PFOS isomer pK_a values are unlikely to affect environmental partitioning since all PFOS isomers will be ionized at environmentally relevant pH, and it is unclear to what extent differential surface activity alone may influence boundary layer (water-air) partitioning of n-PFOS. Surface layer enrichment of n-PFOS could potentially result in water samples collected below the surface layer being enriched to some extent with branched isomers, and while this hypothesis remains tentative at this time, differences have been observed in total PFOS concentrations between surface microlayer and sub-surface water samples[67].

Other possible explanations for branched PFOS isomer enrichment in ocean water include degradation of ECF polymeric material containing unique isomer signatures, or alternatively preferential abiotic degradation [39,68] of

branched PFOS-precursors. This may also explain the relative abundance of branched PFOS isomers in Lake Ontario[13], discussed above. In comparison, PFOS isomer profiles from coastal Asian locations (Shanghai, Tokyo Bay, Tomakomai Bay, and Japan Sea) were fairly consistent with 3M ECF PFOS for all samples[55].

Table 7.4 PFOS isomer composition (%) in humans. Values shown are means unless stated otherwise.

Ref.	Sample (description, location, year collected)	n-	iso-	5m/4m/3m	dm	other branched	Σ branched	Analysis/comment
Karrman et al [12]	PFOS Standard (Fluka)	78 0	14 4[a]	8 0	0 6		23 0	LC-MS (C$_{18}$, m/z 499) Branched content determined using relative peak areas. Separation of several branched isomers and near separation of branched from linear isomers
	Plasma (mixed age/gender, Sweden, 1997-2000)	68.1	18 0[a]	12 6	0 4	0 9	31 9	
	Serum, (mixed age/gender, Australia, 2002-2003,)	58 7	21 3[a]	17 1	0 8	2 9	42.1	
	Plasma, (mixed age/gender, UK, 2003)	59 6	20 4[a]	17 7	0.5	2 5	41 1	
Haug et al [59]	Serum (*range*, mixed age/gender, Norway, 1976-2007)	53 -78					22 – 47	LC-MS/MS (C8 column, m/z 499/499). Branched content determined using relative peak areas. Extent of isomer separation unclear.
	Serum (mixed age/gender, Norway, 1976)	68					32	
	Serum (mixed age/gender, Norway, 2007)	57					43	
Keller et al [8]	Serum (SRM 1957, eight US States, 2004)	59					41	LC-MS/MS (C$_{18}$ column, sum of m/z 80, 99, 130 product ions) Branched content determined using relative sum product ions Extent of isomer separation unclear
	PFOS Standard	77					23	LC-MS/MS (C8 column, m/z 80) Branched content estimated from peak height in chromatograms found in Keller et al 2009 Branched isomers not baseline resolved
	Serum (SRM 1957, eight US States, 2004)	65					35	
	Milk (SRM 1954, several US states, 2006)	73					27	
Riddell et al [2]	Serum (SRM 1589a, Great Lakes region, 1996)	~70					~30	LC-MS/MS (PFO column, m/z 80) Total branched quantified separately from linear using characterized standard Branched isomers baseline resolved from n-PFOS
	Serum (SRM 1957, eight US States, 2004)	~50					~50	
Benskin et al [11]	PFOS Standard (Fluka)	76 0					24 0	LC-MS/MS (PFO column, m/z 80) Concentration using n-PFOS and technical PFOS (Fluka) standards Branched isomers baseline resolved from n-PFOS
	Serum (pregnant women, Edmonton, Canada, 2006)	80 0					20 0	
Rylander et al [4]	Plasma (*median*, delivering women, south central Vietnam, 2005)	83 (range 17-93)					17 (range 7-83)	LC-Q-TOF (C$_{18}$, m/z 498 93) Branched content determined using relative peak areas Branched appears to be separated from linear. Extent of co-elution with linear unclear
Rylander et al [5]	Plasma (male, Norway, 2005)	67 (range 49-100)					33 (range 0-51)	LC-Q-TOF (C$_{18}$, m/z 498.93) Branched content determined using relative peak areas Branched appears to be separated from linear Extent of co-elution with linear unclear
	Plasma (female, Norway, 2005)	70% linear, range 56-100),					30 (range 0-44)	

Table 7.5 PFOS Isomer composition (%) in environmental and wildlife samples. Values shown are means unless stated otherwise.

Ref.	Sample	n-	iso-	5m /4m /3m	1m	tb + dimethyls	other branched	total branched	Analysis/comment
Houde et al [13]	PFOS Standard (unknown supplier)	76 9	10 6	5 1	3 9	3 6		23 2	
	Water (*range*, Lake Ontario, 2004)	43-56	22-28	17-21	3 9-8 0	1 0-2 0		44-57	
	Sediment (*range*, Lake Ontario, 1995-2002)	81-89	4 6-10	2 2-5 9	2 7-4 4			11-19	
	Zooplankton (*range*, Lake Ontario, 2004 & 2006)	95-100	0 1-1 0	0 4-3 0	0			0-5	LC-MS/MS (PFP column, m/z 80 or 99) Quantification using n-PFOS standard (Wellington) adjusted using branched isomer response factors from Riddell et al 2009
	Mysis *Mysis relicta* (*range*, Lake Ontario, 2001)	91-92	3 9-5 2	1 7-2 4	0			8-9	
	Diporeia *Diporeia hoyi* (*range*, Lake Ontario, 2002 & 2003)	95-96	2 0-2 8	0 4-0 6	0 7-1 1			4-5	
	Alewife *Alosa pseudoharengus* (*range*, Lake Ontario, 2002)	90-91	4 2-7 1	2 3-2 4	2 5-2 8			8-9	
	Smelt *Osmerus mordax* (*range*, Lake Ontario, 2002)	88-92	4 6-4 8	1 8-2 3	0 5-0 9	0 4-0 5		8-12	
	Sculpin *Cottus cognatus* (*range*, Lake Ontario, 2002)	91-92	4 6-4 8	1 8-2 3	0 9-1 1	0 2-0 3		8-9	
	Lake trout *Salvelinus namaycush* (*range*, Lake Ontario, 2002)	88-93	2 8-7 1	2 5-4 1	0 9-1 1	0 2-0 3		7-12	
Powley et al [53]	PFOS Standard (Fluka)	74 0						26 0	
	Cod *Arctogadus glacialis* (Western Canadian Arctic, 2004)	50 0						50 0	LC-MS/MS (C8 column, m/z 80) Branched content determined using relative peak areas Extent of isomer separation unclear
	Bearded and Ringed Seal *Erignathus barbatus and Phoca hispida* (Western Canadian Arctic, 2004)	96 0						4 0	
Senthil Kumar et al [7]	Aquatic wildlife (Georgia, USA, 2006-2007)	81 (range 77-89)						19 (11-23)	LC-MS/MS (C_{18} column, m/z 80) Branched content estimated from concentrations of linear/branched isomers in Senthil Kumar et al 2009 Unclear how quantification of branched PFOS was conducted or the extent of isomer separation
Lloyd et al [62]	PFOS Standard (Fluka)	~71						~29	LC-MS/MS (PFO column, m/z 80) Branched content estimated from peak height in chromatograms found in Lloyd et al 2009 Branched isomers not baseline resolved
	Whitebait	~39						~61	
	Roe deer liver	~42						~58	
	Cromer crab	~86						~14	
	Carp roe	~89						~11	
Chu and Letcher [63]	PFOS Standard (T-PFOS, Wellington)	65	11 3	19 7	0 9	1 9	1 1[a]	35	
	Herring gull egg *Larus argentatus* (Great Lakes, 1989)	94 5	2 9	2 2	0 2	0 1	0 1[a]	5 5	GC-MS (DB-5 column, ion monitored dependent on isomer) Branched content determined using isomer-specific quantification
	Double Crested Cormorant egg *Phalacrocorax auritus* (Great Lakes, 2003)	95 9	2 2	1 4	0 3	0 1	0 2[a]	4 1	
	Polar Bear Plasma *Ursus maritimus* (Norwegian Arctic, 2007)	82 4	4 1	10 3	2 8	0 1	0 4[a]	17 6	
	Polar Bear Liver *Ursus maritimus* (Canadian Arctic, 2007-2008)	92 4	4 1	2 8	0 3	0 1	0 4[a]	7 6	

7.4.3 Perfluorocarboxylate Isomer Profiles other than PFOA

The source of branched long chain carboxylates ($>C_8$) is still uncertain. Recent analysis by 3M and in this study (See Chapter 1, Table 1.2) supports the assertion by Prevedouros et al.[22] that branched isomers of $C_4 - C_7$ and $C_9 - C_{13}$ may be present as residuals in both 3M ECF POSF-derived products, and 3M ECF PFOA. Global emissions in 2000 have been estimated for C_6-C_{13} PFCAs, [22], however it is still uncertain whether PFCAs other than C_4, C_6, C_8, and C_9 were ever intentionally produced for large-scale manufacturing. Interestingly, recent data suggests the possibility of long chain (i.e., C_{11}, C_{13}) sources of isopropyl branched isomers[52,54,56]. Unlike ECF which produces a variety of branched isomers, formation of isopropyl perfluoroalkyl compounds are possible via the telomerization reaction pathway of an isopropyl telogen.

De Silva et al.[52] detected no branched PFNA in precipitation, Lake Ontario sediment, or most Lake Ontario Biota (mysis, zooplankton, trout, alewife) but one branched isomer (*iso*-PFNA) in ringed seals from Resolute Bay and a single polar bear from the Canadian arctic. Examination of Arctic lake sediment revealed four branched PFNA isomers, including *iso*-PFNA, along with *n*-PFNA. The surface water of this lake contained only *iso*-PFNA and *n*-PFNA. In Lake Ontario surface water and sediment, only *iso*-PFNA and *n*-PFNA were observed. In contrast, two branched isomers of PFNA have consistently been detected in isomer-specific monitoring of human blood[10,11,52]. Given the large number of patents describing the synthesis of isopropyl branched PFCAs via telomerisation[69-71] (also see supporting info of De Silva et al.[52]), it is realistic to expect that these compounds

have experienced significant production. De Silva et al.[52] suggested that the presence of multiple branched isomers (i.e., isopropyl and monomethyls) was most likely suggestive of ECF inputs, but that detection of only the isopropyl isomer in the absence of other branched isomers was ambiguous with respect to ECF versus an isopropyl telomer source.

The hypothesis of intentional isopropyl PFCA production is supported by PFCA isomer profiles in archived lake trout (1979-2004) from Lake Ontario and archived suspended sediment from the Niagara River (1980-2003)[54], as well as archived sediment cores from Tokyo Bay (1950s-2004)[56]. Of the perfluorocarboxylates monitored in these studies, only PFUnA and PFTrA branched isomers were detected consistently. In Tokyo Bay, a consistent increase in the ratio of branched:linear PFTrA isomers was observed from 1988-2004, suggesting increased in branched isomer production, while the opposite trend was observed in suspended sediment from the Niagara River, where the ratio of branched:linear isomers of PFUnA and PFTrA decreased significantly from 1980-2002. This latter trend was also observed in Lake Ontario trout, however the rate of decrease of branched PFTrA in fish was statistically different than in sediment, in contrast to PFUnA, where trends in fish and sediment were consistent. The presence of branched isomers has typically been interpreted as an ECF contribution, however the authors cite patents describing synthesis of isopropyl PFCAs by telomerisation in both North America[69,70] and Japan[71] as evidence of isopropyl production sources in these regions. While the lack of branched PFOA in lake trout observed by Furdui et al.[54] may be explained by the

230

low bioaccumulation potential of most branched PFOA isomers[51], a subsequent

study observed branched PFOA (2-4 branched isomers) in all samples of Lake

Ontario biota (2002, 2004, 2006), sediment (1998, 2002), and surface water

(2001, 2002)[52]. In addition, *iso*-PFNA was observed in surface water, sediment,

and half of the biota samples (including trout). Interestingly, in this study

isopropyl C_9 - C_{12} PFCAs were also observed, whereby PFUnA had notably

higher branched isomer content (6-12%) than other long chain PFCAs (<2%),

consistent with the observation of the relatively high branched isomer content of

PFUnA observed in Lake Trout[54].

De Silva et al.[52] noted that Lake Ontario biota and dolphins from urban

coastal areas in south-eastern USA, and sporadic human blood samples contained

an abundance of *iso*-PFUnA. Arctic samples, including Char Lake sediment,

ringed seals and polar bears had a different isomer profile in which *iso*-PFDoA (4-

7% of total PFDoA) was dominant compared to *iso*-PFUnA (1-3%). In that study

the authors speculated that atmospheric transport and oxidation of a precursor

containing an isopropyl perfluoroundecyl moiety may be responsible. The same

precursor could, presumably, also undergo biological transformation to yield *iso*-

PFUnA, thus accounting for its presence at mid-latitudes that are heavily

influenced by human activity. In coastal Asian waters a single branched isomer

of PFNA, PFDA, PFUnA, and PFDoA was observed in addition to the respective

linear isomer. There is currently a paucity of isomer-specific long-chain

perfluorocarboxylate data to confirm whether these are consistent trends.

In Chapter 2, (Benskin et al.[11]) perfluorocarboxylate (C9 – C14) isomer profiles were examined in pooled serum from pregnant Edmonton (Alberta, Canada) women. In addition to the linear isomer, two branched isomers of PFNA, and a single branched isomer of PFDA and PFUnA were observed. In contrast, only linear isomers of PFDoA and PFTA were detectable. The peaks corresponding to branched isomers appeared to make up a relatively small component of the total concentrations based on relative LC-MS peak areas in several transitions. This is consistent with the observations by De Silva and Mabury[10], who also detected two minor branched PFNA isomers and one minor branched PFUnA isomer in human serum, representing ~1.6% and 2.3% of total PFNA and PFUnA concentrations, respectively.

7.5 Differences in Toxicity and Bioaccumulation of PFA Isomers

To date, most studies that examine biological properties of PFAs have not differentiated between the branched and linear structures. For PFOS, *in vitro* and *in vivo* experiments have typically relied on standards from Sigma-Aldrich/Fluka (~20% branched)[72,73], or 3M (~30% branched)[74-76], representing a difference in branched isomer content of ~10%. For those studies in which the manufacturer is not identified, or the branched content unknown, it is reasonable to predict that the variability amongst studies is less than 15%, given the difference in branched isomer content in technical standards, (See Chapter 1, Table 1.3) provided a linear standard is not used. Although isomer-specific toxicity information is lost when

using technical standards, this is likely the most environmentally relevant choice of standards for PFOS (and its precursors), considering most exposure sources (water, dust, food, etc.) and the internal dose of organisms (from biomonitoring studies) show that multiple isomers are always present.

Biological testing of PFOA has also made use of standards predominantly from 3M (80% linear) or Sigma/Aldrich (~99% linear). It is unclear which standard is the most relevant for toxicity testing. For example, in humans and higher trophic level organisms, even though linear PFOA dominates the internal dose, this does not necessarily mean that co-exposure does not also occur to the multiple branched isomers via food or house dust (for humans). Nonetheless, the few toxicological comparisons of branched and linear isomers have suggested that there may be only subtle toxicological differences between linear and total branched isomers. Furthermore, it is unclear whether the differences are a function of reduced biological activity, or less bioavailability of the branched isomers. For example, Loveless et al.[77] compared the responses of rats and mice following exposure to either a technical, 77.6% n- / 22.4% branched PFOA isomer mixture, enriched branched isomer dose of 54% 3m-PFOA, 4% 4m-PFOA and 42% iso-PFOA, or a 100% n-PFOA dose. Peroxisomal β-oxidation was least pronounced after administration of the enriched branched dose, results that contrast somewhat to those of Vanden Heuvel et al.[78], in which branched and linear PFOA were both able to activate peroxisome proliferator receptor (PPAR)- α to a similar peak effect in vitro. Body weights of rats and mice in the Loveless et al.[77] study were also approximately 20% lower in rats, exposed to the mixture

233

of linear and branched or pure linear doses, compared to the branched-only dose; this further supports the opinion that *n*-PFOA may be slightly more toxic *in vivo*. However, the authors also observed that *n*-PFOA was preferentially absorbed relative to 3*m*/4*m*, and *iso*-PFOA at increasingly higher doses, suggesting that the increased potency of *n*-PFOA relative to branched, and branched+linear dosing regimens may simply be a result of decreased bioavailability of the branched isomers.

Other isomer-specific data in rodents and fish further corroborate the hypothesis that differences in toxicological response between branched and linear PFAs may be a result of differential bioavailability. For example, rats exposed to lower doses of PFHxS, PFOS, PFOA, and PFNA via a single gavage dose, or through a sub-chronic dietary exposure, showed varying degrees of selective retention of *n*-isomer, compared to the major branched isomers in ECF formulations[49,50]. It should be noted that although most differences in excretion rates of PFOS isomers were not statistically significant, this could be reflective of the experimental design. For example, the single-dose exposure[49] was likely not long enough to detect significant differences among most PFOS isomer rate constants. Likewise, in the subchronic exposure[50] PFOS isomer excretion rate constants were based only on a single animal. Despite these restrictions, some statistically significant differences were observed between *n*-PFOS compared to *tb*-PFOS and 4*m*-PFOS. It is likely that a longer depuration period, along with a larger sample population would suggest preferential linear isomer retention, compared to the major branched isomers in rodents, similar to observations by

Sharpe et al.[64], in fish. Rainbow trout exposed to PFOA and PFNA isomers through the diet showed a similar result, whereby the n-isomer was selectively retained in blood and tissues, relative to the majority of branched isomers[51]. Similarly, Sharpe et al.[64] demonstrated significant preferential accumulation of n-PFOS relative to branched isomers in rainbow trout and zebrafish. More recently, O'Brien et al.[79] demonstrated that the pharamcokientics of PFOS isomers in developing chicken egg are also isomer specific. In that study, the linear isomer was again observed to be the most persistent, consistent with what is observed in rats[4980] and fish[64]. Interestingly, the extent of linear PFOS enrichment was greatest in the lowest dose group, suggesting a dose dependence on isomer fractionation. Also consistent with these results in the observation of a substantial enrichment of n-PFOS in Lake Ontario trout compared to water[13]. Bioaccumulation factors calculated for n-PFOS in this study were estimated to be 3.4 × 10^4 L/kg, compared with 2.9 × 10^3 L/kg for the monomethyl-substituted isomers. The apparent difference in calculated values was attributed to enrichment of branched isomers in Lake Ontario water, however it is not clear what is mediating this phenomenon. Possible explanations include preferential removal of n-PFOS to sediment or aerosols, albeit these hypotheses require further validation. Trophic magnification factors calculated for n-PFOS (4.6 ± 1.0), monomethyl branched isomers (1.3 ± 0.17 to 2.6 ± 0.51), and dimethyl branched isomers (no trophic magnification) also suggest that n-PFOS may preferentially biomagnify through the food chain, relative to branched isomers. Based on these results, it appears that

exposure to any mixture of PFHxS, PFOS, PFOA or PFNA isomers will result in enriched linear isomer profiles in a range of organisms.

Despite this general trend, there were some notable exceptions in which branched isomers were eliminated more slowly than the n-isomer of either PFOS or PFOA. The structure of the biopersistent PFOA isomers has not yet been determined, but the α-branch PFOS isomer ($1m$-PFOS) showed a remarkably long half life (longer than the linear isomer) in male rats following single or sub-chronic dosing, and was not significantly eliminated in female rats following sub-chronic dietary exposure. Interestingly, plots of half life of linear and monomethyl branched PFOS and PFOA isomers, in various species and dosing regimens, revealed a consistent structure/property relationship, whereby a relative decrease in pharmacokinetic half life was observed as the branching point was moved from the perfluoroalkyl chain terminus (n-) to the $4m$-position, whereas an increase in half life was observed as the branching point moved from the $4m$- position closer to the sulfonate or carboxylate group (Figure 7.2).
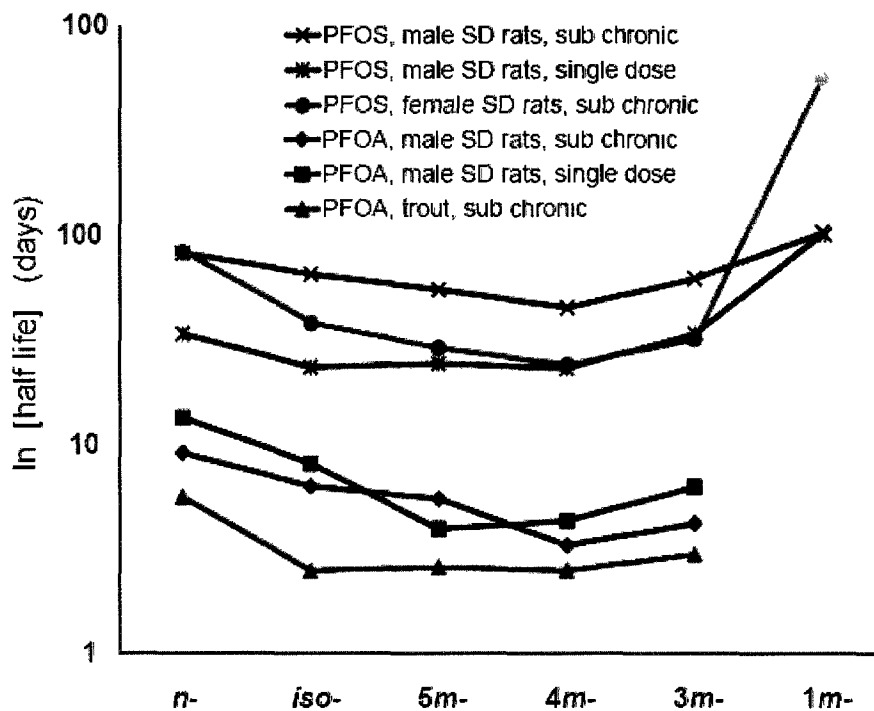
Figure 7.2 Structure-property relationship between PFOS/PFOA isomers observed in rats[49,50] and fish[51]. A relative decrease in half life was observed as the branching point was moved from the perfluoroalkyl chain terminus (*n-*) to the 4*m*-position. In contrast, an increase in half life was observed as the branching point moved from the 4*m*- position closer to the sulfonate or carboxylate group regardless of sex, species, or dosing regimen.

While preferential elimination of branched PFHxS, PFOS, PFOA, and PFNA isomers reportedly occurs via the urine[49], it is still not clear what mechanism mediates this isomer-specific phenomenon. The sex hormone-mediated organic anion transporter (OAT) system plays an important role in the renal elimination of *n*-PFOA from male and female rats[81]. Katakura et al.[82] recently identified some of the specific transporters (oatp1 and OAT3) controlling the elimination of *n*-PFOA in rats, but it is still not clear if substrate-transporter binding is equivalent amongst isomers. In addition, while OAT3 was identified as

237

mediating tubular uptake of *n*-PFOA and oatp1 with tubular reabsorption, the transporter responsible for tubular excretion of this PFA has not yet been identified. Sex-differences in PFOA elimination in orally-dosed fish have also been observed and are thought to be attributable to differences in renal transport activity[83]. Clearly, there are many possibilities, and some transporters may have unique interactions with specific isomers. Only by probing the individual uptake of specific isomers by specific transporters can we obtain an accurate picture of the mechanism of elimination. It may be possible to correlate the preferential elimination of a given isomer *in vivo* to its affinity for renal uptake/excretion transporters and/or a lack of affinity for tubular reabsorption transporters.

Isomer-specific protein binding may also explain differential elimination rates *in vivo*. Branched PFAs with lower affinity for serum proteins could potentially undergo renal elimination to a greater extent than the linear isomer. Although it is known that *n*-PFOS and *n*-PFOA bind strongly to serum proteins [84,85], little is known about the binding affinity of branched isomers. Previous *in vitro* cytochrome P450 assays[65] are suggestive that differential protein binding can occur during the metabolism of PFA-precursor isomers, thus there is reason to suggest this could occur for PFA isomers and serum proteins as well. Such experiments would complement OATP and *in vivo* pharmacokinetic studies to get a better overall picture of the mechanism(s) of isomer-specific biological handling.

7.6 Summary and Conclusions

The overall objectives of this thesis were to assess the extent to which PFOA measured in the environment is a result of historical versus current manufacturing and the extent to which precursors contribute to PFOS concentrations in humans and wildlife. It was hypothesised that isomer profiles could be used as a tool for manufacturing and exposure source determination. To test this hypothesis, a comprehensive method was developed to simultaneously separate and detect PFA and PFA-precursor isomers using LC-MS/MS (Chapter 2). Application of this method to human serum, and comparison with literature data revealed that PFOA isomer profiles are predominantly linear (regardless of species), while PFOS isomer profiles vary widely (enriched or deficient relative to historically manufactured PFOS). Since it was unclear how isomer-specific pharmacokinetics influenced PFA isomer profiles in biological samples, in Chapter 3, a pharmacokinetic study was conducted to assess the influence of perfluoroalkyl chain branching on biological handling. For all PFAs, branched isomers generally had lower blood depuration half-lives than the corresponding linear isomer suggesting that in biological samples, quantitative assessment of PFOA manufacturing source would be difficult, since isomer profiles are unlikely to be conserved. On the other hand, these results were suggestive that PFOS isomer profiles which are similar or deficient in branched content relative to the profile of 3M ECF PFOS, may be a biomarker of direct exposure to PFOS.

While the results of Chapter 3 may partially explain PFOS isomer profiles in human and wildlife samples, they do not explain the apparent enrichment in

branched PFOS which is often observed in humans. Therefore, in Chapter 4, we hypothesised that PFOS isomer profiles might be influenced by isomer specific biotransformation of precursors. An *in vitro* assay using a model PFOS-precursor, CYP isozymes, and human liver microsomes was used to test this hypothesis. Perfluoroalkyl branching geometry significantly influenced the rate of biotransformation, with branched isomers typically biotransformed more rapidly than the linear isomer. These data are suggestive that the relatively high abundance of branched PFOS isomers present in some humans and wildlife, may be a biomarker of exposure to PFOS-precursors. Taken together with the results of Chapter 3, PFOS isomer profiles in humans which are similar to, or deficient in branched content relative to 3M ECF PFOS could be indicative of direct exposure, while profiles which are enriched in branched content are suggestive of significant exposure to precursors.

Since isomer-specific biological handling prevents quantitative assessment of PFOA manufacturing source in humans and wildlife, we sought samples where the isomer profile was more likely to be conserved (i.e. which lacked biological PFA isomer fractionation processes). Seawater was assumed to lack many of these biological isomer fractionation processes; however, PFA concentrations are quite low in these samples. Thus, in Chapter 5, the isomer-specific LC-MS/MS method developed in Chapter 2 was modified to facilitate large-volume injections, and a technique for quantifying the contributions from historical and currently manufactured PFOA was developed. Once validated, this method was applied to more remote locations (Chapter 6). The objective of this work was to assess the

extent to which ECF versus telomer manufacturing contrubtes to PFOA in the Arctic Ocean. Overall, the findings of Chapter 6 support model predictions that ECF manufacturing and slow oceanic transport is the dominant source of PFOA in remote regions. Nonetheless, in some regions, the contributions from telomer manufacturing were significant, and further monitoring in remote sites is warranted.

7.7   Future Work

Despite vast improvements in PFA isomer separation methods, we still lack a single method that can provide high chromatographic resolution of *all* the major PFA isomers and their interferences in a reasonable amount of time (e.g., <30 min). The recent availability of isolated and characterized standards for the major PFOS and PFOA isomers will assist greatly in the further development of quantitative isomer-specific methods. However, another existing deficiency is that commercially available technical PFOS and PFOA standards do not have the same isomer profile as those which were historically manufactured by 3M, thus making comparisons between environmental isomer profiles and historical sources of PFOA and PFOS difficult. Some researchers have obtained standards as gifts from 3M, e.g., ECF PFOS and PFOA, and while these may indeed be very useful as a 'gold standard' for use in source-tracking studies, these are known to contain many impurities which makes them less useful for quantitative analyses.

Another area which requires attention is the analysis of PFOS-precursors. No methods currently exist for monitoring the full suite of PFOS-precursors, and

certainly many precursors are known to have been manufactured in significant quantities (e.g. sulfonamide phosphates, acrylates) but are rarely (if ever) monitored in the environment. Future work should focus on expanding target lists to include these precursors, as well as examining their fate and behaviour in the environment through abiotic and biodegradation studies. If the degradation of these compounds is isomer-specific, this may also be a source of unique PFOS isomer profiles in the environment.

The isomer specific biotransformation of NEtFOSA investigated in Chapter 4 was a proof-of-principle study which requires further validation *in vivo*, and with other PFOS-precursors (including sulfonamide-linked phosphates and acrylates). It is possible that this phenomenon is species-, or precursor-dependent. Knowledge of isomer-specific behaviour for other PFOS-precursors, in conjunction with expanded PFOS-precursor target lists will improve the accuracy of PFOS isomer profile interpretation. Future work with PFOS-precursors should also include abiotic degradation (i.e. atmospheric oxidation) in particular the influence of abiotic sulfonamide degradation on perfluorocarboxylate isomer profiles.

The *in vivo* work presented in Chapter 3 provided strong evidence of isomer-specific pharmacokinetics, several questions still remain. Firstly, the duration of the study was not long enough to obtain many statistically significant differences among PFOS isomer blood elimination rate constants; therefore this study should be repeated with more rats (i.e. to improve statistical power), over a longer duration, and at multiple dosing levels. A multicompartmental model

should be used in future studies to accurately describe PFOS isomer kinetics. It is also unclear whether the isomer-specific behaviour observed in this study is paralleled in other species (e.g. humans). Future studies should investigate isomer-specific behaviour in other mammalian species, as well as avian and aquatic wildlife.

Isomer profiling in seawater from both remote and source regions appears to be the most useful tool in assessing the contributions from current versus historical use and production of PFAs. Latitudinal and longitudinal transects of the Atlantic Ocean, in particular along the eastern seaboard of the United States (where there is minimal data currently available), should be conducted to assess contributions from current production and use of PFOA in this region. The tentative linear-telomer PFOA source in Europe, identified in Chapter 6, should be examined more closely with a larger sample set, focusing on coastal regions of the Baltic Sea. Extensive sampling of the Canadian Archipalego should also be conducted to explain what appears to be a subtle spatial trend in isomer profiles, discussed in Chapter 6.

7.8 References

1. Martin, J.W.; Kannan, K.; Berger, U.; de Voogt, P.; Field, J.; Franklin, J.; Giesy, J.P.; Harner, T.; Muir, D.C.; Scott, B.; Kaiser, M.; Jarnberg, U.; Jones, K.C.; Mabury, S.A.; Schroeder, H.; Simcik, M.; Sottani, C.; van Bavel, B.; Karrman, A.; Lindstrom, G.; van Leeuwen, S. *Environ. Sci. Technol.* **2004**, *38*, 248A-255A.

2.   Riddell, N.; Arsenault, G.; Benskin, J.P.; Chittim, B.; Martin, J.W.; McAlees, A.; McCrindle, R. *Environ. Sci. Technol.* **2009**, *43*, 7902-7908.

3.   Stevenson, L. U.S. Environmental Protection Agency public docket AR-2261150: Comparative analysis of fluorochemicals in human serum samples obtained commercially. U.S. Environmental Protection Agency, Office of Pollution Prevention and Toxic Substances, Washington, DC, **2002**.

4.   Rylander, C.; Phi, D.T.; Odland, J.O.; Sandanger, T.M. *J. Environ. Monit.* **2009**, *11*, 2002-2008.

5.   Rylander, C.; Brustad, M.; Falk, H.; Sandanger, T.M. *J. Environ. Pub. Health.* **2009**, 10 pgs.

6.   Haug, L.S.; Thomsen, C.; Becher, G. *Environ. Sci. Technol.* **2009**, *43*, 2131-2136.

7.   Senthil Kumar, K.; Zushi, Y.; Masunaga, S.; Gilligan, M.; Sajwan, S.S. *Mar. Pollut. Bull.* **2009**, *58*, 601-634.

8.   Keller, J.M.; Calafat, A.M.; Kato, K.; Ellefson, M.E.; Reagen, W.K.; Strynar, M.; O'Connell, S.; Butt, C.M.; Mabury, S.A.; Small, J.; Muir, D.C.; Leigh, S.D.; Schantz, M.M. *Anal. Bioanal. Chem.* **2010**, *397*, 439-451.

9.   Olsen, G.W.; Burris, J.M.; Ehresman, D.J.; Froehlich, J.W.; Seacat, A.M.; Butenhoff, J.L.; Zobel, L.R. *Environ. Health Perspect.* **2007**, *115*, 1298-1305.

10.   De Silva, A.O.; Mabury, S.A. *Environ. Sci. Technol.* **2006**, *40*, 2903-2909.

11.   Benskin, J.P.; Bataineh, M.; Martin, J.W. *Anal. Chem.* **2007**, *79*, 6455-6464.

12.   Karrman, A.; Langlois, I.; van Bavel, B.; Lindstrom, G.; Oehme, M. *Environ. Int.* **2007**, *33*, 782-788.

13.   Houde, M.; Czub, G.; Small, J.M.; Backus, S.; Wang, X.; Alaee, M.; Muir, D.C. *Environ. Sci. Technol.* **2008**, *42*, 9397-9403.

14.   Langlois, I.; Oehme, M. *Rapid Commun. Mass Spectrom.* **2006**, *20*, 844-850.

15.   Arsenault, G.; Chittim, B.; McAlees, A.; McCrindle, R.; Riddell, N.; Yeo, B. *Chemosphere.* **2008**, *70*, 616-625.

16.   Ellis, D.A.; Martin, J.W.; Mabury, S.A.; Hurley, M.D.; Andersen, M.P.; Wallington, T.J. *Environ. Sci. Technol.* **2003**, *37*, 3816-3820.

17.   Butt, C.M.; Muir, D.C.; Stirling, I.; Kwan, M.; Mabury, S.A. *Environ. Sci. Technol.* **2007**, *41*, 42-49.

18. Young, C.J.; Furdui, V.I.; Franklin, J.; Koerner, R.M.; Muir, D.C.; Mabury, S.A. *Environ. Sci. Technol.* **2007**, *41*, 3455-3461.

19. Armitage, J.; Cousins, I.T.; Buck, R.C.; Prevedouros, K.; Russell, M.H.; MacLeod, M.; Korzeniowski, S.H. *Environ. Sci. Technol.* **2006**, *40*, 6969-6975.

20. Armitage, J.M.; MacLeod, M.; Cousins, I.T. *Environ. Sci. Technol.* **2009**, 1134-1136.

21. Armitage, J.M.; Schenker, U.; Scheringer, M.; Martin, J.W.; Macleod, M.; Cousins, I.T. *Environ. Sci. Technol.* **2009**, *43*, 9274-9280.

22. Prevedouros, K.; Cousins, I.T.; Buck, R.C.; Korzeniowski, S.H. *Environ. Sci. Technol.* **2006**, *40*, 32-44.

23. Wania, F. *Environ. Sci. Technol.* **2007**, *41*, 4529-4535.

24. McMurdo, C.J.; Ellis, D.A.; Webster, E.; Butler, J.; Christensen, R.D.; Reid, L.K. *Environ. Sci. Technol.* **2008**, *42*, 3969-3974.

25. Bernett, M.K.; Zisman, W.A. *J. Phys. Chem.* **1967**, *71*, 2075-2077.

26. Goss, K.U. *Environ. Sci. Technol.* **2008**, *42*, 456-458.

27. Goss, K.U. *Environ. Sci. Technol.* **2008**, *42*, 5032.

28. Lopez-Fontan, J.L.; Sarmiento, F.; Schulz, P.C. *Colloid. Polym. Sci.* **2005**, *283*, 862-869.

29. Brace, N.O. *Journal of Organic Chemistry* **1962**, *27*, 4491-4497.

30. Burns, D.C.; Ellis, D.A.; Li, H.; McMurdo, C.J.; Webster, E. *Environ. Sci. Technol.* **2008**, *42*, 9283-9288.

31. Cheng, J.; Psillakis, E.; Hoffmann, M.R.; Colussi, A.J. *J. Phys. Chem. A.* **2009**, 113:8152–8156.

32. Kutsuna, S.; Hori, J. *Atmos. Environ.* **2008**, *42*, 8883-8889.

33. Ellis, D.A.; Webster, E. *Environ. Sci. Technol.* **2009**, *43*, 1234-1231.

34. Rayne, S.; Forest, K.; Friesen, K.J. *J. Environ. Sci. Health. A.* **2009**, *44*, 317-326.

35. Perrin, D.D.; Dempsey, B.; Serjeant, E.P. In: *pKa Prediction for Organic Acid and Bases*; Chapman and Hall: London, **1981**.

36. Benskin, J.P.; Arhens, L.Y.L.W.Y.; Yamashita, N.; Taniyasu, S.; Lam, P.K.S.; Tomy, G.; Muir, D.C.; Scott, B.; Spencer, C.; Rosenberg, B.; Martin, J.W. Society of Environmental Toxicology and Chemistry 30th North American Meeting, New Orleans, LA, USA, November 19-23, **2009**.

37. De Silva, A.O.; Mabury, S.A. *Environ. Sci. Technol.* **2004**, *38*, 6538-6545.

38.   Langlois, I.; Berger, U.; Zencak, Z.; Oehme, M. *Rapid Commun. Mass Spectrom.* **2007**, *21*, 3547-3553.

39.   Ochoa-Herrera, V.; Sierra-Alvarez, R.; Somogyi, A.; Jacobsen, N.E.; Wysocki, V.H.; Field, J.A. *Environ. Sci. Technol.* **2008**, *42*, 3260-3264.

40.   Smart, B.E. *J. Fluorine Chem.* **2001**, *109*, 3-8.

41.   De Silva, A.O.; Stock, N.L.; Bonin, J.; Wong, G.W.Y.; Young, C.; Mabury, S.A. PhD Thesis, Department of Chemistry, University of Toronto, ON, Canada, **2008**.

42.   Gauthier, S.A., MSc Thesis, Department of Chemistry, University of Toronto, ON, Canada, **2004**.

43.   Yamamoto, T.; Noma, Y.; Sakai, S.; Shibata, Y. *Environ. Sci. Technol.* **2007**, *41*, 5660-5665.

44.   Rayne, S.; Forest, K.; Friesen, K.J. *J. Mol. Struct.* **2008**, *869*, 81-82.

45.   D'Eon J, C.; Hurley, M.D.; Wallington, T.J.; Mabury, S.A. *Environ. Sci. Technol.* **2006**, *40*, 1862-1868.

46.   Martin, J.W.; Ellis, D.A.; Mabury, S.A.; Hurley, M.D.; Wallington, T.J. *Environ. Sci. Technol.* **2006**, *40*, 864-872.

47.   Plumlee, M.H.; McNeill, K.; Reinhard, M. *Environ. Sci. Technol.* **2009**, *43*, 3662-3668.

48. Ellis, D.A.; Martin, J.W.; De Silva, A.O.; Mabury, S.A.; Hurley, M.D.; Andersen, M.P.S.; Wallington, T.J. *Environ. Sci. Technol.* **2004**, *38*, 3316-3315.

49. Benskin, J.P.; De Silva, A.O.; Martin, L.J.; Arsenault, G.; McCrindle, R.; Riddell, N.; Mabury, S.A.; Martin, J.W. *Environ. Toxicol. Chem.* **2009**, *28*, 542-512.

50. De Silva, A.O.; Benskin, J.P.; Martin, L.J.; Arsenault, G.; McCrindle, R.; Riddell, N.; Martin, J.W.; Mabury, S.A. *Environ. Toxicol. Chem.* **2009**, *28*, 555-512.

51. De Silva, A.O.; Tseng, P.J.; Mabury, S.A. *Environ. Toxicol. Chem.* **2008**, *28*, 330-337.

52. De Silva, A.O.; Muir, D.C.; Mabury, S.A. *Environ.Toxicol.Chem.* **2009**, *28*, 1801-1815.

53. Powley, C.R.; George, S.W.; Russell, M.H.; Hoke, R.A.; Buck, R.C. *Chemosphere.* **2008**, *70*, 664-668.

54. Furdui, V.I.; Helm, P.A.; Crozier, P.W.; Lucaciu, C.; Reiner, E.I.; Marvin, C.H.; Whittle, D.M.; Mabury, S.A.; Tomy, G.T. *Environ. Sci. Technol.* **2008**, *42*, 4739-4744.

55. Benskin, J.P.; Yeung, L.W.Y.; Yamashita, N.; Taniyasu, S.; Lam, P.K.S.; Martin, J.W. *Environ. Sci. Technol.* **2010**, *44*, 9049-9054.

56. Zushi, Y.; Tamada, M.; Kanai, Y.; Masunaga, S. *Environ. Pollut.* **2010**, *158*, 756-763.

57. Olsen, G.W.; Mair, D.C.; Reagen, W.K.; Ellefson, M.E.; Ehresman, D.J.; Butenhoff, J.L.; Zobel, L.R. *Chemosphere.* **2007**, *68*, 105-111.

58. Reagen, W.K.; Lindstrom, K.R.; Jacoby, C.B.; Purcell R.G.; Kestner T.A.; Payfer R.M.; Miller, J.W.; Platform presentation at Society of Environmental Toxicology and Chemistry 28th North American Meeting, Milwaukee, WI, USA, November 11–15, **2007**.

59. Haug, L.S.; Thomsen, C.; Becher, G. *Environ. Sci. Technol.* **2009**, *43*, 2131-2135.

60. Chan, E.; Sandhu, M.; Benskin, J.P.; Ralitsch, M.; Thibault, N.; Birkholz, D.; Martin, J.W. *Rapid Commun. Mass Spectrom.* **2009**, *23*, 1405-1410.

61. Beesoon S, W.G., Shoeib M, Harner T, Benskin JP, Martin JW. Society of Environmental Toxicology and Chemistry 30th North American Meeting, New Orleans, LA, USA, November 19-23, **2009**.

62. Lloyd, A.S.; Bailey, V.A.; Hird, S.J.; Routledge, A.; Clarke, D.B. *Rapid Commun. Mass Spectrom.* **2009**, *23*, 2923-2938.

63. Chu, S.; Letcher, R.J. *Anal. Chem.* **2009**, *81*, 4256-4262.

64. Sharpe, R.L.; Benskin, J.P.; Laarman, A.L.; MacLeod, S.M.; Martin, J.W.; Wong, C.S.; Goss, G.G. *Environ. Toxicol. Chem.* **2010**, *29*, 1957-1966.

65. Benskin, J.P.; Holt, A.; Martin, J.W. *Environ. Sci. Technol.* **2009**, *43*, 8566-8566.

66. Wang, Y.; Arsenault, G.; Riddell, N.; McCrindle, R.; McAlees, A.; Martin, J.W. *Environ. Sci. Technol.* **2009**, *43*, 8283-8289.

67. Ju, X.; Jin, Y.; Sasaki, K.; Saito, N. *Environ. Sci. Technol.* **2008**, *42*, 3538-3542.

68. Yamamoto, T.; Noma, Y.; Sakai, S.; Shibata, Y. *Environ. Sci. Technol.* **2007**, *41*, 5660-5665.

69. Katsushima, A.; Hisamoto, I.; Nagai, M. United States Patent No. 3,525,758. **1970**.

70. Millauer, H. United States Patent No. 3,829,512. **1974**.

71. Katsushima, A.; Hisamoto, I.; Nagai, M.; Fukui, T.; Kato, T. Japanese Patent No. 0831272 (in Japanese). **1976**.

72. Cui, L.; Zhou, Q.F.; Liao, C.Y.; Fu, J.J.; Jiang, G.B. *Arch. Environ. Contam. Toxicol.* **2009**, *56*, 338-349.

73. Johansson, N.; Eriksson, P.; Viberg, H. *Toxicol. Sci.* **2009**, *108*, 412-418.

74. Hu, W.; Jones, P.D.; Upham, B.L.; Trosko, J.E.; Lau, C.; Giesy, J.P. *Toxicol. Sci.* **2002**, *68*, 429-436.

75. Luebker, D.J.; York, R.G.; Hansen, K.J.; Moore, J.A.; Butenhoff, J.L. *Toxicology.* **2005**, *215*, 149-169.

76. Seacat, A.M.; Thomford, P.J.; Hansen, K.J.; Clemen, L.A.; Eldridge, S.R.; Elcombe, C.R.; Butenhoff, J.L. *Toxicology.* **2003**, *183*, 117-131.

77. Loveless, S.E.; Finlay, C.; Everds, N.E.; Frame, S.R.; Gillies, P.J.; O'Connor, J.C.; Powley, C.R.; Kennedy, G.L. *Toxicology.* **2006**, *220*, 203-217.

78. Vanden Heuvel, J.P.; Thompson, J.T.; Frame, S.R.; Gillies, P.J. *Toxicol. Sci.* **2006**, *92*, 476-489.

79. O'Brien, J.M.; Kennedy, S.W.; Chu, S.; Letcher, R.J. *Environ. Toxicol. Chem.* **2010**, in press.

80. De Silva, A.O.; Benskin, J.P.; Martin, L.J.; Arsenault, G.; McCrindle, R.; Riddell, N.; Martin, J.W.; Mabury, S.A. *Environ. Toxicol. Chem.* **2009**, *28*, 555-512.

81. Kudo, N.; Katakura, M.; Sato, Y.; Kawashima, Y. *Chem.-Biol. Interact.* **2002**, *139*, 301-316.

82.   Katakura, M.; Kudo, N.; Tsuda, T.; Hibino, Y.; Mitsumoto, A.; Kawashima, Y. *J. Health Sci.* **2007**, *53*, 77-76.

83.   Lee, J.J.; Schultz, I.R. *Environ. Sci. Technol.* **2010**, *44*, 491-496.

84.   Jones, P.D.; Hu, W.; De Coen, W.; Newsted, J.L.; Giesy, J.P. *Environ. Toxicol. Chem.* **2003**, *22*, 2639-2649.

85.   Ohmori, K.; Kudo, N.; Katayama, K.; Kawashima, Y. *Toxicology.* **2003**, *184*, 135-140.

Appendix A: Supporting Information for Chapter 2-Simultaneous Characterization of Perfluoroalkyl Carboxylate, Sulfonate, and Sulfonamide Isomers by Liquid Chromatography-Tandem Mass Spectrometry

Experimental Methods
Extraction of Human Serum Samples

Serum samples (5 mL) were added to 6mL of 0.1M formic acid containing ^{13}C-PFOS, ^{13}C-PFOA, ^{13}C-PFNA, ^{13}C-PFDA, ^{13}C-PFDoA, and N-MeFOSA. The solution was vortex-mixed and sonicated for 20 min. PFA levels in Oasis HLB cartridges had less contamination than Sep-Pak (C18) cartridges,[1] therefore the former was chosen for use in this experiment. The Oasis cartridges (200mg, Waters) were conditioned with HPLC grade methanol (6mL) and 0.1M formic acid (6mL). The samples were loaded onto the cartridge and slowly passed through by vacuum. Three 5mL volumes of 0.1M formic acid were also used to rinse the centrifuge tubes, originally containing the serum, and were added consecutively to the Oasis cartridge to ensure volumetric transfer. After passing the serum and sample tube washes, the cartridge was rinsed with 15mL of 0.1M formic acid, 6mL of 50% 0.1M formic acid/ 50% methanol, and 1 mL of 1% NH_4OH in water. The cartridge was then purged with air, and analytes were subsequently eluted with 6 mL of methanol (1% NH_4OH) into 15mL centrifuge tubes. The extracts were evaporated under N_2 to 0.5mL and transferred to methanol rinsed polypropylene microvials (Fisher), with polyethylene caps (Supelco), which are known to have lowest PFA contamination.[1]

Quality Control

All analytes, with the exception of N-EtFOSA, FOSA, and PFHxS, initially had measurable instrumental background levels ranging from 1.7 to 7.4 ng which have previously been attributed to internal fluoropolymer parts on the

255

Agilent 1100 HPLC system.[1] However, with the addition of a guard column inserted upstream of the injector, background levels could be effectively removed so as to drastically improve limits of detection. For example, when the pre-injector guard column was inserted, instrumental PFOA eluted later than the 'total PFA' signal (when analytical column was C8 or C18) and later than the latest eluting isomer (linear) when PFO was used. However, some overlap was inevitable. For example, when response from the sample linear PFOA isomer was approximately equal to the instrumental PFOA response, some coelution was inevitable on the perfluorooctyl column (i.e. resolution = 1.0 min), although this was blank subtracted or integrated separately using manual integration. Once the instrumental signal was separated, injections of blank methanol onto the perfluorooctyl column revealed no traces of analytes at the correct retention times. PFHpA was observed in the instrumental background at even higher levels (~7.4 ng) than PFOA and has been attributed to contamination of injector parts, specifically the graphite injector seal,[1] and unfortunately could not be separated from the injected sample fraction, thus linear PFHpA was not a focus in this work. Nevertheless, this did not prohibit the separation and observation of branched PFHpA isomers. The level of PFA contamination from the method (defined as extraction, clean-up, and concentration) was found to decrease in the order PFHpA>PFNA>PFOA≈PFOS, with the remainder of PFAs being not detectable (Table A-12). PFNA, PFOA, and PFOS levels were at low enough levels that they could be background subtracted. Interestingly, PFOS, PFNA, and PFHpA

contamination introduced by the method consisted of branched and linear isomers, whereas method PFOA contamination was only linear (Table A-12).

Spike/recovery experiments were performed to assess the recovery of both 'total PFA isomer' and individual isomer concentrations and are displayed in Tables A-13, A-14, and A-15. Relative isomer composition was retained through the extraction procedure, and percent recoveries for 'total PFA' analysis were also acceptable (62-82% for most PFAs prior to correction with internal standard). Low recoveries were observed for PFTA, (25%) which may explain why PFTA isomers were difficult to detect in human serum. The low recoveries for PFTA have been reported previously[2] and are thought to be due to poor retention by the HLB cartridge.

MS/MS Optimization

The following instrument parameters were optimized for PFA and PFA precursor isomer detection on the 4000Q: curtain gas, collision gas, ion spray voltage, source temperature, source gas, entrance potential, and collision cell exit potential. For *each* PFA or PFA-precursor, further analyte-specific optimization was conducted: in product-ion mode, declustering potential (DP) was ramped and the value which produced a maximum TIC was determined. The collision energy was subsequently ramped using the optimum DP and the resulting mass spectra over the range of collision energies were examined for product ions. The collision energies for each of these product ions were then optimized in multiple-reaction-monitoring (MRM) mode. CID patterns stated in Tables A-1 to A-11 are the peak

areas of each transition collected in MRM mode, normalized to a percent of the largest fragment.

Prediction of Missing Product Ions for Structural Elucidation of PFOS Isomers

The absence of the following product ions are expect for a given PFOS branched isomer: *iso*-PFOS (380, 119) 5*m*-PFOS (330, 169); 4*m*-PFOS (280, 219); 3*m*-PFOS (230, 269); 2*m*-PFOS (180, 319); and 1*m*-PFOS (130, 369). Similarly, the following missing fragments are expected for perfluoroisobutyl and geminal perfluorodimethyl branched PFOS isomers: *ib*-PFOS (330, 119); 4m_2-PFOS (280, 169); 3m_2-PFOS (230, 219); 2m_2-PFOS (180, 269); 1m_2-PFOS (130, 319). Although not observed here, it is germane to note that Lyons et al.[3] observed '1-series' (*m/z* 361, 311, 261, etc.) fragments and Langlois[4] also detected this, albeit only for 1 isomer.

HPLC-MS Parameters for 'Total PFA' Quantification

HPLC/MS/MS analysis for 'total PFA' (e.g. by integration of a single peak) concentrations was performed by injection (20uL) of methanol extracts onto an Agilent Zorbax C8 3.5 μm (2.1mm x 5cm) column equipped with a Agilent eclipse C8 guard column (4.6 mm x 12.5 mm) using a gradient elution program with 5mM ammonium acetate and 100% methanol at a flow rate of 180 μL/min. The elution program was set initially at 20% methanol, followed immediately by a 1 min linear ramp to 70% methanol then to 100% by 12.5 min. The column was held at 100% MeOH for 7.5 min, returned to initial conditions by 21 min, and

allowed to equilibrate for 20 min prior to the next run. Mass spectra were obtained

using the same instrumentation as in isomer-specific profiling except that only

two MS/MS transitions were monitored for each analyte here.

Product Ion Scanning of Interferences

Structural elucidation of mass spectral interferences in the chromatograms

of PFOS and PFHxS were performed using the 4000Q's enhanced product ion

mode (EPI). For PFOS, the product ions of m/z 499 were monitored from m/z 50

to m/z 550. The declustering potential was set to -80 and the collision energy was

set to -70 with a collision energy spread of ± 25 to allow a range of product ions.

For PFHxS, the product ions of m/z 399 were monitored from m/z 50 to m/z 450.

The declustering potential was set to -70 and the collision energy was set to -30

with a collision energy spread of ± 20 to allow a range of product ions.

Results and Discussion
Fragmentation Assignments of PFOS Mass Spectral Interferences

The product ion spectrum of the PFOS interference was unlike any

perfluorinated analyte (Figure 4a), and the dominant product ion recorded was m/z

80, hence the potential for major interference in the m/z 499→80 MS/MS

transition without separation. Suspecting that this was an endogenous human

metabolite, we searched the Human Metabolome Database (http://www.hmdb.ca/)

to reveal a small list of biomolecules having a negative ion mass of 499±1. This

list included 3 isomers of taurodeoxycholic acid, all of which are sulfonic acid

containing bile acids formed in the liver by conjugation of deoxycholate with

taurine. To confirm that the interferent was indeed taurodeoxycholate (and/or its isomers) an authentic standard of taurodeoxycholate was purchased and its product spectrum recorded by infusion. Fragmentation assignments for taurodeoxycholate are as follows: m/z 499, $[C_{26}H_{44}NO_6S]^-$; m/z 481, $[C_{26}H_{42}NO_5S]^-$; m/z 356, $[C_{24}H_{35}O_2]^-$; m/z 124, $[NH_2C_2H_4SO_3]^-$; m/z 107, $[C_2H_3SO_3]^-$; m/z 80, $[SO_3]^-$. The exact monoisotopic mass of taurodeoxycholate anion is 498.2894 (average 498.7036), compared to 498.9303 for the PFOS anion, thus while these would be easily distinguishable by high-resolution MS, they are difficult to distinguish by low-resolution instruments in common use by investigators in this field.

Fragmentation Assignments of PFHxS Mass Spectral Interferences

The PFHxS interferences eluted at the same location in product ions m/z 80 and 99 as the authentic branched PFHxS isomers in the standard. Again suspecting an endogenous metabolite, we performed a search using the METLIN Metabolite Database (http://metlin.scripps.edu/) to narrow down their possible identity to isomers of pregnenolone sulfate, common steroid sulfates. A detailed mass spectral fragmentation analysis for a variety of neurosteroid sulfates was recently performed by Griffiths et al.[5] that further assisted confirmation of these interferences. Structural assignments for 5-pregnan-3,20-diol-3-sulfate are as follows: m/z 399, $[C_{21}H_{35}O_5S]^-$; m/z 381, $[C_{21}H_{33}O_4S]^-$; m/z 355, $[C_{19}H_{30}O_4S]^-$; m/z 339, $[C_{18}H_{27}O_4S]^-$; m/z 313, $[C_{16}H_{25}O_4S]^-$; m/z 123, $[C_2H_3O_4S]^-$; m/z 97, $[HSO_4]^-$; m/z 80, $[SO_3]^-$.[5] Interestingly, these interferences contain the same 4-ring base

structure as the PFOS interference-not surprising considering their similarities in retention time (~19-24 minutes for the PFHxS interference vs. ~24-27 minutes for the PFOS interference).

Additional PFOS, PFOA Interferences

Another unknown (m/z 499) which was not present in blanks or human serum was observed in the electrochemically fluorinated PFOS standard and eluted *after* the linear isomer (Figure 1). The peak was correlated with the concentration of PFOS and was not observed in the linear PFOS standard or other electrochemically fluorinated standards. Interestingly, Karrman et al.[6] also observed what they identified as a branched PFOS isomer eluting after the linear peak in human serum. However, the fact that this unknown did not show any product ions in our study (including the most common one, a loss of [SO_3]⁻) makes it uncertain if it is indeed an isomer of PFOS. This interferent could presumably hamper quantification of PFOS when using a single quadrupole instrument, it is unlikely that it would present any quantification bias when monitoring the common product ions of PFOS.

Human serum also had nominal mass interferences of PFOA, but only in the m/z 413→169 MS/MS transition. This was identified as an interferent based on the fact that in an electrochemically fluorinated standard (Figure 3), the m/z 413→369 transition was the more sensitive of the two transitions for observation of most branched isomers, while in human serum, the m/z 413→169 transition had significantly more intense peaks (I_1, I_2, I_3) and an absence of branched isomers in

the *m/z* 413→369 transition. The presence of this interference did not preclude the

identification of branched isomers, which could be observed in other transitions.

Table A-1. N-EtFOSA Collision-Induced Dissociation Pattern

N-EtFOSA Isomer	RT (min)	Isomer-specific CID pattern of molecular anion m/z 526 collected in MRM mode. (normalized to % of largest fragment observed) Product ion m/z												
		419	402	362	319	287	269	219	169	126	119	83	69	65
n-[#]	66.56	10.1	1.4	4.8	<0.1	0.7	15.2	31.6	100	17.5	11.2	3.3	1.7	13.6
B_1-[#]	65.55	coelute	<0.1	0.56	---	---	---	10.5	100	coelute	---	0.9	1.6	3.5
B_2-[#]	65.41	100	<0.1	coelute	---	---	---	coelute	---	22.9	0.82	0.28	coelute	coelute
B_3-[#]	65.25	coelute	<0.1	0.63	coelute	---	coelute	100	coelute	14.0	coelute	coelute	14.14	coelute
B_4-[#]	65.05	coelute	<0.1	0.17	25.9	---	100.0	coelute	97.9	---	29.2	3.4	coelute	17.6
B_5/B_6-[#]	64.45	63.1	---	0.03	3.5	---	13.5	100	22.1	13.5	11.0	0.3	1.0	22.7
B_7/B_8-[#]	63.95	9.7	---	---	12.4	---	56.5	20.3	100	9.36	16.9	1.0	17.5	6.0
B_9-[#]	63.65	1.5	---	---	100	---	53.0	---	4.53	---	83.0	1.9	32.3	coelute
B_{10}-[#]	63.55	2.7	---	---	100	---	5.7	34.5	4.72	9.24	---	0.7	38.8	15.20
B_{11}-[#]	63.05	---	---	---	9.5	---	---	100	---	---	---	1.5	8.9	---
B_{12}-[#]	62.85	---	---	---	---	---	58.2	34.93	100	---	---		21.6	---
B_{13}-[#]	62.65	---	---	---	39.1	---	17.6	50.00	---	---	---	9.2	35.3	100
B_{14}-[#]	62.25	---	---	---	100	---	---	---	---	---	---	---	31.2	---

#=found in standard   **coelute** =co-elution may have precluded observation of this ion.

Table A-2. FOSA Collision-Induced Dissociation Pattern

FOSA Isomer	RT (min)	Isomer-specific CID pattern of molecular anion m/z 498 collected in MRM mode. (normalized to % of largest fragment observed)		
		Product ion m/z		
		78	169	119
n-*[#]	60.66	100	1.8	0.4
B$_1$-*[#]	59.33	100	4.4	---
B$_2$-*[#]	59.13	100	1.6	1.5
B$_3$-[#]	58.73	100	2.9	1.4
B$_4$-[#]	57.92	100	100	28.0
B$_5$-[#]	57.72	100	4.4	16.0

*=found in serum   #=found from incubation of technical N-EtFOSA isomers
coelute =co-elution may have precluded observation of this ion.

Table A-3. PFHpA Collision-Induced Dissociation Pattern

PFHpA Isomer	RT (min)	Isomer-specific CID pattern of molecular anion *m/z* 363 collected in MRM mode. (normalized to % of largest fragment observed) Product ion *m/z*		
		78	169	119
n-[#]	42.72	0.30	100	31.5
B_1[#]	36.68	100	48.0	46.9
U_1[#]	35.87	100	---	---
B_2[#]	33.65	100	---	63.6

#=found in standard/ background

265

Table A-4. PFHxS Collision-Induced Dissociation Pattern

| PFHxS Isomer | RT (min) | Isomer-specific CID pattern of molecular anion m/z 399 collected in MRM mode. (normalized to % of largest fragment observed) Product ion m/z |
		99	80	169	130	180	280	230	219	119	69
n-*[#]	26.8	23.5	100	5.4	0.9	0.3	<0.1	0.8	---	9.1	0.8
B_1*[#]	24.3	17.1	100	21.6	4.9	1.1	---	12.4	0.7	8.5	2.9
B_2[#]	23.3	10.0	100	2.3	13.4	3.5	4.5	---	3.6	---	8.5
B_3[#]	23.0	48.0	---	---	---	4.3	---	1.4	---	100	---
B_4[#]	22.6	100	<0.1	82.4	15.6	---	---	---	---	26.2	15.2
U_1[#]	22.4	---	---	---	---	---	100	---	---	---	---
B_5[#]	22.2	---	100	8.5	5.5	3.1	---	---	58.6	---	10.4
B_6[#]	21.4	100	43.4	---	26.2	7.7	---	4.6	15.9	20.6	10.1

*=found in serum   #=found in standard   coelute =co-elution may have precluded observation of this ion.

Table A-5. PFOA Collision-Induced Dissociation Pattern

PFOA Isomer	RT (min)	Isomer-specific CID pattern of molecular anion m/z 413 collected in MRM mode. (normalized to % of largest fragment observed) Product ion m/z					
		369	169	219	119	319	269
n-PFOA*[#]	55.22	100	32.3	13.0	2.8	---	---
B$_1$ *[#]	49.37	100	81.1	62.4	---	---	---
B$_2$*[#]	45.50	coelute	57.0	100	coelute	---	---
B$_3$*[#]	45.50	100	coelute	coelute	56.3	---	---
B$_4$*[#]	43.13	100	44.7	4.0	---	---	---
B$_5$/B$_6$[#]	41.11	14.9	---	100	---	---	---
B$_7$[#]	39.90	100	57.4	3.0	71.3	---	15.2
B$_8$[#]	39.30	---	100	---	---	---	20.0
U$_1$[#]	37.30	---	---	---	---	100	---
U$_2$*	23.00	14.0	100	---	---	---	---

*=found in serum   #=found in standard   coelute =co-elution may have precluded
observation of this ion.

267

Table A-6. PFOS Collision-Induced Dissociation Pattern

Isomer-specific CID pattern of molecular anion m/z 499 collected in MRM mode.
(normalized to % of largest fragment observed)

PFOS Isomer	RT (min)	Product ion m/z												
		169	130	80	99	180	380	280	330	419	230	219	119	69
n-*#	49.98	4.3	2.5	100	22.4	0.9	0.1	0.8	0.3	---	1.9	0.6	2.8	0.6
ip-*#	43.93	19.7	6.3	100	14.4	4.9	---	2.2	3.1	---	10.5	0.9	---	---
5m-*#	40.71	---	35.5	100	5.0	6.8	1.0	10.4	---	---	16.3	2.4	0.6	1.2
4m-*#	39.10	---	5.7	100	4.3	15.9	---	---	5.1	---	19.2	---	1.3	---
B4-*#	38.29	0.1	---	coelute	100	30.1	coelute	coelute	---	8.9	coelute	75.5	---	---
3m-*#	37.89	7.8	38.9	100	19.0	1.7	---	9.6	---	coelute	---	10.3	1.5	0.7
B6-*#	37.40	---	---	---	---	10.3	---	coelute	---	100.0	3.7	15.8	---	---
B7-*#	34.66	coelute	---	100	---	13.4	---	---	11.0	---	5.0	2.5	---	---
B8-*#	34.26	coelute	20.1	100	---	1.8	---	---	1.9	---	---	---	---	---
B9-*#	33.45	100	---	---	85.0	---	---	---	---	13.7	22.1	---	---	---
B10-*#	32.00	---	100	89.2	---	---	---	---	---	---	---	37.3	19.3	---

*=found in serum   #=found in standard   coelute =co-elution may have precluded observation of this ion.

Table A-7. PFNA Collision-Induced Dissociation Pattern

PFNA Isomer	RT (min)	Isomer-specific CID pattern of molecular anion m/z 463 collected in MRM mode. (normalized to % of largest fragment observed) Product ion m/z				
		169	**219**	**419**	**119**	**269**
n-*[#]	60.27	19.6	27.4	100	1.3	4.6
iso-*[#]	58.24	46.4	21.6	100	---	---
B_2-*[#]	57.23	---	100.0	<0.1	---	---
B_3[#]	56.22	55.6	30.0	100.0	---	---
U_1-*[#]	53.70	---	---	---	---	100.0
U_2-*[#]	42.50	---	---	---	100.0	---

*=found in serum   #=found in standard

269

Table A-8. PFDA Collision-Induced Dissociation Pattern

PFDA Isomer	RT (min)	Isomer-specific CID pattern of molecular anion m/z 513 collected in MRM mode. (normalized to % of largest fragment observed) Product ion m/z					
		469	**219**	**169**	**119**	**269**	**319**
n-*[#]	64.09	100	22.4	10.7	2.8	18.5	2.6
B_1-*[#]	62.5	100	---	---	---	14.7	23.3
B_2-[#]	61	---	100	---	---	43.1	---

*=found in serum   #=found in standard

270

Table A-9. PFUnA Collision-Induced Dissociation Pattern

PFUnA Isomer	RT (min)	Isomer-specific CID pattern of molecular anion m/z 563 collected in MRM mode. (normalized to % of largest fragment observed) Product ion m/z				
		519	219	169	119	319
n-*[#]	67.91	55.0	100	80.8	23.8	78.4
B_1-*[#]	66.30	100	8.0	75.9	7.1	12.8
B_2-[#]	65.29	2.4	19.9	1.2	---	100
B_3-[#]	63.88	69.5	---	100	37.4	---
B_4-[#]	63.08	---	---	---	---	100
B_4-/B_5-[#]	62.87	100	11.4	---	---	---
B_5-[#]	62.67	---	---	100	26.8	---

*=found in serum   #=found in standard

Table A-10. PFDoA Collision-Induced Dissociation Pattern

PFDoA Isomer	RT (min)	Isomer-specific CID pattern of molecular anion m/z 613 collected in MRM mode. (normalized to % of largest fragment observed) Product ion m/z							
		569	319	219	169	119	419	319	269
n-*#	70.4	100	17.1	15.7	17.7	5.4	1.4	17.1	16.0
B_1-#	68.92	17.1	---	100	---	0.7	---	---	---
B_2-#	68.40	100	78.0	---	---	---	---	---	---
B_3-#	68.12	---	---	---	3.3	7.1	---	---	100
B_4-#	67.31	---	---	13.6	7.0	44.2	---	---	100
B_5-#	66.91	---	100	3.2	11.5	---	1.6	96.2	2.8
B_6-#	66.10	---	67.5	59.8	---	100	---	66.6	41.1
B_7-#	65.90	100	---	17.1	32.2	---	---	---	---
B_8-#	65.70	---	---	---	---	---	100	---	1.8
U_1-#	64.90	100	---	---	---	---	---	---	---
B_9-#	64.20	63.1	---	---	---	100	60.2	---	---
B_{10}-#	63.90	28.8	---	64.0	---	100	---	---	---
U_2-#	63.20	100	---	---	---	---	---	---	---
B_{12}-#	63.08	<0.01	---	47.7	60.3	---	---	---	100
U_3-#	62.80	20.4	---	---	---	---	100	---	---
U_4-#	61.67	100	---	---	11.9	---	---	---	---
U_5-#	60.05	100	---	---	---	---	---	---	32.7
U_6-#	59.30	73.0	---	---	---	27.1	---	---	---

*=found in serum   #=found in standard   coelute =co-elution may have precluded observation of this ion.

Table A-11. PFTA Collision-Induced Dissociation Pattern

PFTA Isomer	RT (min)	Isomer-specific CID pattern of molecular anion m/z 713 collected in MRM mode. (normalized to % of largest fragment observed) Product ion m/z			
		669	419	169	119
n-*[#]	74.28	100	12.3	27.8	4.7
B_1-[#]	72.95	49.0	---	---	100
B_1-/B_2-[#]	72.75	---	---	100	---
B_2-[#]	72.35	100.0	---	---	52.1
B_3-[#]	71.54	5.1	100	---	---
B_4-[#]	71.34	100	---	17.9	3.5
B_5-[#]	70.94	93.0	---	100.0	9.2
B_6-[#]	70.53	---	33.0	---	100

*=found in serum   #=found in standard

Table A-12. Background levels of PFAs and PFA-precursors

PFA / PFA-precursor	Method Blank PFAs /ng	Isomer Composition	HPLC Pump PFAs /ng
PFHpA	7.0	B_1, U_1, B_2, n-	7.4
PFHxS	---	---	---
PFOS	1.0	$6m$-, $5m$-, $3m$-, n-, others	1.7
PFOA	1.0	n-	5.0
PFNA	1.2	B_3-, n-	3.7
PFDA	---	---	4.0
PFDoA	---	---	2.4
PFUnA	---	---	2.8
PFTA	---	---	2.7
N-EtFOSA	---	---	---
FOSA	---	---	---

Table A-13. Percent Recovery Data for 'Total PFA' Analysis (n=3, 50 ng fortification of human serum)

PFA / PFA-precursor	% Absolute Recovery (95% CI)	% Recovery Corrected for IS (95% CI)
PFHpA*	---	---
PFHxS	63 % (50-76)	99 % (79-119)
PFOS	57 % (41-73)	97 % (79-116)
PFOA	82 % (71-94)	105 % (100-110)
PFNA	79 % (74-85)	101 % (91-111)
PFDA	62 % (40-84)	97 % (91-102)
PFDoA	71 % (43-100)	113 % (101-124)
PFUnA	69 % (44-94)	104 % (101-107)
PFTA	25 % (3-54)	71 % (61-82)
N-EtFOSA[#]	100 %	130 %
FOSA[#]	78 %	100 %

* High background levels precluded quantitation.

[#] n=1, 50 ng fortification.

Table A-14. Percent Recovery Data for Individual PFOS Isomers (n=3)

PFOS Isomer	% Recovery, corrected for IS (95% CI)
n-*[#]	99 % (91-106)
ip -*[#]	108 % (93-124)
$5m$-*[#]	106 % (97-115)
$4m$- *[#]	99 % (94-104)
B_4- *[#]	101 % (92-110)
$3m$- *[#]	103 % (94-113)
B_6-*[#]	102 % (98-106)
B_7-*[#]	109 % (98-120)
B_8-*[#]	116 % (79-154)
B_9-*[#]	102 % (92-113)
B_{10}-*[#]	97 % (86-108)

Table A-15. Percent Recovery Data for Individual PFOA Isomers (n=3)

PFOS Isomer	% Recovery, corrected for IS (95% CI)
n-PFOA*[#]	99 (91-106)
B_1 *[#]	104 (100-108)
B_2[#]/ B_3[#]	103 (94-113)
B_4*[#]	100 (96-104)
B_5/B_6[#]	103 (93-113)
B_7[#]	102 (95-110)
B_8[#]	99 (92-107)
U_1[#]	104 (103-105)
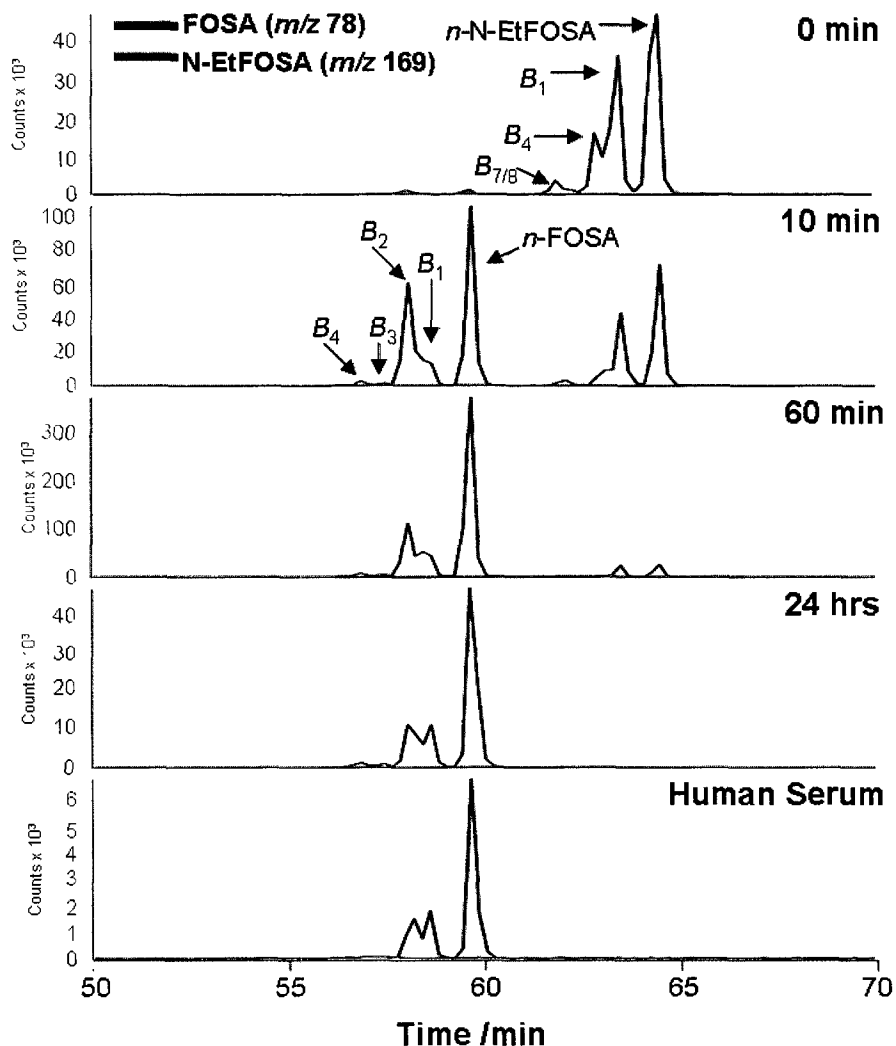
Figure A-1. Metabolism of N-EtFOSA isomers to FOSA isomers (and subsequently to PFOS, not shown) by human liver microsomes over 24 hrs and comparison to profile in human serum. Only a single transition is shown for each, however many other transitions were monitored to fully resolve the isomers. Note the stark contrast of FOSA isomer profile at 10 min vs. 24 hrs. At 24 hrs the FOSA profile is virtually identical to that found in humans.

REFERENCES

1   Yamashita, N.; Kannan, K.; Taniyasu, S.; Horii, Y.; Okazawa, T.; Petrick, G.; Gamo, T. *Environ.Sci.Technol.* **2004**, *38*, 5522-5528.

2   Kuklenyik, Z.; Reich, J. A.; Tully, J. S.; Needham, L. L.; Calafat, A. M. *Environ.Sci.Technol.* **2004**, *38*, 3698-3704.

3   Lyon, P. A.; Tolmer, K. B.; Gross, M. L. *Anal. Chem.* **1985**, *57*, 2984-2989.

4   Langlois, I.; Oehme, M. *Rapid Commun.Mass Spectrom.* **2006**, *20*, 844-850.

5   Griffiths, W. J.; Liu, S. Y.; Yang, Y.; Purdy, R. H.; Sjovall, J. *Rapid Commun.Mass Spectrom.* **1999**, *13*, 1595-1610.

6   Karrman, A.; Jarnberg, U.; van Bavel, B.; Lindstrom, G. *Fluoros Conference*, Toronto, Canada, **2005**.

Appendix B: Supporting Information for Chapter 3-Disposition of Perfluorinated Acid Isomers in Sprague-Dawley Rats Following a Single Dose

Table B-1. Initial body mass, terminal body mass (group 1, day 3; group 2, day 38), and liver somatic index (LSI) for male rats. LSI = liver weight / rat weight x 100%.

	Group 1 Rats		Group 2 Rats	
	Control 1	Dosed n=3 (std error)	Control 2	Dosed n=4 (std error)
Initial mass (g):	402	429 (10.7)	437	434 (5.91)
Terminal Mass (g):	402	427 (11.7)	642	604 (22.5)
LSI at time of sacrifice:	5.97	4.39 (0.21)	4.64	4.05 (0.30)

Table B-2. Percent recovery for perfluorohexane sulfonate (PFHxS), perfluorooctane sulfonate (PFOS), perfluorooctanoic acid (PFOA), and perfluorononanoic acid (PFNA) spiked into blood, tissues, urine, and feces (100ng fortification). Blood data represents the mean of n=3 replicates (± 1 standard error), while tissue data is from n=1 sample. Values in parenthesis represent extraction efficiency (EE). EE =(analyte extracted in 3 MTBE fractions) / (analyte extracted in 4 MTBE fractions) x 100%.

FA Isomer	Blood (1mL)	Brain	Muscle	Fat	Intest.	Testes	Lungs	Heart	Spleen	Kidneys	Liver	Urine	Feces
PFHxS													
n (99)	99±1 97 (100)	37 (100)	96 (100)	38 (ND)	24 (100)	106 (100)	112 (100)	15 (100)	100 (100)	116 (100)	51 (100)	105 (92)	94 (ND)
B₁ (169)	99 1 ±1 98 (100)	45 (ND)	102 (100)	49 (100)	35 (ND)	107 (100)	62 (100)	19 (100)	102 (100)	114 (100)	52 (100)	103 (94)	105 (ND)
B₂ (99)	107± 14 2 (100)	50 (ND)	105 (100)	50 (100)	30 (ND)	101 (100)	71 (100)	17 (100)	110 (100)	106 (100)	65 (100)	105 (94)	105 (ND)
PFOS													
n (80)	100±2 03 (100)	43 (100)	100 (100)	42 (100)	40 (100)	99 (100)	103 (100)	39 (100)	105 (100)	101 (100)	77 (100)	105 (97)	96 (90)
iso (80)	103±8 11 (100)	55 (100)	93 (100)	42 (ND)	46 (100)	105 (100)	81 (100)	30 (100)	103 (100)	98 (100)	80 (100)	105 (96)	110 (89)
5m (130)	110±0 84 (100)	45 (100)	88 (100)	38 (ND)	31 (100)	108 (100)	88 (100)	31 (100)	106 (100)	103 (100)	66 (100)	107 (95)	98 (89)
4m (330)	109±16.80 (100)	43 (ND)	91 (100)	41 (ND)	25 (ND)	104 (100)	85 (100)	34 (100)	110 (100)	115 (100)	69 (100)	100 (96)	99 (ND)
1m (419)	106±2 85 (100)	49 (ND)	110 (100)	74 (ND)	50 (100)	96 (100)	102 (100)	47 (100)	113 (100)	133 (100)	87 (100)	131 (97)	101 (ND)
3m (130)	99±1 91 (100)	42 (100)	90 (100)	35 (ND)	26 (ND)	103 (100)	87 (100)	47 (100)	99 (100)	98 (100)	58 (100)	100 (96)	101 (ND)
tb (130)	- (100)	49 (100)	100 (100)	56 (ND)	27 (100)	105 (100)	74 (100)	30 (100)	93 (100)	95 (100)	62 (100)	91 (96)	91 (ND)
B₇ (169)	100±1 25 (100)	46 (ND)	98 (100)	66 (ND)	52 (100)	97 (100)	102 (100)	30 (100)	163 (100)	111 (100)	97 (100)	127 (97)	94 (ND)
B₈ (130)	- (100)	54 (100)	88 (100)	44 (ND)	33 (100)	102 (100)	99 (100)	30 (100)	98 (100)	99 (100)	73 (100)	96 (97)	110 (ND)
B₉ (419)	- (100)	- (ND)	-(ND)	- (ND)	- (ND)	(ND)	- (100)	-(ND)	- (ND)	- (100)	- (100)	-(ND)	- (ND)
PFOA													
n (369)	106 ± 0.52 (100)	105 (98)	115 (100)	103 (89)	109 (99)	116 (100)	121 (100)	60(99)	116 (100)	112 (100)	100 (100)	111 (95)	109 (94)
iso (369)	103 ± 1 27 (100)	101 (100)	100 (100)	96 (89)	65 (100)	128 (100)	96 (100)	124 (100)	108 (100)	102 (100)	95 (100)	111 (91)	106 (97)
4m (119)	104 ± 5 66(100)	105 (100)	91 (100)	76(100)	48 (100)	114 (100)	75 (100)	149 (100)	95 (100)	90 (100)	77 (100)	101 (92)	103 (100)
5m (219)	110 ± 4 27(100)	106 (ND)	97 (100)	96(100)	52 (100)	115 (100)	83 (100)	147 (100)	98 (100)	101 (100)	97 (100)	110 (99)	114 (100)
3m (169)	105 ± 1 39 (100)	96 (ND)	97 (ND)	95 (ND)	80 (ND)	109 (ND)	89 (100)	135 (ND)	100 (100)	100 (ND)	94 (100)	113 (99)	99 (100)
tb (219)	106 ± 4 39 (100)	95 (ND)	104 (100)	101 (100)	55 (100)	117 (100)	90 (100)	131 (100)	109 (100)	107 (100)	105 (100)	107 (99)	102 (100)
5,3 / 5,4m₂ (169)	106 ± 3 52 (100)	106 (ND)	96 (ND)	96 (ND)	51 (ND)	101 (ND)	83 (100)	150 (ND)	103 (ND)	101 (ND)	99 (ND)	104 (98)	96 (100)
4,4m₂ (269)	104 ± 17 3 (100)	126 (ND)	110 (ND)	93 (ND)	88 (ND)	144 (100)	111 (100)	156 (100)	103 (ND)	116 (100)	116 (100)	105 (99)	102 (ND)
B₈ (319)	104 ± 9 99 (100)	86 (ND)	102 (100)	70 (100)	109 (100)	112 (100)	93 (100)	145 (100)	94 (100)	153 (100)	109 (100)	112 (100)	108 (ND)
PFNA													
n (219)	105 ± 3 7 (100)	96 (99)	110 (100)	87 (90)	106 (100)	126 (99)	118 (100)	90 (100)	112 (100)	106 (100)	92 (100)	114 (86)	117 (97)
iso (219)	99 ± 3 7 (100)	95 (97)	108 (100)	90 (94)	93 (100)	130 (100)	103 (100)	69 (100)	102 (100)	98 (100)	92 (100)	96 (91)	110 (98)

*n=1 for all tissues, urine and feces. n=3 for blood samples.   ND denotes non-detect in first extraction.

Table B-3. Tissue depuration half lives (days) for perfluorohexane sulfonate (PFHxS), perfluorooctane sulfonate (PFOS), perfluorooctanoic acid (PFOA), and perfluorononanoic acid (PFNA). Values were calculated using day 3 and day 38 rats (2 time points). Error represents ± standard error about the mean.

PFA Isomer	Blood	Brain	Muscle	Fat	Intest.	Testes	Lungs	Heart	Spleen	Kidneys	Liver
PFHxS											
n (99)	15 9 (13 29-21 04)	-	7 46 (5 1-14 2)	-	30 5 (21 6-52 2)	19 2 (13 8-22 7)	19 0 (15 6-21 5)	22 4 (16 3-26 7)	20 59 (12 1-20 9)	22 13 (16 2-25 6)	51 8 (29 5 211 4)
B₁ (169)	7 10 (6 3-8 85)	-	-	-	-	-	-	-	-	7 45 (5 2-13)	7 03 (4 6-14 9)
B₂ (99)	3 60 (3 19-4 43)	-	-	-	-	-	-	-	-	-	-
PFOS											
n (80)	33 7 (25 5-49 6)	20 3 (13 8-38 0)	12 4 (9 1-19 5)	10 9 (8 4-15 5)	23 1 (15 4-46 4)	18 5 (13 3-30 3)	17 8 (14 2-23 9)	19 9 (15 1-29 4)	18 9 (15 5-24 3)	23 76 (19-31.8)	51 1 (35 6-90 6)
iso (80)	23 4 (19 1-30 1)	18 5 (12 9-33)	11 6 (8 6-17 9)	11 1 (12 1-20 0)	15 0 (12 1-20 0)	16 9 (11 9-29 2)	16 8 (13 2-23 3)	19 4 (14 4-29 9)	11 8 (8 2-21 1)	18 20 (14 1-25 6)	57 1 (36 8 127 1)
5m (130)	24 4 (19 6-32 2)	-	-	-	20 7 (13 6-44 1)	18 5 (13 1-31 5)	17 9 (14 2-24 0)	19 2 (13 9 30 9)	18 5 (14 6-25 3)	18 70 (14 1-27 9)	59 3 (44 9-327 5)
4m (330)	23 1 (17 5-33 9)		-				8.1 (5 0-21 2)	-		14 86 (9 7-32 1)	60 5 (39 4-130 8)
3m (130)	33 8 (23 0 64 0)	-	-		-	-	16.4 (11 9-26 5)	19 1 (12 7-39 0)	-	-	65 4 (40 6-167 9)
1m (419)	102 (46 2-)	-	-	-	91 4 (37-*)	36 1 (23 3-80 2)	26 2 (20 4 36 5)	36 2 (21 8-105 6)	44 5 (28 6-100 3)	27 9 (22-38 1)	Not eliminated*
tb (130)	19 6 (14 2-31 5)	-	-	-	-	-	-	-	-	14 6 (12 8-17.0)	31 5 (24 1-45 5)
B₇ (169)	15 4 (11 9-21 7)			-	-	-	15 3 (11 9 21 6)	-		18 4 (14 3-25.7)	70 5 (46 3 147 2)
B₈ (130)	11 3 (9 5-13 9)	-	-	-	-	-	-	-	-	18 3 (16 8-20 1)	33 2 (24 7-50 5)
B₉ (419)	11 1 (9 1 14 4)	-	-	-	-	-	-	-	-	-	27 0 (22 2-34 5)
PFOA											
n (369)	13 4 (10 25-19 17)	-	4.76 (4-5 9)	5 83 (5 7)	9 59 (8 6-10 8)	8 89 (8 2-9 7)	8 60 (8 2-9 1)	9 02 (8 3-9 9)	9 00 (8 4-9 7)	10 5 (9 8-11 3)	13 5 (12 1 15 2)
iso (369)	8 11 (6 85 9 96)	-	5 00 (4 3-6 0)	4 97 (4 2-6 2)	8 20 (7.2-9 6)	6 37 (5 9-6 9)	6 35 (6 1-6 6)	6 58 (6 3-6 9)	6 07 (5 9-6 3)	6.62 (6 4-6 8)	7 04 (6 9-7 2)
4m (119)	4 32 (3 87-4 90)	-	-	-	-	-	-	-	-	-	-
5m (219)	3 95 (3.47 4.57)	-	-	-	-	-	8 64 (7 9-9 5)	7 88 (7 4-8 4)		6 04 (5 2-7 1)	-
3m (169)	6 26 (5 47-7 33)	-	-	-	-	-	-	6 16 (5 8 6 6)		4 87 (4 0-6.3)	6 1 (6 0-6 2)
tb (219)	2 25 (1 93-2 71)	-	-	-	-	-	-	-	-	-	-
5,3 / 5,4m₂ (169)	1 79 (1 54-2 14)	-	-	-	-	-	-	-	-	-	-
4,4m₂ (269)	1 28 (0 82-2 91)	-	-	-	-	-	-	-	-	-	-
B₈ (319)	9 10 (7 28-12 12)			-	-	-	-	-	-	-	7 34 (5 6-10 8)
PFNA											
n (219)	40 6 (35 1-48 2)	17 7 (14 5-22 7)	13 5 (10 4 19 5)	13 4 (10 4-18 9)	23 8 (18 0-35 2)	21 0 (15 7 31 5)	17 3 (14 2-22 1)	19 0 (16 1-23 2)	18 4 (14 8-24 5)	23 1 (19 5 28.2)	35 7 (27 1-52 6)
iso (219)	20 7 (18 6-23 3)	12 8 (9 5-19 7)	11 9 (9 1-17 3)	9 5 (7 9-11.9)	18 9 (14 4-27 6)	17 7 (13 8-24 6)	28 6 (20 8-45 9)	18 8 (13 4-31 1)	12 3 (9 4-17 4)	16 4 (12 8-22 9)	18 0 (14 1-25 0)

*Average relative response was identical in liver on day 3 and day 38.
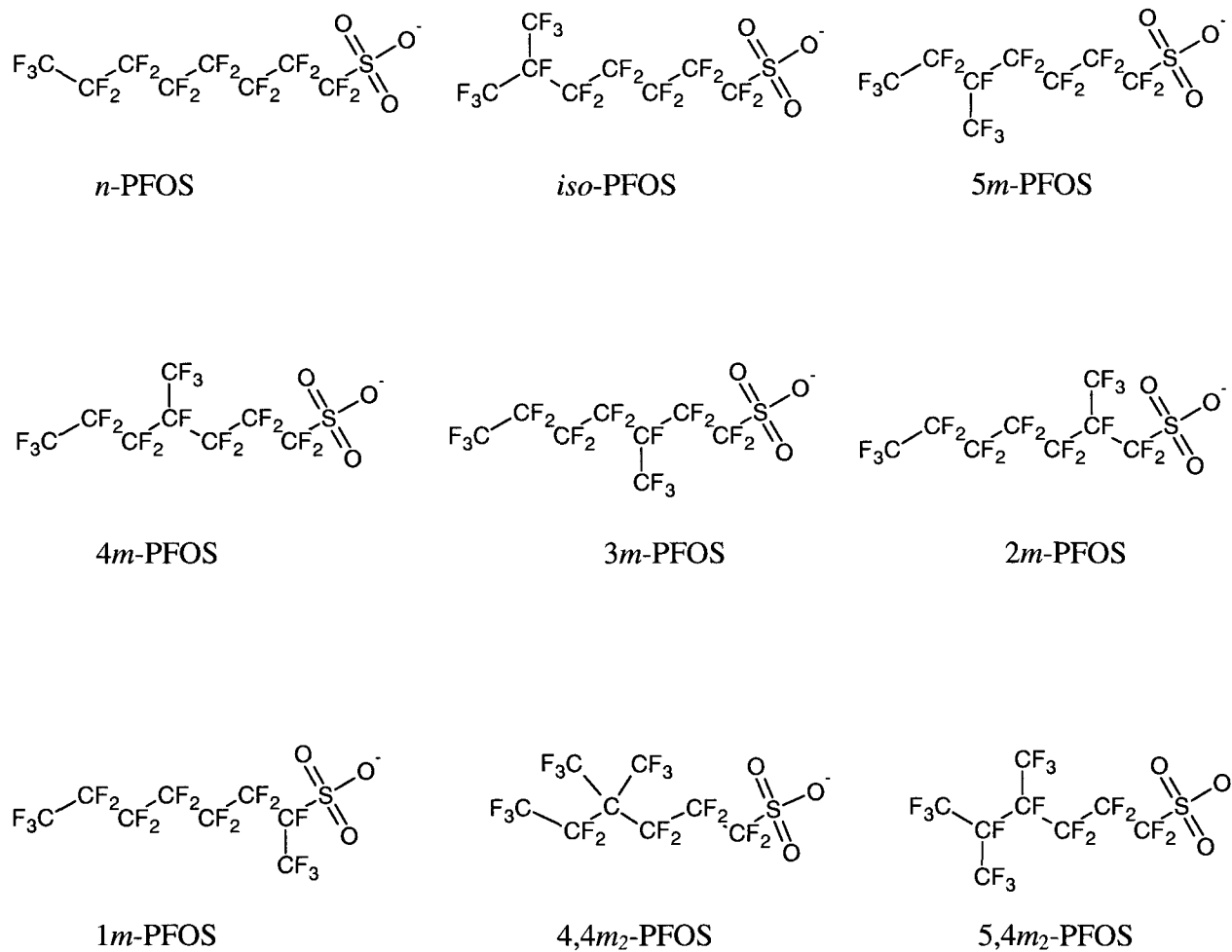
Figure B-1. Structures of perfluorooctane sulfonate (PFOS) isomers. Number represents location of branching point.
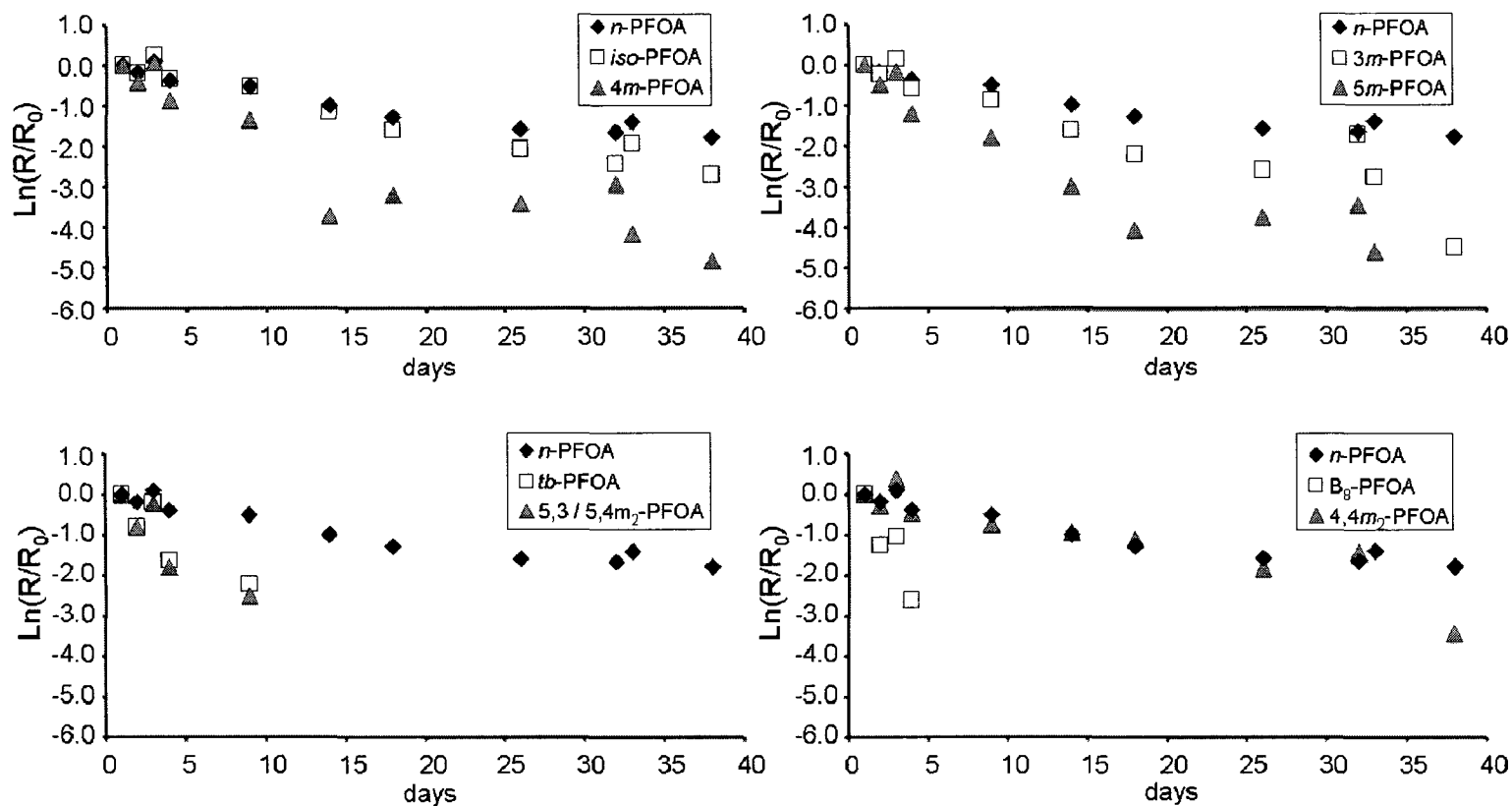
Figure B-2. Depuration of perfluorooctanoic acid (PFOA) isomers in rat blood. Each point represents the average response/mL of blood (R) on a given day normalized to the average response/mL of blood (R_0) on day 1.
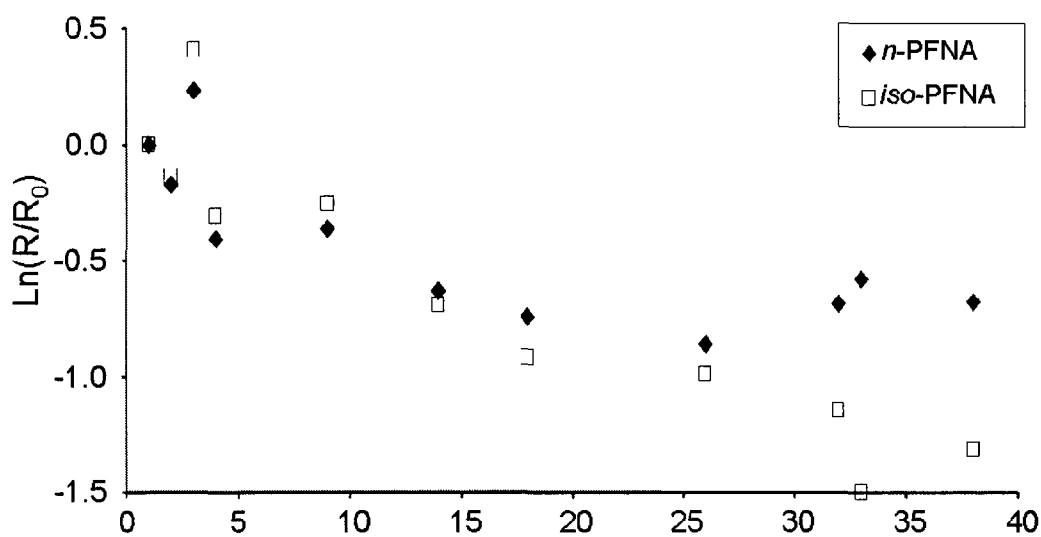
Figure B-3. Depuration of perfluorononanoic acid (PFNA) isomers in rat blood. Each point represents the average response/mL of blood (R) on a given day normalized to the average response/mL of blood (R_0) on day 1.
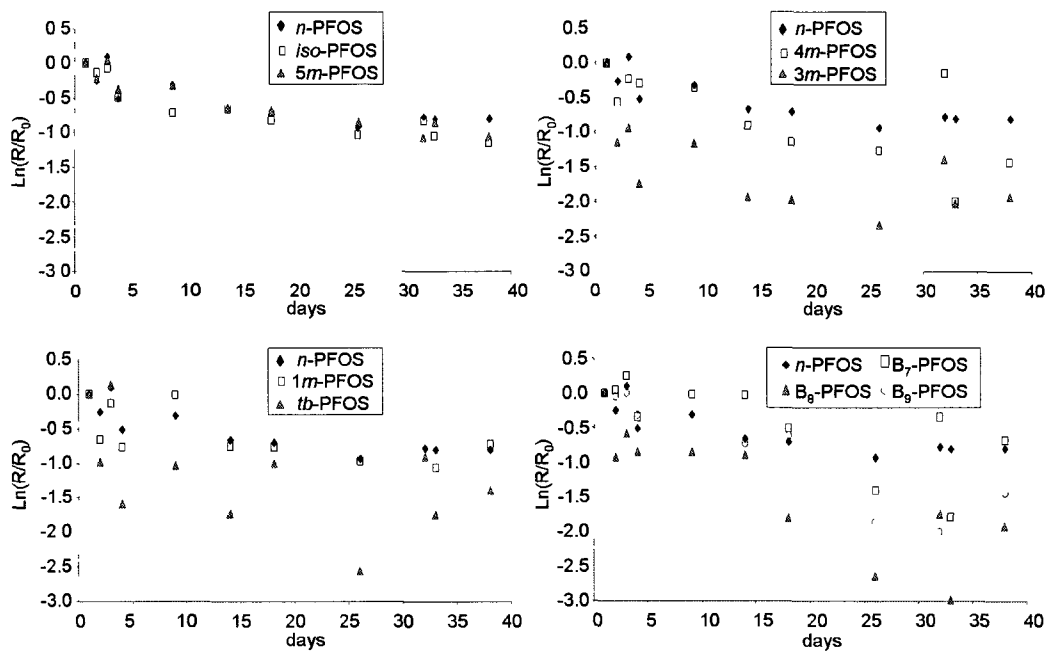
Figure B-4. Depuration of perfluorooctane sulfonate (PFOS) isomers in rat blood. Each point represents the average response/mL of blood (R) on a given day normalized to the average response/mL of blood (R_0) on day 1.
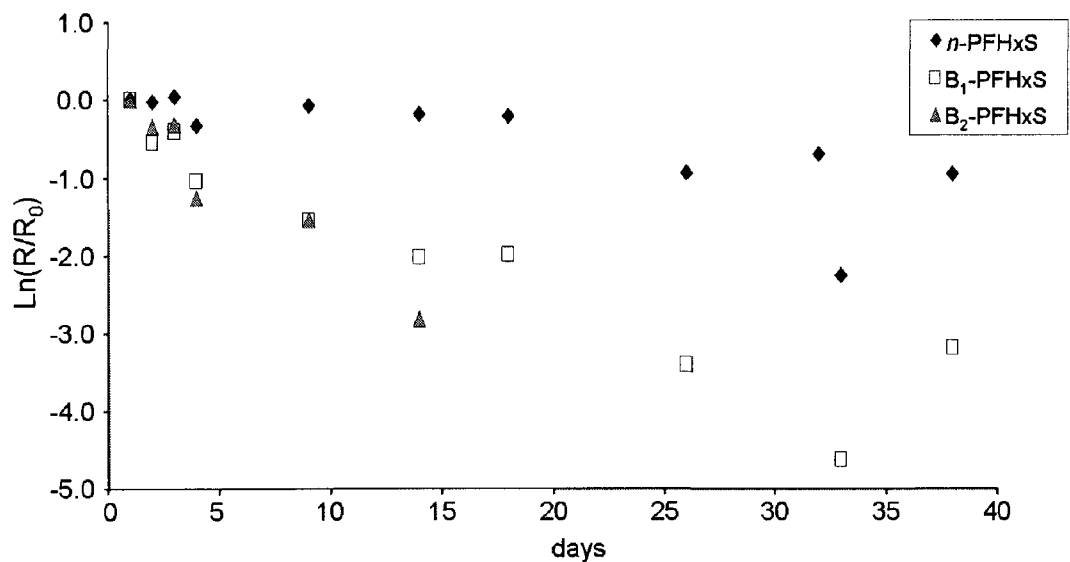
Figure B-5. Depuration of perfluorohexane sulfonate (PFHxS) isomers in rat blood. Each point represents the average response/mL of blood (R) on a given day normalized to the average response/mL of blood (R_0) on day 1
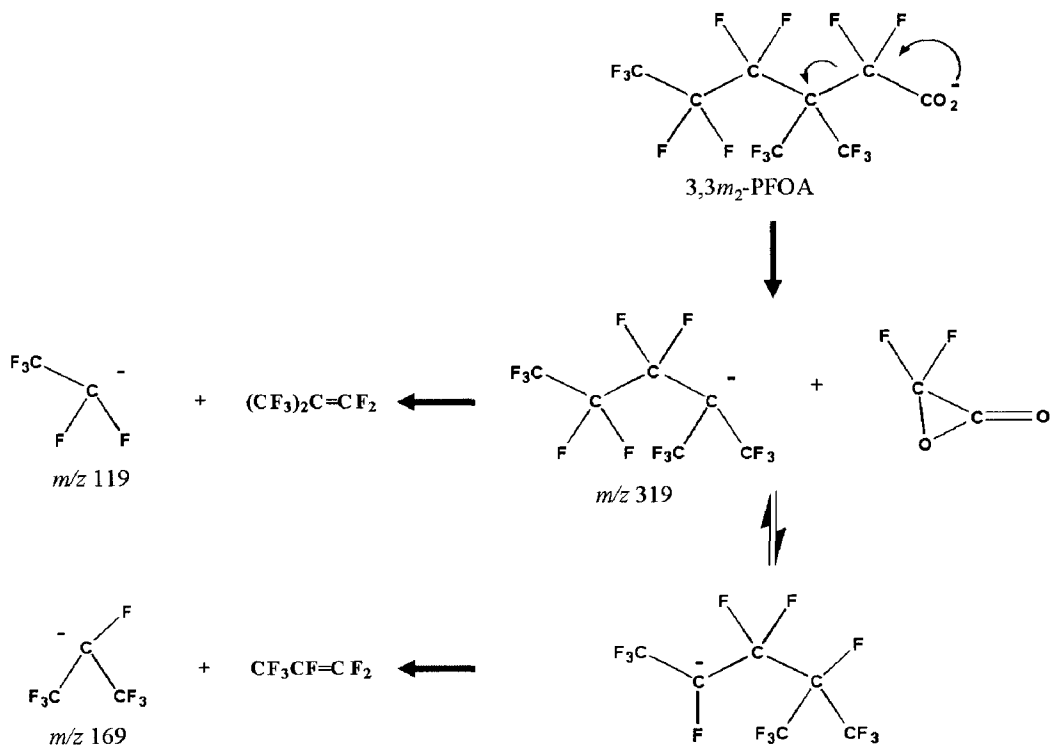
Figure B-6. Proposed reaction mechanism for $3,3m_2$-perfluorooctanoic acid (PFOA) showing formation of m/z 319 product ion (the product ion monitored for B_8-PFOA). This is the only PFOA isomer which could theoretically produce the m/z 319 product ion.
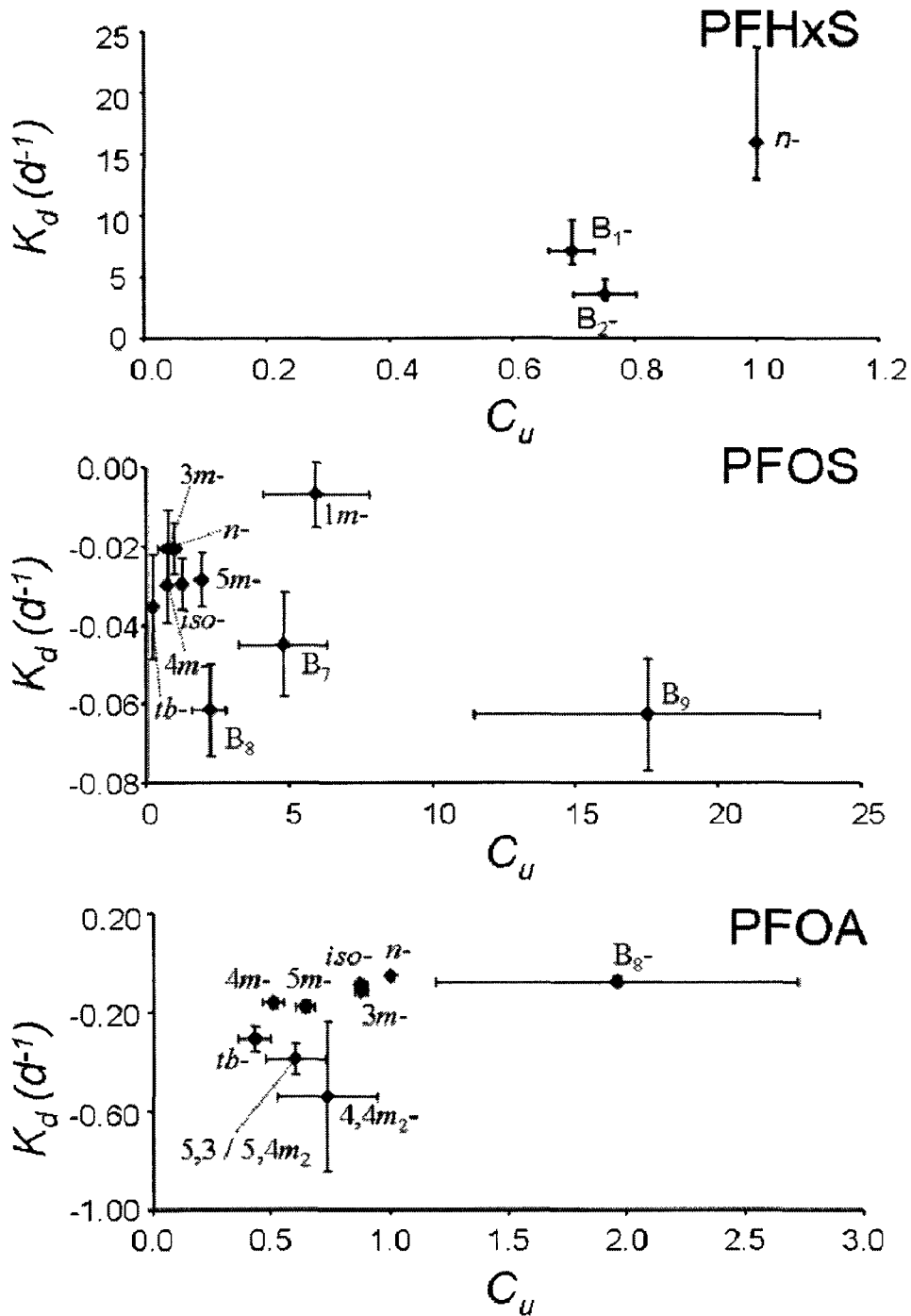
Figure B-7. Plots of blood depuration rate constants (k_d) versus dose-day 1 blood uptake coefficient (C_u), for perfluorohexane sulfonate (PFHxS), perfluorooctane sulfonate (PFOS), and perfluorooctanoic acid (PFOA). No correlation was observed, demonstrating that elimination within the first 24 h had little to no effect on the value of C_u. Error bars represent standard error about the mean.
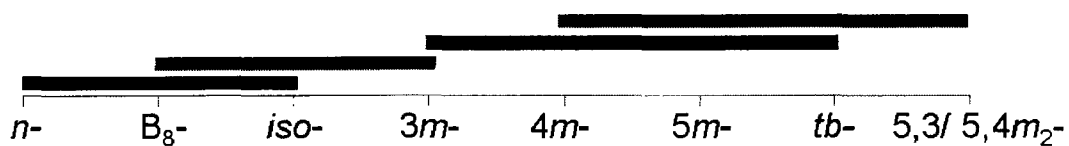
Figure B-8. Diagram showing statistically significant differences among isomers of perfluorooctanoic acid (PFOA) based on pairwise comparisons with Bonferroni correction. Solid lines indicate isomers that were not statistically different from each other. The depuration rate constant (k_d) of $4,4m_2$-PFOA was not found to be statistically different than that of any other PFOA isomer and was therefore not included in this figure.
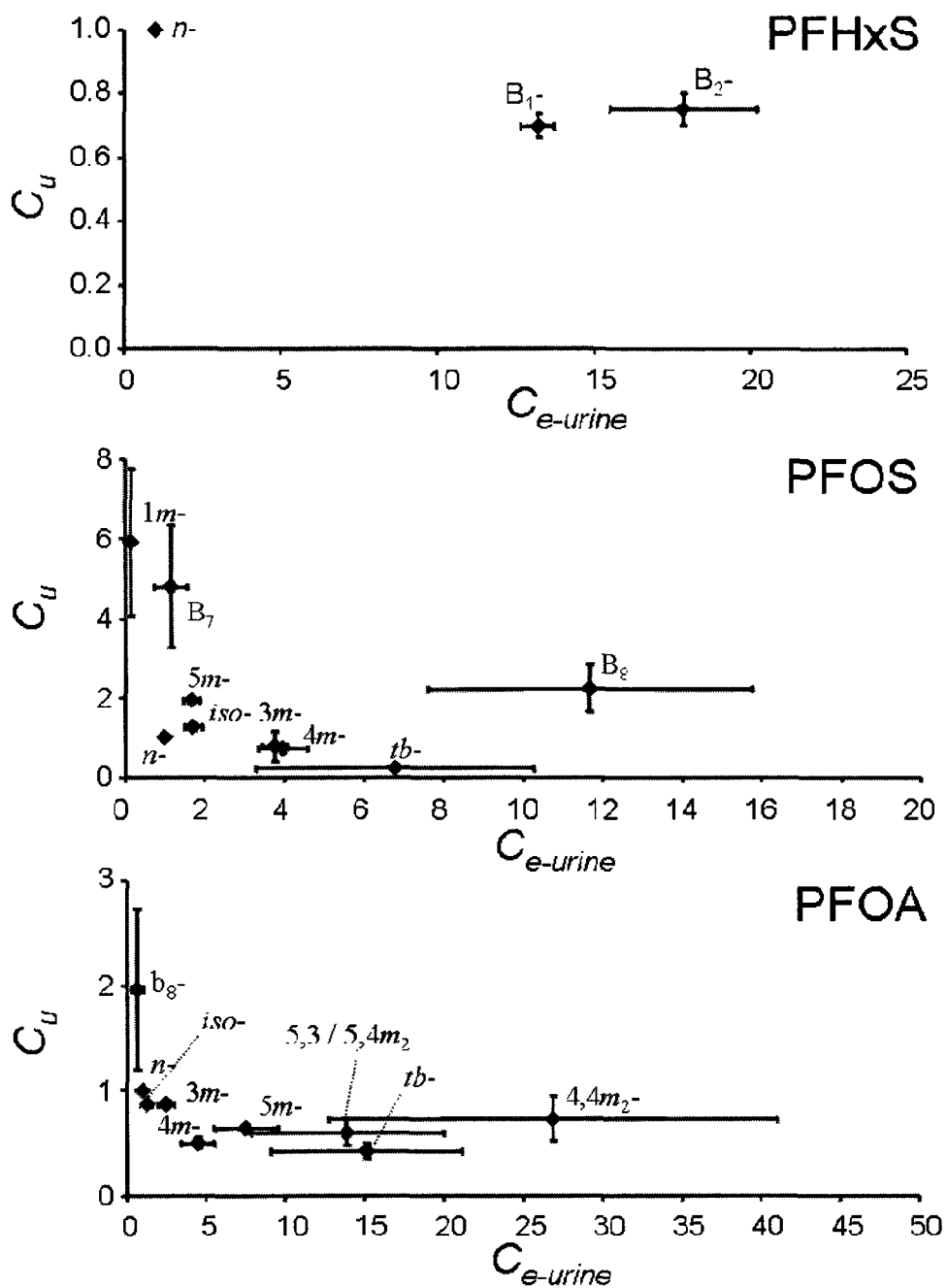
Figure B-9. Plots of dose-day 1 blood uptake coefficient (C_u) versus day 3 blood-urine elimination coefficient ($C_{e\text{-}urine}$) for perfluorohexane sulfonate (PFHxS), perfluorooctane sulfonate (PFOS), and perfluorooctanoic acid (PFOA). Plots of vs $C_{e\text{-}urine}$ for PFHxS (top), PFOS (middle), and PFOA (bottom). No correlation was observed, suggesting that different mechanisms are responsible for preferential uptake and renal elimination of PFA isomers. Error bars represent standard error about the mean.
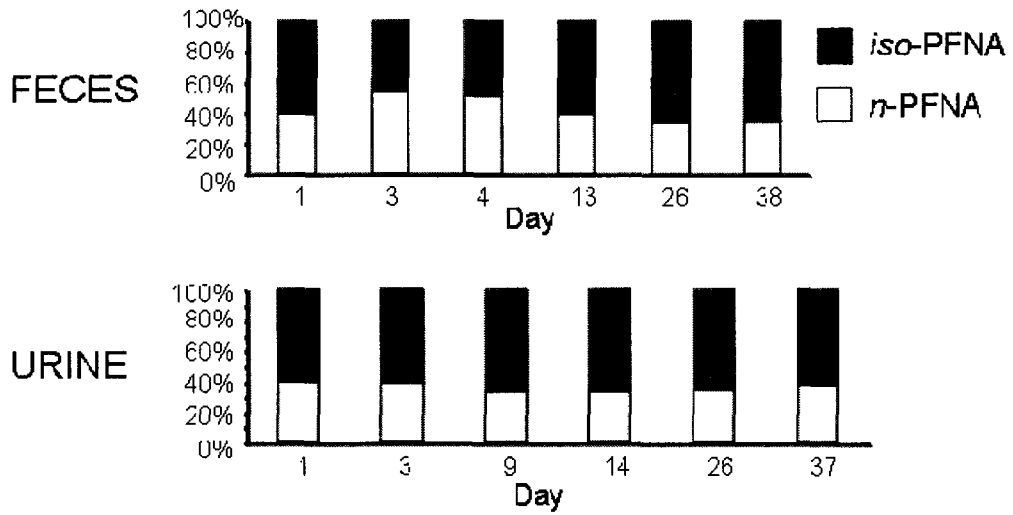
Figure B-10. Composition (%) of perfluorononanoic acid (PFNA) in urine and feces on selected time points over 38 day elimination period.
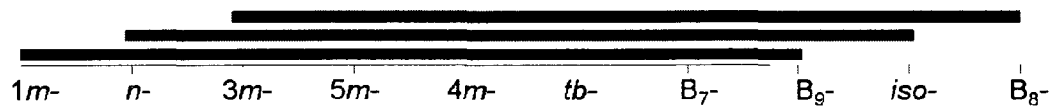
Figure B-11. Diagram showing statistically significant differences among isomers of perfluorooctane sulfonate (PFOS) based on pairwise comparisons with Bonferroni correction. Solid lines indicate isomers that were not statistically different from each other.
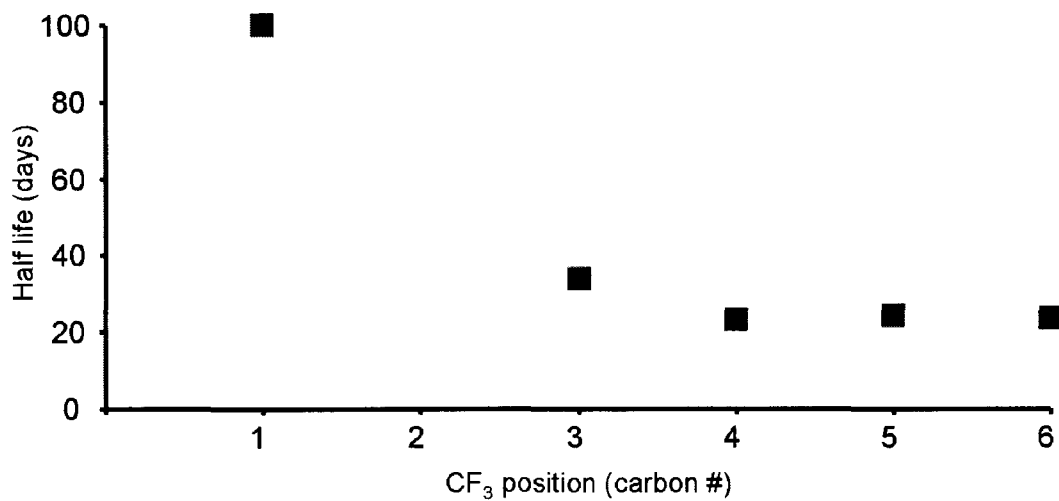
Figure B-12. Plots half life (d) versus perfluoromonomethyl branching point for perfluorooctane sulfonate (PFOS). A weak structure-property relationship was observed whereby branching towards the sulfonate end of the molecule resulted in an elevated half life.
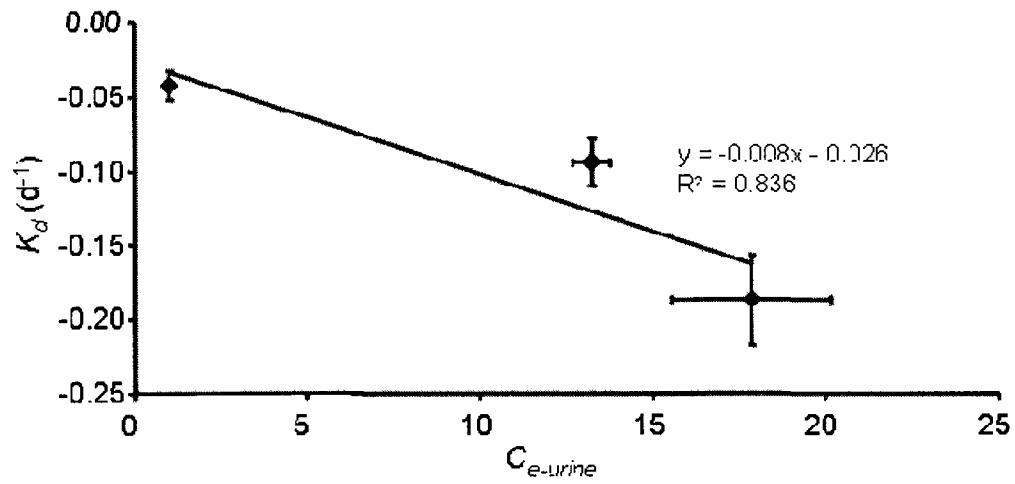
Figure B-13. Plots of blood depuration coefficient (k_d, d^{-1}) versus day 3 blood-urine elimination coefficient ($C_{e\text{-}urine}$) for perfluorohexane sulfoante (PFHxS).

Appendix C: Supporting Information for Chapter 4-Isomer-Specific Biotransformation of a Perfluorooctane Sulfonate (PFOS)-Precursor by Cytochrome P450 Isozymes and Human Liver Microsomes
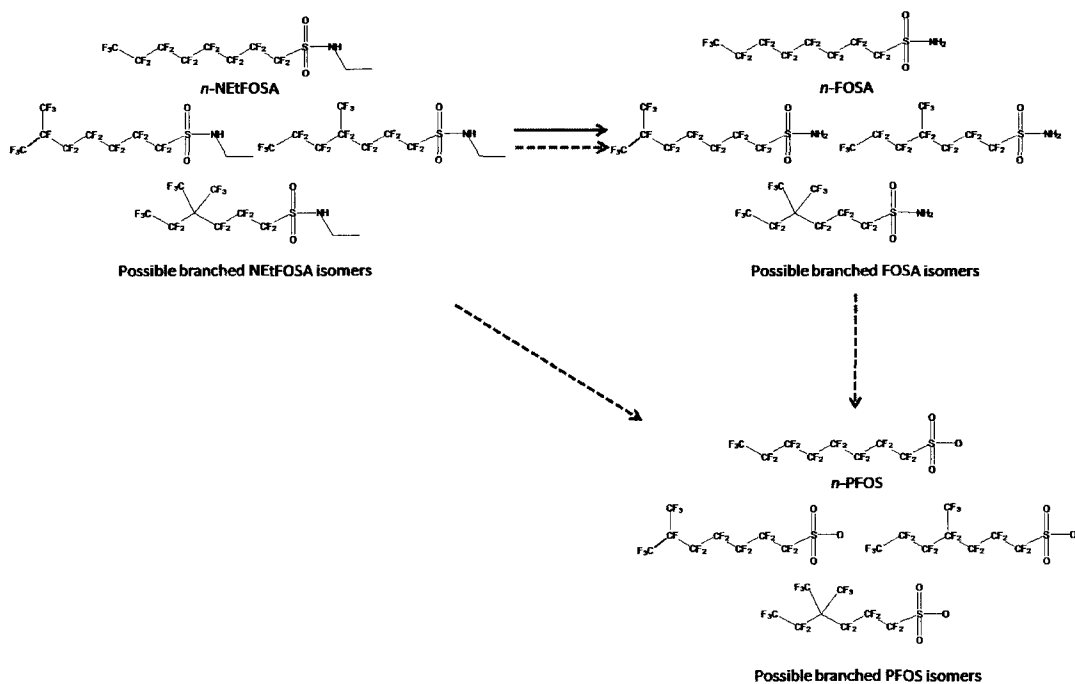
Figure C-1. Biotransformation pathways of NEtFOSA observed in the present study using P450 isozymes and microsomes (⟶), and observed/ discussed by others (·····➤) (1-3). Other products are possible but were not investigated in the present study.
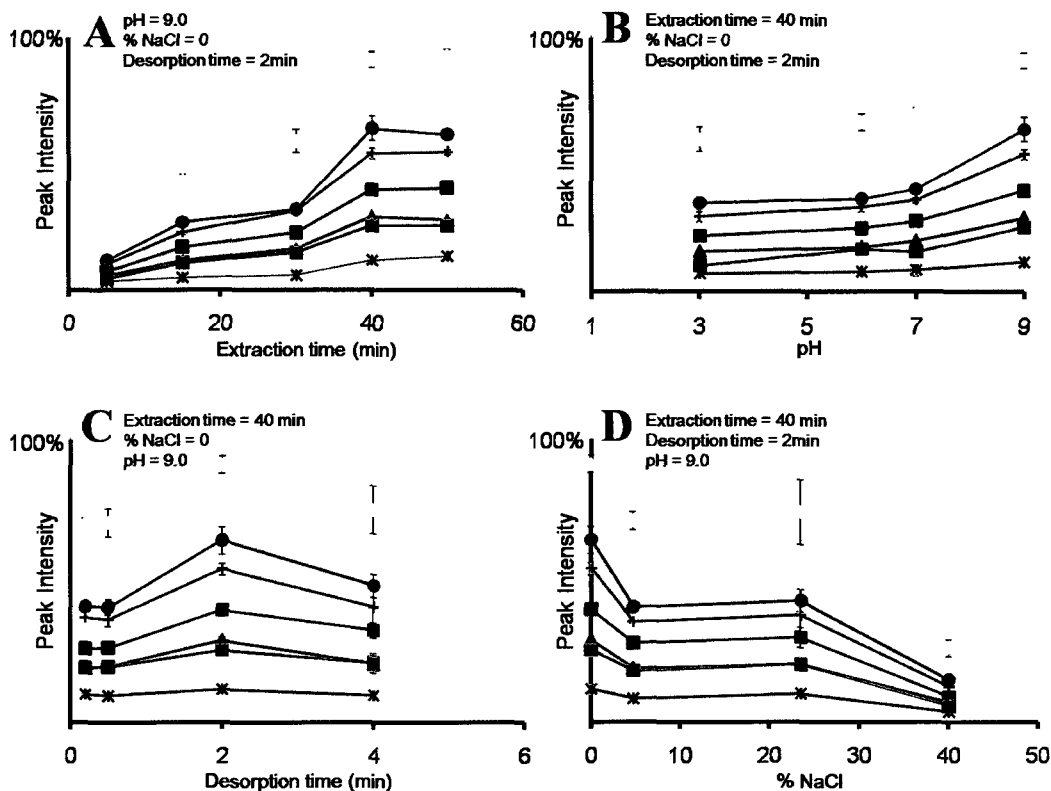
Figure C-2. Optimization of liquid SPME variables extraction time (A), pH (B), desorption time (C), and ionic strength (D). Traces represent the average response (n = 3 replicates) of individual NEtFOSA isomers and internal standard (NMeFOSA) with changes in a particular variable, while holding all other variables constant. NEtFOSA isomer 1 (▲), isomer 2 (✳), isomer 3 (■), isomer 4 (*n*-NEtFOSA, ●), isomer 5 (▪), isomer 6 (+), and internal standard NMeFOSA (   ). Error bars represent ± 1standard deviation about the mean.
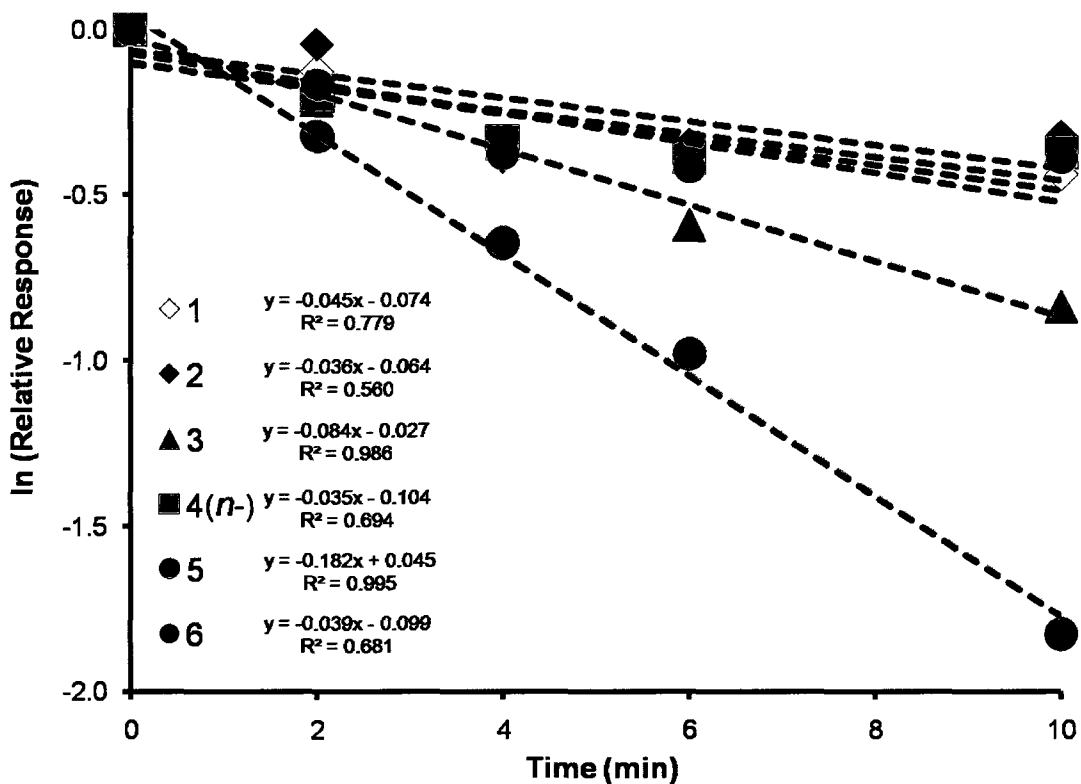
Figure C-3. Example of NEtFOSA isomer depuration curves (ln relative response) for the incubation of CYP 2C9 with 190 nM NEtFOSA (100 ng of NEtFOSA incubated in 1mL total volume). Curves shown represent a single replicate out of a total of 4 used to calculate average rate constants.
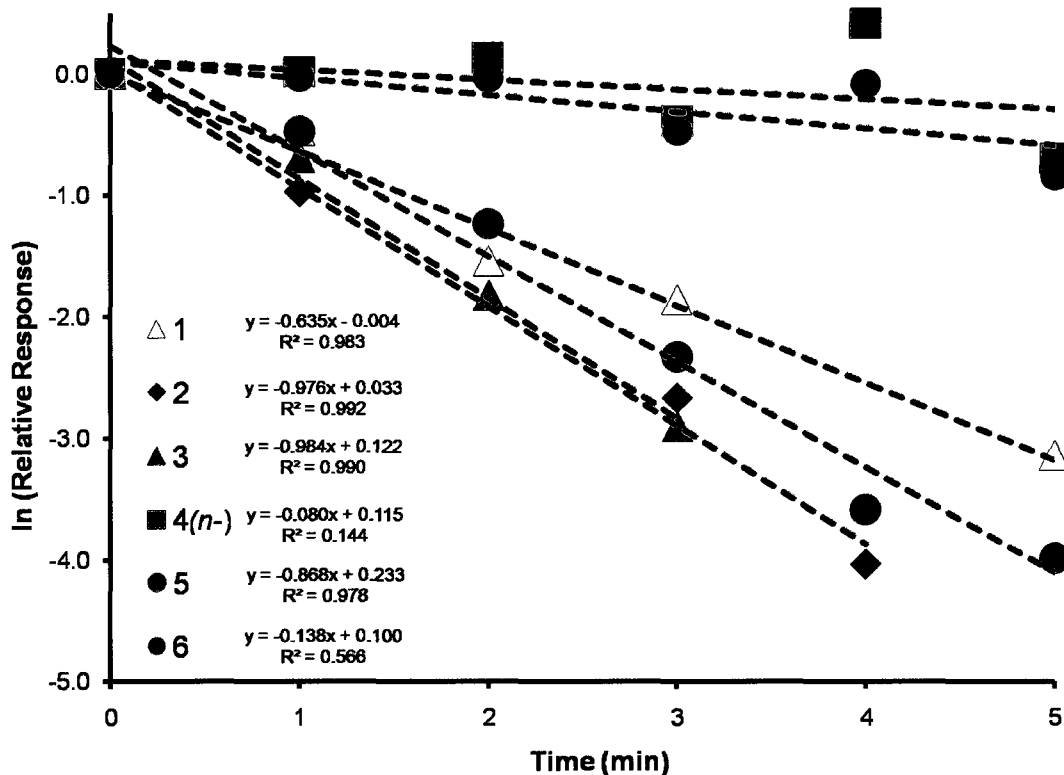
Figure C-4. Example of NEtFOSA isomer depuration curves (ln relative response) for the incubation of CYP 2C19 with 380 nM NEtFOSA (200 ng of NEtFOSA incubated in 1mL total volume). Curves shown represent a single replicate out of a total of 3 that were used to calculate average rate constants.
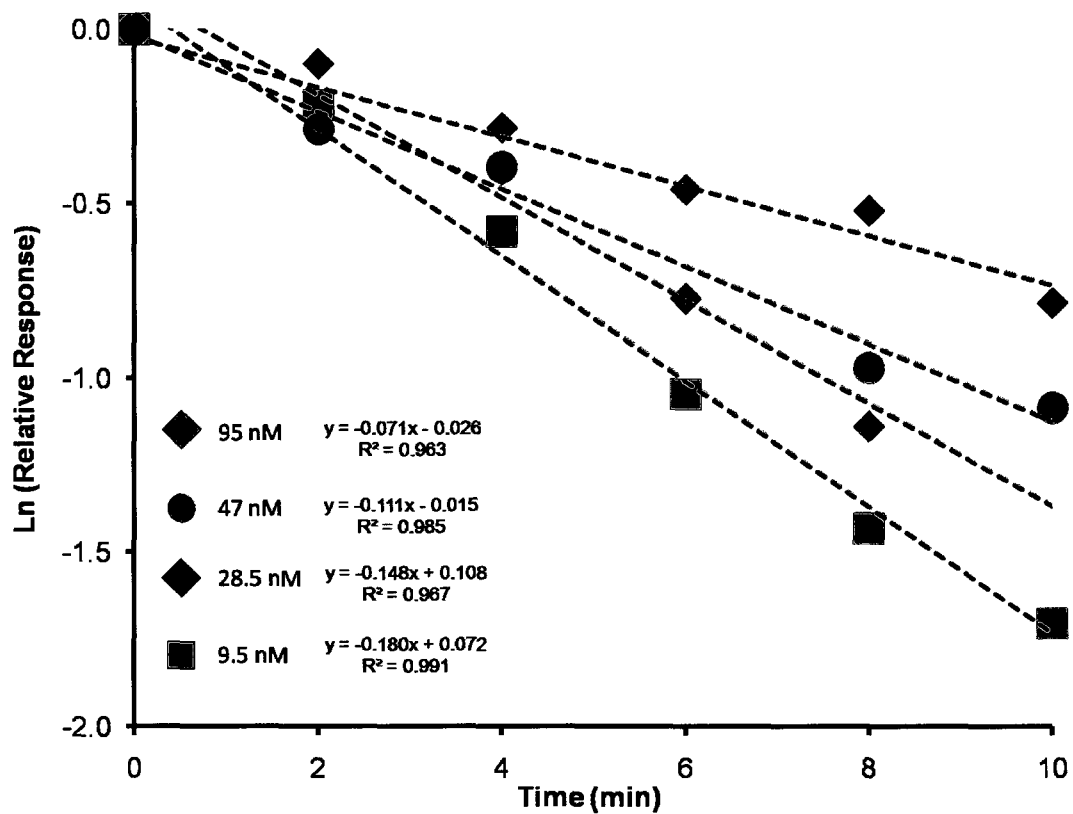
Figure C-5. Example of NEtFOSA isomer depuration curves (ln relative response) for the incubation of CYP 2C9 with n_{pure}-NEtFOSA at several concentrations. Incubations were conducted in 1mL total volume. Curves shown represent a single replicate out of a total of 4 that were used to calculate average rate constants.
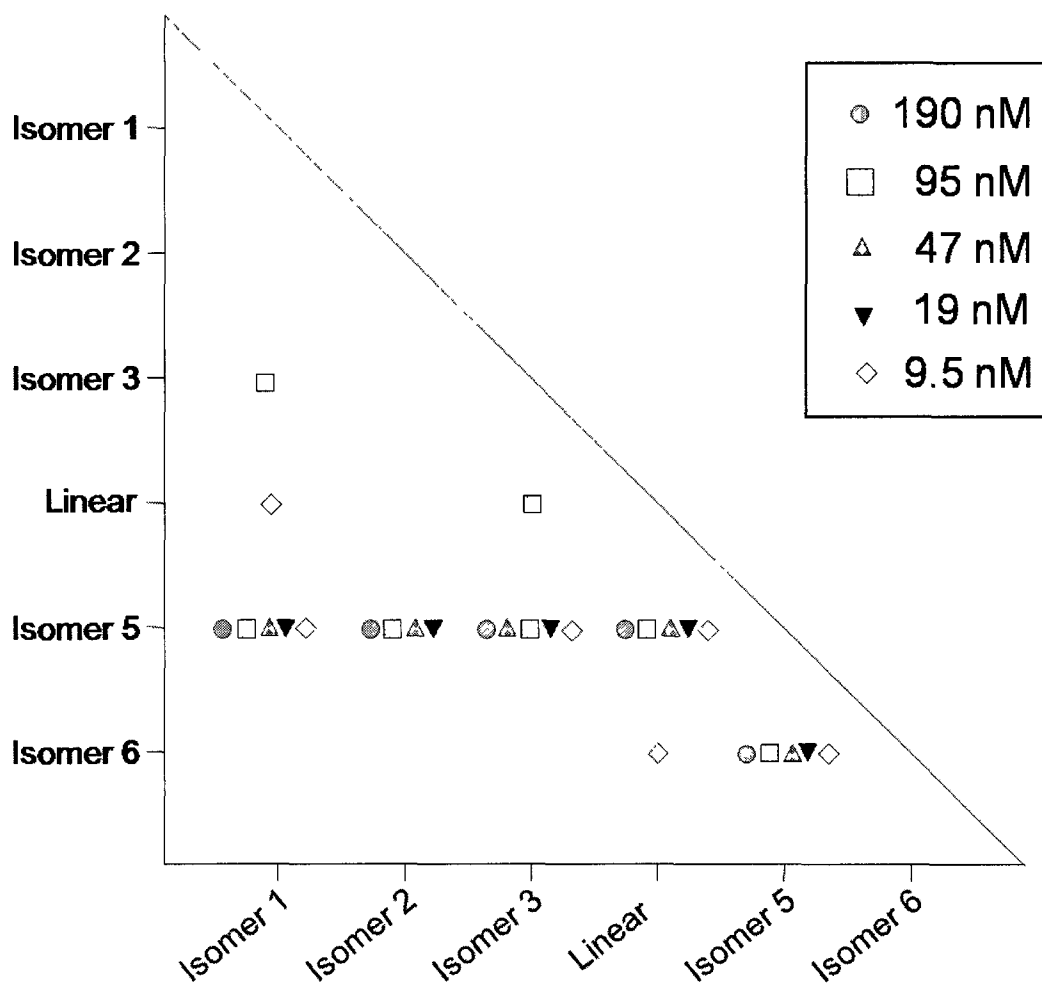
Figure C-6. Statistical significance (Tukey's HSD, $\alpha=0.05$) between biotransformation rate constants of NEtFOSA isomers incubated with CYP 2C9 at several concentrations. The presence of a marker indicates a significant difference between the biotransformation rate constants of two isomers at a given concentration. For example, at 190 nM (grey circles), the biotransformation rate constant of isomer 3 is statistically different from isomer 5, but at 95 nM (squares), it is statistically different from the biotransformation rate constant of linear N-EtFOSA, isomer 5, and isomer 1.
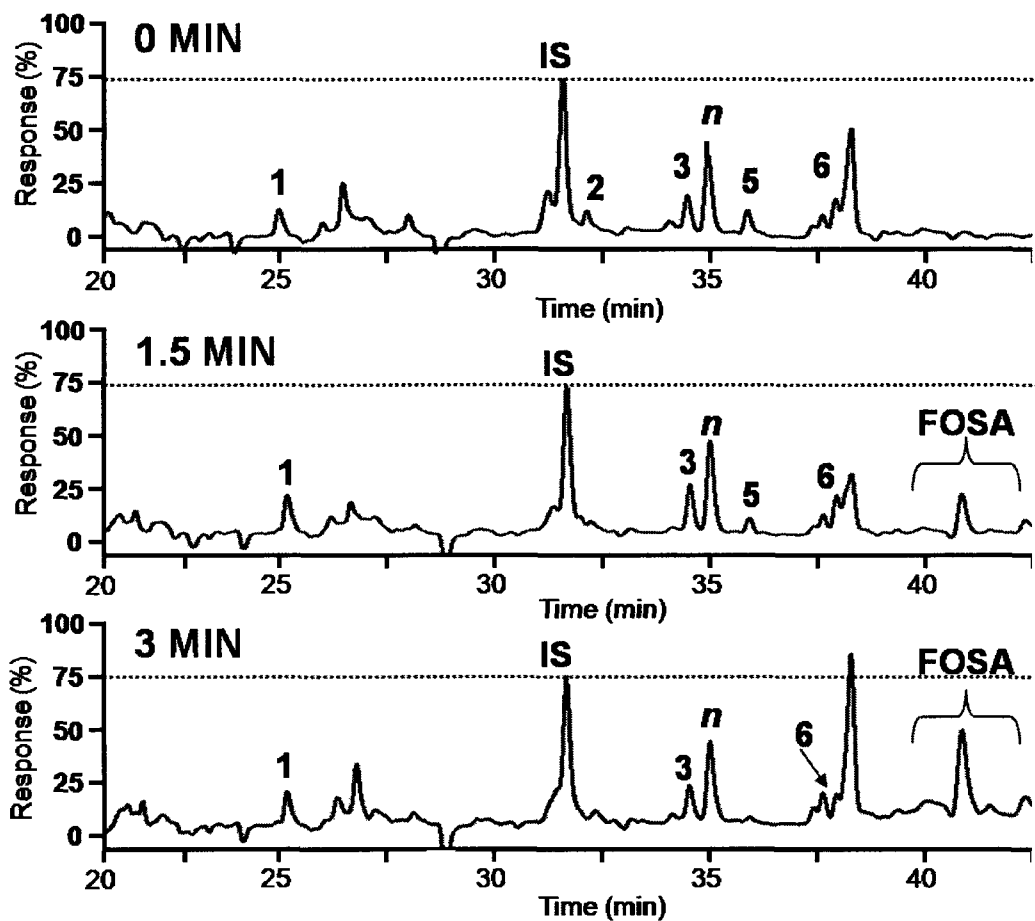
Figure C-7. Representative SPME-GC-ECD chromatograms showing isomer-specific biotransformation of 9.5 nM NEtFOSA by CYP2C9 (n = 4 replicates, 5 ng of NEtFOSA incubated in 1mL total volume). As was observed for incubations at 190 nM, isomer 5 was one of the first isomers to disappear. Note formation of FOSA isomers at ~42min.
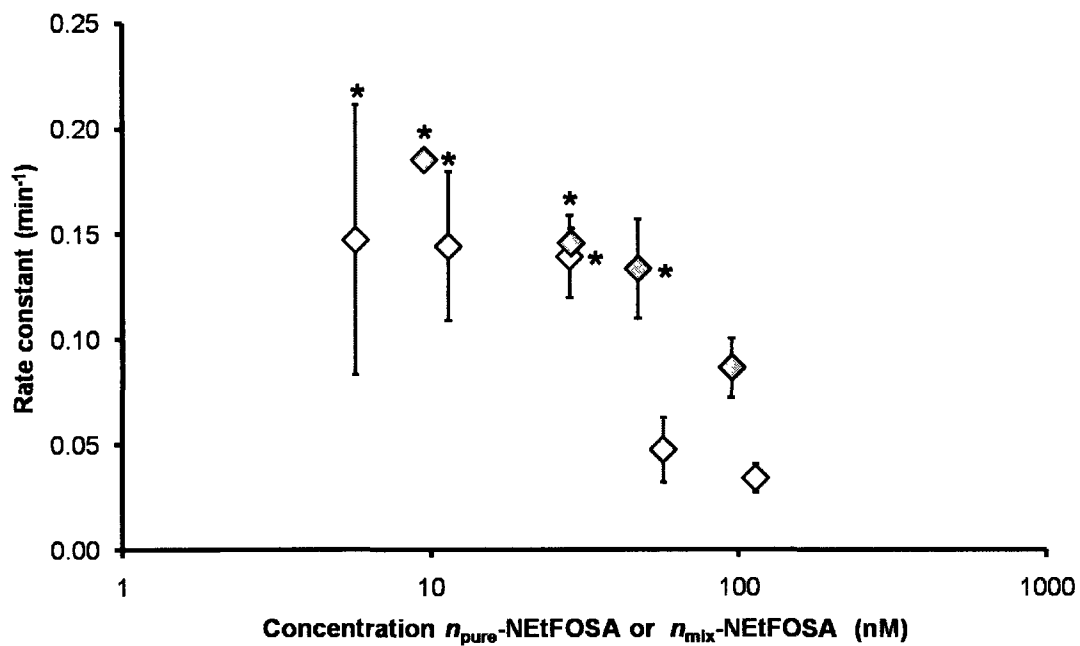
Figure C-8. Rate constants for the biotransformation of n_{mix}-NEtFOSA (hollow diamonds, n = 4 replicates) versus n_{pure}-NEtFOSA (grey diamonds, n = 3 replicates) by CYP2C9. Error bars represent ± 1 standard deviation about the mean. (*) indicates a non-significant difference between rate constants at the 95% confidence level.
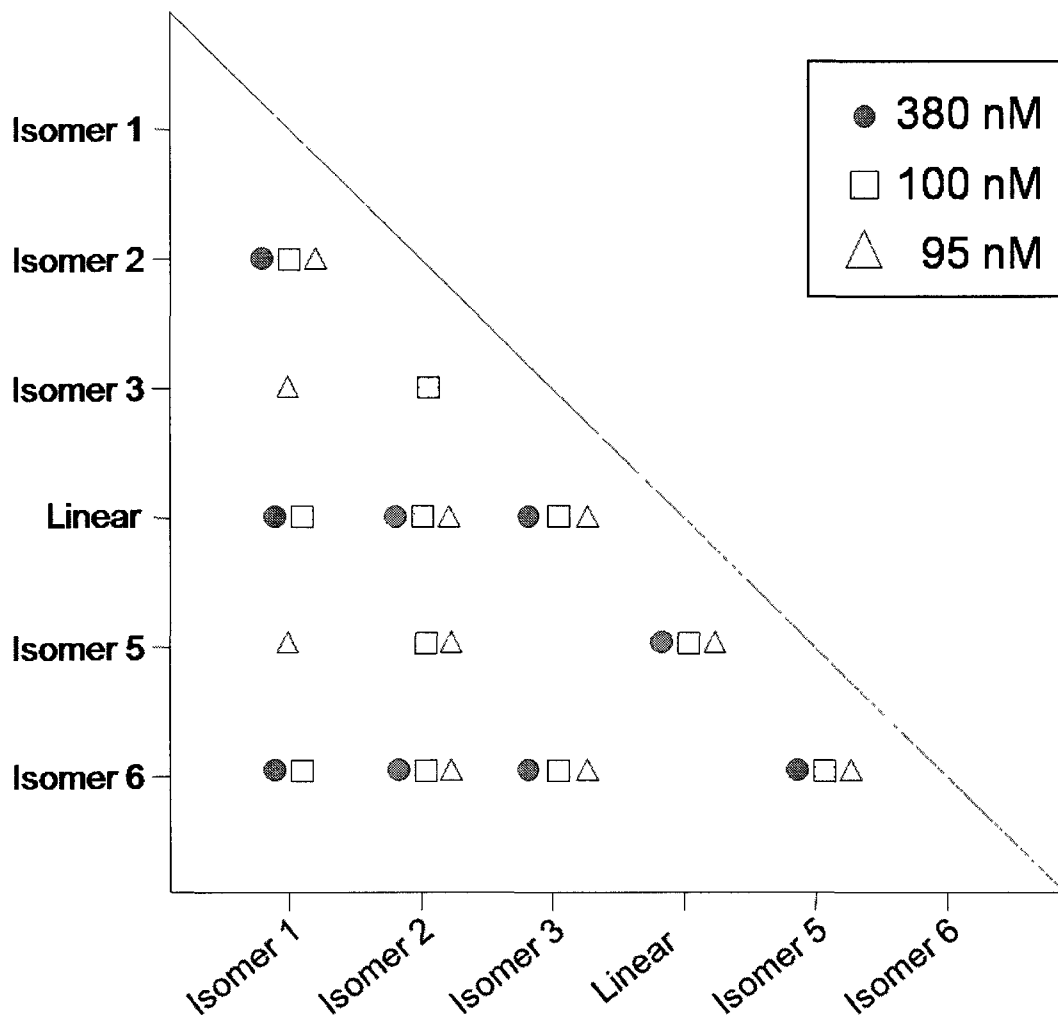
Figure C-9. Statistical significance (Tukey's HSD, α=0.05) between biotransformation rate constants of NEtFOSA isomers incubated with CYP 2C19 at several concentrations. The presence of a marker indicates a significant difference between the biotransformation rate constants of two isomers at a given concentration. For example, at 380 nM (grey circles), the biotransformation rate constant of isomer 6 is statistically different from isomers 1, 2, 3, and 5, but at 95 nM (triangles), it is statistically different from the biotransformation rate constants of isomers 2, 3, and 5.
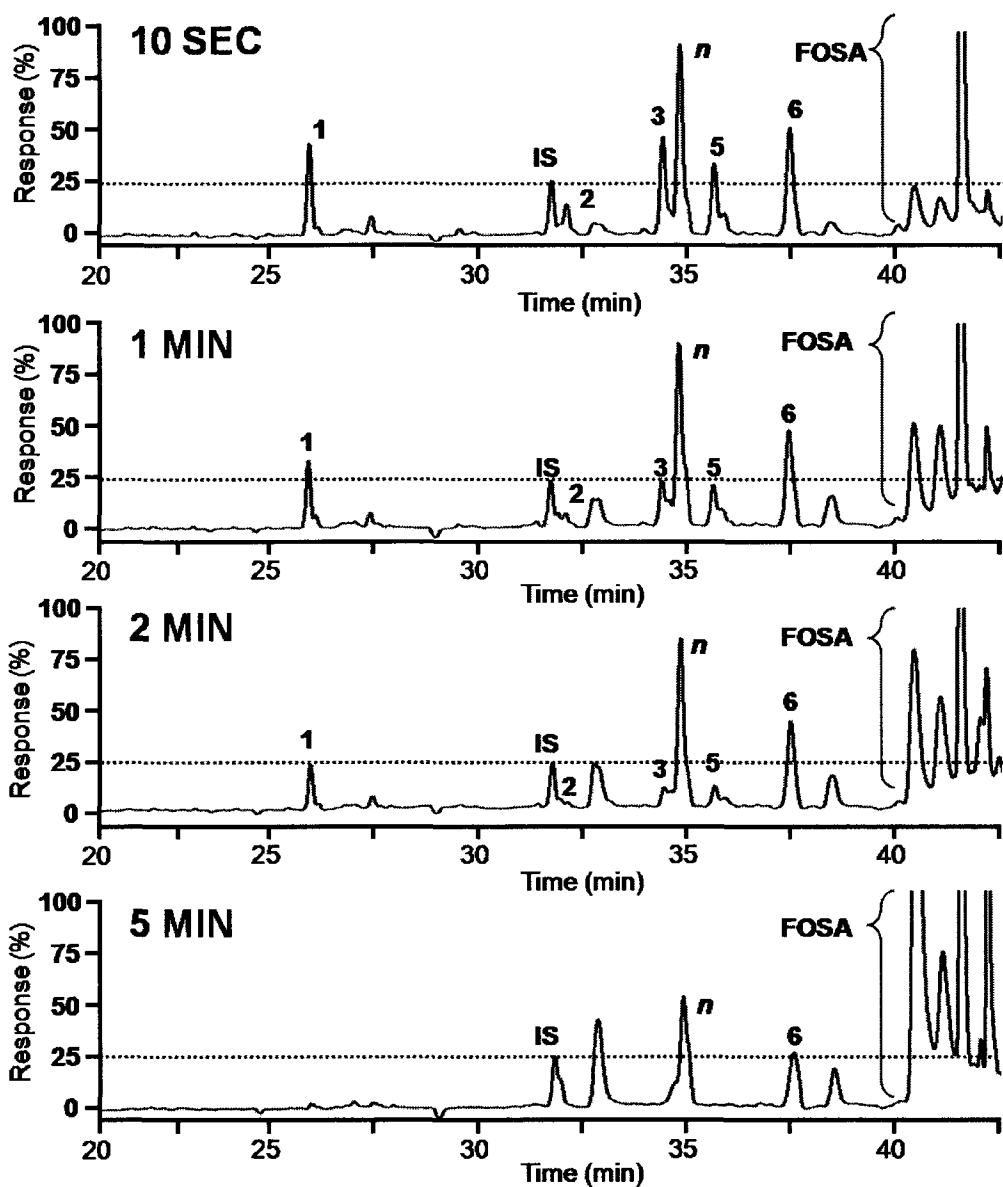
Figure C-10. Representative SPME-GC-ECD chromatograms showing isomer specific biotransformation of 380 nM NEtFOSA by CYP2C19 (n = 3 replicates, 200 ng of NEtFOSA incubated in 1mL total volume). Individual isomer response is relative to the internal standard peak (IS), set arbitrarily at 25%. Note rapid disappearance of isomers 2 and 5 and changes in FOSA isomer profile on right side of chromatogram. The FOSA profile was different than that observed following biotransformation by CYP2C9.

307
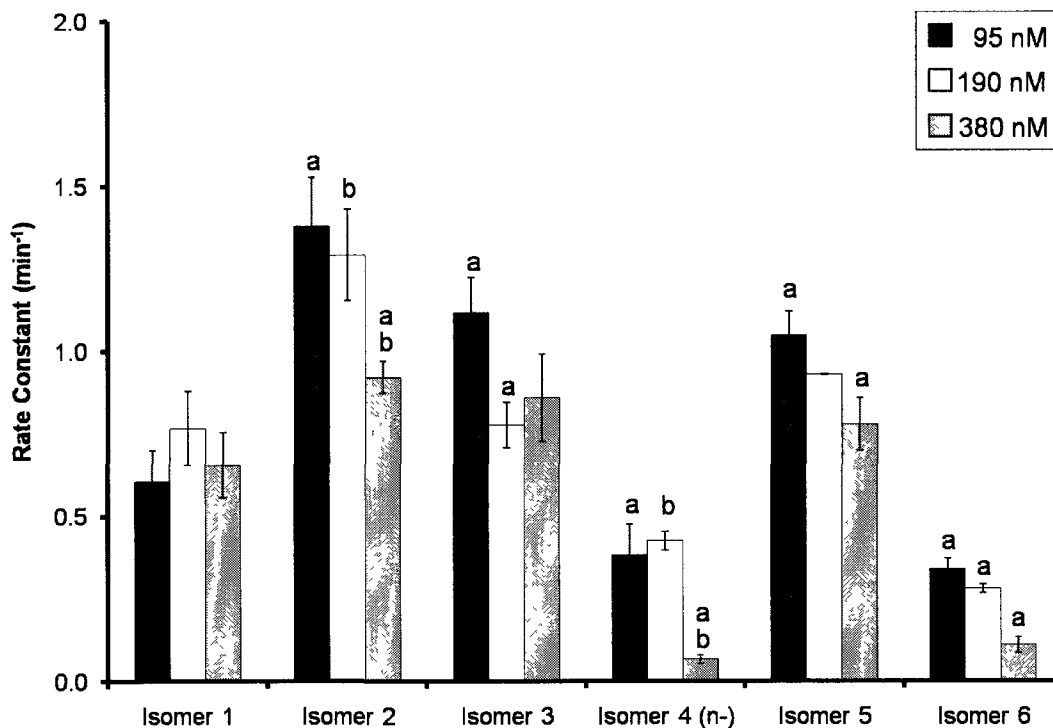
Figure C-11. Mean rate constants for the biotransformation of 95 nM (n = 4 replicates), 190 nM (n = 3 replicates), and 380 nM (n = 3 replicates) NEtFOSA by CYP2C19. Error bars represent ± 1 standard deviation about the mean. Identical letters represent a significant (Tukey's HSD, $\alpha = 0.05$) difference between rate constants obtained for a given isomer. For example, for isomer 4, 'a' represents a statistical difference between rate constants at 95 nM and 380 nM NEtFOSA, while 'b' represents a statistical difference between rate constants at 190 nM and 380 nM.
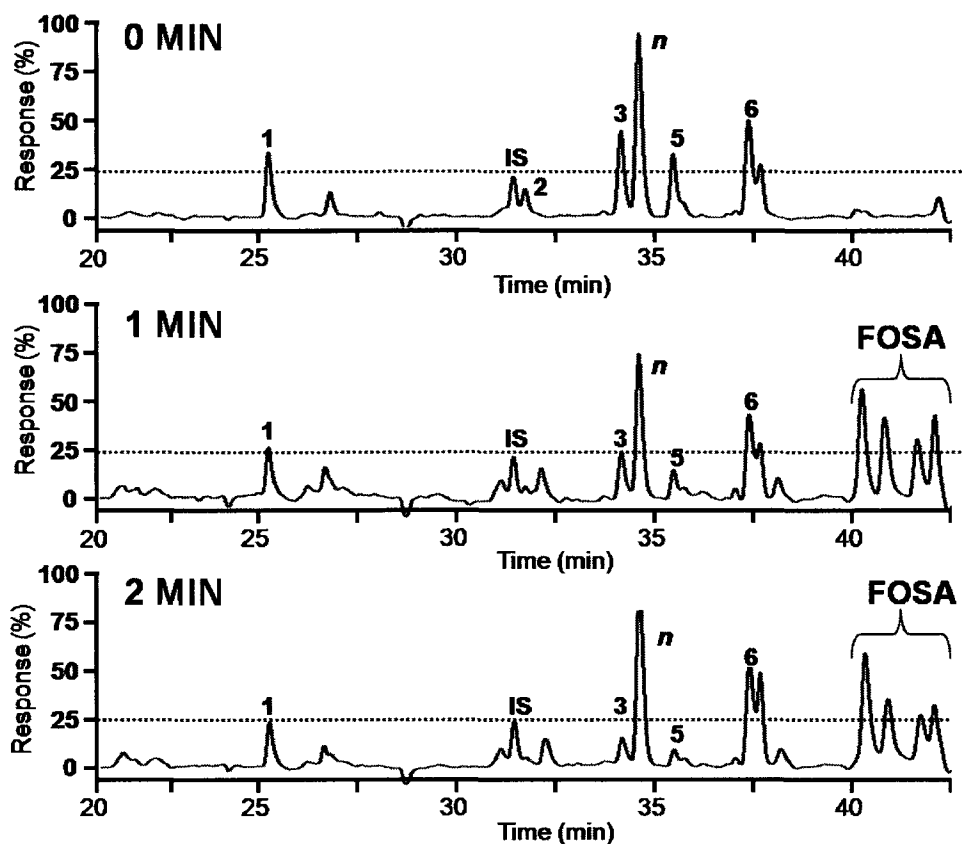
Figure C-12. Representative SPME-GC-ECD chromatograms showing isomer-specific metabolism of 95 nM NEtFOSA by CYP2C19 (n = 4 replicates, 50 ng of NEtFOSA incubated in 1mL total volume). Note rapid disappearance of isomers 3 and 5 and FOSA formation at ~40 min.
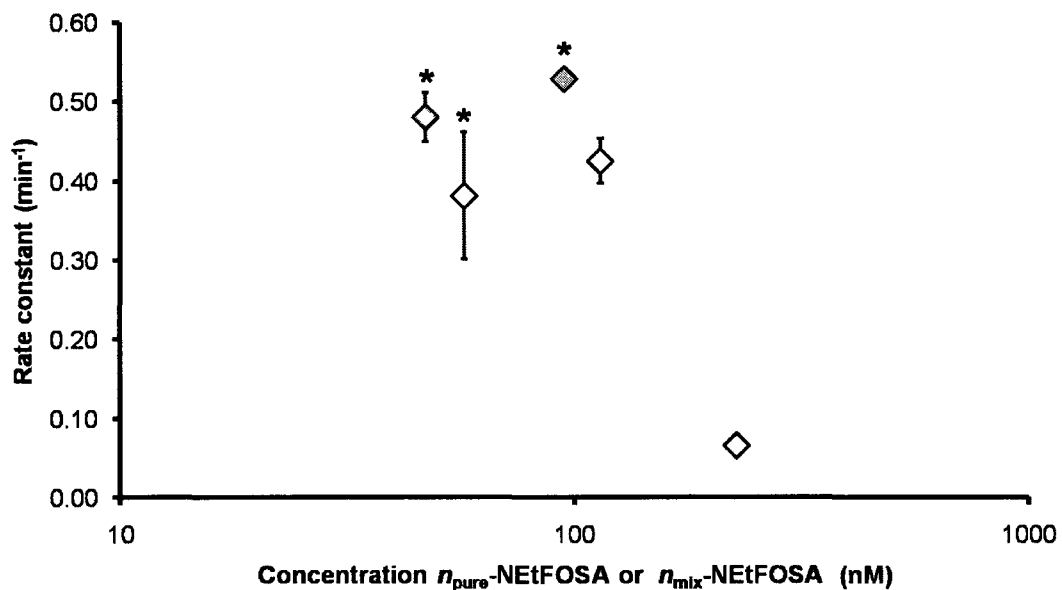
Figure C-13. Rate constants for the biotransformation of n_{mix}-NEtFOSA (hollow diamonds, n = 3 - 4 replicates) versus n_{pure}-NEtFOSA (grey diamonds, n = 3 replicates) by CYP2C19. Error bars represent ± 1 standard deviation about the mean. (*) represents a non significant difference between rate constants at the 95% confidence level.
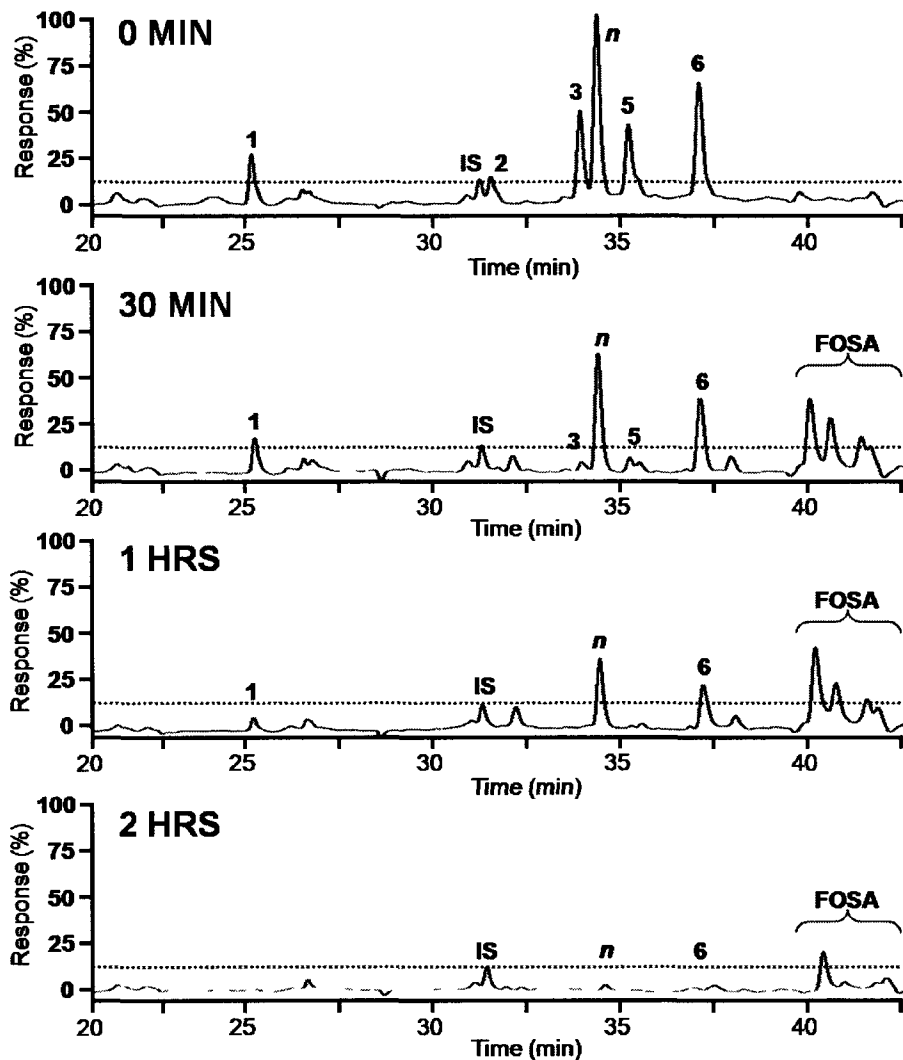
Figure C-14. Representative SPME-GC-ECD chromatograms showing isomer specific biotransformation of 380 nM NEtFOSA by human liver microsomes (n = 3 replicates, 200 ng of NEtFOSA incubated in 1mL total volume). Individual isomer response is relative to the internal standard peak (IS), set arbitrarily at 12.5%. Note slow disappearance of isomer 6 and n-NEtFOSA. Also note changes in FOSA profile, and the apparent disappearance of FOSA at 2 hrs suggesting further biotransformation.
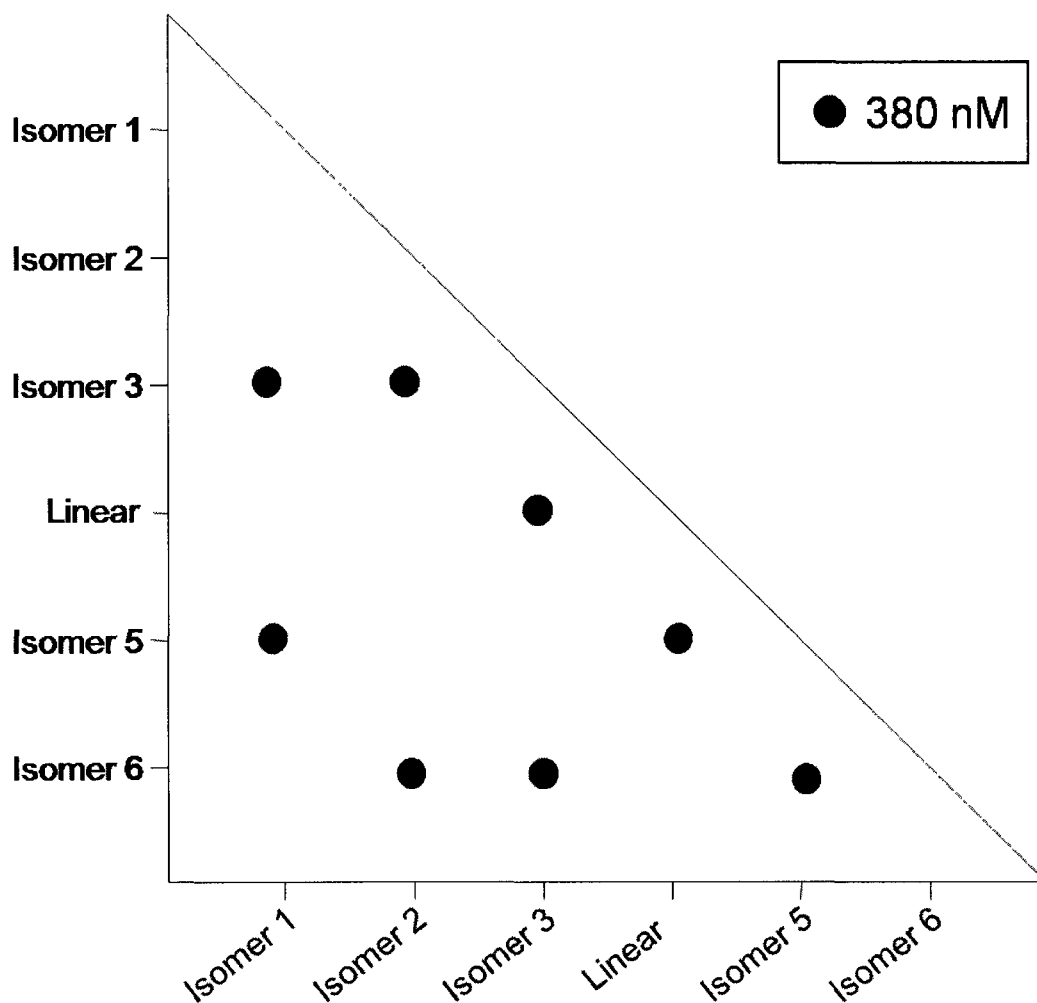
Figure C-15. Figure showing statistical significance (Tukey's HSD, $\alpha=0.05$) between biotransformation rate constants of NEtFOSA isomers incubated with human liver microsomes at 380 nM NEtFOSA. The presence of a marker indicates a significant difference between the biotransformation rate constants of two isomers at a given concentration. For example, at 380 nM NEtFOSA, the biotransformation rate constant of isomer 6 is statistically different from isomers 2, 3, and 5.
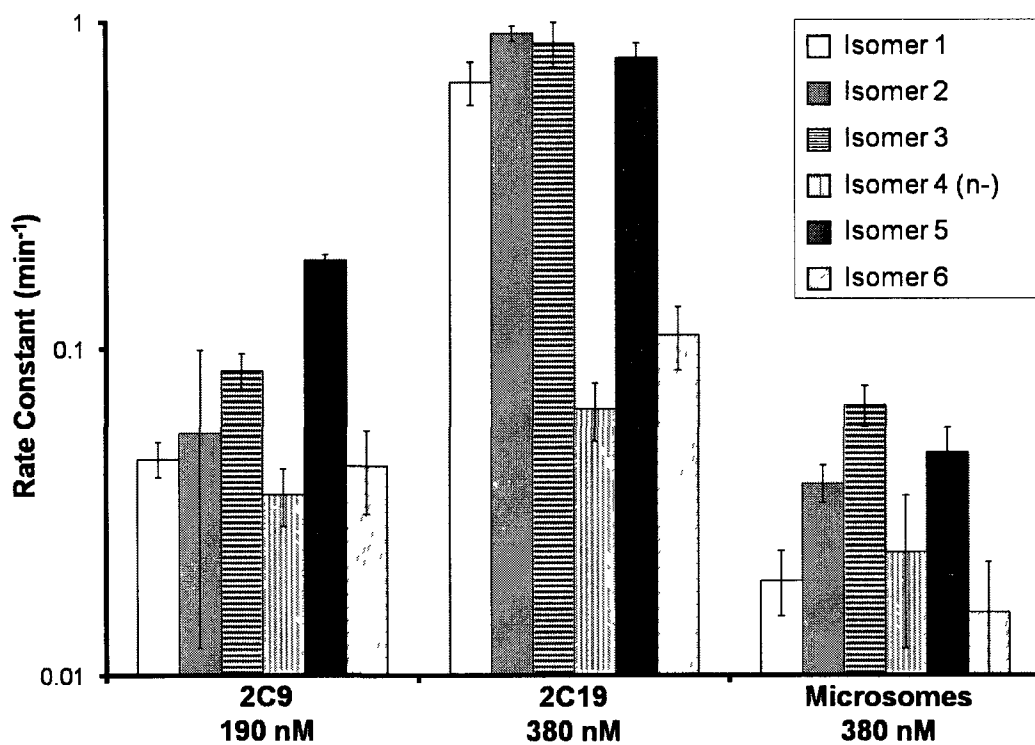
Figure C-16. Rate constants for the biotransformation of NEtFOSA isomers by CYP2C9 (190 nM, n = 4 replicates), CYP2C19 (380 nM, n = 3 replicates) and human liver microsomes (380 nM, n = 3 replicates). Error bars represent ± 1 standard deviation about the mean.
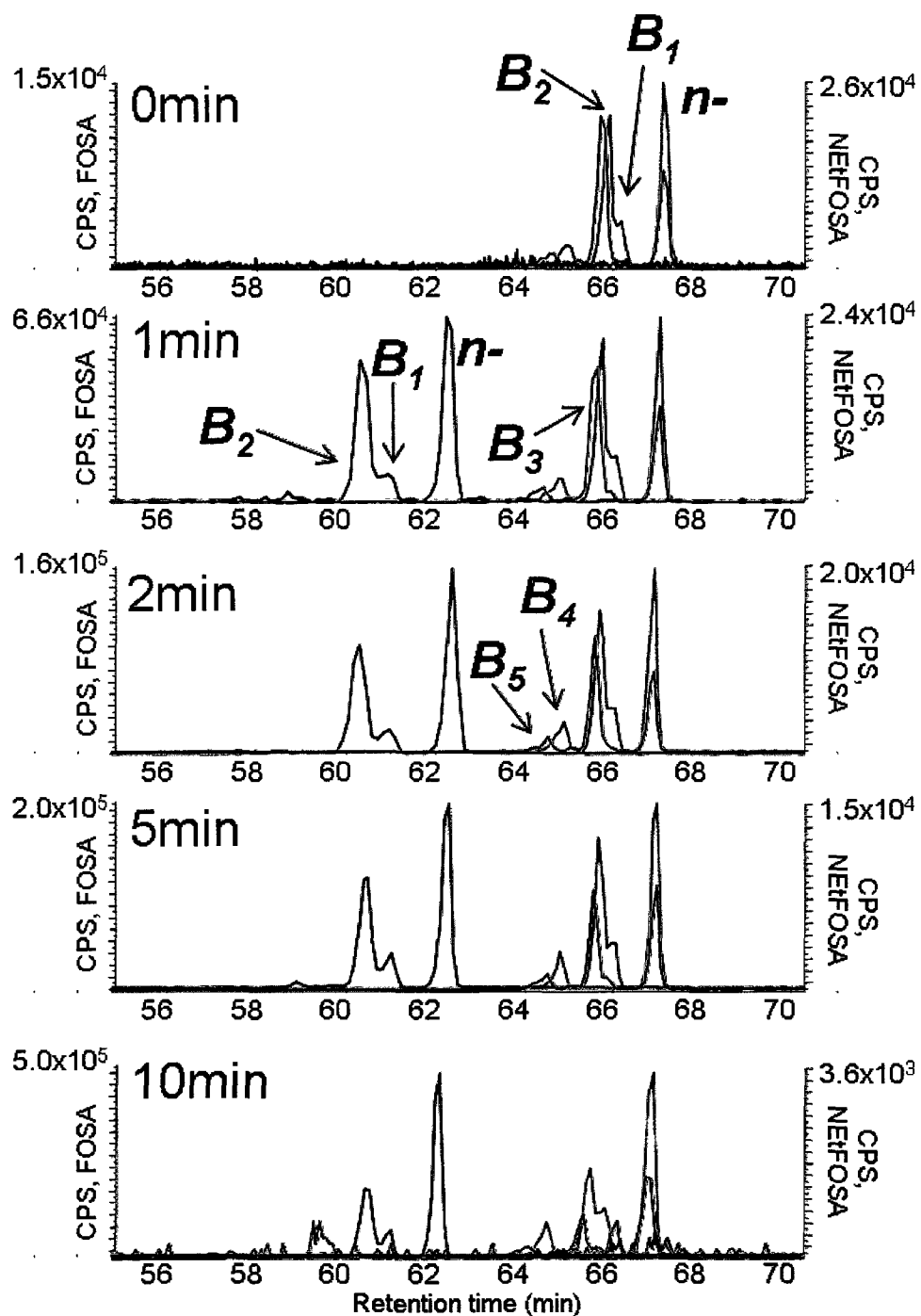
Figure C-17. Representative LC-MS/MS chromatograms showing the biotransformation of 190 nM NEtFOSA (red, m/z 269 and black, m/z 219) to FOSA (blue, m/z 78) by CYP 2C9 (n = 3 replicates, 100 ng of NEtFOSA incubated in 1mL total volume). Note change in NEtFOSA isomer profile and FOSA profile over time.

314
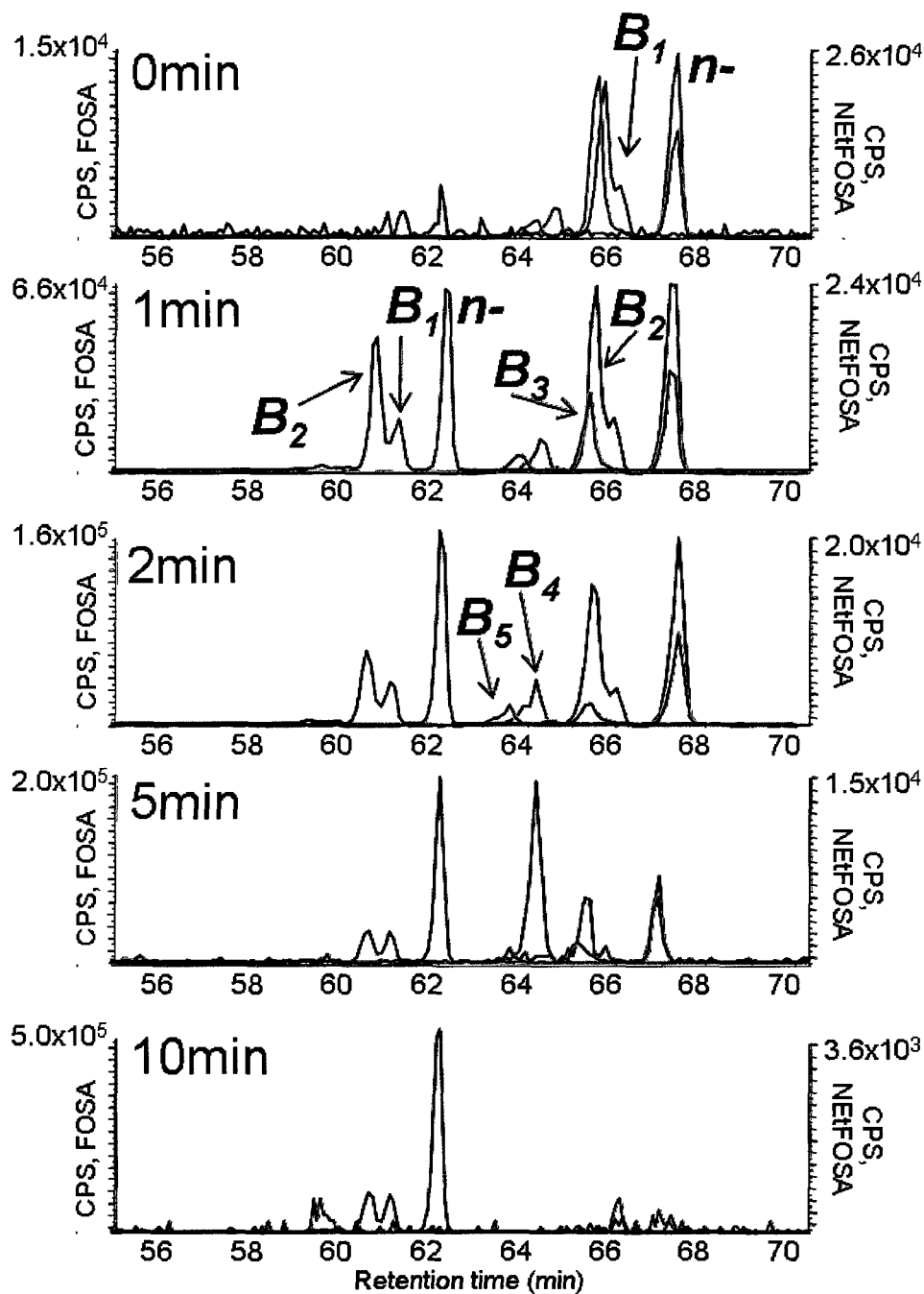
Figure C-18. Representative LC-MS/MS chromatograms showing the biotransformation of 380 nM NEtFOSA (red, *m/z* 269 and black, *m/z* 219) to FOSA (blue, *m/z* 78) by CYP 2C19 (n = 3 replicates, 200 ng of NEtFOSA incubated in 1mL total volume). Note changes in NEtFOSA and FOSA profile over time. Also note differences between profiles as a result of incubation with CYP 2C19 versus CYP 2C9 (Fig C-14).

315

Table C-1. Percent linear PFOS values from literature

Percent linear	Method	Sample description	Reference
78	Peak area	Standard (Fluka)	Karrman et al. 2007 (4)
68		Human plasma (Sweden)	
59		Human serum (Australia)	
60		Human plasma (UK)	
78	Concentration	Standard (Fluka)	Benskin et al. 2007 (5)
80		Human serum (Edmonton, Canada)	
53-78	Peak area	Mixed age/gender human serum (Norway, 1976-2007)	Haug et al. 2009 (6)
~50-70	Concentration	NIST SRM 1589a (Human serum from Great Lakes region), NIST SRM 1957 (Human serum from United States)	Riddell et al. 2009 (7)
70	NMR	3M ECF standard (avg., 10yrs)	Reagan et al. 2007 (8)

Table C-2. Acronyms, formulas, and MRM transitions monitored for PFAs and PFA-precursors

PFA	Acronym	Formula	MRM Transition (m/z) Precursor	MRM Transition (m/z) Product
Perfluorooctanoic acid	PFOA	$C_7F_{15}COOH$	413	369, 319, 269, 219, 169, 119
Perfluorooctane sulfonate	PFOS	$C_8F_{17}SO_3^-$	499	419, 330, 169, 130, 119, 99, 80
N-ethyl perfluorooctane sulfonamide	NEtFOSA	$C_8F_{17}SO_2NHC_2H_5$	526	419, 402, 362, 319, 287, 269, 219, 169, 126, 119, 83, 69, 65, 219
Perfluorooctane sulfonamide	FOSA	$C_8F_{17}SO_2NH_2$	498	478, 410, 269, 219, 169, 119, 78, 48, 69, 83, 419, 319

Storing and Incubation of NEtFOSA

NEtFOSA in aqueous solution was observed to quickly adsorb to many containers tested in this work. Thus, substantial effort was spent on determining optimum conditions for both storing and incubating NEtFOSA. Storing stock methanol solutions of NEtFOSA in polypropylene volumetric flasks resulted in a noticeable change in isomer profiles after ~10 days. Alternatively, stock solutions made up in glass volumetric flasks, or 2 mL amber glass microvials, were stable indefinitely and could be used in all subsequent work. Preliminary experiments in which NEtFOSA was spiked into incubation buffer (isozyme and NADPH were absent) in vessels made of glass, aluminum, or polypropylene, resulted in a sharp decrease in substrate concentration with time, and the substrate could be recovered from the walls by simply rinsing with methanol. Only polystyrene tubes did not result in NEtFOSA adsorption to the walls of the vial; as a result, only this material was used in subsequent incubations.

Validation of Experimental Approach

To validate our experimental approach, arbitrary datasets for a system containing two competing substrates were modelled to equation 1 (9) using GraphPad Prism 5.0 (GraphPad Software, San Diego, CA), where v represents the velocity, V_{max}, represents the maximum velocity, K_m represents the Michaelis constant, and K_i represents the inhibitor dissociation constant. [I] (the concentration of the inhibitor) is equal to a factor (x) of the substrate added ($[S]_{added}$).

Equation 1.

$$\frac{\dfrac{v}{V_{max}}}{(1 + \dfrac{xK_m}{(1-x)K_i})} = \frac{[S]_{added}}{\left[\dfrac{K_m}{(1-x) + \dfrac{xK_m}{K_i}}\right] + [S]_{added}}$$

Equation 1 describes a situation where, as a result of contamination, the contaminant concentration will be higher when substrate concentrations are higher; this situation is analogous to our situation where multiple competing substrates are present in a mixture. Using an arbitrary K_M value of 3, we examined the shapes of v versus [S] curves in the presence of a competing substrate (e.g. a branched isomer) with K_M (K_i) of 0.1, 0.3, 1, 3 or 10 (relative to the K_M of 3 for the substrate of interest) and at various ratios of S2 (the competing substrate) to S (the substrate of interest) between 0 (pure S) and 0.45 (45% competitor) in steps of 5%.

We generated 80 theoretical curves using equation 1 (9) to confirm that effects of contaminants on turnover of S at concentrations of S << KM were negligible. Two important results were obtained from this exercise: 1) the apparent K_M for the substrate of interest falls as the ratio of the competing substrate increases, but, 2) at substrate concentrations that are 10 to 100-fold below K_M (varies, depending on K_i and the S_2 to S ratio), the initial curves are essentially superimposable and there is not a consistent effect of the competing substrate on turnover of the substrate of interest. In other words, one would not see a measurable difference in turnover of the substrate or competitor at very low concentrations of both. Therefore we can expect that by monitoring substrate

depletion at very low concentrations, the biotransformation rate constant for each isomer, determined when $S \ll K_M$, is largely unaffected by the presence of multiple competing isomers. Having confirmed this lack of interference, we simplified this scenario to show the effects of a single contaminating competitive substrate (Scheme 1) to provide an approximate numerical value for the expected degree of inhibition by competing substrates under our experimental conditions.

Scheme 1

$$E + S \underset{}{\overset{K_s}{\rightleftharpoons}} ES \overset{k_{p_s}}{\longrightarrow} E + P_s$$

$$+$$

$$I$$

$$K_i \updownarrow$$

$$EI$$

$$k_{p_i} \downarrow$$

$$E + P_i$$
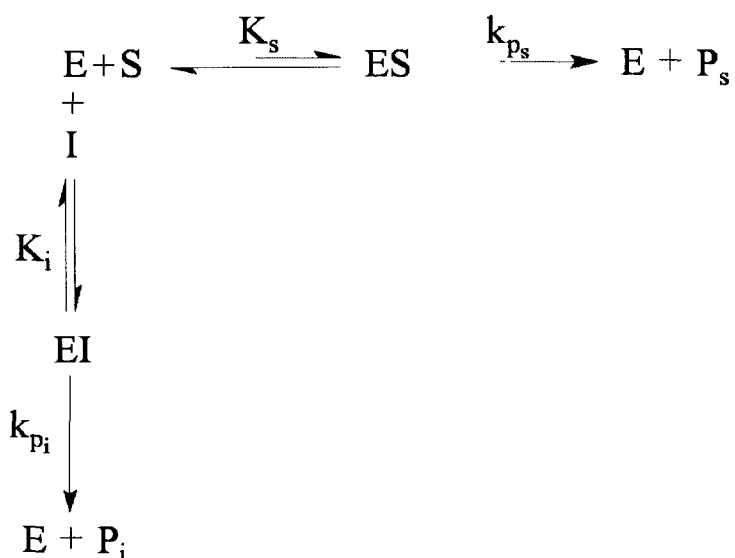
Here, the enzymatic biotransformation of a substrate (S) (e.g. the linear isomer) in the presence of an inhibitor (I) (i.e. a branched isomer) is shown, where E represents the enzyme, P_s and P_i represent products of substrate and inhibitor, respectively, K_s, and K_i are equilibrium constants for binding of substrate and inhibitor, respectively, and k_{ps} and k_{pi} are rate constants for substrate and inhibitor product formation, respectively.

Based on Scheme 1, the inhibition of product formation by the inhibitor can furthermore be described (9) as in Equation 2, whereby K_M is the Michaelis

constant for the biotransformation of S. Assuming that $[S] \ll K_M$, $K_i \approx K_M$, and $[I] = 0.40[S]$, based on the sum GC-ECD response of all branched isomers in the NEtFOSA standard, the % inhibition can be estimated (Equations 3a-c).

Equation 2

$$\% \text{ inhibition} = \frac{[I]}{[I] + K_I\left(1 + \frac{[S]}{K_M}\right)} \times 100\%$$

Equation 3a.

$$\% \text{ inhibition} = \frac{0.40[S]}{0.40[S] + K_M\left(1 + \frac{0.01 K_M}{K_M}\right)} \times 100\%$$

Equation 3b.

$$\% \text{ inhibition} = \frac{0.40(0.01 K_M)}{0.40(0.01 K_M) + 1.01 K_M} \times 100\%$$

Equation 3c.

$$\% \text{ inhibition} = \frac{0.004 K_M}{1.014 K_M} \times 100\% = 0.40\%$$

This suggests that inhibition will indeed be negligible when $[S] \ll K_M$ in our test system with this standard.

REFERENCES

1. Tomy, G.T.; Tittlemier, S.A.; Palace, V.P.; Budakowski, W.R.; Braekevelt, E.; Brinkworth, L.; Friesen, K. Biotransformation of N-ethyl perfluorooctanesulfonamide by rainbow trout (Onchorhynchus mykiss) liver microsomes. *Environ. Sci. Technol.* **2004,** *38,* 758-762.

2. Xu, L.; Krenitsky, D.M.; Seacat, A.M.; Butenhoff, J.L.; Anders, M.W. Biotransformation of N-ethyl-N-(2-hydroxyethyl)perfluorooctanesulfonamide by rat liver microsomes, cytosol, and slices and by expressed rat and human cytochromes P450. *Chem. Res. Toxicol.* **2004,** *17,* 767-775.

3. Manning, R.O.; Bruckner, J.V.; Mispagel, M.E.; Bowen, J.M. Metabolism and disposition of sulfluramid, a unique polyfluorinated insecticide, in the rat. *Drug Metab. Dispos.* **1991,** *19,* 205-211.

4. Karrman, A.; Langlois, I.; van Bavel, B.; Lindstrom, G.; Oehme, M. Identification and pattern of perfluorooctane sulfonate (PFOS) isomers in human serum and plasma. *Environ. Int.* **2007,** *33,* 782-788.

5. Benskin, J.P.; Bataineh, M.; Martin, J.W. Simultaneous characterization of perfluoroalkyl carboxylate, sulfonate, and sulfonamide isomers by liquid chromatography-tandem mass spectrometry. *Anal. Chem.* **2007,** *79,* 6455-6464.

6. Haug, L.S.; Thomsen, C.; Becher, G. Time trends and the influence of age and gender on serum concentrations of perfluorinated compounds in archived human samples. *Environ. Sci. Technol.* **2009,** *43,* 2131-2136.

7. Riddell, N.; Arsenault, G.; Benskin, J.P.; Chittim, B.; Martin, J.W.; McAlees, A.; McCrindle, R. Branched Perfluorooctane Sulfonate Isomer Quantification and Characterization in Blood Serum Samples by HPLC/ESI-MS(/MS). *Environ. Sci. Technol.* **2009,** *43,* 7902–7908.

8. Reagen, W.K.; Lindstrom, K.R.; Jacoby, C.B.; Purcell, R.G. Kestner, T.A.; Payfer, R.M. Miller, J.W. *Environmental characterization of 3M electrochemical fluorination derived perfluorooctanoate and perfluorooctanesulfonate;* Society of Environmental Toxicology and Chemistry 28th North American Meeting platform presentation, Milwaukee, WI, USA, Nov. 11–15, 2007.

9. Segel, I. *Enzyme Kinetics;* John Wiley and Sons: New York, 1975.

Appendix D: Supporting Information for Chapter 5-

Perfluorinated Acid Isomer Profiling in Water and Quantitative

Assessment of Manufacturing Source
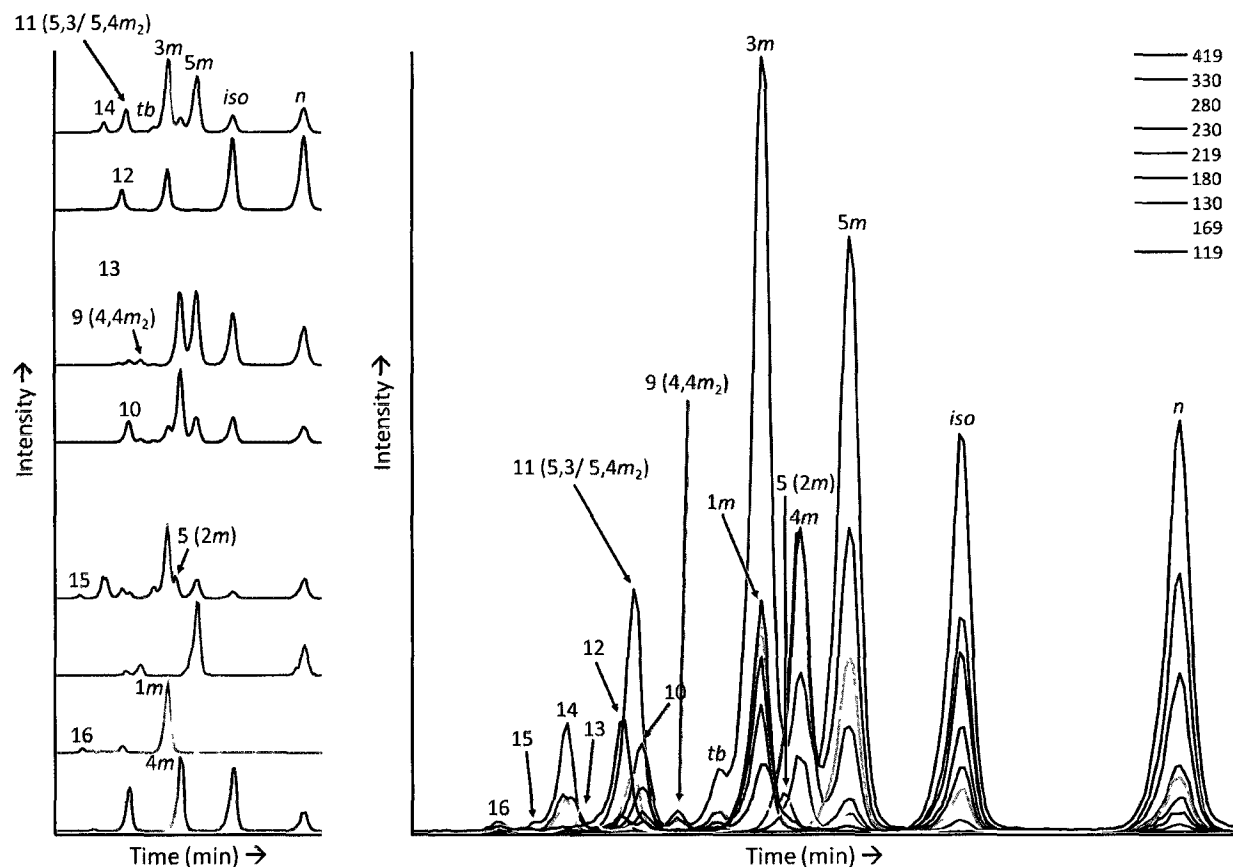
Figure D-1. Stacked (left) and overlaid (right) LC-MS/MS chromatograms showing resolution of 16 PFOS isomers. Only the major isomers, consisting of *n-*, *iso*, *5m*, *4m*, *3m*, *1m*, and dimethyl (*dm*) branches (integrated together in the *m/z* 130 transition) were monitored in this study. Some isomers could not be structurally confirmed using the available isomer standards, however tentative assignments were made based on collision induced dissociation patterns and are stated in parenthesis.
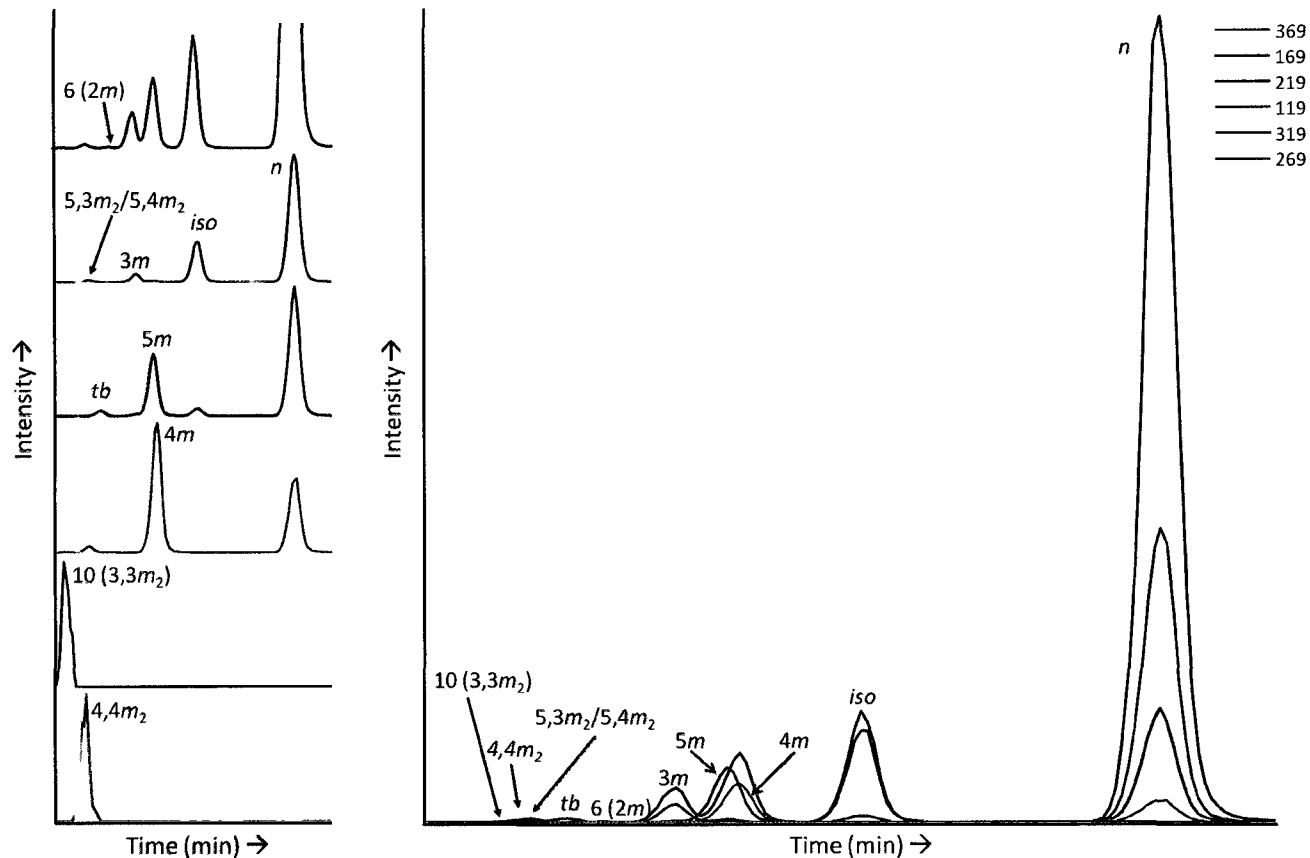
Figure D-2. Stacked (left) and overlaid (right) LC-MS/MS chromatograms showing resolution of 10 PFOA isomers. Only the major isomers, consisting of *n-*, *iso*, 5*m*, 4*m*, 3*m* were used for % ECF calculations. Some isomers could not be structurally confirmed using the available isomer standards, however tentative assignments were made based on collision induced dissociation patterns and are stated in parenthesis.
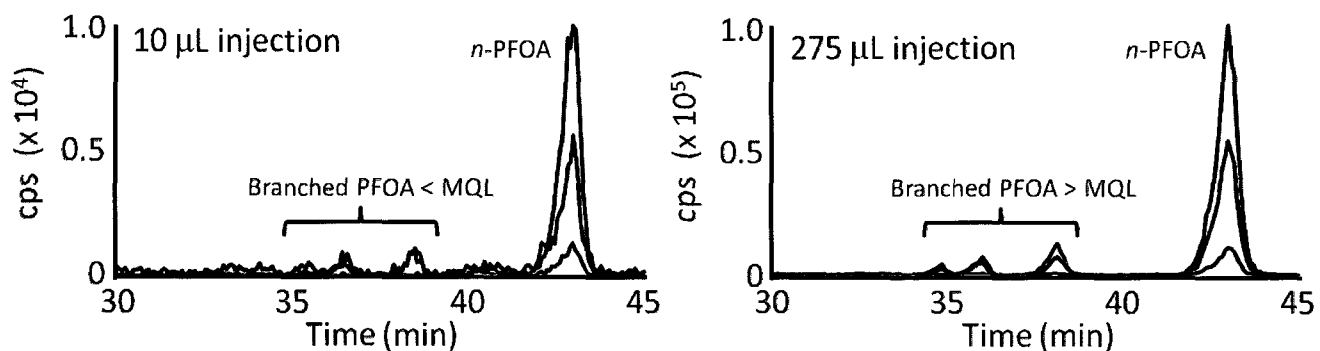
Figure D-3. Figure illustrating the effectiveness of utilizing large volume injections in real samples. Chromatograms shown are PFOA isomers (blue, m/z 413/369; red, m/z 413/169; green, m/z 413/219), following a 10 µL injection (left) or 275 µL injection (right), of Japan Sea site 2 extract. Major isomers were only barely observable and are below method quantification limits (MQLs) when utilizing 10 µL injections, but when 275µL of extract was injected, these isomers are easily observable and above MQLs.
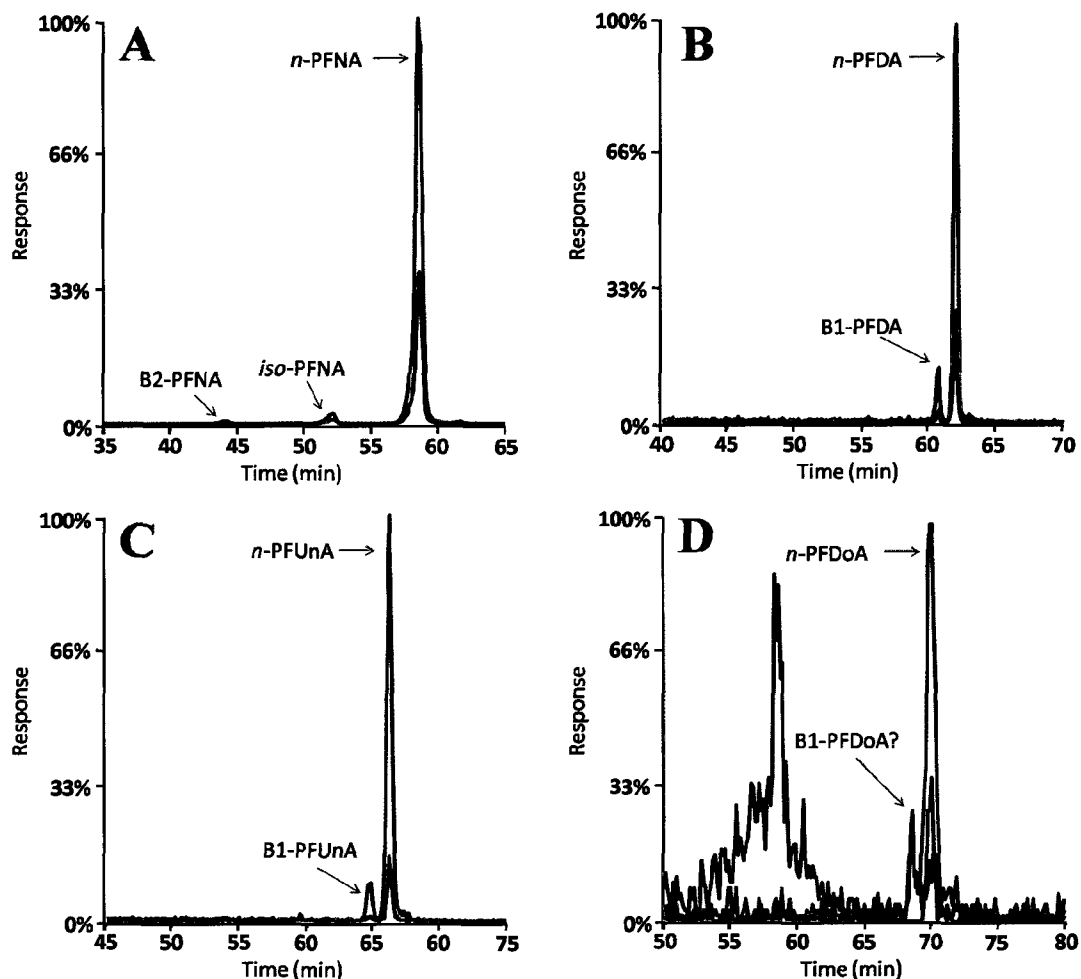
Figure D-4. Long chain perfluorocarboxylate isomers in Tokyo Bay. (A) PFNA, m/z 463/219 (red); m/z 463/169 (green); m/z 463/419 (blue). (B) PFDA, m/z 513/469 (red); m/z 513/269 (green); m/z 513/219 (blue). (C) PFUnA, m/z 563/519 (red); m/z 563/319 (green); m/z 563/219 (blue). (D) PFDoA; m/z 613/569 (red); m/z 613/169 (green); m/z 613/319 (blue). Tokyo Bay was the only coastal Asian location to which branched PFNA, PFDA, PFUnA, and PFDA were observed. With the exception of PFNA, in which the isopropyl branch was confirmed, branched isomers could not be structurally confirmed and were therefore labelled B1 or B2, in order of increasing distance from the linear isomer and depending on the number of branched isomers present.

Table D-1. List of perfluorinated compounds monitored in the present study and their acronyms, chemical formula, and LC-MS/MS parent and product ions.

Perfluorinated compound (acronym)	Chemical Formula	Parent Ion (m/z)	Product Ions (m/z) (specific PFOS and PFOA isomers monitored in a given product ion are stated in parenthesis)
Perfluoroalkyl sulfonates			
Perfluorobutane sulfonate (PFBS)	$C_4F_9SO_3$	299	80, 99, 130
Perfluorohexane sulfonate (PFHxS)	$C_6F_{13}SO_3$	399	80, 99, 119, 169
Perfluorooctane sulfonate (PFOS)	$C_8F_{17}SO_3$	499	80 (n, iso), 130 ($5m$, $3m$, dm), 330 ($4m$), 419 ($1m$), 99, 169, 180, 380, 230, 219, 119
Perfluorodecane sulfonate (PFDS)	$C_{10}F_{21}SO_3$	599	80, 99, 130
Perfluoroalkyl sulfonamides			
Perfluorooctane sulfonamide (FOSA)	$C_8F_{17}SO_2NH_2$	498	78, 169
N-methyl perfluorooctane sulfonamide (NMeFOSA)	$C_8F_{17}SO_2NH(CH_3)$	512	169, 219, 269, 469, 219
N-ethyl perfluorooctane sulfonamide (NEtFOSA)	$C_8F_{17}SO_2NH(CH_2CH_3)$	526	419, 169, 219, 319, 519
Perfluoralkyl carboxylates			
Perfluorohexanoate (PFHxA)	$C_5F_{11}CO_2$	313	69, 119, 269,
Perfluoroheptanoate (PFDA)	$C_6F_{13}CO_2$	363	169, 319
Perfluorooctanoate (PFOA)	$C_7F_{15}CO_2$	413	369 (n), 169 (iso, $3m$), 219 ($5m$), 119 ($4m$), 319, 269
Perfluorononanoate (PFNA)	$C_8F_{17}CO_2$	463	169, 219, 419
Perfluorodecanoate (PFDA)	$C_9F_{19}CO_2$	513	219, 269, 469
Perfluoroundecanoate (PFUnA)	$C_{10}F_{21}CO_2$	563	219, 319, 519
Perfluorododecanoate (PFDoA)	$C_{11}F_{23}CO_2$	613	169, 569, 319
Perfluorotridecanoate (PFTrA)	$C_{12}F_{25}CO_2$	663	119, 269, 619
Perfluorotetradecanoate (PFTA)	$C_{13}F_{27}CO_2$	713	169, 669, 419
Perfluoropentadecanoate (PFTdA)	$C_{14}F_{29}CO_2$	763	219, 269, 719
Internal Standards			
Perfluorohexane[$^{18}O_2$]sulfonate (^{18}O-PFHxS)	$C_6F_{13}S[^{18}O_2]O$	403	84, 103
Perfluoro[1,2,3,4-$^{13}C_4$]octanesulfonate (^{13}C-PFOS)	$C_4F_9[1,2,3,4-^{13}C_4]F_8SO_3$	503	80, 99
$^{13}C_{12}$-perfluorohexanoate (^{13}C-PFHxA)	$C_4F_9[2-^{13}C]F_2{}^{13}CO_2$	315	270, 119
Perfluoro[1,2,3,4-$^{13}C_4$]octanoate (^{13}C-PFOA)	$C_4F_9[2,3,4-^{13}C_3]F_6{}^{13}CO_2$	417	372
Perfluoro[1,2,3,4,5-$^{13}C_5$]nonanoate (^{13}C-PFNA)	$C_4F_9[2,3,4,5-^{13}C_4]F_8{}^{13}CO_2$	468	423
Perfluoro[1,2-$^{13}C_2$]decanoate (^{13}C-PFDA)	$C_8F_{17}{}^{13}CF_2{}^{13}CO_2$	515	470
Perfluoro[1,2-$^{13}C_2$]undecanoate (^{13}C-PFUnA)	$C_9F_{19}{}^{13}CF_2{}^{13}CO_2$	565	520
Perfluoro[1,2-$^{13}C_2$]dodecanoate (^{13}C-PFDoA)	$C_{10}F_{21}{}^{13}CF_2{}^{13}CO_2$	615	570
Perfluoro[1,2,3,4,5,6,7,8-$^{13}C_8$]octanesulfonamide (^{13}C-FOSA)	$C_4F_9[1,2,3,4,5,6,7,8-^{13}C_8]F_8SO_2NH_2$	506	78

Table D-2. Assessment of PFOS and PFOA branched:linear isomer ratios and branched content following SPE extraction. 10 ng or 200 pg 3M ECF PFOA and PFOA was spiked into 0.5 L of Milli-Q water and pumped through a WAX or HLB cartridge.

		ECF standard	10 ng HLB		10 ng WAX		200 pg HLB (Extracted with North Sea Canal Batch)		200pg HLB (Extracted with Mississippi river Batch)	
		Measured value	Measured value	% of value in ECF standard	Measured value	% of value in ECF standard	Measured value	% of value in ECF standard	Measured value	% of value in ECF standard
PFOS Isomer	iso:n	0.191	0.184	96	0.189	99	0.190	100	0.195	102
	5m:n	0.040	0.039	98	0.040	100	0.039	99	0.040	102
	4m:n	0.005	0.005	91	0.005	95	0.005	98	0.005	105
	3m:n	0.042	0.044	106	0.043	102	0.041	98	0.041	99
	1m:n	0.006	0.006	106	0.006	101	0.005	99	0.006	104
	DM:n	0.014	0.015	106	0.015	106	0.014	102	0.014	100
	Avg. ± SEM			100±2.6		101±1.6		104±0.5		100±0.8
	% branched[a]	36.3	36.9	102	37.9	104	37.9	104	36.3	100
PFOA Isomer	iso:n	0.130	0.132	101	0.143	109	0.124	95	0.126	97
	5m:n	0.080	0.074	92	0.076	95	0.074	93	0.086	107
	4m:n	0.060	0.058	97	0.060	99	0.059	98	0.061	101
	3m:n	0.026	0.024	92	0.024	91	0.026	98	0.025	97
	Avg. ± SEM			96±2.1		99±3.9		96±1.2		101±2.4
	% branched[b]	17.8	17.9	101	17.7	99	17.3	97	17.5	98

[a] contribution to total PFOS (peak area, m/z 499/80)
[b] contribution to total PFOA (peak area, m/z 413/369)

Table D-3. Results of PFOS and PFOA isomer standard additions to Tokyo Bay extracts showing conservation of branched: linear isomer regardless of the presence of matrix. Standard addition experiments using Tomakomai Bay Site 1 are also shown for PFOA; PFOS concentrations were too high to assess matrix effects for this extract.

		Spike[a]	Spike + Tokyo Bay (Tomakomai Bay shown in parenthesis for PFOA)[b]	% difference in spike versus spike + matrix
Branched: linear PFOS isomer ratio	iso:n	0.249	0.245	101.4
	5m:n	0.054	0.054	99.3
	4m:n	0.065	0.064	101.7
	3m:n	0.006	0.006	101.0
	1m:n	0.008	0.008	100.2
	dm:n	0.027	0.027	99.9
	Average ± SEM			99.9
	% branched peak area, PFOS (m/z 499/80)	46.841	46.131	101.5
Branched: linear PFOA Isomer ratio	iso:n	0.177	0.176 (0.160)	100.8 (92.6)
	5m:n	0.096	0.098 (0.099)	97.3 (100.6)
	4m:n	0.080	0.082 (0.087)	97.1 (105.9)
	3m:n	0.030	0.031 (0.032)	97.7 (103.1)
	Average ± SEM			98.1±0.9 (100.5±2.9)
	% branched peak area, PFOA (m/z 413/369)	22.5	22.8 (22.6)	101.3 (100.4)

[a]branched: linear isomer ratios and peaks areas reported in spike are not representative of those observed in 3M ECF PFOS and PFOA standards
[b]after subtraction of background levels in Tokyo Bay extract

Table D-4. Concentrations (ng/L) of PFCs in water from coastal Asia, the Mississippi and North Sea Canal. Total and *n*-isomer quantification are displayed. Quantification for both linear and total PFAs was based on linear isomer calibration curves, with the exception of PFOS, which was quantified by isomer-specific quantification. Error represents ± 1 standard error about the mean.

		FOSA	PFHxS	PFOS	PFDS	PFOA	PFNA	PFDA	PFUnA	PFDoA	PFTA
Mississippi River (n=4)	Total	3.29±0.42	1.38±0.07	7.74±0.39	ND	8.66±0.34	3.71±0.09	0.21±0.01	0.11±0.01	ND	ND
	linear	1.38±0.15	1.36±0.08	3.72±0.17		7.35±0.26	3.67±0.09	0.21±0.01	0.10±0.01		
Tokyo Bay, Japan (n=3)	Total	NQ	0.74±0.001	2.89±0.09	NQ	1.76±0.14	3.40±0.06	0.26±0.02	1.25±0.02	0.65±0.01	ND
	linear		0.70±0.001	1.87±0.002		1.42±0.01	3.01±0.06	0.22±0.01	1.20±0.01	0.65±0.01	
Tomakomai Bay 1, Japan (n=2)	Total	NQ	208.6±55	525±139	NQ	14.8±0.72	58.2±13.0	5.36±0.13	7.67±0.55	ND	ND
	linear		167±42	321.8±2.25		12.8±0.25	58.2±13.0	5.36±0.13	7.67±0.55		
Tomakomai Bay 2, Japan (n=2)	Total	NQ	6.1±0.91	7.91±0.32	NQ	12.5±2.8	6.73±0.15	5.76±0.05	6.35±0.09	ND	ND
	linear		3.9±0.03	5.43±0.0002		10.3±2.4	6.73±0.15	5.76±0.05	6.35±0.09		
Japan Sea 1 (n=1)	Total	NQ	0.02	0.78	NQ	4.86	1.39	1.96	2.33	ND	ND
	linear		0.02	0.47		4.05	1.39	1.96	2.33		
Japan Sea 2 (n=1)	Total	NQ	ND	0.85	NQ	2.93	2.62	2.28	2.53	ND	ND
	linear			0.52		2.55	2.62	2.28	2.53		
Shanghai, China (n=2)	Total	NQ	0.35±0.01	7.15±0.44	NQ	242±19	12.0±1.34	5.25±0.33	4.81±0.332	ND	ND
	linear		0.32±0.01	4.95±0.02		200±17	12.0±1.34	5.25±0.33	4.81±0.332		
Hangzhou, China (n=2)	Total	NQ	ND	1.52±0.17	NQ	11.1±0.3	0.92±0.27	2.12±0.12	2.29±0.12	ND	ND
	linear			1.08±0.002		9.12±0.18	0.92±0.27	2.12±0.12	2.29±0.12		
North Sea Canal (n=3)[a]	Total	1.4±0.01	7.6±0.11	18.7±1.5	ND	18.6±0.60	0.73±0.002[b]	0.50±0.03	0.08±0.004[b]	0.04±0.003	ND
	linear	0.98±0.01	6.01±0.10	12.1±0.7		15.9±0.46	0.65±0.02	0.50±0.03	0.06±0.003	0.04±0.003	
North Sea Canal[6]	Total	1.00	6.30	19.50	-	19.40	*8.70[c]*	0.42	*10.40[c]*	-	-

[a]triplicate 10µL injection of single extract
[b]duplicate 100µL injection of single extract
[c]Assigned values in italics are based on arithmetic means, rather than model data. See Van Leeuwen et al.[6] for details.
NQ-not quantified   ND-not detected

331

Table D-5. Comparison of PFOS and PFOA isomer method quantification limits (MQLs) for large and small volume injections. Number in paranethesis represents product ion monitored.

	Major PFOA isomers (product ion)						
	n (369)	*iso* (169)	5*m* (219)	4*m* (119)	3*m* (169)		
275μL MQL (pg)	0.6	2.4	2.6	2.9	11		
10μL MQL (pg)	81	270	330	320	1200		

	Major PFOS isomers (product ion)						
	n (80)	*iso* (80)	5*m* (130)	4*m* (330)	3*m* (130)	1*m* (419)	DM (130)
275μL MQL (pg)	0.7	3.5	22.5	10.6	28	34	95
10μL MQL (pg)	73	250	1107	439	1580	974	7000

MQL: Method Quantification limit. The minimum absolute quantity of total PFOS or PFOA (pg) required in any volume of water for quantification (i.e. S/N=10) of a given isomer, assuming pre-concentration down to 300μL and injection of 275 μL (large volume injection) or 10 μL (low volume injection).

Table D-6. PFOA isomer profiles based on the ratio of *iso:n*, 5*m:n*, 4*m:n*, 3*m:n*, *tb:n*, and 5,3*m₂:n*. Tokyo Bay, Japan Sea 2, and Tomakomai Bay 1 contained significantly different ($p < 0.05$) ratios compared to 3M ECF PFOA (grey shading). Statistical tests were only performed on the ratios of the major isomers (*iso:n*, 5*m:n*, 4*m:n*, 3*m:n*).

	PFOA isomer (product ion)					
	iso:n	*5m:n*	*4m:n*	*3m:n*	*tb:n*	*5,3m₂:n*
Mississippi (n=4)	0.10	0.07	0.05	0.02	0.005	0.006
Shanghai (n=2)	0.13	0.08	0.07	0.02	0.009	0.007
Hangzhou (n=2)	0.14	0.08	0.07	0.02	0.010	0.008
Japan Sea 1 (n=1)	0.12	0.07	0.06	0.02	0.007	0.007
Japan Sea 2 (n=1)	0.09	0.05	0.04	0.01	0.004	0.004
Tomakomai Bay 1 (n=2)	0.06	0.04	0.03	0.01	0.004	0.002
Tomakomai Bay 2 (n=2)	0.10	0.06	0.06	0.02	0.007	0.010
Tokyo Bay (n=3)	0.08	0.02	0.02	0.01		
North Sea Canal (n=3)[a]	0.09	0.07	0.05	0.02	0.007	0.007
3M PFOA (n=4)	0.13	0.08	0.06	0.03	0.007	0.007
Defu PFOA (n=5)	0.10	0.06	0.05	0.02	0.006	0.005

[a] n=3 injections of single extract

333

Table D-7. Ratios of $5m{:}iso$, $4m{:}iso$, and $3m{:}iso$ PFOA isomers. Tokyo Bay was the only sample which contained significantly different ($p<0.05$) ratios compared to 3M ECF PFOA (grey shading).

	$5m{:}iso$	$4m{:}iso$	$3m{:}iso$
Mississippi (n=4)	0.66	0.47	0.21
Shanghai (n=2)	0.62	0.51	0.15
Hangzhou (n=2)	0.58	0.47	0.15
Japan Sea 1 (n=1)	0.61	0.49	0.17
Japan Sea 2 (n=1)	0.56	0.45	0.13
Tomakomai Bay 1 (n=2)	0.60	0.45	0.12
Tomakomai Bay 2 (n=2)	0.62	0.53	0.21
Tokyo Bay (n=3)	0.23	0.18	0.09
North Sea Canal (n=3)[a]	0.70	0.54	0.24
3M PFOA (n=4)	0.61	0.46	0.20
Defu PFOA (n=5)	0.63	0.48	0.22

[a]n=3 injections of single extract

Table D-8. Ratio of $4m:5m$ and $3m:5m$ PFOA isomers. No significant ($p<0.05$) differences were observed between ratios in samples and 3M ECF PFOA.

	$4m:5m$	$3m:5m$
Mississippi (n=4)	0.72	0.32
Shanghai (n=2)	0.82	0.24
Hangzhou (n=2)	0.82	0.27
Japan Sea 1 (n=1)	0.81	0.27
Japan Sea 2 (n=1)	0.81	0.24
Tomakomai Bay 1 (n=2)	0.75	0.20
Tomakomai Bay 2 (n=2)	0.86	0.34
Tokyo Bay (n=3)	0.79	0.38
North Sea Canal (n=3)[a]	0.77	0.34
3M PFOA (n=4)	0.74	0.33
Defu PFOA (n=5)	0.76	0.34

[a]n=3 injections of single extract

Table D-9. Total, *n*- and branched-PFOA concentrations and contribution of individual manufacturing sources (ECF, *n*-telomer, *iso*-telomer) to total PFOA concentrations

	[PFOA]total (ng/L)	[*n*-PFOA] (ng/L)	[branched PFOA] (ng/L) ([*iso*-PFOA] is shown in parenthesis)	% branched (wt)	% contribution of ECF to [PFOA]total	% contribution of *n*-telomer to [PFOA]total (*iso*-telomer contribution is shown in parenthesis)
Japan Sea site 1 (n=1)	4.86	4.05	0.81	16.7	94	6
Japan Sea site 2 (n=1)	2.93	2.55	0.39	13.2	74	26
Hangzhou, China (n=2)	11.1	9.12	1.97	17.8	100	0
Shanghai, China (n=2)	242	200	42.0	17.4	98	2
Tomakomai Bay site 1, Japan (n=2)	14.8	12.8	1.96	13.3	75	25
Tomakomai Bay site 2, Japan (n=2)	12.5	10.3	2.17	17.4	98	2
Mississippi River, New Orleans, USA (n=4)	8.66	7.35	1.31	15.1	85	15
Tokyo Bay, Japan (n=3)	1.76	1.42	0.35 (*iso* = 0.29)	19.6	33	53 (*iso*-telomer = 14)
North Sea canal, The Netherlands (n-3)[a]	18.6	15.9	2.64	14.2	80	20
3M ECF PFOA (n=4)				18 +/- 0.3		

[a]triplicate injections of same extract.

Table D-10. Weight distribution of PFOS isomers in commercial products and comparison to water from coastal Asia, Mississippi river, and North Sea Canal. Error Represents ± 1 standard error about the mean (SEM).

SAMPLES	n (80)	iso (80)	5m (130)	4m (330)	3m (130)	1m (419)	dm (130)	∑branched (sum isomer specific)	∑ branched (80)
Mississippi River, (n=4)	48.1±0.5	13.3±0.1	7.9±0.1	14.5±0.3	7.9±0.2	4.0±0.1	4.4±0.1	51.9±0.5	50.8±0.54
North Sea Canal, (n=3)[a]	66.1±1.2	10.9±0.1	6.0±0.1	5.9±0.3	6.0±0.4	2.6±0.3	2.5±0.2	33.9±1.2	34.8±1.5
Tokyo Bay, (n=3)	64.6±0.1	10.7±0.1	4.5±0.1	7.2±0.2	5.8±0.2	4.3±0.1	2.9±0.1	35.4±0.09	37.6±0.1
Tomakomai Bay site 1, (n=2)	61.3±0.7	10.3±0.05	5.9±0.1	8.2±0.3	6.1±0.2	4.5±0.1	3.6±0.1	38.7±0.7	40.4±0.7
Tomakomai Bay site 2, (n=2)	68.6±0.004	7.3±0.03	4.6±0.2	6.7±0.3	6.1±0.01	3.8±0.4	2.9±0.1	31.4±0.004	34.4±0.4
Japan Sea 1 (n=1)	60.4	11.9	6.8	6.8	8.1	3.5	2.5	39.6	43.0
Japan Sea 2 (n=1)	61.2	12.7	6.0	5.8	5.9	5.4	3.0	38.8	42.4
Shanghai, (n=2)	69.3±0.4	11.2±0.1	4.6±0.2	5.7±0.6	4.5±0.1	2.2±0.03	2.4±0.02	30.7±0.4	34.7±0.3
Hangzhou, (n=2)	70.8±1.7	11.4±0.4	4.1±0.2	5.6±0.5	3.5±0.3	2.6±0.1	2.0±0.4	29.2±1.7	33.3±1.5
3M PFOS (n=5)	72.8±0.9	9.4±0.1	4.2±0.2	4.1±0.2	5.2±0.1	2.1±0.02	2.2±0.1	27.2±0.9	28.5±0.2
Defu PFOS (n=4)	78.2±0.5	9.2±0.2	4.5±0.1	2.4±0.1	2.8±0.4	1.2±0.1	1.7±0.1	21.8±0.5	22.5±0.3
Jinfu K-PFOS (n=3)	69.1±1.5	11.2±0.2	7.1±0.4	3.9±0.3	4.1±0.4	2.2±0.1	2.3±0.1	30.9±1.5	32.0±1.4
Jinfu TEA-PFOS (n=3)	69.2±0.9	11.3±0.1	7.5±0.3	4.3±0.3	3.7±0.2	1.8±0.1	2.2±0.1	30.8±0.9	31.3±1.1

[a]triplicate injections of single extract.

Extraction and treatment of samples

Extraction of water samples utilized Oasis® weak anion exchange (WAX; 6 cc, 150 mg, 30 μm; for Coastal Asian samples) or Oasis® hydrophilic-lipophilic balance (HLB; 6 cc, 200 mg, 30 μm; for Coastal Asian, Mississippi river, and North Sea Canal water samples) cartridges, which have been previously shown to give consistent results for the quantification of total PFOS and PFOA[1]. Briefly, HLB cartridges were preconditioned with 5 mL of methanol, followed by 5 mL of water, while WAX cartridges were preconditioned with 4 mL of 0.1% NH4OH in methanol, 4 mL of MeOH and finally 4 mL of water. Samples (0.2 – 1 L) were passed through the cartridges at a rate of approximately 1 drop per second. HLB cartridges were washed with 5 mL of 40% MeOH/60% water and then eluted with MeOH, while WAX cartridges were washed with 4 mL of 25 mM ammonium acetate buffer at pH 4 and then eluted with 4 mL of MeOH and 4 mL of 0.1% NH4OH in methanol, respectively, as described elsewhere.[1-2] The volume of extract was reduced under nitrogen and then diluted with water (final composition 50:50 MeOH/water) and then transferred to a 300 μL polypropylene microvials for analysis.

Instrumental modification

An Agilent 1100 liquid chromatograph (LC) was used which was equipped with a standard analytical head assembly, for use with a 100 μL injector loop. However, this injection volume was too small to allow adequate detection limits for branched isomers. Pre-concentration of extract was considered, however

338

this could introduce contamination to the extracts we were receiving, thus we wanted to avoid sample manipulation as much as possible. Ultimately we required a flexible method, in which the injection volume could be increased or decreased depending on the type, volume, or concentration of extract received. We considered replacing both the analytical head assembly and injector loop with ones designed for large volume injections; however, this was costly and not recommended for the pressures typically reached in our LC method (up to 260 bar). To facilitate injection volumes greater than 100 µL, a 400 µL loop was placed between the needle seat and the injector valve, and the LC was set to "valve by-pass" for the duration of the injection method. The injector was programmed to draw a maximum sample volume of 100 µL and to inject this onto the extended needle seat capillary. This procedure was repeated, using multiple injection stacking, until the desired volume of injected sample was reached; depending on the concentration and volume of extract. Once the desired volume was reached, the valve was set to "main pass" to send the contents of the extended needle seat capillary to the column. This modification has the potential to accommodate injections of up to 500 µL (100 µL in the injector loop + 400 µL in the expanded needle seat), which is comparable to other large volume injection methods for perfluorinated compounds[3-4] however it was only validated for injections up to 275 µL, for use with 300 µL sample vials in the present study.

Instrumental analysis

Isomer separation and total PFOS quantification was adapted from Benskin et al.[5]. Briefly, extracts (10-275 µL) were injected onto a FluoroSep RP Octyl column (3µm, 100A, 15 cm × 2.1 mm, ES Industries, West Berlin, NJ) equipped with an Agilent Eclipse C8 guard column (4.6 mm x 12.5 mm) which were both maintained at 35°C. An Agilent Eclipse XDB-C18 column (5 µm, 15 cm x 4.6 mm), at ambient temperature was placed directly upstream of the injector to trap all PFAs originating from the LC pump. The starting mobile phase composition was 60% A (water adjusted to pH 4.0 with ammonium formate) - 40% B (100% MeOH). Initial conditions were held for 0.3 min, ramped to 64% B by 1.9 min, increased to 66% B by 5.9 min, 70% B by 7.9 min, 78% B by 40.0 min, 88% B by 42.0 min, followed by 100% B by 60 min. The gradient was maintained at 100% B until 70.0 min, and then returned to initial conditions by 71 min, after which time the column was equilibrated for a further 25 min. Flow rate was kept constant at 200 µL/min. A diverter valve (VICI Valco Canada, Inc., Brockville, ON) was placed downstream of the analytical column to divert flow to waste for the first 18 min of the run, after which time the flow was redirected to the mass spectrometer. Mass spectral data were collected using a triple-quadrupole mass spectrometer (API 5000Q, MDS Sciex, Concord, ON, Canada) with negative ion electrospray ionization, and all data were collected in multiple reaction monitoring (MRM) mode.

QA/QC

Results of isomer-specific spike/recovery experiments are shown in Table D-2 of Appendix D. PFOS and PFOA n:branched isomer ratios following extraction were, on average, within 4% of unextracted standards, demonstrating that PFOS and PFOA isomer profiles are well conserved regardless of the extraction method (WAX or HLB). A comparison of total branched PFOS and PFOA isomers (based on the sum of branched isomer peaks in the m/z 499/80 and 413/369 transitions, respectively) also indicated less than 4% difference in extracted versus unextracted standards. Further validation of our extraction and quantification methods was conducted by comparing measured versus interlaboratory assigned values[6] for the North Sea Canal extract (Table D-4, Appendix D). Measured concentrations were very close to assigned values for PFHxS (7.6 ng/L quantified vs 6.3 ng/L assigned), PFOS (18.7 ng/L quantified vs 19.5 ng/L assigned), PFOA (18.6 ng/L quantified vs 19.4 ng/L assigned), and PFDA (0.50 ng/L quantified vs 0.42 assigned). Assigned values reported by Van Leeuwen et al.[6] for PFNA and PFUnA were based on arithmetic means (not model data, as with the other values) and were subject to considerable variability, which likely explains the inconsistencies in PFNA and PFUnA concentrations in the present study versus the interlaboratory results. Overall, these results indicate that our extraction and quantification methods produced reliable and accurate data.

Large volume injections vastly reduced the minimum quantity of PFOS and PFOA required in any given volume of water (assuming preconcentration to 300 µL) for quantification of individual isomers, with PFOS MQLs ranging from

0.7 - 95 pg using 275 μL injections versus 73 - 7000 pg for 10 μL injections, and

PFOA MQLs ranging from 0.6-11 pg using 275 μL injections versus 81 – 1200

pg for 10 μL injections (Table D-5, Appendix D).

Standard addition experiments with the Tokyo Bay extract demonstrated

that PFOS and PFOA isomer profiles were not influenced by matrix affects, with

<3% difference in both total branched content and individual branched:linear

isomer ratios in the presence or absence of matrix (Table D-3, Appendix D). A

standard addition experiment was also performed with Tomakomai Bay site 1

extract, and while PFOA isomer profiles again showed an absence of matrix

effects, PFOS concentrations in this sample were too high (i.e. beyond 'percent

branched' dynamic range, see discussion below) to assess matrix effects using

large volume injections. Standard addition experiments to other extracts could not

be performed due limited volume of sample extract.

Isomer identification and quantification

A total of 16 isomers in the standard of 3M ECF PFOS (Figure D-1) can

be resolved by the current method, and of these, linear, isopropyl, internal

monomethyl (5m, 4m, 3m, 2m, 1m) tert-butyl, and dimethyl (4,4m_2, 5,3m_2, and

5,4m_2) reportedly make up over 99% of the total isomer composition[7]. To prevent

bias in the calculation of total PFOS concentrations, which can occur when the

isomer profile in the sample is different from the standard used to quantify it, we

quantified the major isomers, n, iso, 5m, 4m, 3m, and 1m-PFOS individually,

using a characterized technical standard and isomer specific transitions (Table D-

1). Dimethyl branched isomer peaks in the m/z 130 product ion chromatogram were integrated together and quantified using a dimethyl branched isomer calibration curve, as reported in Riddell et al.[8] For comparison purposes, we also quantified total branched content using the sum of all branched isomer peaks in the m/z 80 product ion, and compared the results with isomer-specific quantification. Total branched isomer quantification using the m/z 80 product ion is expected to give similar results as isomer specific quantification, provided the isomer profile in the sample is similar to that of the technical standard.[8]

The method was also capable of chromatographically resolving 10 isomers in a standard of 3M ECF PFOA (Figure D-2), but like for ECF PFOS, not all branched isomers are detectable in environmental samples. A quantitatively characterized technical ECF PFOA standard is not commercially available, therefore total PFOA concentrations were based on integration of all isomers in the m/z 369 product ion, and by quantification relative to a linear isomer standard. To prevent bias from occurring when certain branched isomers dropped below detection limits (see Results and Discussion section), only the major isomers of PFOA (n, iso, $5m$, $4m$, $3m$) were summed, which were always detectable in samples reported here.

For all other PFAs, only pure linear standards were commercially available, therefore both linear and "total" (i.e. branched + linear isomer) concentrations were determined using calibration curves based only on the linear isomer standard. Thus, some inaccuracies in these "total" concentrations are anticipated due to varying response factors between branched and linear isomers.

While peaks eluting within 10 min of the linear isomer were examined as possible branched isomers, only those with at least two MRM transitions were integrated for "total" PFA quantification.

Limitations of % ECF calculation

Two limitations of the methods application are discussed briefly here. Firstly, we cannot rule out that abiotic or biological fractionation (reviewed elsewhere[9]) has altered the observed profiles, and if this had occurred it would introduce error to our reported source contributions. However, evidence for such fractionation was not apparent in any sample. The various branched isomers have distinct physical properties and pharmacokinetics[10-13] which could affect their relative fractionation (e.g. sedimentation on suspended particles, or volatilization), but the ratios of individual monomethyl branched isomers (i.e. *5m:iso, 4m:iso,* and *3m:iso*-PFOA) were not statistically different in samples, compared to standards (with the exception of Tokyo Bay, where an isopropyl-telomer source was identified), thus it is unlikely that the profiles of branched isomers were affected by fractionation, and by extension it is unlikely that the linear isomer was affected. Secondly, the use of an *n*-PFOA standard for quantification of total PFOA and *iso*-PFOA is recognized as a potential source of error, but there is currently no alternative to this practice. If the relative response factors of *iso*-PFOA and *n*-PFOA are significantly different, this would result in over- or under-reporting of concentrations. When we used this technique to quantify isopropyl and total branched PFOA in our 3M ECF PFOA standard, we obtained values of 7

and 18%, respectively, the latter of which is within 1% of the value reported for LC-MS/MS analysis of 3M ECF PFOA (19% branched) by Reagen et al.[14]. These values are also within 4% of isopropyl and total branched PFOA content determined by ^{19}F NMR, (9 and 22%, respectively) in the same study. Isopropyl and total branched PFOA content determined in the present study may therefore vary 2-4% from the true weight percentages, but this is unlikely to have affected our % ECF determinations, since branched content was measured and compared the same way in samples and our 3M ECF PFOA standard (i.e. using LC-MS/MS and an *n*-PFOA standard), as opposed to comparison with literature % branched values for 3M ECF PFOA (i.e. 22%), which could lead to an underestimation of the true ECF contribution.

REFERENCES

1.   Taniyasu, S.; Kannan, K.; So, M. K.; Gulkowska, A.; Sinclair, E.;
        Okazawa, T.; Yamashita, N., Analysis of fluorotelomer alcohols,
        fluorotelomer acids, and short- and long-chain perfluorinated acids in
        water and biota. *J. Chrom. A.* **2005,** *1093*, 89-97.

2.   Yamashita, N.; Kannan, K.; Taniyasu, S.; Horii, Y.; Petrick, G.; Gamo, T.,
        A global survey of perfluorinated acids in oceans. *Marine Pollut. Bull.*
        2005, *51*, 658-668.

3.   Schultz, M. M.; Barofsky, D. F.; Field, J. A., Quantitative determination of
        fluorinated alkyl substances by large-volume-injection liquid
        chromatography tandem mass spectrometry-characterization of municipal
        wastewaters. *Environ. Sci. Technol.* **2006,** *40*, 289-95.

4.   Holm, A.; Wilson, S. R.; Molander, P.; Lundanes, E.; Greibrokk, T.,
        Determination of perfluorooctane sulfonate and perfluorooctanoic acid in
        human plasma by large volume injection capillary column switching liquid
        chromatography coupled to electrospray ionization mass spectrometry. *J.
        Sep. Sci.* **2004,** *27*, 1071-1079.

5.   Benskin, J. P.; Bataineh, M.; Martin, J. W., Simultaneous characterization
        of perfluoroalkyl carboxylate, sulfonate, and sulfonamide isomers by
        liquid chromatography-tandem mass spectrometry. *Anal. Chem.* **2007,** *79*,
        6455-6464.

6.   van Leeuwen, S. P.; Karrman, A.; van Bavel, B.; de Boer, J.; Lindstrom,
        G., Struggle for quality in determination of perfluorinated contaminants in
        environmental and human samples. *Environ. Sci. Technol.* **2006,** *40*, 7854-
        7860.

7.   Arsenault, G.; Chittim, B.; McAlees, A.; McCrindle, R.; Riddell, N.; Yeo,
        B., Some issues relating to the use of perfluorooctanesulfonate (PFOS)
        samples as reference standards. *Chemosphere* **2008,** *70*, 616-625.

8.   Riddell, N.; Arsenault, G.; Benskin, J. P.; Chittim, B.; Martin, J. W.;
        McAlees, A.; McCrindle, R., Branched perfluorooctane sulfonate isomer
        quantification and characterization in blood serum samples by HPLC/ESI-
        MS(/MS). *Environ. Sci. Technol.* **2009,** *43*, 7902-7908.

9.   Benskin, J. P.; De Silva, A. O.; Martin, J. W., Isomer profiling of
        perfluorinated substances as a tool for source tracking: A review of early
        findings and future applications. *Rev. Environ. Contam. Toxicol.* **2010,** *in
        press.*

346

10. Benskin, J. P.; De Silva, A. O.; Martin, L. J.; Arsenault, G.; McCrindle, R.; Riddell, N.; Mabury, S. A.; Martin, J.W. Disposition of perfluorinated acid isomers in Sprague- Dawley rats; part 1: single dose. *Environ. Toxicol. Chem.* **2009**, *28*, 542–554.

11. De Silva, A. O.; Benskin, J. P.; Martin, L. J.; Arsenault, G.; McCrindle, R.; Riddell, N.; Martin, J. W.; Mabury, S. A., Disposition of perfluorinated acid isomers in Sprague-Dawley rats; part 2: subchronic dose. *Environ. Toxicol. Chem.* **2009**, *28*, 555-567.

12. De Silva, A. O.; Tseng, P. J.; Mabury, S. A., Toxicokinetics of perfluorocarboxylate isomers in rainbow trout. *Environ. Toxicol. Chem.* **2009**, *28*, 330-337.

13. Sharpe, R. L.; Benskin, J. P.; Laarman, A. L.; MacLeod, S. M.; Martin, J. W.; Wong, C. S.; Goss, G. G., An Investigation of perfluorooctane sulfonate (PFOS) toxicity, isomer-specific accumulation and maternal transfer in Zebrafish (*Danio rerio*) and Rainbow Trout (*Oncorhynchus mykiss*). *Environ. Toxicol. Chem.* **2010,** *in press.*

14. Reagen, W. K.; Lindstrom, K. R.; Jacoby, C. B.; Purcell, R. G.; Kestner, T. A.; Payfer, R. M.; Miller, J. W. **2007.** *Environmental characterization of 3M electrochemical fluorination derived perfluorooctanoate and perfluorooctanesulfonate,* Society of Environmental Toxicology and Chemistry 28th North American meeting, Milwaukee, WI, USA, 11–15 Nov.

Appendix E: Supporting Information for Chapter 6-Perfluorinated Acid Isomer Profiles in Water from Remote Locations

Figure E-1. ECF Standards showing relative ratios of branched isomers : linear PFOA and the corresponding change in % ECF. Calibration curves for total branched content versus ECF were based on quantification using the m/z 369 product ion, which showed good sensitivity for all branched isomers.
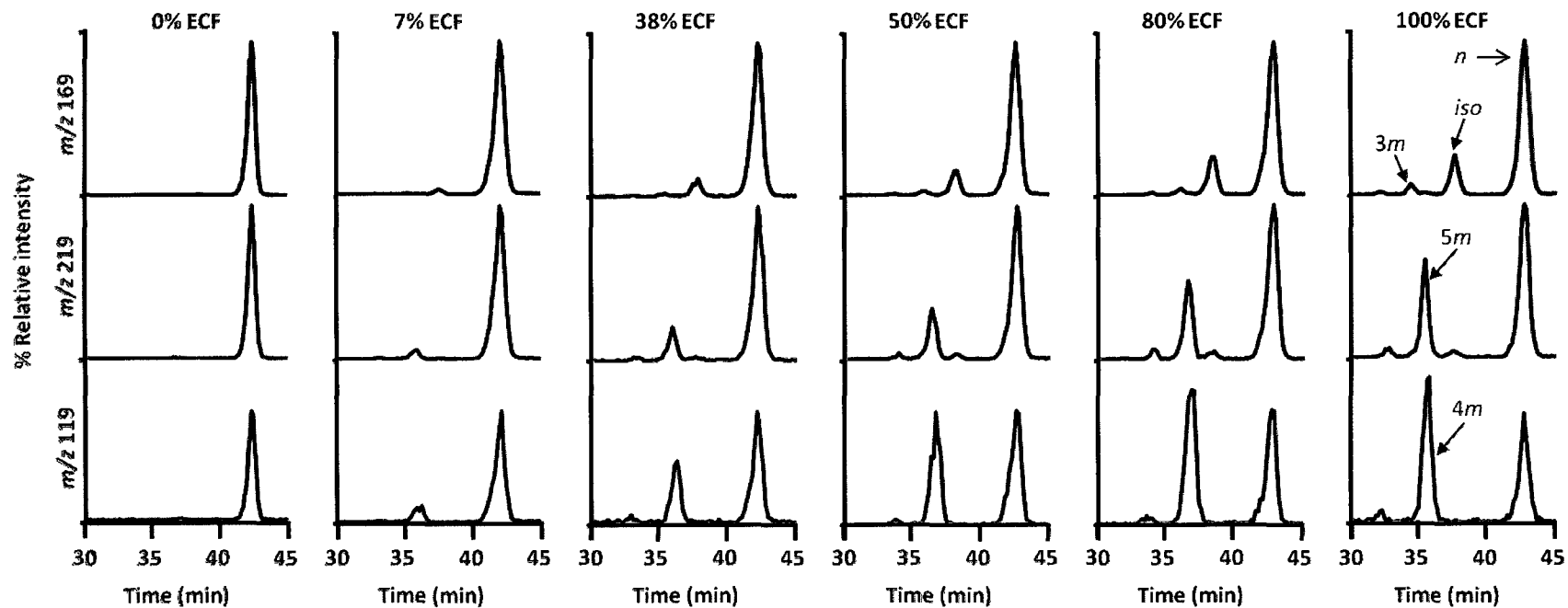
Figure E-2. PFOA chromatograms showing increase in telomer contribution to ECF signature from Norwegian sea (samples I, II) to North Sea (III, IV), to mouth of the Baltic Sea (V, VI).
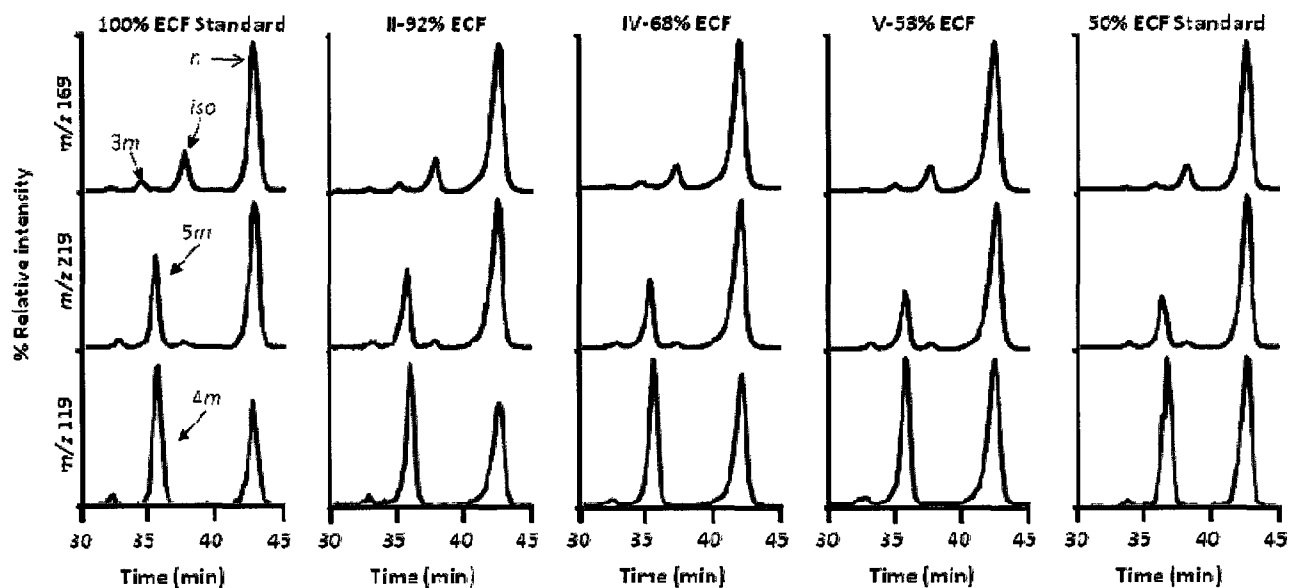
Figure E-3. PFOA chromatograms from Baffin Bay/ Lancaster Sound sampling locations and comparison to 100% ECF and 80% ECF standards.
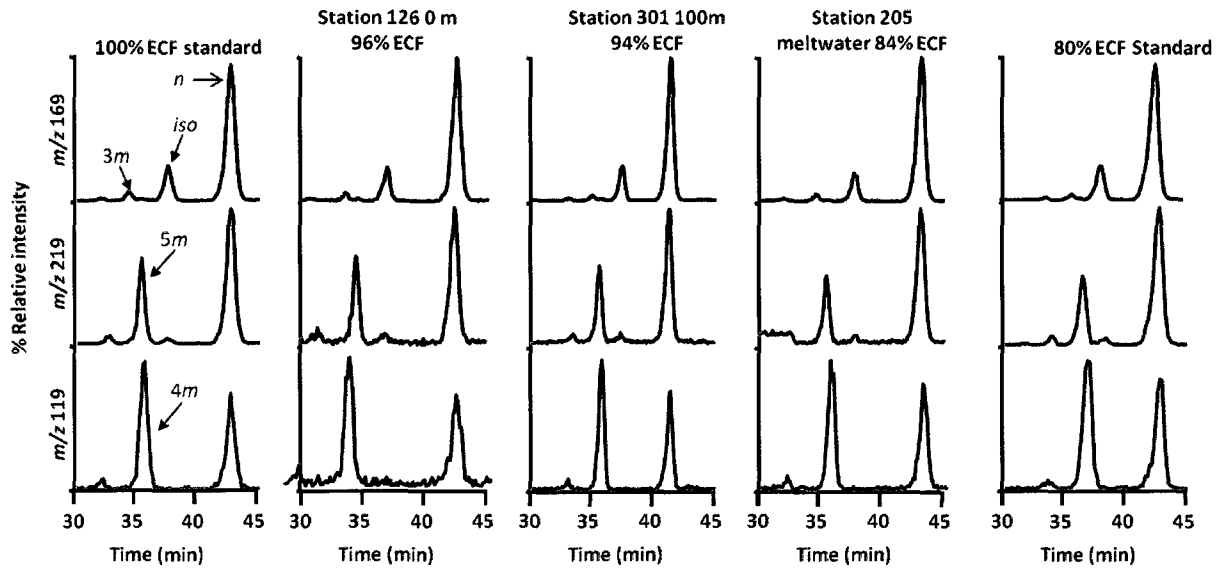
Figure E-4. PFOS Isomer chromatograms from Baffin Bay/ Lancaster Sound sampling locations. Note presence of interference eluting directly before branched isomers in m/z 499/80 product ions. This interference co-eluted with branched isomers in most samples, and was only observable in Arctic samples.
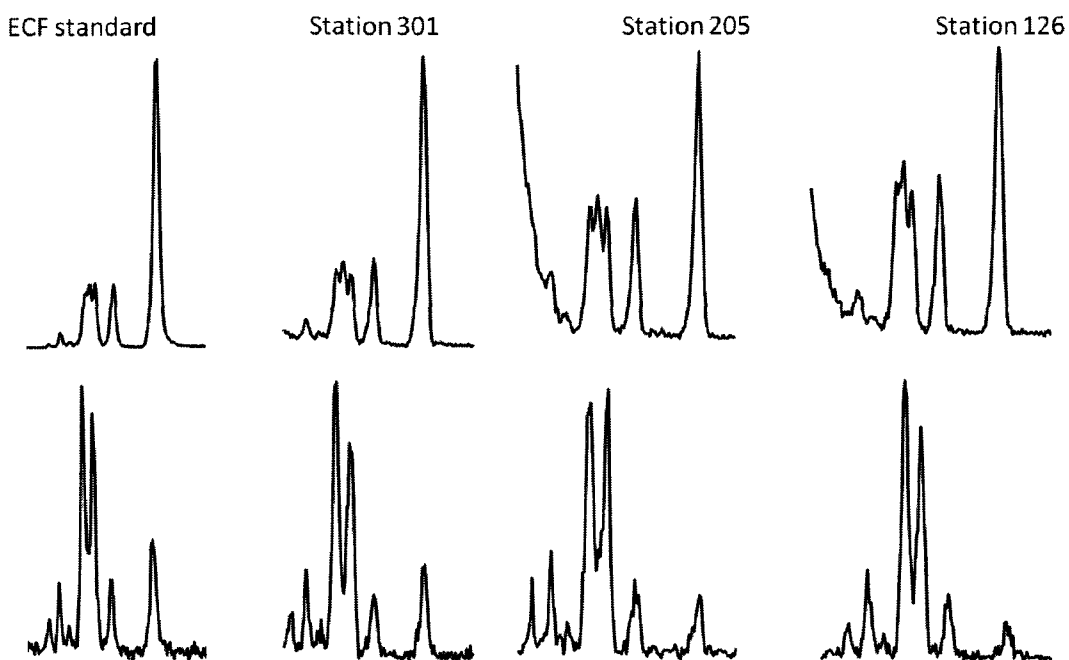
Table E-1. PFCs monitored in the present study and their acronyms, chemical forumula, and LC-MS/MS parent and product ions.

	Perfluorinated compound (acronym)	Chemical Formula	Parent Ions (m/z)	Product Ions (m/z)[a]
Perfluoroalkyl sulfonates	Perfluorobutane sulfonate (PFBS)	$C_4F_9SO_3^-$	299	80, 99, 130
	Perfluorohexane sulfonate (PFHxS)	$C_6F_{13}SO_3^-$	399	80, 99, 119, 169
	Perfluorooctane sulfonate (PFOS)	$C_8F_{17}SO_3^-$	499	80 (n, iso), 130 ($5m$, $3m$, dm), 330 ($4m$), 419 ($1m$), 99, 169, 180, 380, 230, 219, 119
	Perfluorodecane sulfonate (PFDS)	$C_{10}F_{21}SO_3$	599	80, 99, 130
Perfluoroalkyl sulfonamides	Perfluorooctane sulfonamide (FOSA)	$C_8F_{17}SO_2NH_2$	498	78, 169
	N-methyl perfluorooctane sulfonamide (NMeFOSA)	$C_8F_{17}SO_2NH(CH_3)$	512	169, 219, 269, 469, 219
	N-ethyl perfluorooctane sulfonamide (NEtFOSA)	$C_8F_{17}SO_2NH(CH_2CH_3)$	526	419, 169, 219, 319, 519
Perfluoralkyl carboxylates	Perfluorohexanoate (PFHxA)	$C_5F_{11}CO_2^-$	313	69, 119, 269,
	Perfluoroheptanoate (PFDA)	$C_6F_{13}CO_2^-$	363	169, 319
	Perfluorooctanoate (PFOA)	$C_7F_{15}CO_2^-$	413	369 (n), 169 (iso, $3m$), 219 ($5m$), 119 ($4m$), 319, 269
	Perfluorononanoate (PFNA)	$C_8F_{17}CO_2^-$	463	169, 219, 419
	Perfluorodecanoate (PFDA)	$C_9F_{19}CO_2^-$	513	219, 269, 469
	Perfluoroundecanoate (PFUnA)	$C_{10}F_{21}CO_2$	563	219, 319, 519
	Perfluorododecanoate (PFDoA)	$C_{11}F_{23}CO_2$	613	169, 569, 319
	Perfluorotridecanoate (PFTrA)	$C_{12}F_{25}CO_2$	663	119, 269, 619
	Perfluorotetradecanoate (PFTA)	$C_{13}F_{27}CO_2^-$	713	169, 669, 419
	Perfluoropentadecanoate (PFTdA)	$C_{14}F_{29}CO_2^-$	763	219, 269, 719
Internal Standards	Perfluorohexane[$^{18}O_2$]sulfonate (^{18}O-PFHxS)	$C_6F_{13}S[^{18}O_2]O$	403	84, 103
	Perfluoro[1,2,3,4-$^{13}C_4$]octanesulfonate (^{13}C-PFOS)	$C_4F_9[1,2,3,4-^{13}C_4]F_8SO_3^-$	503	80, 99
	$^{13}C_{1,2}$-perfluorohexanoate (^{13}C-PFHxA)	$C_4F_9[2-^{13}C]F_2^{13}CO_2^-$	315	270, 119
	Perfluoro[1,2,3,4-$^{13}C_4$]octanoate (^{13}C-PFOA)	$C_4F_9[2,3,4-^{13}C_3]F_6^{13}CO_2^-$	417	372
	Perfluoro[1,2,3,4,5-$^{13}C_5$]nonanoate (^{13}C-PFNA)	$C_4F_9[2,3,4,5-^{13}C_4]F_8^{13}CO_2^-$	468	423
	Perfluoro[1,2-$^{13}C_2$]decanoate (^{13}C-PFDA)	$C_8F_{17}^{13}CF_2^{13}CO_2^-$	515	470
	Perfluoro[1,2-$^{13}C_2$]undecanoate (^{13}C-PFUnA)	$C_9F_{19}^{13}CF_2^{13}CO_2^-$	565	520
	Perfluoro[1,2-$^{13}C_2$]dodecanoate (^{13}C-PFDoA)	$C_{10}F_{21}^{13}CF_2^{13}CO_2$	615	570
	Perfluoro[1,2,3,4,5,6,7,8-$^{13}C_8$]octanesulfonamide (^{13}C-FOSA)	$C_4F_9[1,2,3,4,5,6,7,8-^{13}C_8]F_8SO_2NH_2$	506	78

a. (specific PFOS and PFOA isomers monitored in a given product ion are stated in parenthesis)

Table E-2. Total, *n*- and branched-PFOA concentrations and contribution of individual manufacturing sources (ECF, *n*-telomer, *iso*-telomer) to total PFOA concentrations. Upper values (total, *n*-PFOA concentrations and ECF) represent subtraction of highest blank, while lower values represent subtraction of lowest blank. Quantification using % ECF vs %branched. Samples 1, 3, 19, 26 had unique isomer profiles which could not be accounted for contributions from n-telomer or *iso*-telomer sources, therefore % ECF could not be calculated.

Sample	Total PFOA (Ahrens et al. 2009[1], 2010[2]; pg/L)	Total PFOA (This study; pg/L)	*n*-PFOA (pg/L)	% branched	%ECF	% *n*-telomer (% *iso*-telomer shown in parenthesis)
3M ECF PFOA				18.0 ±0.3	100 (99-102)	0
1	229	263	213	18.7		
2	209	167	138	17.4	95	5
3	99	117	95	19.2		
4	147	126	104	17.4	97	3
5	97	100	83	17.3	97	3
6	115	92	70	23.9	88	4 (8)
7	94	79	65	16.8	94	6
8	108	110	91	17.0	95	5
9	80	73	61	16.6	93	7
10	88	70	57	17.5	98	2
11	65	70	58	16.6	93	7
12	62	78	66	16.0	89	11
14	69	78	65	17.3	97	3
16	72	83	64	23.0	93	1 (6)
19	77	92	73	20.6		
25	87	102	85	16.5	93	7
26	82	121	93	23.4		
27	65	92	73	17.3	97	3
I	10	92	77	16.8	94	6
II	10	94	78	16.3	92	8
III	70	169	149	11.7	65	35
IV	350	378	332	12.1	68	32
V	340	304	275	9.4	53	47
VI	240	313	282	9.7	55	45

Table E-3. Branched: *n*-PFOA isomer ratios in Atlantic, North, and Norwegian Sea water samples relative to 3M ECF PFOA. Statistically significant differences ($P < 0.05$) between samples and the ECF PFOA standard are highlighted in grey.

Sample	*iso:n*	*5m:n*	*4m:n*	*3m:n*
3M ECF PFOA	0.13	0.08	0.06	0.03
1	0.14	0.10	0.08	0.03
2	0.12	0.08	0.06	0.02
3	0.15	0.09	0.07	0.02
4	0.14	0.08	0.06	0.02
5	0.13	0.08	0.06	0.02
6	0.19	0.07	0.06	0.03
7	0.10	0.06	0.05	0.02
8	0.11	0.06	0.05	0.02
9	0.10	0.06	0.05	0.02
10	0.13	0.08	0.06	0.02
11	0.10	0.06	0.05	0.02
12	0.09	0.06	0.05	0.02
14	0.12	0.08	0.06	0.03
16	0.19	0.08	0.06	0.02
19	0.13	0.10	0.09	0.03
25	0.10	0.07	0.05	0.02
26	0.20	0.12	0.09	0.04
27	0.12	0.08	0.06	0.02
I	0.10	0.06	0.04	0.02
II	0.10	0.07	0.05	0.02
III	0.07	0.05	0.04	0.02
IV	0.07	0.05	0.03	0.01
V	0.06	0.04	0.03	0.01
VI	0.06	0.05	0.03	0.01

Table E-4. Branched: *iso*-PFOA isomer ratios in Atlantic, North, and Norwegian Sea water samples relative to 3M ECF PFOA. Statistically significant differences (P < 0.05) between samples and the ECF PFOA standard are highlighted in grey.

Sample	5*m*:iso	4*m*:iso	3*m*:iso
3M PFOA	0.61	0.46	0.20
1	0.71	0.57	0.19
2	0.66	0.53	0.18
3	0.58	0.46	0.17
4	0.58	0.45	0.16
5	0.60	0.46	0.18
6	0.40	0.31	0.14
7	0.59	0.48	0.17
8	0.55	0.45	0.20
9	0.66	0.53	0.18
10	0.60	0.45	0.19
11	0.61	0.48	0.24
12	0.62	0.51	0.20
14	0.64	0.50	0.21
16	0.40	0.30	0.12
19	0.82	0.70	0.21
25	0.67	0.53	0.18
26	0.61	0.43	0.22
27	0.67	0.51	0.19
I	0.60	0.47	0.18
II	0.68	0.47	0.21
III	0.73	0.51	0.22
IV	0.74	0.53	0.20
V	0.66	0.48	0.18
VI	0.72	0.53	0.20

Table E-5. $4m{:}5m$ and $3m{:}5m$-PFOA isomer ratios in Atlantic, North, and Norwegian Sea water samples relative to 3M ECF PFOA. Statistically significant differences (P < 0.05) between samples and the ECF PFOA standard are highlighted in grey.

Sample	*4m:5m*	*3m:5m*
3M PFOA	0.74	0.33
1	0.81	0.27
2	0.81	0.28
3	0.80	0.29
4	0.78	0.27
5	0.78	0.30
6	0.77	0.35
7	0.81	0.28
8	0.83	0.36
9	0.81	0.27
10	0.76	0.31
11	0.79	0.39
12	0.82	0.33
14	0.79	0.33
16	0.75	0.29
19	0.86	0.25
25	0.79	0.27
26	0.71	0.36
27	0.77	0.28
I	0.78	0.30
II	0.69	0.32
III	0.71	0.30
IV	0.71	0.27
V	0.72	0.27
VI	0.74	0.27

Table E-6. Weight distribution of PFOS isomers in Atlantic and North/Norwegian Seas sampling locations. Error represents ± 1 standard error about the mean (SEM).

Sample	Total PFOS concentration (pg/L)		% Composition (wt)						
	This study	Ahrens et al. 2009[1], 2010[2]	*n-*	*iso-*	*5m*	*4m*	*3m*	*1m*	*dm*
3M PFOS (n=5)			72.8 ±0.9	9.4 ±0.1	4.2 ±0.2	4.1 ±0.2	5.2 ±0.1	2.1 ±0.02	2.2 ±0.1
1	295	291	65	13	7	4	7	1	3
2	104	114	69	12	6	4	6	1	2
3	33	40	70	12	5	4	6	0.78	2
4	ND	<10							
5	ND	<10							
6	ND	<10							
7	ND	<10							
8	7	<10	66	12	7	5	7	ND	3
9	10	<10							
10	ND	<10							
11	ND	<10							
12	14	<10	70	10	5	4	8	ND	2
14	15	<10	69	13	6	3	6	ND	2
16	ND	<10							
19	ND	<10							
21	ND	<10							
22	ND	<10							
23	ND	<10							
24	ND	<10							
25	ND	<10							
26	31	60	65	10	7	5	7	3	3
27	ND	<10							
32	ND	<10							
36	ND	<10							
42	ND	<10							
I	6	ND	60	14	6	4	9	3	3
II	16	ND	66	11	7	6	6	ND	3
III	59	ND	60	13	8	5	8	2	3
IV	190	ND	64	11	8	4	8	2	3
V	141	ND	68	10	6	4	7	2	3
VI	143	ND	63	11	8	4	8	2	3

Table E-7. FOSA Concentration (pg/L) in Atlantic and North, and Norwegian Sea water and branched content.

Sample	Total FOSA (Ahrens et al. 2009[1], 2010[2]; pg/L)	% Linear	% branched (sum 3 isomers)
1	302	82.2	17.8
2	307	88.2	11.8
3	97	85.6	14.4
4	183	85.5	14.5
5	143	89.7	10.3
6	104	89.3	10.7
7	97	90.9	9.1
8	71	87.9	12.1
9	32	88.1	11.9
10	44	88.8	11.2
11	37	84.2	15.8
12	39	88.1	11.9
14	45	85.3	14.7
16	37	85.8	14.2
19	<17	ND	ND
21	110	88.5	11.5
22	72	84.6	15.4
23	<17	ND	ND
24	60	87.0	13.0
25	<17	ND	ND
26	<17	ND	ND
27	<17	ND	ND
32	37	ND	ND
36	<17	ND	ND
42	<17	ND	ND
I	ND	85.0	15.0
II	ND	81.9	18.1
III	280	96.9	3.1
IV	210	89.9	10.1
V	120	81.2	18.8
VI	200	87.7	12.3

Table E-8. PFA Concentrations (pg/L) in Atlantic and North/Norwegian Sea water and Comparison to Ahrens values. PFDoA and PFTA were not detected.

Sample	PFHxS	PFNA	PFNA (Ahrens)	PFDA	$3,7m_2$-PFDA	PFUnA
1	19	110[a]	107	51	42	11
2	12	82[a]	100	25	16	59
3	17	55	65	ND	ND	ND
4	ND	69[a]	69	ND	ND	ND
5	ND	60[a]	63	ND	ND	ND
6	6	57[a]	73	ND	ND	ND
7	ND	46	65	ND	ND	ND
8	ND	62	68	ND	ND	ND
9	ND	63[a]	66	ND	ND	ND
10	ND	43	52	ND	ND	ND
11	ND	39[a]	31	ND	ND	ND
12	ND	43	16	ND	ND	ND
14	ND	50[a]	23	ND	ND	ND
16	ND	33[a]	29	ND	ND	ND
19	ND	34[a]	13	ND	ND	ND
21	ND	37[a]	40	ND	ND	ND
22	ND	37	42	ND	ND	ND
23	ND	21[a]	28	ND	ND	ND
24	ND	21	29	ND	ND	ND
25	ND	20[a]	29	ND	ND	ND
26	ND	27[a]	35	ND	ND	ND
27	ND	25[a]	30	ND	ND	ND
32	ND	ND	<5.1	ND	ND	ND
36	ND	10	<5.1	ND	ND	ND
42	ND	2	<5.1	ND	ND	ND
I	ND	44	ND	3	ND	ND
II	ND	53	ND	ND	ND	ND
III	3	83	10	10	ND	60
IV	25	137	40	19	ND	32
V	15	114	20	13	ND	29
VI	16	105	10	3	ND	ND

[a]Potential branched isomer detected in m/z 169 and 219 product ions, always at or near limits of detection (<1% of peak area of linear isomer).

Table E-9. Total, n- and branched-PFOA concentrations and contribution of individual manufacturing sources (ECF, n-telomer) to total PFOA concentrationsin Arctic Sampling locations.

Station	Depth (m)	Total PFOA	n-PFOA	% branched	% ECF
101	0	95	81	14.9	84
108	0	80	69	13.9	78
115	0	46	38	15.8	89
	0	38	32	17.1	96
	50	39	32	17.7	99
126	100	76	63	17.2	96
	200	29	24	17.2	96
	319	31	26	17.2	96
	0	57	48	16.0	90
	0	30	25	17.3	97
	50	41	35	14.6	82
137	100	59	50	15.4	86
	200	37	31	17.3	97
	200	54	45	16.9	95
	400	11	9	16.8	94
	484	15	12	17.2	96
	Glacier surface	14	11	18.4	-
205	Glacier meltwater	72	62	15.0	84
	0	78	68	13.6	76
	50	81	68	15.9	89
	100	77	66	14.3	80
	0	19	15	16.5	93
	0	21	18	16.0	89
	50	66	55	16.7	94
301	100	145	121	16.8	94
	200	43	36	16.4	92
	400	30	24	17.8	-
	600	78	65	16.5	93
303	0	76	64	16.1	90

Table E-10. Branched: *n*-PFOA isomer ratios in Baffin Bay sampling locations.

Station	Depth	*iso:n*	*5m:n*	*4m:n*	*3m:n*
		0.13	0.08	0.06	0.03
301	0	0.10	0.06	0.05	0.02
301	0	0.09	0.05	0.05	0.02
301	50	0.10	0.07	0.05	0.02
301	100	0.11	0.07	0.05	0.02
301	200	0.11	0.06	0.05	0.01
301	400	0.14	0.10	0.08	0.03
301	600	0.10	0.07	0.05	0.02
137	0	0.09	0.06	0.05	0.01
137	0	0.11	0.07	0.05	0.02
137	50	0.08	0.06	0.04	0.01
137	100	0.09	0.06	0.04	0.02
137	200	0.10	0.07	0.05	0.02
137	200	0.10	0.06	0.04	0.01
137	400	0.11	0.06	0.06	0.02
137	484	0.12	0.07	0.05	0.02
205	Glacier surface	0.11	0.08	0.07	0.03
205	Glacier meltwater	0.09	0.06	0.05	0.02
205	0	0.08	0.05	0.04	0.01
205	50	0.10	0.06	0.05	0.02
205	100	0.08	0.06	0.04	0.01
126	0	0.11	0.06	0.05	0.02
126	50	0.12	0.09	0.06	0.02
126	100	0.10	0.06	0.05	0.01
126	200	0.10	0.07	0.05	0.02
126	319	0.10	0.07	0.05	0.02
303	0	0.11	0.06	0.04	0.02
115	0	0.09	0.07	0.04	0.02
108	0	0.08	0.06	0.04	0.02
101	0	0.09	0.06	0.05	0.02

362

Table E-11. Branched:*iso*-PFOA ratios for Baffin Bay/Lancaster Sound samples. Grey shading indicates a statistically significant difference relative to 3M ECF PFOA.

	Depth	5m:iso	4m:iso	3m:iso
		0.63	0.46	0.20
301	0	0.65	0.50	0.19
301	0	0.58	0.53	0.17
301	50	0.65	0.53	0.18
301	100	0.61	0.46	0.14
301	200	0.55	0.42	0.13
301	400	0.75	0.59	0.22
301	600	0.68	0.49	0.15
137	0	0.68	0.56	0.17
137	0	0.64	0.49	0.17
137	50	0.69	0.42	0.16
137	100	0.73	0.48	0.18
137	200	0.67	0.53	0.17
137	200	0.62	0.42	0.14
137	400	0.55	0.51	0.17
137	484	0.61	0.46	0.15
205	Glacier surface	0.79	0.67	0.24
205	Glacier meltwater	0.65	0.52	0.22
205	0	0.63	0.47	0.17
205	50	0.61	0.49	0.18
205	100	0.67	0.48	0.16
126	0	0.60	0.51	0.16
126	50	0.70	0.50	0.17
126	100	0.58	0.47	0.15
126	200	0.71	0.53	0.19
126	319	0.66	0.51	0.20
303	0	0.56	0.40	0.15
115	0	0.73	0.49	0.21
108	0	0.74	0.53	0.22
101	0	0.66	0.49	0.20

Table E-12. FOSA Concentrations and isomer profiles.

Station	Depth	Total FOSA	*n*-FOSA	% branched
301	0	2	1	29
301	200	5	3	33
137	10	2	1	35
137	100	1	1	36
137	200	1	1	39
205	Glacier surface	1	1	20
205	Glacier meltwater	1	1	24
126	10	2	1	26
126	50	2	1	32
303	0	12	9	26
115	0	1	1	35
108	0	2	1	37

REFERENCES

1.   Ahrens L.; Barber, J. L.; Xie, Z.; Ebinghaus, R. *Environ. Sci. Technol.*
        2009, *43*, 3122-3127.

2.   Ahrens, L.; Gerwinski, W.; Theobald, N.; Ebinghaus, R, *Mar. Pollut.*
        Bull., **2010**, *60*, 255-260.